The Dynamics of the Acetylcholine Receptor and the Receptor-Associated Rapsyn Scaffolding Protein Studied *In Vitro* and *In Vivo*
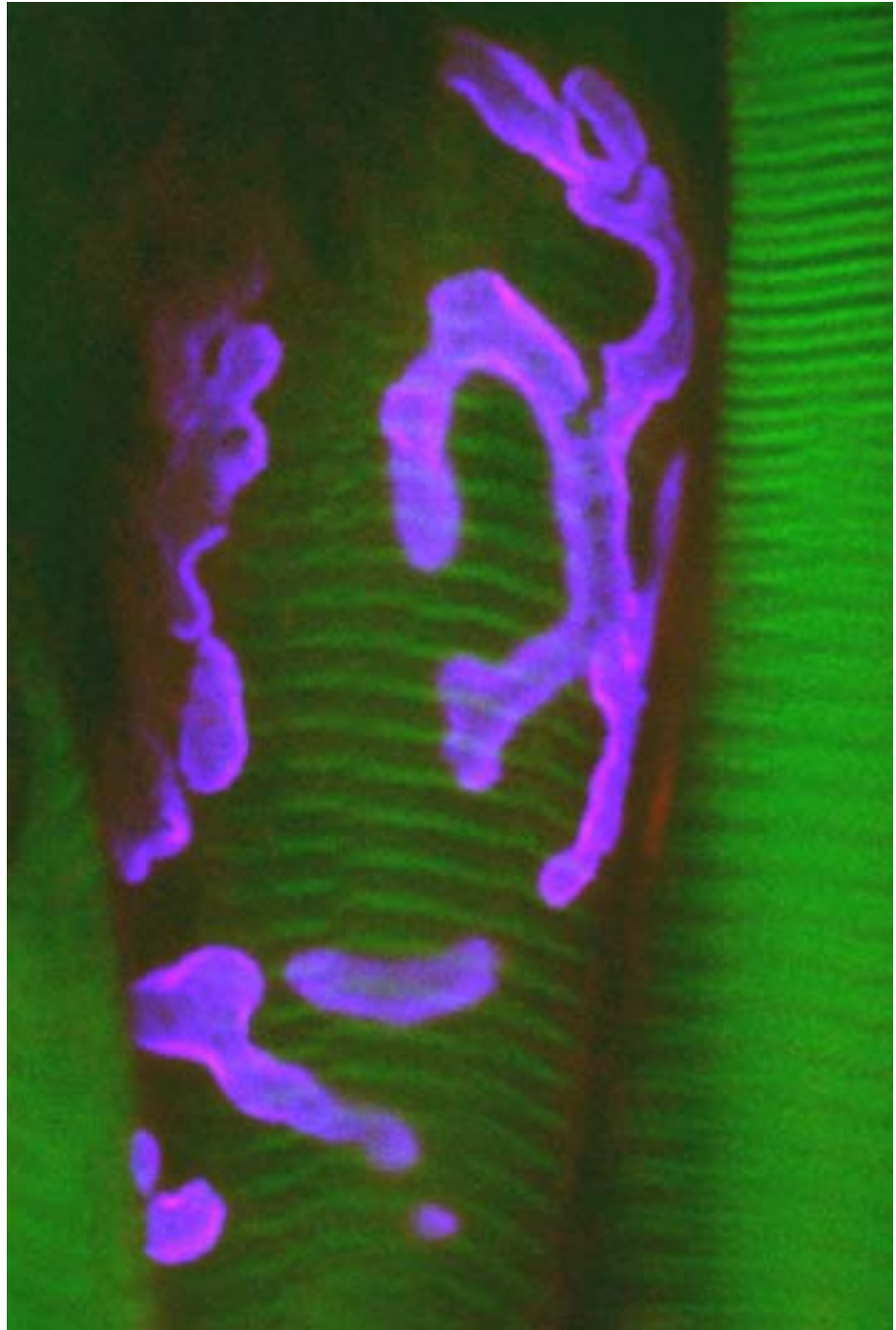
by

Emile G. Bruneau

A dissertation submitted in partial fulfillment
of the requirements for the degree of
Doctor of Philosophy
(Neuroscience)
in The University of Michigan
2008

Doctoral Committee:

      Professor Mohammed Akaaboune, Chair
      Professor Daniel J. Goldman
      Professor Richard I. Hume
      Professor John Y. Kuwada
      Assistant Professor Jose A. Esteban

Dedication

To my mother who has led me on a continual journey to understand how our magnificent and delicate brains provide us with such convincing yet divergent versions of reality. This has been the latest stop. Many more await.

Acknowledgements

To my motivations for entering into neuroscience: Robert Sapolsky for bringing science and humanism together for me. The children who I taught over the years whose process of learning so fascinated me.

To the forces that kept me here: A neuroscience program that was at once helpful and familiar. An advisor in Mohammed whose enthusiasm and clear thinking provided a wonderful guide to my education. The many professors in the greater neuroscience community here who have, in ways both modest and grand, helped me become a better scientist: John Kuwada, Israel Liberzon, Roger Albin, Gisela Wilson, Hao Shing Hsu, Jose Esteban, Dan Goldman, Gina Poe, and especially Richard Hume, who set the tone for my graduate experience and provided help, support, belief and guidance the entire way through. The friends I have made here in Michigan, in particular Mary, who provided me with continual reminders of what 'determined effort' and 'playfulness' really mean. Finally, my family, whose unqualified support has always provided the best context in which to grow into my own.

Table of Contents

List of Figures

Chapter I

Introduction

In the mammalian nervous system, synaptic transmission is largely mediated by ligand-gated ion channels which are aggregated in high density in the membrane of the post-synaptic target cell in direct apposition to nerve terminals. In the central nervous system (CNS), the majority of excitatory input is mediated by glutamatergic α-**a**mino-3-hydroxy-5-**m**ethylisoxazole-4-**p**ropionic **a**cid (AMPA) and *N*-**m**ethyl *D*-**a**spartate (NMDA) receptors, while inhibitory transmission is governed almost entirely by glycine and γ-**a**mino**b**utyric **a**cid (GABA$_A$) receptors. In the peripheral nervous system (PNS), cholinergic transmission is mediated at the neuromuscular junction (NMJ) by acetylcholine receptors (AChRs) clustered on the muscle cell surface. In all synapses, the efficiency of synaptic transmission is largely controlled by the density of neurotransmitter receptors, and changes in receptor density have been shown to be crucial for synaptic development and synaptic plasticity.

Although neuromuscular synapses and synapses within the CNS differ markedly in a number of respects, the list of striking similarities between peripheral cholinergic synapses and central glycinergic, GABAergic and glutamatergic synapses is growing: the role of receptor recycling in maintaining receptor density, the activity-dependence of receptor dynamics, the rapid dynamics of receptor-associated proteins and the differential

regulation of receptor and receptor-associated proteins are all ways in which the machinery of the NMJ has recently been shown to behave similarly to synapses in the CNS. It therefore seems likely that similar cellular and molecular mechanisms may be regulating the clustering, maintenance and stability of post-synaptic receptor densities. These similarities are intriguing enough to justify the use of the NMJ as a model synapse that may inform processes occurring at synapses in the central nervous system.

The simple question still remains, however: why use the NMJ as a model synapse? First, the neuromuscular synapse is large and easily accessible, allowing repetitive imaging in the living animal. Second, the extremely high-affinity AChR ligand, bungarotoxin, can be used to selectively label AChRs at the post-synaptic membrane. Finally, the large number of receptors and associated proteins at the post-synaptic membrane allows protein number and density to be accurately quantified. Together, these characteristics enable the investigation of receptor dynamics at individual synapses *in vivo* over long periods of time. It is our hope, therefore, that the robust findings in the NMJ can provide insights and potential new avenues of research, either methodologically or conceptually, for studies of protein dynamics in the central nervous system. Indeed, in this thesis I show a number of ways in which the post-synaptic protein dynamics of the NMJ are similar, in ways not previously thought, to the dynamics of PSD proteins at inhibitory and/or excitatory synapses in the CNS. Before engaging these studies, however, it is necessary to first put them in context.

The body of work contained in this thesis focuses on two critical protein components of the post-synaptic scaffolding complex at the NMJ which allow synaptic transmission to occur: the acetylcholine receptors and the **r**eceptor-**a**ssociated **p**rotein of

the **syn**apse (rapsyn), which underlies the receptor and anchors it in place at the muscle surface. Accordingly, the introduction will be broken into two parts that each serve as a separate reviews: the first ("Running to stand still: ionotropic receptor dynamics at central and peripheral synapses") will focus on the current state of our understanding of ionotropic receptor dynamics in synapses both in the central and peripheral nervous systems, and the second ("The role of dynamic receptor-associated proteins in the development and plasticity of the synapse") will outline the emerging research focus on the role of receptor-associated proteins in the regulation of receptor dynamics in these synapses.

A note on the use of the term "turnover". "Turnover" has been used to describe protein dynamics for decades. The definition now has come to refer to a number of different protein properties. One definition of turnover is the time that it takes for a protein to be synthesized, inserted into the membrane, removed and degraded. This is normally referred to as "metabolic turnover". Experiments using radioactive ligands such as bungarotoxin-^{35}I, on the other hand, label acetylcholine receptors already on the membrane surface at the time of incubation, and so "turnover" in these experiments (found by measuring the radioactivity remaining in the membrane at later time points) is a determination of the time it takes for surface receptors to be internalized, degraded and ejected from the cell. This might be called "surface dwell-time". The types of experiments performed in our lab deal almost exclusively with synaptic receptors. Therefore, when we measure changes in receptor number using fluorescent ligands, we are determining the dwell-time of receptors in the synapse. In this dissertation this last

definition of turnover is used and is referred to as "synaptic dwell-time", "synaptic turnover" or simply "receptor turnover".

Running to Stand Still: Ionotropic Receptor Dynamics at Central and Peripheral Synapses

Emile G. Bruneau and Mohammed Akaaboune

Abstract

In order for synapses to form and function, neurotransmitter receptors must be recruited to a location on the post-synaptic cell in direct apposition to pre-synaptic neurotransmitter release. Once inserted into the post-synaptic membrane, receptors are not fixed in place, however, but are permanently exchanged between synaptic and extra-synaptic regions, and cycle between the surface and intracellular compartments. In this review, we will highlight and compare the current knowledge about the dynamics of acetylcholine receptors at the vertebrate peripheral neuromuscular junction and AMPA, NMDA, and GABA receptors in central synapses.

Introduction

Much of our understanding about rapid changes in receptor trafficking in response to activity has come from studies on the AMPA receptor (Bredt and Nicoll, 2003; Malenka, 2003; Collingridge et al., 2004). Using primary neuronal cultures and organotypic hippocampal slice preparations a large body of work has found that AMPARs are inserted and removed rapidly from the synapse in response to different stimulation protocols. These changes in receptor density are involved in the processes of

long-term potentiation and long-term depression, which have long been thought to be cellular mechanisms of learning and memory (Bliss and Lomo, 1973; Bear and Malenka, 1994). Interestingly, many of the characteristic behaviors of AMPA receptors have been found to apply to NMDA and GABA receptors in the central nervous system (CNS) and acetylcholine receptors (AChRs) in peripheral neuromuscular junctions (NMJs).

Just as findings in the CNS have directed investigation in peripheral synapses, work in the NMJ has given great insights into the processes of pre-synaptic vesicular release, synaptic pruning, receptor clustering and surface mobility that have proved to be applicable to synapses in the central nervous system. This is due largely to the accessibility of the neuromuscular junction and the availability of the highly specific acetylcholine receptor ligand bungarotoxin, which has allowed the analysis of *in vivo* synapse formation and maintenance in living animals. More recently, much work has been done to understand the trafficking of acetylcholine receptors at the neuromuscular junction. The NMJ is dramatically larger than a central synapse and has the extremely high synaptic receptor density of >10,000 receptors/μm^2. Building on research begun over 3 decades ago into the dynamics of AChRs, more recent studies using conjugated bungarotoxin, fluorescent labeling and time-lapse imaging in the living mouse have given us great insights into synaptic receptor dynamics *in vivo*.

While each receptor has its own complement of accessory proteins and regulatory elements to enable receptor trafficking and activity-dependent changes in trafficking to occur, some interesting commonalities between excitatory and inhibitory synapses of the central nervous system, and cholinergic synapses in the peripheral nervous system have emerged that will also be explored in this review.

Regulation of AMPAR dynamics at excitatory central synapses:

The AMPA receptor is a tetrameric ionotropic glutamate receptor composed of Glu1-4 subunits (Hollmann and Heinemann, 1994), which are expressed as GluR1/2 and GluR2/3 heteromers in most brain regions (Zhu et al., 2000). A number of studies in recent years have used both direct and indirect methods to measure basal dynamics (removal, insertion, recycling and lateral mobility) of AMPARs (Figure 1A). These studies have shown that the half-life of AMPARs varies widely depending on cell type and technique used (optical, biochemical or electrophysiological), ranging from minutes to days. For example, $[S]^{35}$ uptake experiments have estimated the turnover of AMPARs in cerebellar granule cells to be 18-23 hours for GluR2/3 and GluR4 subunits (Huh and Wenthold, 1999), and 48 hours for the GluR1 subunit (Archibald et al., 1998), while biotinylation assays have estimated surface GluR1 expression to have a $t_{1/2}$ of 30 hours on cultured cerebellar granule cells (Archibald et al., 1998), 11-43 hours on spinal cord cultures (depending upon culture age) (Mammen et al., 1997; O'Brien et al., 1998) and ~1-2 hours on cultured hippocampal neurons (Ehlers, 2000; Passafaro et al., 2001; Park et al., 2004). Using fluorescent bungarotoxin to bind to recombinant AMPARs and fluorescent AMPAR antibodies, however, the insertion and removal of AMPARs under basal conditions has been shown to occur very rapidly, on the order of minutes (Lin et al., 2000; Sekine-Aizawa and Huganir, 2004). Similar results were obtained when electrophysiological recording were used: the run down or run up of synaptic AMPAR EPSCs in response to pharmacological blockade of either exocytosis or endocytosis was found to occur rapidly over a time course of minutes (Nishimune et al., 1998; Luscher et al., 1999; Luthi et al., 1999; Lee et al., 2004).

One limitation of most of these studies is that they are not able to resolve synaptic and extra-synaptic receptor pools. Most recently, an elegant study using photoinactivation of AMPARs with the compound ANQX allowed a more complete analysis of AMPA receptors dynamics (Adesnik et al., 2005). This technique has the power to specifically determine AMPAR turnover at distinct neuronal regions (synaptic, extrasynaptic and soma). Interestingly, this study found that AMPAR insertion at the soma was rapid ($t_{1/2}$ <15 minutes), while AMPAR recovery at extra-synaptic and synaptic sites on the dendrites was much slower, on the order of hours. Although the average half-life on the neuronal surface is reasonably consistent with the average surface half-life estimated in previous work, this study is still at odds with a number of previous studies showing fast synaptic insertion and removal of AMPARs.

Although the above-mentioned estimates of AMPAR half-life under basal conditions vary widely from minutes to days, it is almost universally accepted that rapid and significant changes in AMPAR number can occur within seconds at synaptic sites in response to activity. For example, during long-term depression (LTD) or long-term potentiation (LTP), the endocytosis, exocytosis or recycling of receptors can be altered by the regulated association of AMPARs with a number of intracellular proteins which increase or decrease synaptic AMPAR expression (Bredt and Nicoll, 2003; Gomes et al., 2003; Malenka, 2003; Collingridge et al., 2004; Palmer et al., 2005). LTP and LTD, which have been most extensively studied in the hippocampus, have been shown to involve changes in the GluR1/2 receptors which are expressed at a low basal level synaptically and are then inserted into the synapse rapidly in response to LTP induction protocols (Shi et al., 1999; Ehlers, 2000; Hayashi et al., 2000; Lu et al., 2001; Passafaro

et al., 2001; Shi et al., 2001; Lee et al., 2004). Conversely, GluR1/2 receptors are removed rapidly in response to LTD or de-potentiation (Ehlers, 2000; Lin et al., 2000; Lee et al., 2002; Brown et al., 2005). Consistent with this, GluR2 and GluR2/3 knockout mice show no deficits in LTP or LTP-dependent learning (Jia et al., 1996; Meng et al., 2003) while the targeted deletion of GluR1 significantly impairs LTP (Zamanillo et al., 1999) and hippocampus-dependent learning (Reisel et al., 2002; Schmitt et al., 2003), which can be rescued by the delivery of GluR1 into the hippocampus (Schmitt et al., 2005). Further, rapid experience-dependent insertion of GluR1/2 receptors has been shown to occur *in vivo* after fear conditioning in the amygdala (Rumpel et al., 2005), and the rapid removal of GluR1/2 receptors has been observed *in vivo* after monocular deprivation in the visual cortex (Heynen et al., 2003) or activity deprivation in the barrel cortex (Takahashi et al., 2003).

AMPAR dynamics are regulated by a host of accessory proteins that facilitate or inhibit the insertion and removal of AMPARs. For example, the TARP family of proteins (γ-3, γ-4, γ-8 and Stargazin (γ-2)) bind AMPARs to the post-synaptic density protein, PSD-95 to mediate AMPAR synaptic clustering (Hashimoto et al., 1999; Chen et al., 2000; Schnell et al., 2002; Rouach et al., 2005; Tomita et al., 2005a; Nicoll et al., 2006). TARP-AMPAR association is activity-dependent, as glutamate binding has been shown to dissociate TARPs from AMPARs (Tomita et al., 2004), and Stargazin phosphorylation has been shown to mediate the expression of both LTP and LTD (Tomita et al., 2005b). It has been suggested that TARP-AMPAR dissociation might facilitate lateral diffusion of AMPARs out of synapses and into the extra-synaptic space, where they could be internalized by clathrin-coated pits (Triller and Choquet, 2003; Tomita et al., 2005a). In

fact, a mechanism of receptor delivery and removal from synapses by extra-synaptic endo- and exocytosis and lateral diffusion was first described for acetylcholine receptors in the neuromuscular junction (Axelrod et al., 1976) and has since been found to occur similarly for AMPARs. In glutamatergic synapses, endocytic zones have been identified in the extra-synaptic area close to the PSD (Blanpied et al., 2002), and pH-sensitive GFP-conjugates have shown that internalization occurs in this area in response to NMDAR activation (Ashby et al., 2004). The lateral movement of AMPARs between synaptic and extra-synaptic spaces is regulated by calcium (Borgdorff and Choquet, 2002), and single particle imaging shows that receptor mobility within the PSD and extra-synaptic area is increased with treatments that stimulate neuronal activity (Tardin et al., 2003; Groc et al., 2004). Finally, transient internalization of extracellular receptors appears to precede synaptic loss of receptors (Ashby et al., 2004) and diffuse extra-synaptic staining of inserted AMPARs has also been observed to precede AMPAR aggregation at the PSD (Passafaro et al., 2001), indicating that the extra-synaptic area may be involved both in endo- and exocytotic events.
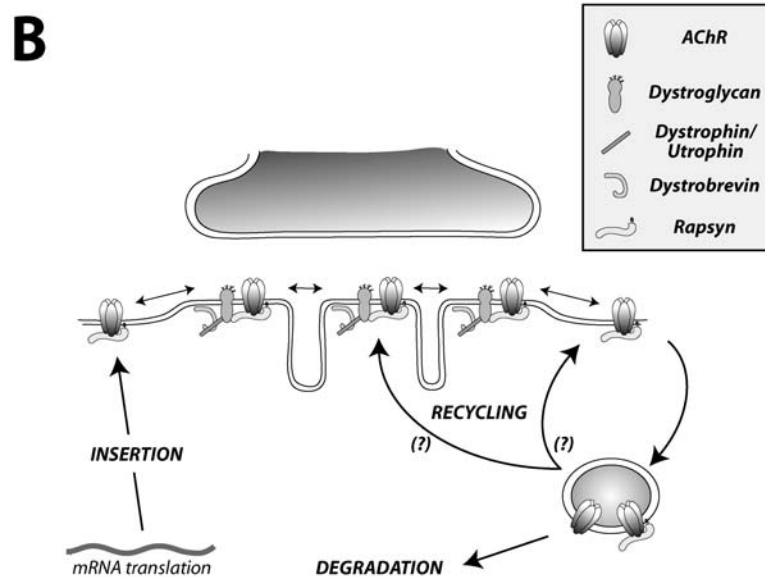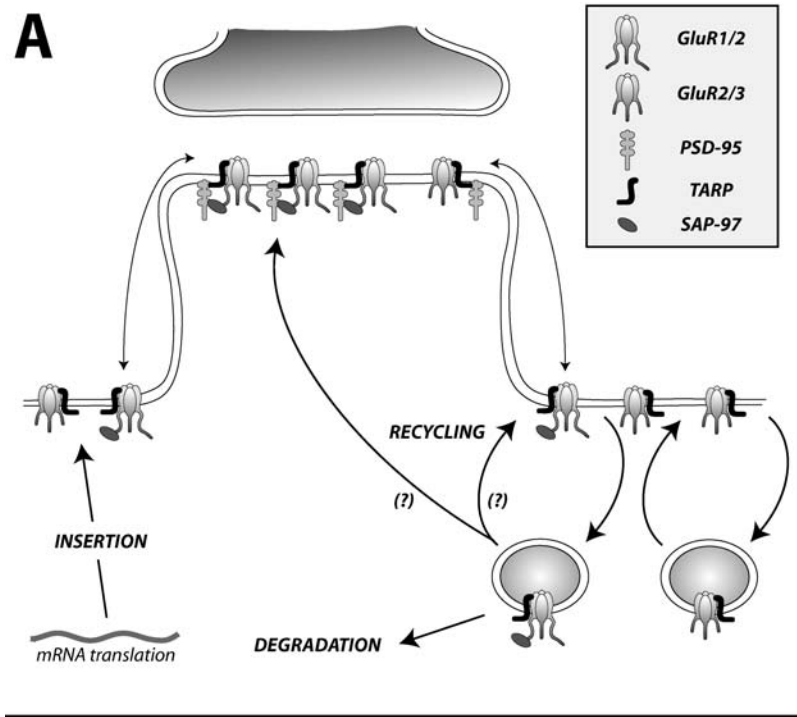
Figure 1.1. A model of post-synaptic receptor dynamics at glutamatergic and cholinergic synapses. (A) Receptor dynamics at excitatory glutamatergic synapses in the central nervous system. At glutamatergic synapses the density of AMPARs at synaptic sites is controlled by the insertion, lateral migration, degradation and recycling of receptors. These dynamics can be altered by a number of different events, including activity and phosphorylation, and are regulated by intracellular scaffolding proteins. (B) Receptor dynamics at excitatory cholinergic synapses in the peripheral neuromuscular junction. Similar to receptors in the central nervous system, the density of AChRs at synaptic sites in the NMJ is controlled by the insertion, lateral migration, degradation and recycling of receptors. AChR dynamics are also controlled by activity and phosphorylation, as well as by proteins in the intracellular scaffold.

A number of proteins have also been shown to be involved in subunit-specific regulation of AMPAR dynamics. The "short-tailed" AMPAR subunits, including GluR2 and GluR3, are stabilized at synapses by the binding of GRIP or its homologue ABP, and GluR2 subunits are additionally stabilized by NSF (Dong et al., 1997; Osten et al., 2000; Braithwaite et al., 2002; Hanley et al., 2002; Lee et al., 2002). Disruption of GRIP/ABP binding by PICK1 and the replacement of NSF with the clathrin adaptor protein AP-2 induce the endocytosis of GluR2/3 AMPARs (Chung et al., 2000; Perez et al., 2001; Hanley et al., 2002; Chung et al., 2003; Seidenman et al., 2003; Hayashi and Huganir, 2004; Hanley and Henley, 2005; Lu and Ziff, 2005). The "long-tailed" AMPAR subunits, including GluR1 and GluR4, have quite different intracellular binding domains, which allow another complement of proteins to regulate their dynamics. SAP-97, for example, links GluR1 to PSD-95, a protein that localizes specifically to synapses (Leonard et al., 1998; Valtschanoff et al., 2000; Gardoni et al., 2003; Rumbaugh et al., 2003; Cai et al., 2006; Jin et al., 2006). The AMPAR-SAP-97 interaction has been shown previously to be essential for activity-dependent delivery of GluR1 into spines (Mauceri et al., 2004; Nakagawa et al., 2004) (however, see (Kim et al., 2005)), and PSD-95 has been shown to modulate AMPAR incorporation during LTP *in vivo* (Ehrlich and Malinow, 2004).

Regulation of NMDAR dynamics at excitatory central synapses:

The NMDAR is a heterotetramer composed of NR1, NR2(A-D) and NR3(A-B) subunits, all of which have endo- and exocytosis motifs that allow binding of regulatory proteins. In the mammalian forebrain NMDARs are predominantly expressed as NR1/2A and NR1/2B diheteromers (Kew et al., 1998; Vicini et al., 1998; Rumbaugh and Vicini, 1999; Tovar and Westbrook, 1999). Although the discovery that AMPA receptors

undergo rapid changes in response to activity has driven much of the research on receptor dynamics at the glutamatergic synapse towards the AMPA receptor, focus has more recently turned towards the trafficking of the NMDAR (Carroll and Zukin, 2002; Wenthold et al., 2003; Nong et al., 2004; Perez-Otano and Ehlers, 2005). Similar to the AMPAR, NMDAR half-life estimates vary depending upon experimental method, ranging from hours to days, and NMDAR half-life also changes significantly through development. For example, in cultures from early stage neurons, a surface biotinilation assay found that over 20% of NMDARs are internalized after 30 minutes ($t_{1/2}$ < 2 hours) (Roche et al., 2001), which is comparable to 15% internalization of surface AMPARs after 30 minutes (Ehlers, 2000). In more mature neurons the turnover of NMDARs slows dramatically (Roche et al., 2001) to a rate that is 2-3 fold slower than AMPARs (Huh and Wenthold, 1999; Ehlers, 2000; Lin et al., 2000; Nong et al., 2003; Sharma et al., 2006b).

As with AMPARs, the synaptic delivery and removal of NMDARs in response to activity can be much more rapid than indicated above, with significant changes in NMDAR number occurring within minutes. For example, glycine/glutamate treatment causes an ~25% decrease in surface NMDAR expression after 15 minutes in cultured hippocampal cells (Nong et al., 2003), and LTP-induction in adult hippocampal cells results in an ~20% increase in NMDARs in the same time period (Grosshans et al., 2002). Similarly, dark-reared neo-natal rats show rapid and persistent increases in NR2A subunit expression in the visual cortex *in vivo* within an hour of light exposure (Quinlan et al., 1999). As with the AMPAR, the dynamics and resulting changes in surface

expression of the NMDAR can be controlled at the level of insertion, removal or recycling.

Several studies have shown that the insertion of the NMDAR is strongly regulated by the NR1 subunit. NMDA export is first regulated at the level of translation, as the NR1 subunit can be spliced to produce alternate C-terminal tails, with activity blockade resulting in a C'-cassette that allows rapid export and chronic stimulation resulting in down-regulation of this isoform (Standley et al., 2000; Scott et al., 2001; Xia et al., 2001; Mu et al., 2003). An ER retention signal on the NR1 C-terminal region also serves as a control point for exocytosis and surface expression and has been shown to be regulated by PKC (Scott et al., 2003). PKC, a kinase that is also implicated in the dynamics of AMPARs (Chung et al., 2000; Kim et al., 2001; Seidenman et al., 2003) and GABARs (Connolly et al., 1999b), has been shown to increase NMDAR surface expression (Lan et al., 2001), and is essential for LTP expression in hippocampal slices from older mice (Grosshans et al., 2002). Since the NR1 subunit is obligatory for the surface expression of NMDARs, the activity-dependent alternate splicing and PKC masking of a retention signal allow NMDAR exocytosis to be altered by activity to control surface expression.

While the NR1 subunit also contains signals that are potentially involved in internalization (Scott et al., 2004), NMDAR endocytosis appears to be controlled largely by signals on the intracellular tails of NR2A and NR2B. The NR2 subunits bind to the homologous PDZ-containing proteins PSD-95 and SAP102 (Lau et al., 1996; Muller et al., 1996; Barria and Malinow, 2002; Sans et al., 2003; Chung et al., 2004; Sans et al., 2005), which play a role in anchoring or stabilizing NMDARs rather than facilitating their delivery to synapses. For example, the delivery of NR2B to neonatal synapses

13

precedes PSD-95 (Washbourne et al., 2004) and PSD-95 knockouts still express surface NMDARs (Migaud et al., 1998). Instead, the association of PSD-95 with the NR2 subunit of the NMDAR appears to regulate internalization, as activity-dependent de-phosphorylation of NR2 results in the replacement of PSD-95 with the clathrin adaptor protein, AP-2, which initiates endocytosis (Roche et al., 2001; Lavezzari et al., 2003; Chung et al., 2004; Prybylowski et al., 2005). This interaction is mediated by a number of different factors. For example, the NMDAR co-agonist glycine is able to recruit AP-2 to synapses, and subsequent binding of both glycine and NMDA/glutamate initiates rapid internalization of NMDARs, which results in LTD at synapses (Nong et al., 2003).

After endocytosis, NR2A and NR2B receptors are trafficked along different pathways: the NR2A-containing receptors appear mostly in late endosomes on the way to lysosomal degradation while the NR2B-containing receptors are found in recycling vesicles, which are able to deliver ~15% of internalized receptors back to the surface after 1 hour (Lavezzari et al., 2004; Scott et al., 2004). While changes in NMDAR expression have traditionally been thought to mediate homeostatic plasticity changes through slow cycling mechanisms (Perez-Otano and Ehlers, 2005), the rapid cycling of NMDARs observed more recently suggests a method by which very rapid changes in NMDAR surface expression could be modulated. Indeed, while AMPAR dynamics have been shown to control much of the activity-dependent changes observed in early post-natal neurons, changes in NMDAR number have been associated with LTP in older cells (Grosshans et al., 2002). Also in support of this idea is the finding that in older cultures of rat hippocampal neurons, the internalization of NMDAR subunits occurs just as rapidly

as AMPAR subunits after the stimulation of mGluRs and the initiation of LTD (Snyder et al., 2001).

Between exocytosis and endocytosis lies a robust mechanism allowing for the surface exchange of receptors between the synaptic and extrasynaptic spaces (Triller and Choquet, 2003). Elegant single-particle tracking experiments have shown that the NMDAR mobility is high outside of synapses and decreases markedly once it enters the synapse (Tovar and Westbrook, 2002; Groc et al., 2004). This mobility has also been shown to be altered by activity, which could potentially be due to the activity-dependent up-regulation of synaptic PSD-95 (Ehrlich and Malinow, 2004).

Regulation of GABA receptor dynamics at inhibitory central synapses:

The $GABA_A$ receptor is a pentameric ionotropic receptor that is constructed from seven subunit classes. However, it seems likely that the majority of GABARs *in vivo* are composed of two α, two β and one γ subunit (Rabow et al., 1995; Sieghart and Sperk, 2002), and are anchored to the intracellular cytoskeleton by the GABA receptor associated protein (GABARAP) and gephyrin (Wang et al., 1999a; Hanus et al., 2004; Luscher and Keller, 2004). The $GABA_A$ receptor is responsible for the majority of inhibitory transmission in the adult brain, and GABAR surface expression is regulated *in vivo* by a number of endogenous and exogenous factors including ethanol, insulin and agonist binding (Wan et al., 1997; Kneussel, 2002; Kumar et al., 2003). The lifetime of GABAR has been shown to have two phases: one rapid with a $t_{1/2}$ of ~ 4 hours, and one more slow with a $t_{1/2}$ of ~ 32 hours (Borden et al., 1984). More recently GABAR lifetime was estimated to be ~ 12 hours (Kittler et al., 2005). The surface dwell time has been measured with biotinylation assays, which show 25% internalization after 30 minutes ($t_{1/2}$

15

~ 1 hour) (Kittler et al., 2005). However, this assay is not able to resolve recycled receptors or distinguish between synaptic and extrasynaptic zones and therefore may underestimate the lifetime of GABA receptors.

Although comparatively little is known about GABAR dynamics, much work shows that GABARs share characteristics with both AMPA/NMDARs and AChRs. For example, as with the ionotropic glutamate receptors, constitutive endocytosis of surface GABARs is initiated by clathrin-mediated endocytosis and is regulated by the phosphorylation state of the adaptor protein AP-2 (Kittler et al., 2001; Herring et al., 2003; Kittler et al., 2005). After internalization, GABARs are either targeted to lysosomes for degradation, or are recycled back into the plasma membrane (Connolly et al., 1999b; Connolly et al., 1999a; Barnes, 2000). This recycling mechanism is able to insert 50% of internalized receptors back to the surface after internalization (Kittler et al., 2005). Also potentially involved in the cycling of internalized GABARs is the ubiquitin-like molecule, Plic-1, which prevents proteosomal degradation and potentially increases the size of the available intracellular pool of GABARs (Bedford et al., 2001). Recently, the proteins NSF and GRIP-1 have also been found at GABAergic post-synaptic sites (Kittler et al., 2001; Kittler et al., 2004; Goto et al., 2005), raising the possibility that these two proteins, which regulate ionotropic receptor trafficking in glutamatergic synapses, may play a key role in GABAR dynamics. Finally, while GABARs share a number of trafficking proteins with glutamatergic receptors, they also have a cytoskeletal anchoring framework in common with AChRs. Namely, the intracellular cytoskeleton complex to which both of these receptors bind is the dystrophin-glycoprotein complex (DGC). The role of the DGC in regulated trafficking of GABARs is poorly understood,

though disruption of a number of DGC proteins results in a reduction both in the size of GABAR clusters and the overall number of surface GABARs (Knuesel et al., 1999).

Regulation of AChR dynamics at excitatory peripheral neuromuscular synapses:

At the adult NMJ, the acetylcholine receptor is composed of two α, one β, one δ and one ε subunit (Mishina et al., 1986; Gu and Hall, 1988; Missias et al., 1996). Early in development the γ subunit is highly expressed and is capable of forming functional channels, but is replaced completely by ε subunit-containing receptors in the adult (Gu and Hall, 1988). Because of the availability of a snake toxin alpha-bungarotoxin (BTX) that selectively and irreversibly labels AChRs, the turnover of AChRs at developing, mature and denervated NMJs has been studied extensively using radioactively-labeled BTX. These studies primarily used I^{125}-BTX to determine the loss of receptors from muscle cells. Using this approach, the time course of AChR loss was estimated by comparing radioactivity between muscles from different animals that were examined at varying times after applying the radioactive toxin. These studies found that the half-life of receptors on mature, innervated muscle cells ranges from ~ 7-13 days (Bevan and Steinbach, 1983; Stanley and Drachman, 1983; Salpeter and Loring, 1985). Although the I^{125}-BTX approach forged the first inroads into estimating ionotropic receptor turnover *in vivo*, it had some drawbacks. First, by summing radio-labeled ligands from the entire muscle it could not reveal the receptor dynamics at individual neuromuscular junctions. For example, muscles with different populations of muscle fiber types may have different turnover rates. Second, the inactivation of AChRs with BTX could greatly affect the way that AChRs are removed from synapses. Lastly, the density of postsynaptic molecules can change enormously when the junction expands or shrinks during growth or

denervation, which could give erroneous estimates when counting radio-labeling on muscle cross-sections.

The subsequent development of fluorescently-conjugated bungarotoxin and quantitative fluorescence microscopy largely circumvented these limitations. Studies utilizing this tool have been able to more directly study the turnover of AChRs by assaying the intensity of fluorescently tagged BTX that is irreversibly bound to AChRs at individual identified junctions viewed more than one time in living mice (Green et al., 1975; Fambrough, 1979). This approach has led to a substantially different view of AChR dynamics than was provided by previous studies (Figure 1B). For example, they showed that when neuromuscular transmission was functional, receptor lifetime in the junctional membrane was quite long (~ 2 weeks). However when all AChRs were inactivated by BTX or another AChR inhibitor, curare, receptor lifetime decreased substantially to a $t_{1/2}$ of several hours (Akaaboune et al., 1999).

Recently, we have devised a novel labeling method that has revealed that AChRs at the NMJ are not simply degraded upon internalization, as previously thought (Gardner and Fambrough, 1979). Instead, a significant number of receptors, rather than being metabolized upon internalization, recycle back into the postsynaptic membrane (Bruneau et al., 2005a). The unexpectedly high contribution of recycled AChRs at synapses implies that the classical concept of "metabolic stability" of junctional AChRs as previously defined (Salpeter and Loring, 1985) must be revised. Specifically, earlier work did not consider the possibility that receptors continuously recycle back to the postsynaptic membrane with their bungarotoxin tag to contribute to the junctional receptor population. This work has led to the idea that previous experiments using fluorescently labeled BTX

must be re-interpreted (Salpeter and Loring, 1985; Andreose et al., 1993; Caroni et al., 1993; Akaaboune et al., 1999; Akaaboune et al., 2002). This also argues that junctional AChRs are being internalized from the surface at a significantly faster rate ($t_{1/2} \sim 4$ days after a one-time blockade) than previously thought. Since recycled and pre-existing AChRs can be labeled with different fluorophores, we have also monitored the lifetime of recycled and pre-existing AChRs from the same postsynaptic membrane and found that recycled AChRs turn over ~4 times more rapidly than pre-existing AChRs (Bruneau and Akaaboune, unpublished data).

In sharp contrast to innervated synapses, AChRs on mouse-derived C2C12 myotubes do not recycle (Bruneau et al., 2005a), despite the short half-life of AChRs in the postsynaptic membrane (Bruneau et al., 2005b). This suggests that a nerve factor(s) is required for triggering the recycling of AChRs and indicates that the insertion of newly synthesized AChR is the main source for maintaining normal receptor density at any given time in aneural muscle cells. We are now in the process of exploring the nature of the nerve factors that may be involved in the initiation of receptor recycling.

As with other ionotropic receptors in central synapses, the turnover rate of AChRs at the NMJ is also subject to synaptic activity. For example following muscle denervation, AChR lifetime decreases substantially to a $t_{1/2}$ of ~1-3 days (Gu and Hall, 1988; Shyng and Salpeter, 1989; Rotzler et al., 1991). Interestingly, the blockade of synaptic transmission not only increases the turnover rate of AChRs, but also depresses the insertion of recycled AChRs into the postsynaptic membrane (Bruneau et al., 2005a). However, blocking synaptic potentials with TTX does not affect AChR dynamics, suggesting that spontaneous release of neurotransmitter is sufficient to maintain normal

AChR turnover (Akaaboune et al., 1999). In support of this idea, the loss of AChRs can be prevented in denervated muscle by the restoration of synaptic activity or direct muscle stimulation (Rotzler and Brenner, 1990; Rotzler et al., 1991; Andreose et al., 1993; Akaaboune et al., 1999).

Previous studies have shown that the nerve clustering factor agrin not only causes aggregation of AChRs but also may increase the stability of AChRs at denervated neuromuscular junctions (Bezakova et al., 2001). Work with mouse-derived C2C12 aneural myotubes, however, shows that agrin does not alter receptor turnover (Bruneau et al., 2005b), which suggests that other factors present at the mature NMJ in conjunction with agrin may be implicated in AChR stability. The lifetime of AChRs can also be controlled by postsynaptic scaffolding proteins. For example in mice lacking alpha dystrobrevin, a protein of the dystrophin glycoprotein complex (DGC), dramatic changes occur in the NMJ, including a severe reduction in the number and the density of postsynaptic receptors as well as a rapid rate of removal ($t_{1/2}$ ~2.7 days vs. ~2 weeks in control) (Akaaboune et al., 2002). Similar reductions in AChR number and density are observed in mice lacking alpha syntrophin (Adams et al., 2000), although the lifetime of AChRs was not assessed in this study. Recent work from the Phillips lab has further implicated the receptor-associated protein rapsyn in controlling the lifetime of AChRs: electroporation of rapsyn into mouse muscle *in vivo* decreased the loss of AChRs (Gervasio and Phillips, 2005). From our unpublished results, it appears that rapsyn does not play an important role in AChR dynamics at clusters on the surface of aneural myotubes, however (Bruneau and Akaaboune, unpublished results). The investigation of the role of other scaffolding proteins on AChR dynamics is currently underway.

Future Directions

Although a large body of work now exists on ionotropic receptor dynamics in the central nervous system, this work is limited by the inaccessibility of these synapses and has therefore been done almost exclusively in culture or organotypic slice preparations outside of the intact system. The peripheral neuromuscular junction, on the other hand, is highly accessible in the living animal. The fundamental question, therefore, is whether the NMJ is similar enough to provide insights into synapses in the CNS. In the past 30 years the NMJ has proved its utility on this score by driving the understanding of synapse elimination, pre-synaptic quantal release, extra-synaptic endo- and exocytosis and lateral migration of receptors. In the field of receptor dynamics, however, the applicability of information gained about AChRs from *in vivo* studies seemed to be of limited applicability to ionotropic receptors in the CNS because of a few key apparent differences: namely a synaptic AChR turnover at least 2 orders of magnitude slower than AMPARs, and a lack of AChR recycling. Over the last few years these apparent differences have been slowly dismantled as estimates of AMPAR lifetime have decreased with new methods while the estimates of AChR dynamics have increased. The discovery that receptor recycling, which is a hallmark of receptor dynamics in central synapses, also takes place at the NMJ has further brought central and peripheral receptor dynamics into closer relation (Figure 1). Finally, as the components of the intracellular scaffolds of each of the ionotropic receptors have become resolved, structural homologies between AMPA/NMDAR and GABARs, as well as GABARs and AChRs have begun to appear. It will be most interesting to see if understanding the functional role of these proteins at

the accessible NMJ can help to continue the trend of *in vivo* investigation at peripheral synapses informing our understanding and directing research into processes that occur at central synapses *in vivo*. It is a productive tradition that will hopefully continue to carry forward our understanding of ionotropic receptor dynamics in the intact, living animal.

The Role of Dynamic Receptor-Associated Proteins in the Development and Plasticity of the Synapse

Introduction

The recruitment and maintenance of a high density of ionotropic receptors at post-synaptic sites is necessary for proper synaptic function. Changes in receptor density which are crucial both for synaptic development and synaptic plasticity are controlled by several factors ranging from electrical activity to postsynaptic scaffolding proteins. For example, genetic knock-outs of one of a number of intracellular scaffolding proteins result in the prevention or disruption of post-synaptic receptor aggregation. Necessary for the clustering of ionotropic receptors are a class of receptor-associated proteins that link receptors to the intracellular scaffold and stabilize them at post-synaptic sites.

At the cholinergic neuromuscular junction (NMJ), the acetylcholine receptor (AChR)-associated protein rapsyn is responsible for receptor anchoring and is crucial for the initiation of AChR clustering (Maimone and Enigk, 1999; Bartoli et al., 2001). Analogously, at inhibitory synapses in the central nervous system, the receptor-associated protein gephyrin is necessary for the aggregation of glycine (Kirsch et al., 1993; Feng et al., 1998b) and many subtypes of **γ-a**mino**b**utyric **a**cid (GABA$_A$) receptors (Essrich et al., 1998; Kneussel et al., 1999). In excitatory central synapses, the glutamatergic AMPA and

NMDA receptors are similarly anchored in place. Anchoring at glutamatergic synapses, however, is not mediated by a single receptor-associated protein, but instead by a family of proteins including the most prevalent member, PSD-95, which binds directly to NMDA receptors and indirectly to AMPA receptors (Kim and Sheng, 2004).

In addition to their role in receptor anchoring, each of these receptor-associated proteins is involved in the regulation of intracellular signaling and the maintenance of the scaffolding complex. Through their many protein-interacting domains, they are able to bind proteins that regulate scaffold dynamics and protein transcription, implicating receptor-associated proteins as central organizers of the post-synaptic apparatus.

Finally, mounting evidence points to the potential role of transient inter-molecular interactions in mediating receptor stability at individual synapses. Recent work has therefore focused on characterizing the collective dynamics of receptors and their associated scaffolding proteins. Interestingly, the picture emerging from this work is a post-synaptic structure in which receptor-associated proteins are highly dynamic and involved in regulating changes in receptor density both during development and at the mature, dynamic post-synaptic structure.

In this review, we will review emerging literature on the dynamics of receptor-associated proteins and their role in maintaining the post-synaptic apparatus at both peripheral and central synapses. Although we will largely focus our analysis on the functionally homologous rapsyn and gephyrin receptor-associated proteins, we will visit the major receptor-associated proteins in the excitatory glutamatergic synapse as well.

Rapsyn

At the neuromuscular junction (NMJ), pentameric acetylcholine receptors (AChRs) mediate the activation of muscle action potentials. AChRs bind directly to the **r**eceptor **a**ssociated **p**rotein of the **syn**apse (rapsyn), which is thought to anchor receptors to the intracellular protein scaffold. The importance of a number of these scaffolding proteins has been elucidated using genetic tools. For example, it has been found that mice deficient in the muscle specific kinase (MuSK) or Dok-7 fail to form AChR clusters both *in vitro* and *in vivo* (DeChiara et al., 1996; Beeson et al., 2006; Okada et al., 2006), while dystrobrevin, dystroglycan and utrophin knock-out mice show decreases in the number of junctional receptors (Deconinck et al., 1997; Grady et al., 1997; Sanes, 1997; Cote et al., 1999; Grady et al., 2000; Jacobson et al., 2001; Grady et al., 2003). These genetic studies, along with biochemical experiments, have led to a model for AChR anchoring at the post-synaptic density in which AChRs link directly to rapsyn, rapsyn binds to β-dystroglycan, β-dystroglycan binds to utrophin and utrophin forms a connection to the intracellular actin cytoskeleton (James et al., 1996; Sanes and Lichtman, 2001; Galkin et al., 2002; Huebsch and Maimone, 2003; Dobbins et al., 2006).

The essential role of rapsyn in the anchoring of AChRs to the scaffold and the clustering of receptors at post-synaptic sites *in vivo* is illustrated by the complete lack of clustered receptors at nerve endplates in rapsyn$^{-/-}$ mice and the lack of receptor clusters on myotubes generated from these mice (Gautam et al., 1995; Gautam et al., 1999). Depletion of rapsyn expression with RNAi in adult rat muscle fibers *in vivo* also results in the rapid disappearance of AChR clusters, showing that rapsyn is necessary for both

the formation and the maintenance of AChR clustering (Kong et al., 2004). Together this genetic data points to rapsyn as an indispensable receptor anchoring protein.

Although the tertiary structure of rapsyn has not been solved, it contains multiple binding domains (Figures 1.2 and 1.3). The activation of MuSK/Dok7 by neural agrin results in the increased association of rapsyn to AChR and concomitant receptor clustering (Reist et al., 1992; Sanes and Lichtman, 2001; Moransard et al., 2003; Okada et al., 2006). Recently it has been shown that the stabilization of receptor clustering at post-synaptic sites is at least partly mediated by the increased association of rapsyn (which is almost exclusively synthesized at the synapse) to calpain, a protease that initiates AChR dispersal when unbound (Chen et al., 2007). Additionally, post-synaptic sites on muscles from rapsyn^{-/-} mice show disruptions of the dystrophin-glycoprotein complex, with near complete lack of utrophin and syntrophin, while the synaptically-localized laminin β2 extracellular matrix protein is present (Gautam et al., 1995). This indicates that rapsyn is involved, at least indirectly, in the formation of the intracellular scaffolding complex rather than simply serving to tether receptors to a pre-formed scaffold. This implicates rapsyn not only as an anchor to AChRs, but also as a modulator of signaling cascades which are, themselves, capable of modulating AChR clustering.

Rapsyn
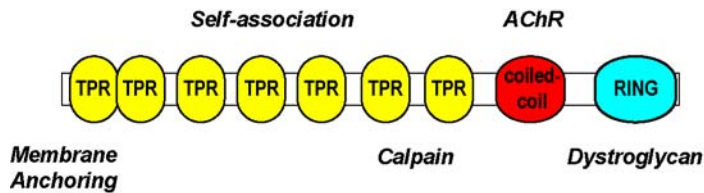
Gephyrin
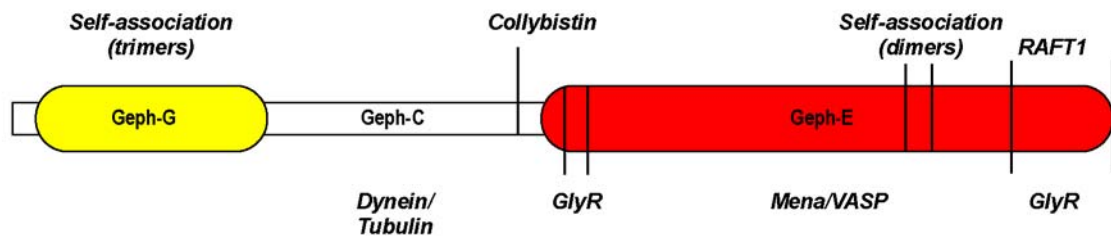
Figure 1.2. Primary structures and known interacting domains of rapsyn and gephyrin receptor-associated proteins. Both rapsyn and gephyrin have distinct domains involved in self-association and protein binding. (A) The N-terminal region of rapsyn is sufficient to traffic rapsyn to the cell surface, and N-terminal myristoylation is responsible for anchoring rapsyn to the membrane (Ramarao and Cohen, 1998). Seven putative tetratricopeptide repeat (TPR) regions mediate rapsyn self-association and the association of rapsyn with the protease calpain (Ramarao and Cohen, 1998; Ramarao et al., 2001; Chen et al., 2007). A coiled-coil domain (codons 297-330) binds directly to the intracellular loops of all of the AChR subunits, and a RING-H2 domain associates with β-dystroglycan (Cartaud et al., 1998; Maimone and Enigk, 1999; Bartoli et al., 2001). β-dystroglycan in turn binds to the intracellular cytoskeleton through its interaction with utrophin and to the extracullar matrix protein laminin via α-dystroglycan (Henry and Campbell, 1996; Montanaro et al., 1998; Henry and Campbell, 1999). Rapsyn is therefore thought to mechanically stabilize receptors at the synapse by serving as the protein linker between the AChR and beta-dystroglycan (Sanes and Lichtman, 2001). (B) Analysis of crystallized gephyrin has found that glycine receptor binding occurs after folding of the protein and multimerization. Gephyrin contains a G-domain and an E-domain that mediate the formation of a hexagonal gephyrin lattice in sub-synaptic aggregates (Sola et al., 2001; Saiyed et al., 2007). The G- and E-domains are connected by a linker region, which is thought to contain the binding sites for tubulin and the tubulin-interacting motor protein, dynein (Fuhrmann et al., 2002). Gephyrin also associates with the actin-interacting proteins mena/VASP and profilin (Giesemann et al., 2003; Neuhoff et al., 2005), as well as the signaling factor collybistin (Kins et al., 2000; Harvey et al., 2004) and transcriptional regulator RAFT1 (Sabatini et al., 1999).

Since many proteins of the dystrophin-glycoprotein complex are present in the central nervous system, the potential role of rapsyn in clustering of CNS pentameric

receptors has also been investigated. When co-expressed with neuronal AChRs in heterologous cells, rapsyn has been shown to cluster and increase the metabolic stability of neuronal nicotinic receptors (Kassner et al., 1998). Similarly, rapsyn has been shown to bind to and cluster GABA$_A$Rs when co-expressed in heterologous cells (Yang et al., 1997; Ebert et al., 1999). Despite rapsyn's ability to bind to these pentameric receptor types, however, rapsyn does not appear to play a functional role in the formation of CNS synapses as rapsyn expression is inessential for the clustering of neuronal nicotinic AChRs in neurons (Feng et al., 1998a).

The regulation of receptor density at synaptic sites has been extensively studied at the NMJ, and the insertion, removal, recycling and lateral migration of receptors into and out of the post-synaptic membrane have all been shown to be involved in maintaining a dynamic equilibrium of synaptic AChRs (Akaaboune et al., 1999; Akaaboune et al., 2002; Bruneau et al., 2005b; Bruneau and Akaaboune, 2006a). Given that the AChR associates intimately with rapsyn, an increasing focus has turned towards the role of rapsyn in regulating AChR density at the synapse. However, little is known about the behavior of the rapsyn molecule over time. Recently our lab has begun to examine the dynamics of rapsyn itself, yielding interesting observations about the stability and regulation of this protein.

Although rapsyn is clearly necessary for the induction of receptor clustering, its involvement in regulating AChR density at the developing or mature synapse is not well understood. While the availability of high-affinity fluorescent bungarotoxin conjugates have allowed AChR dynamics to be extensively studied, the inaccessibility of

intracellular rapsyn to extracellular ligands has prevented the study of rapsyn dynamics in living cells. Recently, we have used a rapsyn-GFP construct to circumvent this limitation. By transfecting muscle cells with the rapsyn-GFP fusion construct we have shown that rapsyn-GFP is able to take the place of endogenous rapsyn at cluster sites to keep overall rapsyn density constant, and that the presence of rapsyn-GFP at cluster sites has no effect on AChR density or turnover (Bruneau and Akaabourne, 2007), a result which has been seen with our recent work *in vivo*, as well (Bruneau and Akaaboune, unpublished data). This is in contrast to previous studies which have found that over-expressing rapsyn through electroporation or injection in adult mouse muscles slightly but significantly increases receptor density and stability at post-synaptic sites (Phillips et al., 1997; Wang et al., 1999b; Gervasio and Phillips, 2005; Gervasio et al., 2007). This discrepancy may be explained by the observation that in our *in vitro* system the total concentration of rapsyn was the same at clusters containing or devoid of rapsyn-GFP, likely because rapsyn-GFP is able to replace endogenous rapsyn to keep overall rapsyn density constant (Bruneau and Akaabourne, 2007).

Using fluorescent recovery after photobleaching (FRAP) to investigate rapsyn-GFP dynamics, we found that rapsyn turns over more rapidly than AChRs *in vitro* and that rapsyn is unaffected by protein phosphatase inhibition that causes significant changes in receptor removal and insertion (Bruneau and Akaabourne, 2007). Ongoing work in our lab has taken this investigation into the living mouse muscle *in vivo*. Using electroporation we have been able to successfully introduce the rapsyn-GFP construct into individual NMJs without damaging the muscle fibers. Consistent with our *in vitro* results we have found that rapsyn also turns over more rapidly than receptors *in vivo*

(Bruneau and Akaaboune, unpublished data). While AChR turnover and trafficking are dramatically altered by activity (Akaaboune et al., 1999; Bruneau et al., 2005a; Bruneau and Akaaboune, 2006a), rapsyn turnover appears to be unaffected by pharmacological post-synaptic activity blockade or by surgical muscle denervation (Bruneau and Akaaboune, unpublished data), indicating that both *in vitro* and *in vivo* the turnover of rapsyn and AChRs are regulated by different mechanisms. It is possible that changing the turnover of receptor-associated proteins at cluster sites may be a factor regulating receptor density, and this intriguing possibility is currently under investigation in our lab. At the very least, the fast turnover of receptor-associated proteins could allow for rapid changes in rapsyn density within the synapse, which could drive alterations in the intracellular scaffold morphology during development and aging.

In humans, rapsyn has been implicated in muscular dystrophies including myasthenic syndrome. One hallmark of this illness is a dramatic decrease in post-synaptic AChR density, and mutations in the rapsyn gene or promoter region have been shown to be the primary cause of synaptic pathogenesis in a number of reported cases (Ohno et al., 2002; Maselli et al., 2003; Ohno et al., 2003; Banwell et al., 2004). In addition to the disruption of junctional folding caused by rapsyn mutations or deficiencies, mutations in the rapsyn protein cause a decrease in the number of post-synaptic rapsyn and receptor proteins. The use of mutant rapsyn-GFP fusion proteins should enable a very complete investigation of the molecular-level pathophysiology of these muscular dystrophies.

Finally, a number of studies have shown that rapsyn, and not dystrophin or dystrobrevin, accompanies AChRs in the same intracellular vesicles during exocytosis both in heterologous cells and in the modified neuromuscular junction that is the torpedo

electric organ (Marchand et al., 2000; Marchand et al., 2001; Marchand et al., 2002). While this indicates that rapsyn and AChRs can potentially be delivered in the same intracellular compartments, the possibility that rapsyn accompanies receptors during endocytosis or recycling (as a regulatory chaperone or a non-regulatory binding partner) is currently being investigated. At the least, the fact that the surface expression of AChRs is decreased but not abolished in rapsyn knock-out mice indicates that even though rapsyn may accompany receptors to the cell surface it is not essential for receptor exocytosis (Gautam et al., 1995).

Gephyrin

In inhibitory synapses of the brain and spinal cord, the synaptic clustering and localization of glycine and $GABA_A$ receptors is mediated by the scaffolding protein gephyrin (Kirsch et al., 1993; Essrich et al., 1998; Feng et al., 1998b; Kneussel et al., 1999). Gephyrin is a 93-kD tubulin binding protein that associates directly with the intracellular loop of the glycine receptor β-subunit, and indirectly through a putative linker protein to the intracellular portion of gamma-subunit containing $GABA_A$ receptors (Meyer et al., 1995). Similar to rapsyn knockouts, glycine receptor clustering is absent in mice that are lacking gephyrin either because of genetic deletion or RNAi (Kirsch et al., 1993; Feng et al., 1998b; Levi et al., 2004); at the same time α_2- and γ_2-containing $GABA_A$ receptor clustering is dramatically decreased in gephyrin knockout mice (Kneussel et al., 1999; Jacob et al., 2005; Yu et al., 2007), even though overall $GABA_AR$ surface expression remains unaffected (Kneussel et al., 1999; Kneussel et al., 2001). Further, it has been shown that GABAergic inhibitory post-synaptic currents, synaptic

plasticity and performance on learning tasks are all significantly compromised when gephyrin expression or clustering is disrupted (Papadopoulos et al., 2007; Yu et al., 2007), while whole cell GABA-mediated currents are unaffected (Yu et al., 2007). This indicates that gephyrin may be necessary for both the initiation and maintenance of inhibitory receptor clustering which is required for proper synaptic function.
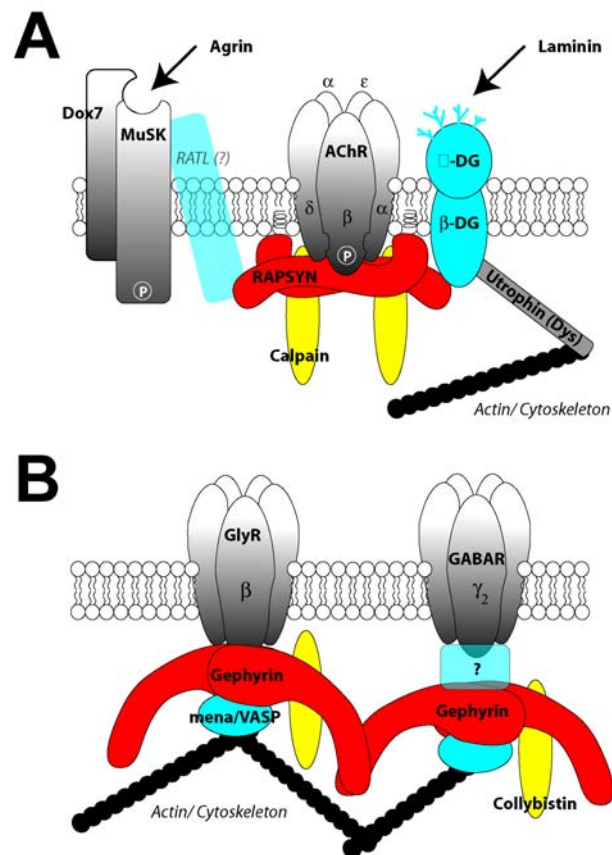
Figure 1.3. A model illustrating the central role of receptor-associated proteins in the clustering complex. (A) At acetylcholine receptor clusters rapsyn binds the intracellular portion of the receptor subunits. The activation of rapsyn and the clustering of receptors is initiated by agrin or laminin, and rapsyn stabilizes receptors through a direct association with beta-dystroglycan. Cytoskeletal re-organization is controlled by the association of rapsyn to calpain. (B) At inhibitory synapses glycine and/or GABA receptors mediate neurotransmission. The activation of gephyrin clustering requires glycine receptor activity, and gephyrin binds directly to the intracellular loop of the glycine receptor beta-subunit. Direct binding of gephyrin to the GABA receptor has not been observed, but gephyrin is required for γ_2-GABA receptor subunit clustering. Like rapsyn, gephyrin links receptors to the intracellular cytoskeleton (through mena/VASP) and regulates signaling through interactions with collybistin.

In addition to a number of functional binding domains on gephyrin which allow self-association and the association of gephyrin with scaffolding proteins (Figures 1.2 and 1.3), gephyrin binds to a number of signaling molecules which may help regulate synaptic structure. Collybistin is a guanine nucleotide exchange factor that binds to gephyrin and, similar to calpain in AChR clusters at the NMJ, has been proposed to modulate cytoskeletal remodeling and be involved in gephyrin and GABA$_A$R clustering (Kins et al., 2000; Erickson and Cerione, 2001; Papadopoulos et al., 2007). Collybistin knockout mice display dramatic decreases in GABA$_A$R clustering in amygdala and hippocampus and show deficits in synaptic plasticity and learning (Papadopoulos et al., 2007). Also on the list of regulatory proteins which bind to and are potentially modulated by gephyrin is RAFT1 (mTOR), which is a regulator of mRNA translation that has been shown to be active only if bound to gephyrin (Sabatini et al., 1999). Finally, gephyrin binds to the actin-associating mena/VASP (**va**sodilator **s**timulated **p**rotein) and profilin proteins (Giesemann et al., 2003), which are involved in actin regulation, implying that gephyrin not only relies on the cytoskeleton for anchoring but may be directly involved in regulating cytoskeletal dynamics and thereby altering synaptic structure.

The dynamics of the glycine receptor have recently been investigated in a series of elegant single-particle tracking experiments. Twenty-five years ago, investigation of AChR lateral diffusion led to the 'diffusion-trap' model of synaptic receptor accumulation (Young and Poo, 1983). Single particle imaging studies have allowed a more direct investigation of this hypothesis at glycinergic synapses. Using coated beads, rapidly bleaching protein fluorophores and non-bleaching quantum dots it has been

shown that individual glycine receptors move with near-Brownian motion outside of synaptic sites but slow considerably once they are within the synaptic region (Meier et al., 2001; Dahan et al., 2003; Charrier et al., 2006). Gephyrin appears to be critical for the trapping and stabilization of glycine receptors, as co-transfection of glycine receptors and gephyrin in heterologous cells or the over-expression of gephyrin in neuronal cells dramatically decreases receptor lateral mobility (Meier et al., 2001). Similarly, when gephyrin surface expression is decreased with shRNA or with a dominant negative gephyrin, glycine receptor mobility increases (Charrier et al., 2006).

Although the dynamics of $GABA_A$ receptors have not been examined as extensively as ACh or glycine receptors, studies using recombinant $GABA_ARs$ containing either the bungarotoxin binding site (Bogdanov et al., 2006) or a tag allowing electrophysiological identification (Thomas et al., 2005) have found that $GABA_ARs$ are rapidly inserted and removed at the neuronal membrane, and that they transfer rapidly between synaptic and extra-synaptic regions by lateral diffusion. As with glycine receptors, gephyrin appears to play a critical role in the regulation of $GABA_AR$ dynamics as disruption of gephyrin with RNAi decreases the number and density of $GABA_AR$ clusters while increasing $GABA_AR$ cluster mobility on the surface of cultured hippocampal neurons (Jacob et al., 2005).

The dynamics of gephyrin itself have also just recently begun to be investigated. These studies have used a recombinant gephyrin fused to a fluorescent marker and introduced it into cultured spinal cord neurons (Hanus et al., 2006). Using time-lapse imaging this group investigated the overall movement of individual gephyrin clusters following pharmacological manipulation. By examining intra-cluster fluctuations over

short time periods and the movement of the entire cluster over longer time periods they found that gephyrin dynamics within clusters were decreased when F-actin was disrupted, while movements of the entire clusters were tubulin dependent. Interestingly, synaptic activity specifically stabilized the intra-cluster movement of gephyrin. Although these studies did not examine the insertion, removal or lateral mobility of gephyrin into or out of individual synaptic sites as has been done with rapsyn, it nevertheless supports a similar model of receptor-associated protein dynamics potentially playing a role in regulating changes in receptor density at post-synaptic sites.

PSD-95

Most excitatory transmission in the mammalian brain is mediated by glutamate. At glutamatergic synapses, anchoring of the main receptor types is mediated by a family of PDZ binding proteins. Most ubiquitous and best characterized of these glutamatergic PSD proteins is PSD-95, which binds directly to NMDARs through the C-terminus of the NR2 subunit, and indirectly to AMPARs through interactions with SAP-97 and Stargazin (Rutter and Stephenson, 2000; Chetkovich et al., 2002; Choi et al., 2002; Schnell et al., 2002; Cai et al., 2006). Unlike rapsyn or gephyrin, PSD-95 does not appear to be necessary for NMDA receptor clustering: genetic knock-outs do not prevent post-synaptic receptor accumulation, and time-lapse imaging indicates that NMDA receptors actually begin to cluster at post-synaptic site prior to the arrival of PSD-95 (Washbourne et al., 2002). This protein is involved, however, in regulating AMPA receptor density changes and, like rapsyn and gephyrin, is highly dynamic.

Similar to rapsyn and gephyrin, PSD-95 has multiple interaction domains capable of mediating self-association and also of binding structural proteins (Kim et al., 1997;

34

Colledge et al., 2000) and signaling molecules (Kim et al., 1998; Tezuka et al., 1999; Penzes et al., 2001; Kalia and Salter, 2003) in the intracellular scaffold. Although PSD-95 clusters NMDARs when the two proteins are co-expressed in heterologous cells (Kim et al., 1995), it is not necessary for NMDAR clustering, and gain- and loss-of function constructs have no effect on NMDAR-mediated excitatory post-synaptic currents (EPSCs) (Barria and Malinow, 2002; Prybylowski et al., 2005).

As with rapsyn and gephyrin, recent work has also focused on the turnover of PSD-95 as a means of controlling the synaptic localization and density of receptors. Using a PSD-95 fusion construct and FRAP experiments similar to the ones used to examine rapsyn turnover, it has been shown that PSD-95 turns over rapidly at glutamatergic synapses in hippocampal cultures *in vitro* (Kuriu et al., 2006; Sharma et al., 2006a). This fast constitutive turnover could allow for very rapid changes in PSD-95 expression at synapses, which would in turn dramatically alter AMPA receptor levels. Indeed, the over-expression or knockdown of PSD-95 has been shown to dramatically alter AMPAR-mediated currents by altering synaptic expression of AMPA receptors (Hayashi et al., 2000; Ehrlich and Malinow, 2004; Nakagawa et al., 2004). These synaptic changes driven by the alteration of PSD-95 density have further been shown to mediate LTP in slice cultures *in vitro* (Stein et al., 2003; Bingol and Schuman, 2004; Lin et al., 2004), and the expression of PSD-95 has also been linked to enhanced learning *in vivo* (Ehrlich and Malinow, 2004; Yao et al., 2004) [however, see (Migaud et al., 1998)]. Finally, the active clustering function of PSD-95 requires palmitoylation (Topinka and Bredt, 1998), and the cycling of palmitate on synaptic PSD-95 is also able to alter

synaptic PSD-95 levels, potentially adding another layer of control to synaptic PSD-95 expression (El-Husseini Ael et al., 2002).

The rapid cycling of post-synaptic density proteins illustrated by rapsyn, gephyrin and PSD-95 appears to be the rule rather the exception. Along with PSD-95, other PDZ proteins studied as GFP fusion proteins with FRAP have proven to be very dynamic both at the drosophila NMJ and in hippocampal neuronal cell cultures, turning over even more rapidly than PSD-95 (Rasse et al., 2005; Kuriu et al., 2006; Sharma et al., 2006a). Together these emerging data challenge a view of the post-synaptic scaffold as a static structure. Given the important role that many of these scaffolding proteins play in the density, turnover and localization of post-synaptic receptors, this also indicates that changes in scaffolding protein turnover may have dramatic effects on synaptic structure, development and plasticity.

Chapter II

The Effect of Agrin and Laminin on Acetylcholine Receptor Dynamics *In Vitro*

Emile G. Bruneau, Peter C. Macpherson, Daniel Goldman, Richard I. Hume, Mohammed Akaaboune

Abstract

Using optical imaging assays, we investigated the dynamics of acetylcholine receptors (AChRs) at laminin-associated clusters on cultured myotubes in the absence or presence of the nerve-derived clustering factor, agrin. Using fluorescence recovery after photobleaching (FRAP) on fluorescent bungarotoxin-labeled receptors, we found that ~ 9% of original fluorescence was recovered after 8 hours as surface AChRs were recruited into clusters. By quantifying the loss of labeled receptors and the recovery of fluorescence after photobleaching, we estimated that the half-life of clustered receptors was ~ 4.5 hours. Despite the rapid removal of receptors, the accumulation of new receptors at clusters was robust enough to maintain receptor density over time. We also found that the AChR half-life was not affected by agrin despite its role in inducing the aggregation of AChRs. Interestingly, when agrin was added to myotubes grown on laminin-coated substrates, most new receptors were not directed into preexisting laminin-induced clusters but instead formed numerous small aggregates on the entire muscle

surface. Time-lapse imaging revealed that the agrin-induced clusters could be seen as early as 1 hour, and agrin treatment resulted in the complete dissipation of laminin-associated clusters by 24 hours. These results reveal that while laminin and agrin are involved in the clustering of receptors they are not critical to the regulation of receptor metabolic stability at these clusters, and further argue that agrin is able to rapidly and fully negate the laminin-substrate clustering effect while inducing the rapid formation of new clusters.

Introduction

Through the course of neuromuscular development the most prominent emerging feature of the postsynaptic membrane surface is the high density of acetylcholine receptors (AChRs) at the nerve endplate. In rodents, early in embryonic development AChRs are distributed evenly over the muscle surface (Bevan and Steinbach, 1977). By around E13, nerve-independent clustering of receptors occurs in the general region of eventual innervation (Lin et al., 2001). Upon innervation a few days later, the receptor clusters that lie outside of muscle innervation sites disappear and new clustering of receptors is rapidly induced in direct and tight apposition to each nerve endplate (Lin et al., 2001). The receptor clusters continue to morphologically differentiate post-natally, resulting in a dramatic increase in AChR density to $> 10,000/\mu m^2$ at the mature neuromuscular junction (NMJ) that drops to $< 10/\mu m^2$ within a few microns of the NMJ boundary (Fertuck and Salpeter, 1974; Fambrough, 1979).

The metabolic stability of AChRs has been extensively studied both *in vivo* and *in vitro*. Using conjugates of bungarotoxin (a snake venom that binds specifically and quasi-irreversibly to AChRs), it has been shown that AChR turnover in cultured aneural

myotubes is rapid, with a half-life of 7-24 hours depending on experimental conditions (Devreotes and Fambrough, 1975; Wang et al., 1999b; Trinidad and Cohen, 2004). At innervated and functional adult neuromuscular junctions, however, receptor stability dramatically increases ($t_{1/2}$ ~10-14 days) (Salpeter and Loring, 1985; Akaaboune et al., 1999). What remains unclear is the dynamics of receptors during the early stages of embryonic development and whether these dynamics are modulated by neuronal factors.

A crucial factor that affects AChR clustering during development *in vivo* is agrin, a nerve-derived heparin sulphate proteoglycan that activates both a muscle specific kinase (MuSK), and rapsyn, an intracellular protein that is found in 1:1 stoichiometry with AChRs (Burden et al., 1983; Sealock et al., 1984; Valenzuela et al., 1995; Sanes and Lichtman, 2001). Indeed, mice deficient in either MuSK or rapsyn fail to form any AChR clusters either during development or on dissociated myotubes (Gautam et al., 1995; DeChiara et al., 1996). Agrin knockout mice, however, do form receptor clusters in the endplate zone by E14.5, but these clusters disappear after failing to stabilize or reform under nerve endplates after innervation (Lin et al., 2001). Based on these observations it was suggested that agrin may act to stabilize AChR clusters rather than initiate their formation.

Since it would be difficult to study receptor dynamics *in utero* directly, we have used a culture system that produces post-synaptic receptor clusters that are remarkably similar in morphology and maturation to those seen during post-synaptic apparatus development *in vivo* (Kummer et al., 2004). This culture system was developed by growing myotubes on another factor known to influence receptor clustering *in vitro*: the nerve-independent extracellular matrix protein laminin (Vogel et al., 1983). In this work

we sought to study the effect of agrin on AChR dynamics directly using fluorescence imaging assays, and used the same assay to analyze the effect of laminin per se on the metabolic stability of clustered AChRs. This approach has led to the observation that agrin and laminin do not alter AChR metabolic stability, and it unexpectedly revealed that agrin is able to induce the accumulation of new receptors into new cluster sites while preventing the maintenance of receptor density at preexisting laminin-associated clusters.

Materials and Methods

Cell culture. C2C12 myotubes obtained from American Type Cell Culture were grown in DMEM supplemented with 20% fetal bovine serum at 37° C, split into 35-mm culture dishes and differentiated 2 days later at cell confluence by replacing the media with DMEM supplemented with 5% horse serum. Media was then changed every two days and cells were imaged 4-6 days after differentiation. For laminin-coated cultures, culture dishes were coated with 5 µg/ml polyornathine (Sigma-Aldrich) in distilled water, air dried and then incubated overnight at 37°C with EHS laminin (10 µg/ml) (Invitrogen) in L-15 media supplemented with 0.5% sodium bicarbonate. Dishes were then aspirated of excess laminin media immediately before plating cells. Laminin coated plates caused rapid differentiation and growth of muscle cells. Consequently, imaging of AChRs on myotubes grown on laminin substrate was done at time points slightly earlier than those for non-laminin substrate myotubes (3-5 days).

Fluorescence Microscopy. Images were taken with a digital CCD camera (Retiga EXi, Burnaby, BS, Canada) using a water immersion objective (20X UAPO 0.7 NA Olympus BW51, Optical Analysis Corporation, NH). Images were captured at 25% light intensity through a neutral density filter (to limit photobleaching effects) on an Olympus51

microscope using IPLab, and images were then quantified using Matlab and converted into figures in Photoshop.

To study the rate of AChR removal from receptor clusters, cells were incubated with α-bungarotoxin conjugated to an Alexa fluorophore (BTX-Alexa 594) (5 μg/ml, 1 h) and washed gently 3 times in differentiation media; a second dose of BTX-Alexa 488 was added to ensure that all receptors were saturated and then cultures were washed gently 3 times and imaged at time 0. Residual BTX left in the culture media for the duration of the experiment after time 0 was therefore primarily BTX-Alexa 488 and not BTX-Alexa 594. This ensured that any new receptors that were inserted into the membrane would bind residual BTX-488 and therefore would not contribute to BTX-Alexa 594 fluorescence detected at later time points. From 2-8 hours later the same clusters were re-imaged and their fluorescence intensity was assayed using a quantitative fluorescence imaging technique, as described by Turney and colleagues (Turney et al., 1996), with minor modifications. Control myotubes were saturated with BTX-594, imaged, and then immediately incubated in BTX-488 until imaging at 8 hours. Loss of fluorescence at the clusters on these myotubes was indistinguishable from the loss of fluorescence at tubes subjected to the BTX-488 labeling only immediately before imaging at 8 hours. This implies both that the unbinding and re-binding of BTX conjugates does not occur at a measurable rate over 8 hours, and that blocking new functional receptors does not affect receptor removal. This last point was supported by the fact that the addition of the sodium channel blocker tetrodotoxin also did not alter the removal of receptors from clusters over the same time period.

To study the rate of AChR insertion into receptor clusters, cells were saturated with BTX-Alexa 594 as described above, washed gently 3 times and then immediately imaged. Four and/or 8 h later the same clusters were re-imaged and their fluorescence intensity was assayed, and then a second dose of the same BTX-Alexa 594 was added to saturate the new AChRs inserted at each time point, and fluorescence intensity was again determined. Clusters that had "rolled" over to the edge of the tube as it grew and therefore existed in multiple focal planes, or clusters on myotubes that were dying or shrinking at the later time point were discarded. This did not present a problem on laminin-coated dishes as the clusters in these preparations were large and easy to differentiate from each other, and they always formed at the laminin-muscle cell boundary and therefore were consistently in a single focal plane.

To study the lateral migration of AChRs, cells were saturated with BTX-Alexa 488 and washed gently 3 times. Immediately after imaging, the fluorescence of single clusters was carefully removed with a 10mW argon laser emitting at 488 nm and passed through neutral density filters that blocked 87.5% of the laser emission. Photobleaching typically took less than 5 seconds/cluster. At later time points the bleached and non-bleached neighboring "sister" clusters were found and re-imaged. The FRAP experiments were done in the presence of either unlabeled BTX or BTX-Alexa 594 to prevent rebinding of photo-unbound BTX-Alexa 488 (Akaaboune et al., 2002).

Agrin treatment. Either 100 ng/ml or 500 ng/ml of C-terminal agrin (R&D Systems, Minneapolis, MN) was added to culture dishes either 16 hours prior to initial imaging or immediately before the initial images were taken. After all washing steps, additional agrin was added to maintain the concentration throughout the imaging session.

Laminin treatment. Cell cultures were treated with a soluble laminin (10μg/ml) immediately before initial imaging and through the imaging period. After all washing steps, additional laminin was added to maintain the concentration throughout the imaging session. Cells were labeled and imaged as describe above.

Results

Substrate laminin does not affect the rate of receptor removal.

To estimate the receptor removal rate at individual spontaneous AChR clusters over time, C2C12 myotube cultures were labeled with BTX-Alexa 594 (5 μg/ml, 1 h), and then incubated in BTX-Alexa 488 (5 μg/ml, 10 min) to ensure that saturation was achieved. The fluorescence intensities of clusters were then assayed immediately after saturation and then 4 and/or 8 hours later. 4 hours after initial labeling, fluorescent intensity had decreased to 56% ±19 SD (n=94 cluster/5 cultures) of original fluorescence, and had decreased further to 38% ±20 SD (n=39 clusters/4 cultures) of original fluorescence at 8 hours (Figure 2.1 A,C). We next wanted to determine if receptor removal is altered in clusters found on the surface of myotubes that are grown on a laminin substrate. These clusters show some striking similarities to mature neuromuscular junctions in terms of size, topology and the general morphological development from "plaque" to "open" to "pretzel-like" shapes, as described by Kummer et al., 2004. Further, these clusters form between muscle and dish and so lie in a single focal plane and do not tend to change location as muscles grow or even contract, making these clusters relatively easy to image when labeled with fluorescent molecules. When the fluorescence intensity of labeled receptor clusters was assayed at 4h, we found that

61% ±12 SD (n=92 clusters/4 cultures) of original fluorescence remained, and at 8h 44% ±14 SD (n=71 clusters/4 cultures) of original fluorescence remained (Figure 2.1 B,C). This loss was not due to the photobleaching of fluorescent bungarotoxin bound to receptors, as the same control cluster imaged several times experienced little if any loss of fluorescence (<1% fluorescence loss at each sequential image). The loss of fluorescence was also not dependent upon spontaneous unbinding of BTX from AChRs, since BTX-labeled receptor complexes that remained bound to the laminin as "ghost" clusters (after the muscle they were originally clustered on had died) did not bind to new BTX-Alexa of a different color added days later. This is in agreement with studies that have shown that the BTX-AChR bond is essentially irreversible (Devreotes and Fambrough, 1975, Sanes and Lichtman, 2001). Therefore these results suggest that while substrate laminin dramatically alters receptor cluster size and morphology, it does not increase AChR half-life at these clusters.

Since the effect of c-terminal agrin on increasing the number of spontaneous clusters is well documented (Ferns et al., 1993), we wanted to investigate whether the clustering activity of agrin is also involved in altering the rate of receptor removal. To examine this possibility, cultured myotubes were grown either on a laminin substrate or non-coated culture dishes and incubated with c-terminal agrin (100 ng/ml) either the night before imaging (t = −16 h) or immediately prior to initial imaging (t = 0 h). In both cases, agrin concentration was maintained in the culture through the duration of the experiment and BTX-Alexa labeling was done as detailed above. When we measured receptor loss from spontaneous clusters at 4 hours in the presence of agrin, we found that 48% ±20 SD (n=39 clusters/4 cultures) of the original fluorescence was retained, and that

the fluorescence dropped to 38% ±20 SD (n=12 clusters/3 cultures) at 8h, which was nearly identical to the rate of fluorescence lost from clusters on myotubes in the absence of agrin (Figure 2.1 C). In many cases it was difficult to accurately identify or quantify the original clusters at later time points either because clusters often "rolled" over the side of the muscle out of a single focal plane as the myotube grew, or because they fragmented over time. We therefore only used clusters in this study that could be clearly distinguished from neighboring clusters and accurately quantified at 4 h and 8 h.

When myotube cultures expressing laminin-induced clusters were treated with c-terminal agrin (hereafter referred to as "agrin", unless otherwise noted) and fluorescence loss was examined at both 4 h and 8 h, we found that the agrin had no effect on the rate of receptor removal: at 4 h the fluorescent intensity was 63% ±13 SD (n=74 clusters/4 cultures) of original fluorescence, and at 8 h fluorescent intensity was 37% ±14 SD (n=74 clusters/4 cultures) of original fluorescence (Figure 2.1 C). While agrin did cause clear and dramatic increases in receptor cluster number (consistent with previous studies), these results indicate that agrin does not affect AChR stability at spontaneous clusters or laminin-induced clusters on C2C12 myotubes.

Lateral Migration of AChRs.

Given that the rate of receptor removal from receptor clusters was nearly identical for myotubes grown in the presence or absence of laminin substrate, and since laminin-induced clusters are larger, easier to identify and lie in the same focal plane, we carried out most of the following experiments only on myotubes grown on laminin substrate. First we were interested to know whether the diffusible AChRs contribute to cluster density. If lateral migration of receptors accounts for an appreciable amount of

fluorescence over time then measurements of fluorescence at later time points would not allow an accurate computation of receptor half-life. To determine the contribution of laterally migrating AChRs to cluster density, we saturated all preexisting AChRs on the myotube surface with BTX-Alexa 488 and then used an argon laser to selectively remove the fluorescence from all the receptors at single laminin-induced clusters. In this way, only the pre-existing diffusible AChRs on the membrane remained fluorescently labeled. All photobleaching experiments were performed in the presence of unlabeled bungarotoxin or BTX-Alexa 594 to prevent the rebinding of any BTX-Alexa 488 that may have been induced to unbind by the laser (Akaaboune et al., 2002).

Since photobleaching was done on living myotubes we performed a number of controls to confirm that the argon laser did not have deleterious effects in our experimental design *in vitro*. We found that myotube growth was normal, and nuclei under photobleached regions appeared healthy, even on myotubes that were completely photobleached over their entire surface. Bleached clusters themselves also appeared to be unaffected by the bleaching process, as the accumulation of new receptors measured with a distinctly colored BTX-Alexa at later time points revealed that the addition of new receptors at bleached clusters was equal to that at non-bleached neighboring "sister" clusters on the surface of the same myotube. Photobleaching therefore had no observable deleterious effect on the muscle cell or bleached cluster. Bleaching of sister clusters by residual laser light was also minimal.

From 2 hours to 8 hours after photobleaching the recovery of fluorescence was monitored. We found that the fluorescence recovery was circumferential around the original cluster area, consistent with a diffusion-trap process, and that bleached clusters

46
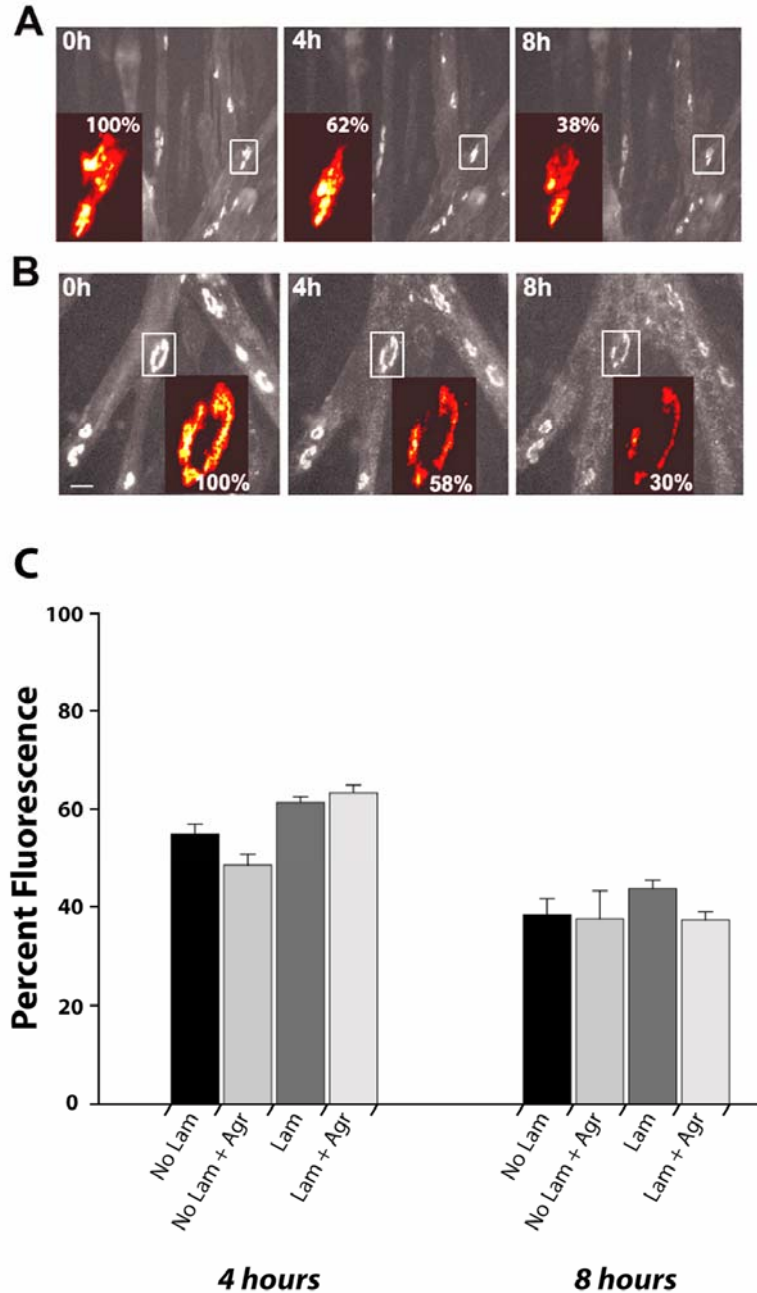
Figure 2.1. Receptor removal at single acetylcholine receptor clusters in vitro is unaffected by laminin or agrin. (A) Example of a number of myotubes displaying small, spontaneous AChR clusters. Receptors were labeled once with BTX-Alexa 594 and the loss in fluorescence was assayed at 4 and 8 hours. (B) Example of a single fused myotube grown on a laminin substrate displaying multiple laminin-induced AChR clusters and assayed for fluorescent loss as in (A). Note that these clusters are larger and more topologically complex than the non-laminin clusters in (A). Scale bar = 20 μm. (C) A Histogram summarizing the fluorescence at 4 and 8 hours of clusters on myotubes grown in the presence or absence of laminin substrate and in the presence or absence of agrin. Receptors at clusters on the surface of myotubes grown on a laminin substrate show approximately the same stability as receptors at clusters on myotubes lacking substrate. Agrin treatment 16 hours prior to or immediately after initial imaging had little effect on the removal rate of clustered receptors on myotubes grown in the presence or absence of a laminin substrate. All plots represent mean ±S.E.M.

gradually gained back ~ 9% (9.4% ±4 SD, n = 49) of their original fluorescence intensity after 8 hours (Figure 2.2 A). Since previous work indicates that recycling does not occur in cultured myotubes (Gardner and Fambrough, 1979), we assume that these laterally migrating receptors diffuse solely through the membrane surface. After 2, 4 and 6 hours, fluorescence recovery was 5.6% (±2 SD, n = 39), 9.4% (±4 SD, n = 23) and 9.7% (±5 SD, n = 21), respectively. These data were fit well by a single exponential curve (Figure 2.2 B) with R^2 = 0.98. When sister clusters were not laser illuminated, 44% of fluorescence remained after 8 hours, consistent with our calculations of fluorescence loss at clusters on myotubes not exposed to the laser (Figure 2.2 A). Since the remaining fluorescence at a non-bleached sister cluster is a combination of both the preexisting labeled receptors and the recovery from laterally migrating receptors, we subtracted out the amount of fluorescence signal due to lateral migration to determine the amount of fluorescence due only to originally clustered receptors (44% - 9% = 35% of receptors remaining after 8 hours). After collecting data for the loss of fluorescence at unbleached clusters at the 2, 4, 6 and 8 hour time points (78% ±13 SD, n = 42; 61% ±11 SD, n = 92; 48% ±8 SD, n = 20; 44% ±14 SD, n = 71, respectively), this correction for lateral migration was done at each data point to give a new curve that allowed us to estimate receptor half-life (Figure 2.2 B). This curve was fit well by a single exponential with R^2 = 0.99. Interestingly, the only point that was slightly elevated compared to the exponential fit was the 8-hour time point, which was also the time at which aggregations of intracellular fluorescent puncta became prevalent. Although every effort was made to only image clusters that did not have these puncta near them, it seems likely that this intracellular fluorescence might have contributed to the total cluster fluorescence, thus

causing this slight elevation above the actual fluorescence from clustered receptors at this time point. The receptor half-life of 4.5 hours derived from this corrected decay is far more rapid than the uncorrected half-life calculated from our experiments that measured fluorescence loss only ($t_{1/2} \sim 7$ hours), and approximately two times shorter than previous estimates that have ignored lateral migration and trapping of diffusible surface AChRs.
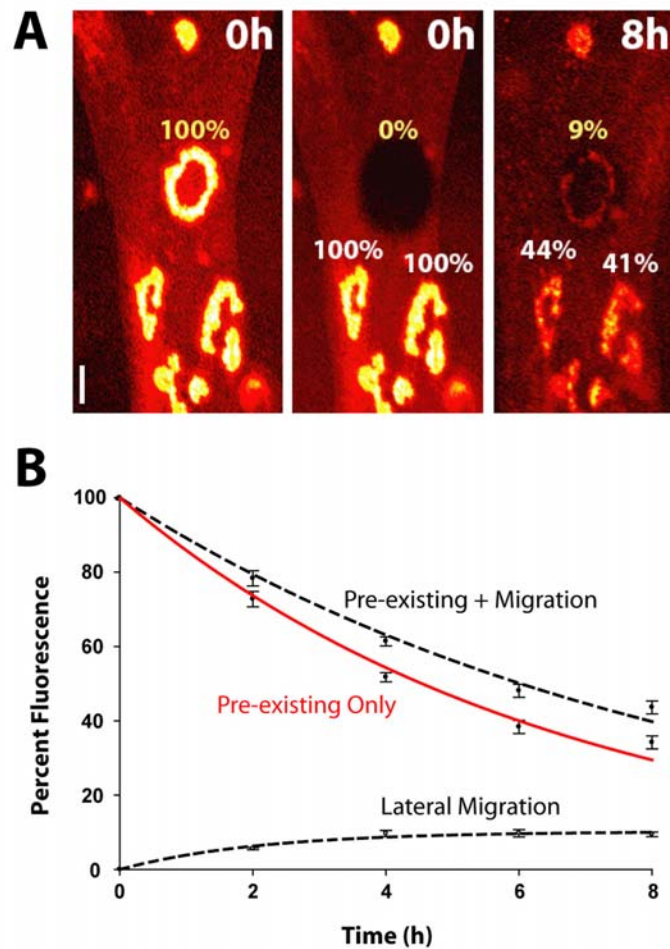
Figure 2.2. Contribution of diffusible acetylcholine receptors to laminin-induced clusters. (A) Example of a single myotube grown on laminin substrate that was imaged prior to, immediately after and 8 hours after photobleaching. At 8 hours the fluorescence recovery at bleached clusters was ~ 9%, indicating that a significant number of diffusible preexisting labeled receptors had moved into the bleached cluster. "Sister" clusters on the myotube that were not exposed to the laser lost more than half of their fluorescence after 8 hours, as expected (see Figure 1). Scale bar = 20 μm. (B) Data from a number of experiments performed at 2, 4, 6 and 8 hour time points. At each time point the average fluorescence due to lateral migration was subtracted from the total average fluorescence remaining to obtain the number of preexisting receptors remaining at a cluster. All data were fit by single exponential curves. All points represent mean ±S.E.M.

Accumulation of new receptors compensates for removal of old receptors to maintain receptor density at AChR clusters.

While the rapid loss of receptors from laminin-induced AChR clusters is partially offset by the trapping of laterally migrating receptors, we wanted to determine whether the accumulation of new receptors at myotube clusters is able to provide enough additional receptors to match receptor removal and maintain receptor density over time. To determine the amount of new receptor accumulation at clusters, myotubes were labeled with BTX-Alexa 594 (5 μg/ml, 1 h), and clusters were imaged immediately. Four hours later, the same clusters were imaged to determine the amount of fluorescence lost, and new BTX-Alexa 594 was then added to the myotube culture to saturate all new receptors that had accumulated at clusters since the initial BTX-Alexa 594 saturation. We found that on myotubes grown on laminin substrate and on myotubes grown without substrate, accumulation of new receptors at existing clusters allowed receptor density to be maintained: laminin-associated clusters were at 101% of original fluorescence at 5 h ±21% SD (n = 72 clusters/5 cultures) (Figure 2.3 A, B), and non-laminin clusters were at 95% of original fluorescence at 5 h (±20 SD, n=22 clusters/3 cultures) (Figure 2.3 B). These results suggest that the accumulation of new receptors at clusters on myotubes grown on both laminin- and non-laminin substrates is rapid and robust enough to maintain receptor density at individual clusters even as muscle and cluster morphology often change over time. Similar results were obtained at 8 hours, see figure 2.6.
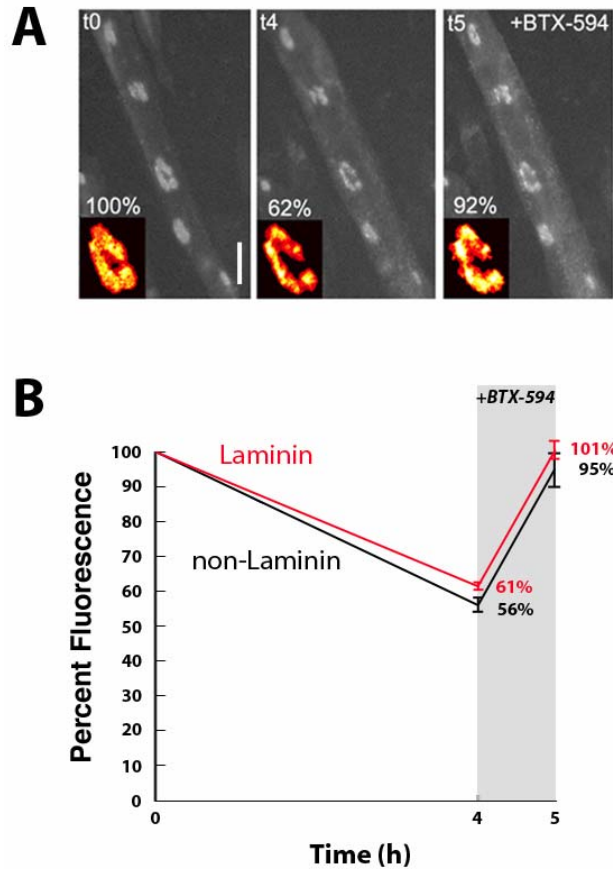
Figure 2.3. Accumulation of new receptors at single acetylcholine receptor clusters in vitro. (A) Myotubes grown on a laminin substrate that were saturated with BTX-Alexa 594 immediately before the first image. A sample cluster is shown in the inset that was quantitatively imaged at time 0 and 4 hours later. The loss of fluorescence was assayed, and then the cluster was imaged a third time after new BTX-Alexa 594 was added to label new AChRs. Note that even though the overall morphology of laminin-associated clusters can change markedly over 4 hours, the receptor density is maintained by the accumulation of new receptors. Scale bar = 20 μm. (B) Summary of data from multiple experiments with both laminin and non-laminin substrates. Note that insertion allows both laminin-associated and non-laminin clusters to maintain receptor density over a 5 hour time period. All points represent mean ±S.E.M.

Agrin causes new cluster formation and disrupts laminin substrate-associated clusters.

Although the experiments above showed that laminin substrate and soluble agrin alone do not alter receptor half-life at individual AChR clusters, laminin and agrin are known to interact directly and indirectly to induce receptor clustering (Denzer et al., 1997; Sugiyama et al., 1997; Montanaro et al., 1998). We therefore wanted to determine if the

51

clustering effect of laminin is affected by the addition of agrin. To do this, myotubes grown on a laminin substrate were saturated with BTX-Alexa 594 (5μg/ml, 1.5) and exposed to a high dose of agrin (100 – 500 ng/ml). Either 16 hours after or immediately following agrin treatment, initial images for each condition were taken to identify clusters saturated with BTX-Alexa 594 (Figure 4, "preexisting", pseudo-color). For each condition, 8 hours after initial imaging the same myotubes were re-imaged and then incubated with BTX-Alexa 488 to label all new receptors. On control myotubes grown on laminin substrate and not treated with agrin, no new clusters formed over the 8-hour time period (Figure 2.4 A) while old receptors were selectively removed from the inside of developing cluster (Figure 2.4 A), as previously described by Kummer et al, 2004. Interestingly, on the myotubes incubated with agrin, immediately after initial imaging we found that while the fluorescence from preexisting laminin-induced clusters labeled with BTX-Alexa 594 (red) disappeared over time at a normal rate (37% ±14 SD, n=74 clusters/4 cultures fluorescence remaining at 8 hours), numerous small clusters formed from pre-labeled AChRs on the surface of the myotubes (Figure 2.4 B, arrowheads). This is consistent with previous studies that have found that agrin-induced receptor aggregation is independent of new protein synthesis (Wallace, 1988). However, new AChRs that were identified with BTX-Alexa 488 (green) were also found to be concentrated at these clusters (Figure 2.4 B, arrowheads). Cells pre-incubated in agrin the night before initial imaging displayed many of these small clusters, but lacked discernible laminin-induced clusters when imaged the next day (Figure 4C, time 0 "preexisting"). The agrin-induced clusters, however, were stable over 8 hours and no new clusters appeared at 8 hours that had not existed at time 0 (Figure 2.4 C). This implies that the c-

terminus of agrin induces either a preferential targeting of new AChRs to agrin-induced

clusters over laminin-induced clusters, or that receptors, once inserted randomly into the

membrane, are trapped by agrin-induced clusters more effectively than laminin-induced

clusters as they diffuse laterally in the membrane.
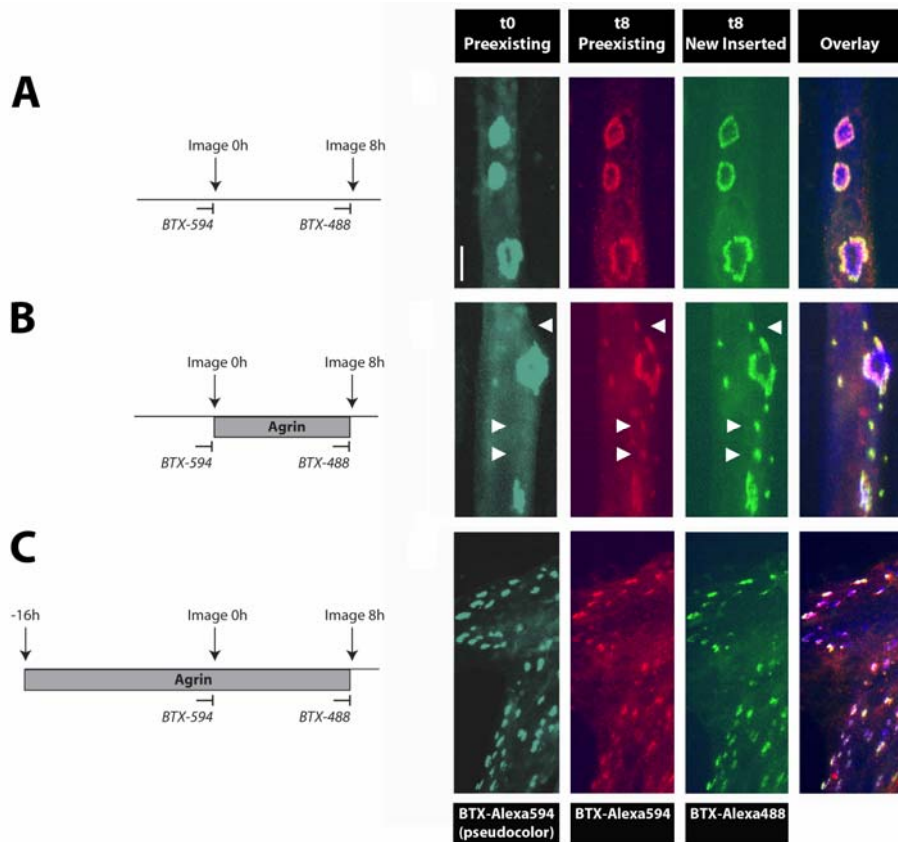
Figure 2.4. Agrin decreases the accumulation of new receptors at laminin-associated clusters and induces clustering of preexisting and new receptors at novel cluster sites. (A-C) Labeling schemes and sample images for control myotubes and myotubes incubated with a high dose of agrin either at the time of initial imaging or 16 hours prior to initial imaging, and then re-imaged 8 hours later. (A) In non-agrin treated cells, laminin-associated myotubes display large clusters (left panel), typical removal of preexisting receptors (second panel) and a normal pattern of receptor insertion (third panel). Overlay (right panel) reveals that preexisting receptors are preferentially removed from the center of the developing cluster and new receptors accumulate around the entire cluster. (B) When agrin is added to the culture immediately before the first image is taken, preexisting receptors can be seen to aggregate into new clusters after 8 hours that did not exist at the time of initial imaging (second panel, arrowheads). New receptors are also preferentially added to these new agrin-induced clusters (third panel, arrowheads). (C) When incubated in agrin for 16 hours prior to initial imaging (and then for the duration of the experiment), myotubes are devoid of laminin-induced clusters at time 0 (left panel), the small agrin clusters are maintained over the next 8 hours (second panel) and new receptors accumulate only at these preexisting clusters (third panel). Scale bar = 20 μm.

In order to gain a better temporal resolution of the agrin effect on the redirection of new receptors, we examined the agrin effect over a 3-hour time period using time-lapse imaging. Myotubes were grown on a laminin substrate and incubated with agrin at the time of initial imaging, and then re-imaged 1 and 3 hours later (Figure 2.5 A). After only one hour, small clusters of preexisting receptors labeled with BTX-Alexa 488 could be detected, and these clusters became more defined by 3 hours (Figure 2.5 B, first panels). While some of the clustering of preexisting receptors clearly occurred at places where AChR cluster "seeds" existed at 0 h (arrowheads), others appeared at regions that were not obviously seeded by receptors (arrows). When BTX-Alexa 594 was added to label new receptors, labeling was clearly visible at laminin-induced clusters but was not able to be resolved at the agrin-induced clusters at 1 hour. However, when the same myotube was re-imaged again at 3 hours after new BTX-Alexa 594 incubation, new receptors were clearly visible at the agrin-induced clusters (Figure 2.5 B, second panels). These results indicate that the effect of agrin is rapid, occurring within one hour of incubation. This effect was also specific to agrin, as soluble laminin (10 µg/ml) added in the same manner as agrin failed to induce new cluster formation over the same time period (Figure 2.5 C).
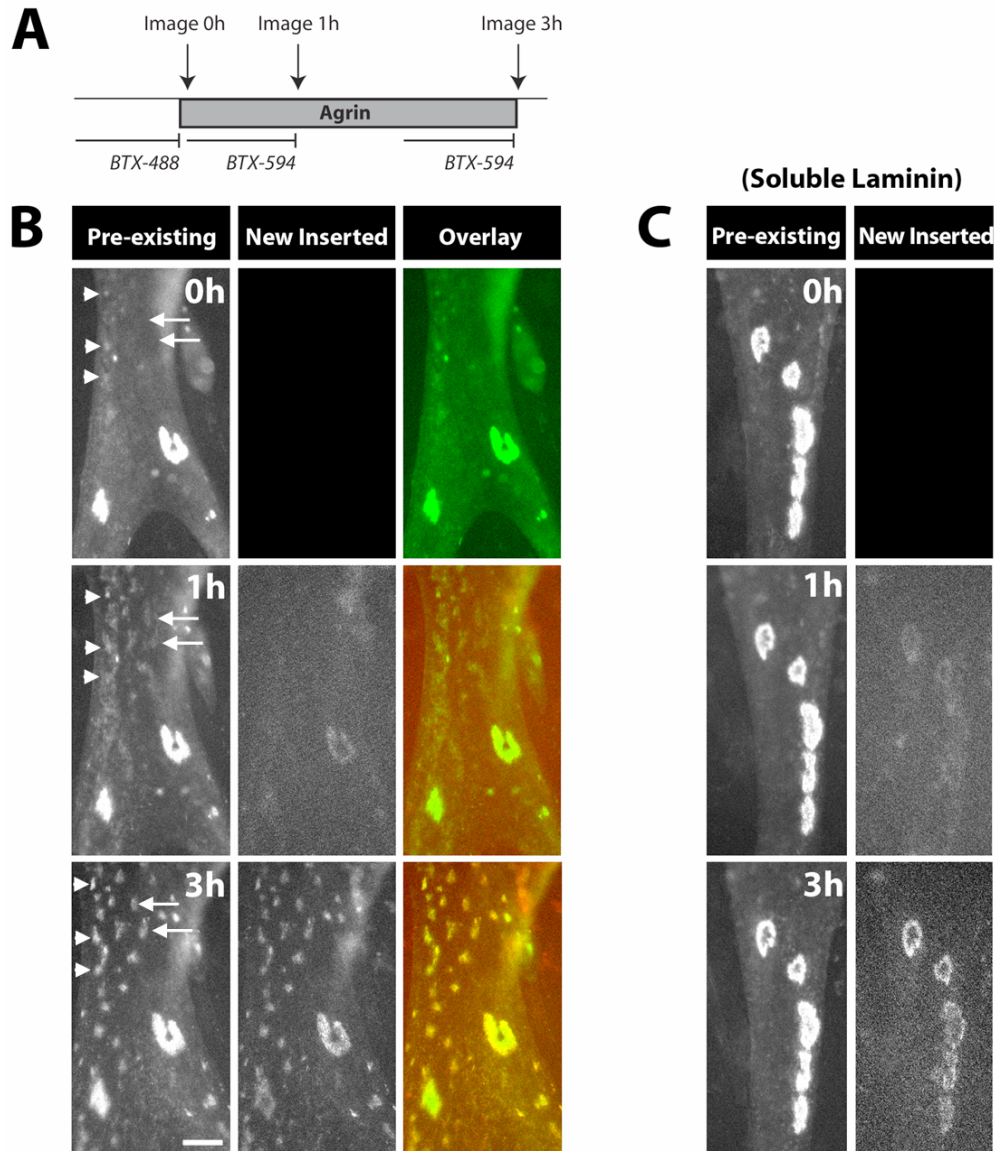
Figure 2.5. Time-lapse imaging of agrin-induced cluster formation on the surface of myotubes grown on laminin substrate. (A) Scheme for the BTX-Alexa labeling and agrin treatment of myotubes. (B) Example of a single myotube treated with 100 ng of agrin and imaged 3 times. First panels (left) represent preexisting receptors labeled at time 0 and imaged at 0, 1 and 3 hours later. Second panels (from the left) show the same myotube labeled with BTX-Alexa 594 to stain new receptors that have accumulated at the clusters between time 0 and each of the later time points. Third panels are overlays of the first two panels at each time point. Note that by 1 hour small receptor aggregates can be detected on the muscle surface and that at 3 hours these preexisting receptors have clustered and new receptors are clearly visible and co-localized at these agrin-induced clusters. Arrowheads indicate clusters that formed where cluster "seeds" existed at time 0; arrows indicate clusters that formed at regions on the surface where no receptor cluster seeds could be seen at time 0. (C) When soluble laminin was added instead of agrin to myotubes grown on laminin substrate no new clusters could be detected, indicating that the formation of new clusters is specific to agrin-treatment. Scale bar = 20 µm.

Effect of agrin on the accumulation of new receptors at agrin-induced and laminin substrate-induced clusters.

Having found that agrin does not alter the rate of receptor removal rate from membrane clusters (see Figure 2.1), we wanted to determine whether agrin modulates the accumulation of new AChRs into clusters. To do this we continually labeled all receptors with the same fluorescent BTX conjugate and quantified the amount of fluorescence at new agrin-induced clusters and large distinct laminin substrate clusters over time. Myotubes were saturated with BTX-Alexa 594 and then imaged in the presence of agrin (100 ng/ml). The same clusters were re-imaged 4 and 8 hours later after being re-saturated with new BTX-Alexa 594 (5μg/ml, 1h) to label any new receptors that had accumulated at clusters over each time period (Figure 2.6 A). In this way the full complement of clustered receptors (both preexisting and new) was imaged at each time point. While total fluorescence at 4 and 8 hours remained near 100% at laminin-associated myotube clusters in the absence of agrin, we found that the total receptor number at laminin-induced clusters treated with agrin decreased to 89% ±17 SD (n=71 clusters/3 cultures) of original fluorescence at 4 hours and 61% ±23 SD (n=78 clusters/3 cultures) of original fluorescence at 8 hours (Figure 2.6 B). In addition we found that less than 5% of original fluorescence was recovered after photobleaching at laminin-induced clusters in the presence of agrin compared to approximately 10% in the absence of agrin, indicating that the lateral migration of diffuse preexisting AChRs into preexisting clusters was altered by agrin treatment.

We next wanted to estimate the number of new receptors that were integrated into clusters by lateral migration versus targeted insertion. To do this we first calculated the contribution in original fluorescence of new receptors by subtracting the preexisting

receptors remaining at clusters after 8 hours from the full complement of receptors (preexisting + new) found at clusters at this time. For example, at 8 hours preexisting + new receptors at laminin-associated clusters account for 97% of original fluorescence, and preexisting receptors alone account for 44% of original fluorescence. Therefore 53% of the original fluorescence is due to new receptors at 8 hours. Assuming that < 10% of original fluorescence is due to the lateral diffusion of new receptors > 43% must be due to direct insertion of new receptors. However, in agrin-challenged cultures, only 24% of original fluorescence is contributed by new receptors (61% - 37%) at 8 hours. Assuming that < 5% of original fluorescence is due to the lateral diffusion of new receptors, direct insertion of new receptors must account for at least 15% of original fluorescence at 8 hours. Therefore, while laminin-associated clusters disappear over time and are absent 24 hours after agrin treatment, this appears not to be the result of increased receptor removal or cluster fragmentation, but rather because the accumulation of new receptors through both diffusion/trap and targeted insertion is decreased markedly within 8 hours of agrin treatment, presumably dropping to undetectable levels within 24 hours.

Finally, we observed that this agrin effect occurred even if the agrin was removed after imaging at 8 hours. Indeed a single 30 minute incubation with agrin was sufficient to produce an effect similar to that seen when agrin was used for the duration of the experiment, albeit at a reduced effect, suggesting that a single agrin treatment is sufficient to activate downstream machinery necessary for the redirection of new AChRs and the formation of new clusters.
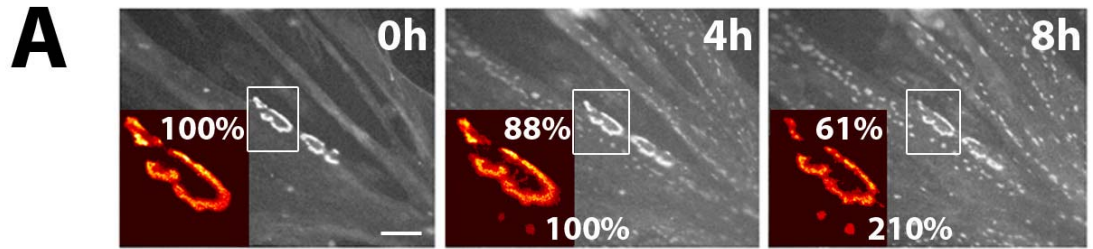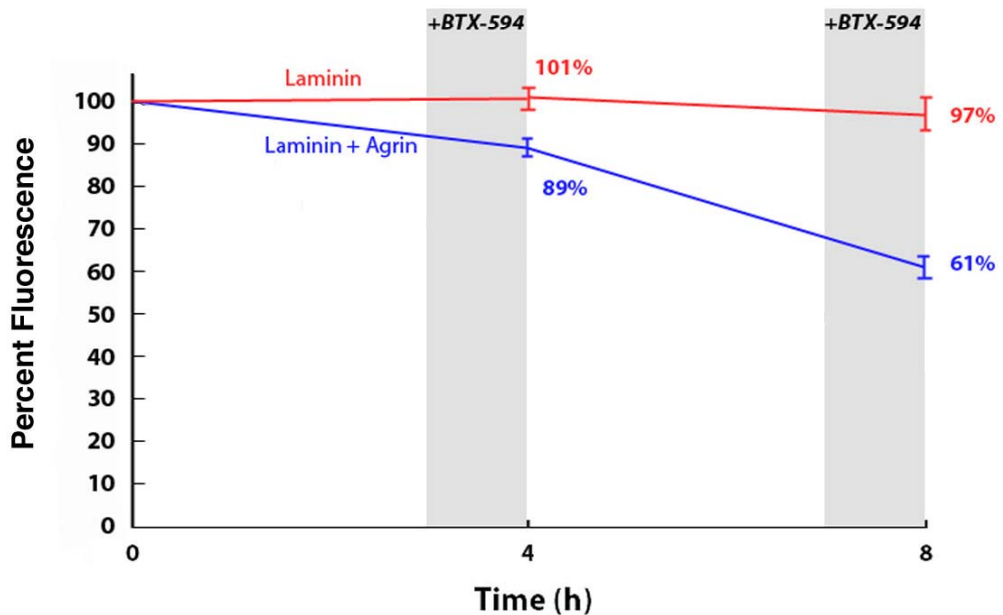
Figure 2.6. Agrin treatment decreases the accumulation of new receptors at preexisting laminin-induced clusters and increases insertion of new receptors into agrin-induced clusters, as revealed by quantitative fluorescence imaging. (A) A sample image shows the decrease in total receptor number at laminin-associated clusters and the subsequent appearance and increase in total receptor number at agrin-clusters beginning at 4 hours. Scale bar = 20 μm. (B) AChR clusters on myotubes grown on a laminin substrate were saturated with the same fluorescent bungarotoxin three times (before each of the three imaging time points at 0 h, 4 h and 8 h) to ensure that all receptors (both preexisting and new) were quantitatively imaged. This showed that receptor density is maintained at control clusters formed on myotubes grown on laminin substrate over 8 hours (red trace). Agrin treatment immediately before initial imaging resulted in a marked decrease in total receptor number at laminin-induced clusters over 8 hours (blue trace); since agrin does not increase receptor removal (see figure 1), this must be due to a decrease in receptor insertion. At the same time, agrin resulted in a marked increase in new receptor aggregation at agrin-induced clusters that had appeared by 4 hours. All points represent mean ±S.E.M.

58

Discussion

In this work, we used quantitative fluorescence imaging and FRAP techniques to study AChR dynamics at single spontaneous and laminin-induced clusters over time. While receptors on myotubes grown on a laminin substrate aggregate into large, differentiated clusters, we demonstrated that receptor half-life at these clusters was hardly affected, having a $t_{1/2}$ of about 4.5 hours. In addition we found that the total number of receptors at individual laminin-induced and non-laminin clusters remained nearly constant over time. Furthermore, we found that c-terminal agrin is not involved in regulating the metabolic stability of receptors, although its critical role in clustering receptors is undisputed. Finally, agrin treatment of laminin-induced clusters resulted in the formation of numerous small agrin clusters on the myotube surface while the accumulation of new receptors at preexisting laminin clusters was significantly decreased.

The metabolic stability of surface AChRs on developing cultured myotubes has been studied previously and these receptors were found to have a $t_{1/2}$ of 7-24 hours, depending on cell type and experimental design. Most of these previous studies used radio-labeled bungarotoxin (I^{125}-BTX), estimating the time course of AChR removal by comparing the amount of radioactivity released into the media to the total amount of the radioactivity at the time of initial labeling. However this method does not distinguish between diffuse and clustered receptors and the estimate of receptor half-life is derived by pooling together all receptors from the entire population of cells in a culture (Devreotes and Fambrough, 1975; Miller, 1984; O'Malley et al., 1993). In addition this technique does not distinguish between the surface AChRs and the receptors that are

59

removed from the membrane but not yet degraded (Devreotes and Fambrough, 1975), potentially inflating the calculations of surface receptor half-life. More recently a few attempts have been made to study the removal of receptors from individual clusters in cultured myotubes using fluorescence assays. These studies have found that the $t_{1/2}$ of removal of clustered receptors ranges from 7-20 hours (Kim and Nelson, 2000; Trinidad and Cohen, 2004). These studies did not, however, take into account the pool of diffuse receptors that are able to laterally migrate into the receptor clusters over time. In our work we also used fluorescent bungarotoxin to assay receptor removal, but we used FRAP to determine the amount of lateral migration into individual clusters over time. Before taking into account the contribution of laterally diffusing AChRs to cluster density we found that receptor half-life was ~ 7 hours, and after correcting for lateral migration we estimated the half-life of AChRs at clusters to be ~ 4.5 hours. This rate is more rapid than previous estimates that have ignored the migration of diffuse AChRs.

Our work also demonstrated that the accumulation of new receptors at preexisting clusters was quite rapid, matching receptor removal to maintain receptor density over time. It further implied that a significant number of these new receptors are targeted directly to the clusters: since results from our FRAP experiments clearly show that the diffusion of preexisting receptors accounts for < 10% of original fluorescence accumulated at clusters over 8 hours, one would assume that new receptors would laterally migrate at a similar rate, also contributing < 10% of original fluorescence after 8 hours. If this assumption is correct, then a significant number of new AChRs, which account for > 50% of original fluorescence after 8 hours, must be inserted directly into the preexisting clusters. This result is consistent with previous studies that showed that a

significant number of new inserted receptors are targeted directly to clusters (Bursztajn et al., 1985).

One interesting finding demonstrated by this work is that c-terminal agrin is not involved in the maintenance of receptors at either spontaneous or elaborated laminin-induced clusters on myotubes, even when a large dose of agrin (100 – 500ng/ml) was added to the cultures. Previously it has been shown that the initiation of receptor clustering occurs in agrin deficient mice, but that these clusters disappear later on which suggests that agrin might have a role in maintaining receptor clusters rather than initiating them (Lin et al., 2001). In transfected denervated muscle, too, agrin has been shown to stabilize receptors at ectopic clusters (Bezakova et al., 2001). This could be due to the fact that this study used full-length agrin rather than the c-terminal agrin that was used in the present study. While the c-terminal region of agrin is known to be responsible for the receptor aggregation affect seen *in vitro*, it is possible that other regions on agrin might alter receptor stability at those clusters.

While some studies hint at the action of agrin on receptor stability *in vivo*, most of the studies that have investigated the effect of c-terminal agrin on clustering *in vitro* have quantified clustering by the number of clusters per myotube (Nitkin et al., 1987; Gesemann et al., 1995; Cornish et al., 1999), using an increase in the number of clusters as an indirect indicator of increased AChR "stability" rather than examining agrin's effect on receptor turnover at the clusters themselves. Here, by showing explicitly that c-terminal agrin has no effect on AChR metabolic stability at individual clusters, we provide direct evidence that the clustering region of agrin is not involved in regulating

AChR half-life in myotube clusters, suggesting that c-terminal agrin does not act as a stabilizer of metabolic stability in this culture system, but only as a cluster inducer.

Since agrin and laminin are clustering factors known to effect the aggregation of AChRs during development in living animals, an obvious question arises from the current work: does the laminin/agrin interaction observed here potentially shed light on any developmental phenomenon *in vivo*? While speculative, there are some interesting parallels between our observations and the development of the nerve-endplate region during embryonic development. The initial clustering of AChRs on muscle fibers at the future endplate region is induced by nerve-independent factors. One such factor that is able to induce cluster formation is laminin, which when added in solution to muscle cell cultures does not induce large, complex clusters, but when allowed to form as a substrate on laminin-coated dishes does result in such formation (Sugiyama et al., 1997; Kummer et al., 2004). As laminin exists as a part of the extracellular matrix that forms a layer in between muscle fibers *in vivo*, it seems plausible that the substrate laminin represents a more likely mimic of endogenous laminin deposition than soluble laminin applied to dissociated muscle cells. As such, laminin becomes a candidate for the factor responsible for the early, nerve-independent clustering observed at ~E14 in mice, as has been suggested (Sugiyama et al., 1997). By E18.5, nerve endplates have contacted the muscle cells and released high local concentrations of agrin. Subsequent to this innervation are the disappearance of extra-synaptic clusters and then the formation of clusters directly under the nerve endplate. While our observations of decreased AChR accumulation in laminin-induced clusters after agrin treatment is consistent with this developmental progression, it must be stressed that the agrin used in our study is c-terminal agrin, which

contains the receptor aggregation activity of agrin but lacks the laminin-binding site, so the applicability of the laminin and agrin clustering interactions to *in vivo* remains highly speculative. Still, it will be interesting to see if these factors do indeed interact during this intriguing developmental transition.

In sum, while agrin appears to induce the formation of multiple new clusters, even while it causes the degradation of existing laminin clusters, it does not contribute to receptor stability at these clusters. Agrin does have a rapid and dramatic effect on clusters that form on myotubes grown on laminin-substrate, however, significantly decreasing accumulation into these clusters and eventuating in their dissolution after 24 hours, while resulting in the simultaneous induction of numerous small clusters at novel clustering sites. These results therefore support the "induction" but not the "stabilizing" hypothesis of c-terminal agrin action on clustered acetylcholine receptors.

Acknowledgements

Chapter III

Identification of Nicotinic Acetylcholine Receptor Recycling and its Role in Maintaining Receptor Density at the Neuromuscular Junction *In Vivo*

Emile Bruneau[1], David Sutter[1], Richard I Hume, and Mohammed Akaaboune

Abstract

In the central nervous system, receptor recycling is critical for synaptic plasticity; however, the recycling of receptors has never been observed at peripheral synapses. Using a novel imaging technique, we show here that nicotinic acetylcholine receptors (AChRs) recycle into the postsynaptic membrane of the neuromuscular junction (NMJ). By sequentially labeling AChRs with biotin-bungarotoxin and streptavidin-fluorophore conjugates, we were able to distinguish recycled, pre-existing and new receptor pools at synapses in living mice. Time-lapse imaging revealed that recycled AChRs were incorporated into the synapse within hours of initial labeling, and that their numbers increased with time. At fully functional synapses AChR recycling was robust and comparable to the insertion of newly synthesized receptors, while chronic synaptic activity blockade nearly abolished receptor recycling. Finally, using the same sequential labeling method we found that acetylcholinesterase, another synaptic component, does

not recycle. These results identify an activity-dependent AChR recycling mechanism that enables the regulation of receptor density, which could lead to rapid alterations in synaptic efficacy.

Introduction

The density of neurotransmitter receptors is an important parameter in regulating the efficacy of synaptic transmission. In both the central (O'Brien et al., 1998; Carroll et al., 1999a) and peripheral (Fambrough and Hartzell, 1972; Akaaboune et al., 1999; Sanes and Lichtman, 2001) nervous systems, alterations in synaptic transmission cause changes in postsynaptic receptor density. Such changes are important in many forms of synaptic plasticity, which lead to the strengthening or weakening of synaptic connections (Carroll et al., 1999b; Luscher et al., 1999). Several mechanisms at central nervous synapses, including receptor recycling, are known to be involved in regulating synaptic plasticity (Nishimune et al., 1998; Noel et al., 1999; Ehlers, 2000; Kim and Lisman, 2001; Malinow and Malenka, 2002; Bredt and Nicoll, 2003; Park et al., 2004). In peripheral cholinergic neuromuscular junctions, however, it is not known whether acetylcholine receptors are stable until they are removed and degraded in a one-way trip to the lysosomes, or if they are in constant movement between internal compartments and the plasma membrane. To address this issue, we have developed a novel imaging technique that enables us to study new aspects of AChR dynamics at neuromuscular junctions *in vivo.* By selectively labeling different AChR pools (pre-existing, recycled and new) within a single synapse in the living mouse we were able to provide an estimate of the contribution of each pool to the NMJ over time. We found that a significant number of

65

these receptors undergo recycling back to the NMJ, and that this recycling is dramatically affected by alterations in synaptic activity.

Material and Methods

In vivo imaging. All animal usage followed methods approved by the University of Michigan Committee on the Use and Care of Animals. Adult female mice (20-27 grams, NSA, Harlan Sprague Dawley, Indianapolis, IN) were anesthetized with an intra-peritoneal injection of ketamine and xylazine (17.38 mg/ml). Sternomastoid muscle exposure and neuromuscular junction imaging was done as previously described in detail (Lichtman et al., 1987; van Mier and Lichtman, 1994; Akaaboune et al., 1999). Briefly, the anesthetized mouse was placed on its back on the stage of a customized epifluorescence microscope, and neuromuscular junctions were viewed under a coverslip with a water immersion objective (20X UAPO 0.7 NA, Olympus BW51, Optical Analysis Corporation, NH) and a digital CCD camera (Retiga EXi, Burnaby, BC, Canada). Mice were intubated and ventilated for the duration of the imaging sessions. For imaging at multiple time points, the mouse was sutured after each session and allowed to fully recover before the next imaging session.

Labeling of distinct AChR pools. After exposure of the sternomastoid muscle, AChRs were saturated first with fully substituted BTX-biotin (5 µg/ml, 1.5 h, Molecular Probes, Eugene, OR) and then with streptavidin conjugated to Alexa 660 (10 µg/ml, 2.5 h, Molecular Probes, Eugene, OR) to saturate all biotin sites. To ensure that all receptors and all biotin sites were saturated, distinct colors of tetramethyl-rhodaminated BTX conjugate (TMR-BTX) and streptavidin-Alexa (streptavidin-Alexa 488) were added to the sternomastoid muscle. Superficial synapses were then immediately imaged (IPLAB

software, Scanalytics, VA). Hours or days later the mouse was re-anesthetized, and the sternomastoid muscle was re-exposed and bathed with streptavidin-Alexa 488 to label the recycled AChRs and TMR-BTX to label the new AChRs. The muscle was washed, and the same synapses were relocated and imaged. In this way, we were able to distinguish the preexisting, new and recycled receptor pools. To rule out the possibility that streptavidin-Alexa binds directly to receptors, sternomastoid muscles were lightly labeled with TMR-BTX (5 μg/ml, 2 min application) to identify synapses. Streptavidin-Alexa 488 (green) (10 μg/ml) was then applied to the sternomastoid muscle for 2.5 h. In these junctions no green labeling was observed, indicating that streptavidin does not bind directly to receptors.

Denervation. The sternomastoid muscle was denervated by excising a 5 mm piece of nerve to prevent its regeneration. 10 days later the mouse was anesthetized and labeled as described above.

Muscle stimulation. Denervated muscle was stimulated by placing stimulating electrodes at either end of the muscle (3-ms bipolar pulses of 10-13 V at 10 Hz for 1-s duration every 2 s for the entire 8 hour period).

Continuous blockade of activity. To study the effect of muscle postsynaptic activity blockade on the insertion of recycled and new receptors, curare (2.5 mg/ml), a poison that binds reversibly to AChRs, was applied to the sternomastoid muscle to block neuromuscular transmission. For the duration of the experiment a coverslip was placed over the exposed muscle to prevent it from drying. Every two hours, additional curare solution was applied to the muscle. Animals were intubated with a ventilator for the duration of the experiment to prevent asphyxiation.

Cell culture. C2C12 cells (obtained from American Type Culture Collection, VA) were cultured on laminin coated dishes in medium containing 20% FBS and then switched after 2 days to 5% HS to induce differentiation into myotubes. 3-5 days after differentiation cultures were labeled and imaged as with muscles in vivo. We used the appearance of the cells under phase contrast illumination to distinguish receptor clusters on living muscle cells from ghost receptor clusters.

Immunocytochemistry. Longitudinal sections (20 μm) of fixed (2% PFA) sternomastoid muscle that was labeled 4 days earlier with BTX-biotin (5 μg/ml, 1.5 h) followed by a saturating dose of fluorescent or unlabeled streptavidin (10 μg/ml, 2.5 h) were blocked with 10% BSA and goat serum, permeabilized with 1% triton X-100 and incubated with primary antibodies for 1-2 h at room temperature in blocking solution. The primary antibodies used were as follows: antibody to biotin (1:200, monoclonal 2F5, anti-biotin-Alexa 488/594, Molecular Probes, OR); rat anti-acetylcholine receptor (1:500, mAb35 or mAb210, Sigma, St. Louis); rabbit anti-early endosomal antigen (1:300, EEA1, Abcam, Cambridge, MA). The sections were then washed extensively in PBS and incubated for 1 hour with secondary goat anti-rat antibody conjugated to either Alexa 594 or Alexa 488 (Molecular Probes, OR), and/or with secondary sheep anti-rabbit antibody conjugated to Texas Red (Abcam, Cambridge, MA).

Confocal microscopy. The analysis of intracellular and extracellular colocalization was carried out using a 60X oil immersion lens and laser illumination on a confocal Zeiss LSM 510 microscope. A series of optical planes were collected in the z dimension (z-stack), and collapsed into a single image. Images presented in the Results section were produced and adjusted for brightness and contrast using Adobe Photoshop CS.

Quantitative fluorescence imaging. In experiments involving multiple color fluorescent ligands (such as the one illustrated in Figure 1), the camera gain was adjusted to give a nicely exposed image on each color channel, but because of differences in the extent of labeling of the different ligands and the quantum efficiency of different fluorophores, it was not possible to compare the relative number of molecules labeled with each ligand. When such comparisons were essential (Figures 4.7 and 4.8) the fluorescence intensity of labeled receptors at neuromuscular junctions was assayed using a quantitative fluorescence imaging technique, as described by Turney and colleagues (Turney et al., 1996), with minor modifications. This technique incorporates compensation for image variation that may be caused by spatial and temporal changes in the light source and camera between imaging sessions by calibrating all images with a non-fading reference standard. A key feature of the quantitative imaging approach used in the current study is that it involves three sequential labeling steps with the same ligands (BTX-biotin and streptavidin-Alexa 594). Thus, as long as we verified that labeling had reached saturation and that the image pixel intensity was not saturated, it was simple to get an accurate quantitative measurement corresponding to the number of AChRs in each pool.

Results

Recycling of AChRs at the neuromuscular junctions of live animals

Experiments such as the one illustrated in Figure 3.1 suggested that AChRs are recycled at the postsynaptic membrane of the neuromuscular junction. The sternomastoid muscle of this mouse was labeled with a saturating dose of biotin-labeled α-bungarotoxin (BTX-biotin) (5 μg/ml, 1.5 h), which binds with extremely high affinity to AChRs (Green et al., 1975; Fambrough, 1979). BTX-biotin bound receptors were then saturated

with streptavidin conjugated to a fluorescent Alexa dye (10 µg/ml, 2.5 h), which in turn forms a noncovalent, very high affinity bond with biotin (Weber et al., 1989; Green, 1990). To test whether all receptors were saturated with BTX-biotin and all biotins saturated with streptavidin-Alexa, immediately after the unbound BTX-biotin and streptavidin-Alexa 660 were washed away (pseudo color, blue) the muscle was exposed to alternately colored streptavidin-Alexa (streptavidin-Alexa 488 (green), 10 µg/ml) and fluorescent α-BTX (tetramethyl-rhodamine tagged (BTX-TMR) (red), 5µg/ml). The superficial synapses were then imaged (Figure 3.1 A). The absence of red and green fluorescence indicates that saturation was achieved (Figure 3.1 B,C). When the same synapse was exposed 24 hours later to streptavidin-Alexa 488 and BTX-TMR, much of the original fluorescence from the streptavidin-Alexa 660 remained (Figure 3.1 D) but there was also significant fluorescence on the green (streptavidin-Alexa 488) and red (α-BTX-TMR) channels (Figure 3.1 E,F). The blue label at 24 hours indicates that the majority of receptors were still bound to both of the original ligands. The red label at 24 hours indicates those receptors that appeared on the surface after the initial labeling period (whether newly synthesized or from an internal storage pool) as well as any surface receptors that had lost their BTX-biotin label. For the rest of this paper, all receptors that stain with fluorescent BTX after an initial saturating dose of BTX will be referred to as part of the pool of "new" receptors. The green fluorescence present at 24 hours indicates receptors that remained bound to BTX-biotin, but that had lost their streptavidin-Alexa 660 label. Given the expected high affinity of the streptavidin-biotin bond, we were surprised by the extent of loss of streptavidin. This matter is further considered below and in the discussion.

70
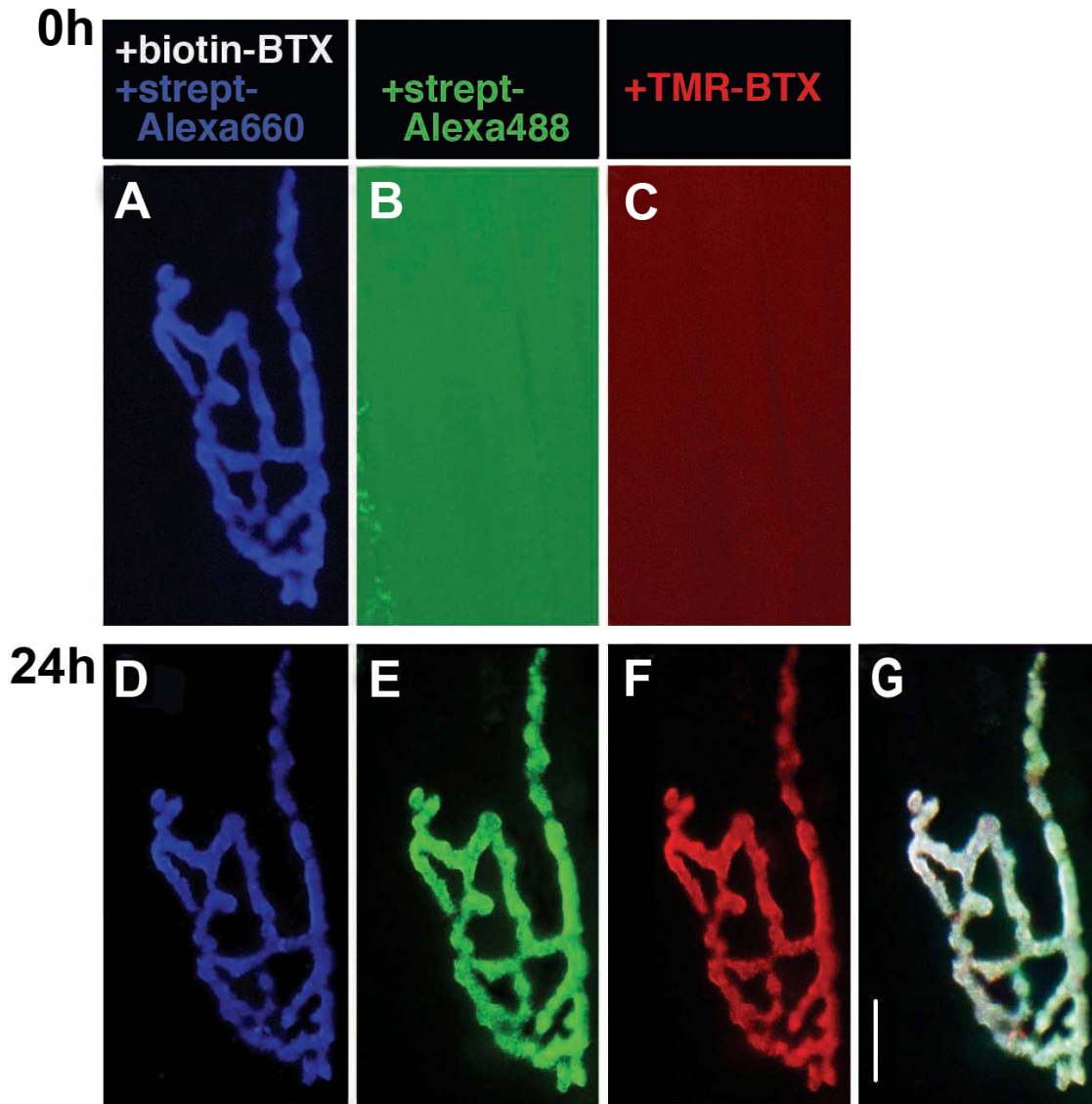
Figure 3.1. Multiple AChR pools are present at synapses on sternomastoid muscles of living mice.
(**A**) In a living adult mouse, a neuromuscular junction of the sternomastoid muscle was labeled with a saturating dose of BTX-biotin followed by a saturating dose of streptavidin-Alexa 660 (blue, pseudo-color). (**B-C**) The junction was then immediately bathed with a saturating dose of streptavidin-Alexa 488 (green) and TMR-BTX (red). The absence of any labeling (even when camera exposure was increased significantly) indicates that all receptors and biotin sites were saturated by the initial applications. (**D-G**) The same neuromuscular junction imaged 24 hours later, after application of new streptavidin-Alexa 488 (green) and TMR-BTX (red) to the sternomastoid muscle. The remaining pre-existing receptors were still labeled with BTX-biotin/streptavidin-Alexa 660 (blue, pseudo-color). The streptavidin-Alexa 488 labeling indicates the presence of receptors that retained BTX-biotin sites but lost their streptavidin-Alexa 660. These free sites are unlikely due to the loss of streptavidin on the surface (see Figures 2-5) and therefore referred to as "recycled" receptors. The TMR-BTX labeling indicates receptors that were not bound to either BTX-biotin or streptavidin and are referred to as "new" receptors. Scale bar, 20 μm.

Dissociation of streptavidin from the AChR-bungarotoxin-biotin complex does not occur on the muscle surface

We carried out a series of experiments to test whether the dissociation of streptavidin from biotin-BTX-AChR could occur on the cell surface. First, to estimate the intrinsic rate of dissociation of streptavidin from the biotin-BTX-AChR complex at the neuromuscular junction, mice were perfused with 2-4% paraformaldehyde in PBS and the sternomastoid muscle was removed and placed in a dish. We then labeled these muscles with saturating doses of BTX-biotin and then streptavidin-Alexa, as described above. Three to five days later, the muscle was bathed with a second color of fluorescent streptavidin. In contrast to the result obtained for receptors at synapses in living animals at this time (where a significant amount of the signal intensity was attributable to receptors that had lost their original streptavidin-Alexa tag and were then able to be relabeled with a new streptavidin-Alexa at a later time point, see Figure 3.1), no fluorescence from the second streptavidin fluorophore was observed (data not shown). Thus under these conditions the rate of biotin-streptavidin dissociation is negligible. As both the BTX-biotin and the streptavidin-Alexa were applied after fixation and extensive washing, this protocol likely accurately reflects the extremely slow intrinsic rate of biotin-streptavidin dissociation in the absence of processes associated with living cells.

Another possibility is that factors released from living muscle may increase the dissociation of streptavidin on the muscle cell surface. To test this possibility, we took advantage of "ghost" clusters observed in aneural myotube cultures grown on laminin. C2C12 myotubes grown on laminin display large, complex AChR clusters that often remain bound to the laminin, even after the muscle cell that used to hold them on its surface has died (Kummer et al., 2004). Sequentially saturating these ghost clusters with

BTX-biotin and streptavidin-Alexa 594 therefore enabled the analysis of AChR-BTX-biotin-streptavidin complexes isolated from muscle membranes but still surrounded by living muscle cells in a normal extracellular milieu. When these ghost clusters were labeled with either streptavidin-Alexa 488 or anti-biotin 488 5 days later no green fluorescence was observed (Figure 3.2 A-C). Thus there was no detectable dissociation of streptavidin over a five-day period when receptors are surrounded by medium, but not on living cells. We also tested for the dissociation of streptavidin from BTX-biotin on the surface of living myotubes. When receptor clusters on the myotube surface were labeled with BTX-biotin and saturated with streptavidin-Alexa 660, and then relabeled 12 hours later with (green) streptavidin-Alexa 488 and BTX-Alexa 594 (Figure 3.2 D-G), considerable red staining, but no green staining was observed. This indicated that despite a significant loss of fluorescence (due to the turnover rate of AChR) over this time period and significant insertion of new receptors, biotin-streptavidin dissociation did not occur under these conditions. We also found that there is no significant difference in the rate of internalization of receptors on cultured C2C12 myotubes that were labeled with either fluorescent bungarotoxin (38% ±12.0 SD, of fluorescence remaining after 8 hours, n= 2 cultures) or BTX-biotin-streptavidin-Alexa (33% ±10.0 SD, of fluorescence remaining, n= 2 cultures, p>0.1) (see supplemental figure S3.2). Together these results indicate that biotin-streptavidin dissociation does not occur even in a normal extracellular environment, and implies that recycling does not occur in aneural myotubes and that streptavidin does not significantly increase internalization.
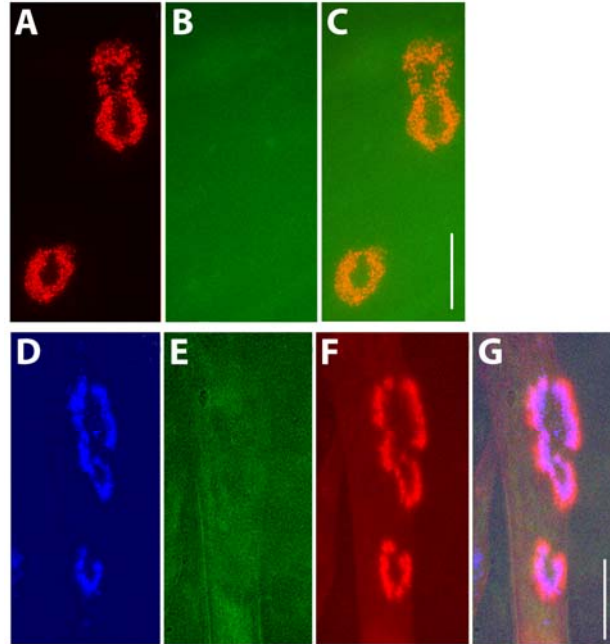
Figure 3.2. Streptavidin does not dissociate from AChR-BTX-biotin clusters on muscle cells in culture. (A) In C2C12 myotube cultures, "ghost" clusters (as described by Kummer et al., 2004) that were no longer associated with myotubes were labeled with BTX-biotin followed by streptavidin-Alexa 594. (B) 5 days later, the same clusters were treated with streptavidin-Alexa 488 (to identify receptors that retained BTX-biotin and lost streptavidin). (C) Overlay of images in (A) and (B). The absence of green labeling in (B) indicates that there was no dissociation of streptavidin from receptor-bungarotoxin-biotin complexes on ghost clusters after 5 days. (D) AChRs on a living C2C12 myotube that were labeled with a saturating dose of BTX-biotin followed immediately by a saturating dose of streptavidin-Alexa 660 (pseudo-color blue) and then imaged 12 hours later. (E and F) The same cells were then incubated with streptavidin-Alexa 488 (green) to label receptors that retain BTX-biotin and lose streptavidin, and BTX-Alexa 594 (red) to label new AChRs. The absence of green labeling in (E) indicates that no detectable streptavidin-biotin dissociation occurred over this time period, while the red labeling indicates the addition of new receptors. (G) Overlay of (D-F). Scale bar, 20 μm.

While the previous experiments show that the dissociation of streptavidin from biotin does not occur from the surface of fixed muscle or AChR clusters on living or dead cultured myotubes, it is still possible that biological processes could occur at the surface of the NMJ of an intact muscle *in vivo* that might cause streptavidin-biotin dissociation from the surface of synapses (such as the secretion of proteases by infiltrating immune cells). To examine this possibility, we transplanted a portion of a sternomastoid muscle that was first fixed with 2% PFA and then labeled with BTX-biotin/streptavidin-Alexa

594 into the neck of a host mouse directly next to the living sternomastoid muscle. In this way the BTX-biotin/streptavidin bound to immobilized receptors after fixation was exposed to a fully active and living sternomastoid muscle environment. As in the previous *in vivo* labeling studies described above, the mouse was then allowed to recover. Seven days later we quantified the amount of biotin-streptavidin dissociation at the NMJs of the fixed and transplanted muscle. We found that the original fluorescence of the transplanted muscles decreased by less than 3%, and we found no evidence of new streptavidin-Alexa binding, compared to normal levels of new streptavidin-Alexa binding observed at NMJs in the live host muscle. These experiments indicate that extracellular proteases do not cause biotin-streptavidin dissociation on the surface of the muscle.

To further rule out the possibility of extracellular dissociation of streptavidin from biotin, we used the same sequential labeling protocol on another synaptic component *in vivo*. Due to the availability of the snake toxin Fasciculin2, which selectively and specifically labels acetycholinesterase (AChE), we monitored the dissociation of streptavidin from Fasciculin2-biotin over 4 days. AChEs were labeled with biotinylated Fasciculin2 (7 µg/ml, 1 h), and then saturated with streptavidin-Alexa 594 (10 µg/ml, 2.5 h). The mouse was allowed to recover and after 4 days the sternomastoid muscle was exposed to a new saturating dose of streptavidin-Alexa 488 (green). In sharp contrast to AChR recycling (Figure 3.3 A,B), we found that AChEs originally labeled with Fasciculin2-biotin/streptavidin-Alexa 594 showed barely detectable green labeling and therefore negligible biotin-streptavidin dissociation after 4 days (Figure 3.3 C,D). These results show that the dissociation of streptavidin from biotin does not occur on the surface of the synapses and rules out the possibility that extracellular proteases or other unknown

cellular processes at the cell surface are responsible for such dissociation, suggesting that

this dissociation likely occurs in intracellular compartments after being internalized.
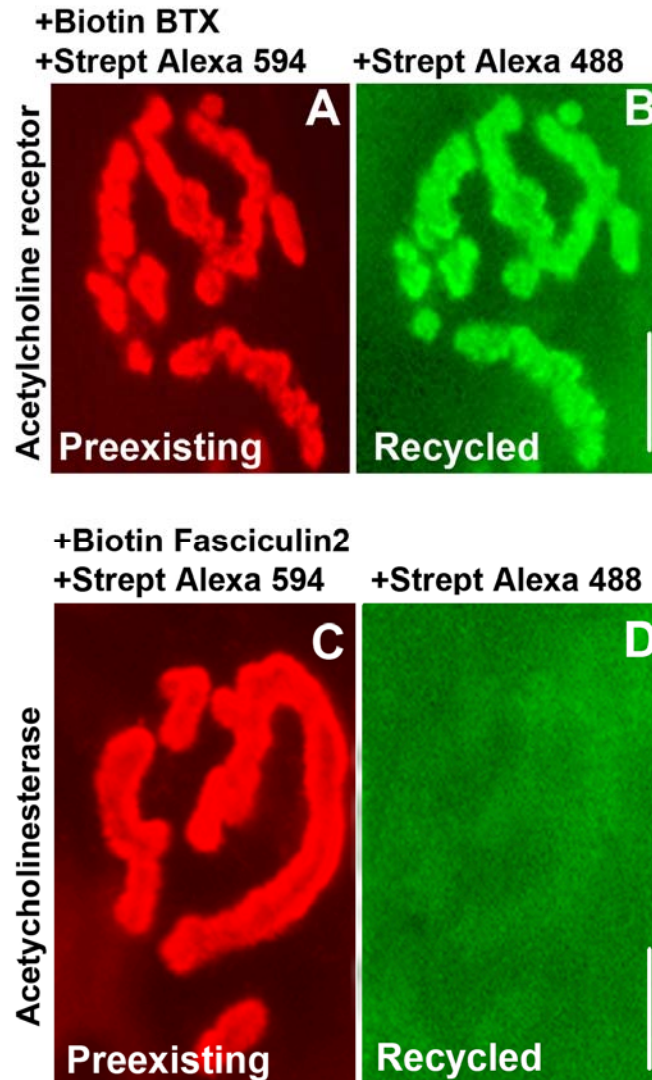
Figure 3.3. Lack of streptavidin dissociation from AChE-Fasciculin2-biotin *in vivo*. (A) Example of a living adult mouse neuromuscular junction previously labeled with BTX-biotin (to label AChRs) followed by a saturating dose of streptavidin-Alexa 594 (red) at time 0 and imaged at 4 days. Red signal indicates the pre-existing receptors still remaining on day 4. (B) The same neuromuscular junction imaged after application of streptavidin-Alexa 488 (green). Green signal indicates the AChRs that were recycled over 4 days. (C) Example of a NMJ labeled with Fasciculin2-biotin (to label AChEs) followed by a saturating dose of streptavidin-Alexa 594 (red) at time 0 and imaged at 4 days. Red signal indicates the pre-existing acetycholinestrase remaining on day 4. (D) The same neuromuscular junction imaged after application of new streptavidin-Alexa 488 (green) and viewed with much higher camera gain than used in B. The weak green signal indicates that there is very little streptavidin dissociation after 4 days. If the same gain was used as in B, the fluorescence was almost undetectable. Scale bar, 20 μm.

In denervated muscle, receptors are known to turn over at an accelerated rate and muscle stimulation has been shown to prevent this increase in receptor loss (Salpeter and Loring, 1985; Andreose et al., 1993; Caroni et al., 1993; Akaaboune et al., 1999). If dissociation does not occur on the surface but only after the AChR-BTX-biotin-streptavidin complex is internalized, one would predict that decreasing the rate of internalization of receptors would also decrease the streptavidin-biotin dissociation. To test this possibility, we labeled synaptic AChRs on denervated muscle with BTX-biotin followed by streptavidin and then directly stimulated the sternomastoid muscle by placing stimulating electrodes at either end of the muscle for the entire 8 hour experiment. As predicted, 8 hours after stimulation we found no evidence of receptor loss (see supplemental figure S3.2). When we added a second dose of streptavidin-Alexa and then quantified the recovery of fluorescence, we did not see any evidence for new streptavidin-Alexa binding (see supplemental data). In contrast, binding of new streptavidin-Alexa was easily measurable in control, unstimulated muscle during the same time window. This result argues strongly that the dissociation of streptavidin from AChR-BTX-biotin does not occur spontaneously on the muscle surface, but rather only after internalization.

Evidence for the intracellular dissociation of streptavidin from the AChR-bungarotoxin-biotin complex

If streptavidin dissociates from the AChR-BTX-biotin-Streptavidin-Alexa complex at an intracellular site, it should be possible to observe Alexa fluorescence in intracellular vesicles. It should also be possible to observe intracellular vesicles with biotin freed from streptavidin. To test the first possibility, muscles were initially labeled with a saturating dose of BTX-biotin (5 μg/ml, 1.5 h) followed by a saturating dose of

77

fluorescent streptavidin-Alexa 488. After an appropriate waiting time (4 days), the mouse was perfused with 2% paraformaldehyde. The sternomastoid muscle was then dissected and cut in longitudinal sections parallel to the axis of the muscle fibers to allow visualization of both the cell surface and the region below it, using confocal microscopy.

In control muscles that were labeled with BTX-biotin/streptavidin-Alexa 488 and then immediately fixed and sectioned (rather than waiting 4 days), the antibody mediated AChR-labeling was intense at the surface receptors of the synapse, plus a number of small spots (puncta), while the streptavidin-Alexa labeling was also intense on the cell surface, but not visible in puncta. This is the expected result, because the AChR immunocytochemistry detects all receptors, including those present internally, while the streptavidin-Alexa staining procedure initially detects only surface receptors, and some time must elapse before they become internalized. However, when four days were allowed between labeling and fixation, we found that most of the initial streptavidin label colocalized with receptors on the surface and in intracellular puncta (Figure 3.4 A-F). Z-stack analysis of the images confirmed that these colocalized fluorescent spots were beneath the muscle surface indicating that AChR-BTX-biotin-streptavidin was internalized as a complex. A significant number of the intracellular AChR-containing puncta were also labeled only by the anti-receptor antibody. These could be receptors that have lost their streptavidin label and are either in the process of recycling or degradation, or unlabeled newly synthesized receptors yet to be inserted. A small number of green fluorescent spots were also observed which did not colocalize with receptors, perhaps corresponding to accumulation of fluorescence in degradative vesicles.

It seemed likely that many of the puncta were intracellular vesicles. To test this possibility, muscle fibers were fixed and then processed so that AChR and the early endosome marker EEA1 could be detected immunocytochemically (Figure 3.4 G-O). The EEA1 labeling was present in a profusion of small spots located below the cell surface, while the AChR labeling consisted of intense labeling of the surface receptors of the synapse, plus a modest number of small spots. Although many EEA1 spots were negative for AChR, the vast majority of AChR positive spots were also positive for EEA1. Thus puncta of AChR staining represent a reliable marker of internalized AChR. Given the high correlation between AChR labeling of puncta and EEA1 labeling of puncta, the presence of puncta that were labeled both for AChR and for streptavidin in the experiments shown in Figure 3.4 A-F demonstrates that fluorescent Alexa from surface AChRs labeled with BTX-biotin-streptavidin-Alexa is internalized. The puncta that stained only with the anti-receptor antibody but were negative for Alexa most likely represent newly synthesized receptors yet to be inserted, while the puncta that stained for Alexa, but not for AChR seem likely to correspond to degradative vesicles that have completely consumed their AChR.
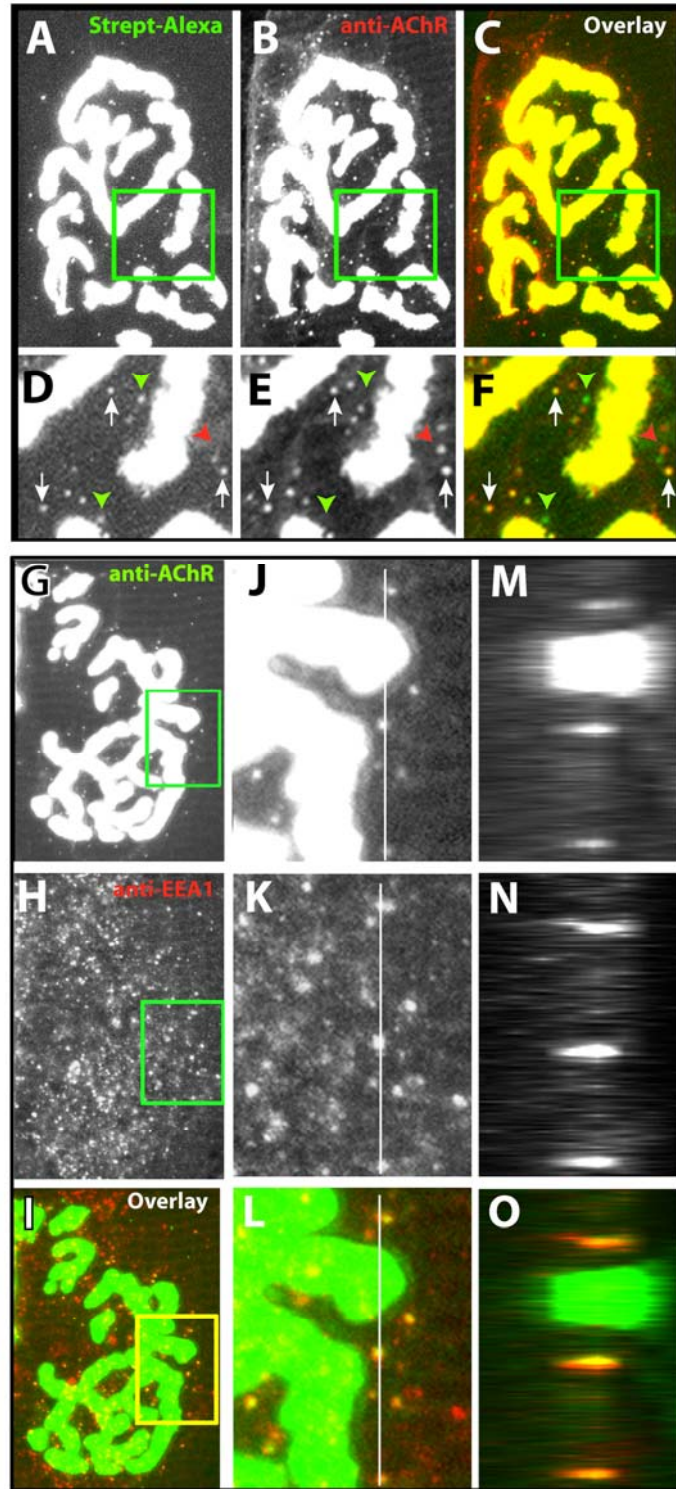
Figure 3.4. Confocal imaging of AChR-bungarotoxin-biotin-streptavidin complexes in intracellular compartments. Sternomastoid muscles were labeled in living mice with BTX-biotin and saturated with streptavidin-Alexa 488. After 4 days the muscles were fixed, sectioned longitudinally and then processed for immunocytochemical detection of AChRs with an Alexa 594 conjugated secondary antibody. (A) Example of a stack of 20 confocal images (0.5 μm intervals) of a NMJ that was

initially labeled with BTX-biotin/streptavidin-Alexa 488 and collapsed onto a single plane. The small green fluorescence puncta could represent either the accumulation of fluorescent streptavidin still attached to AChR-BTX-biotin complexes, or the accumulation of fluorescent streptavidin in intracellular compartments. (B) Immunostaining with anti-AChR and secondary antibody conjugated to Alexa 594. These puncta could represent the presence of receptors that are newly synthesized, internalized and recycling, or internalized and in the process of degradation. (C) Overlay of the Alexa 488 fluorescence colored green, and the anti-AChR fluorescence colored red. (D-F) Detail from the boxed regions in (A-C). Arrows indicate colocalization of original streptavidin-Alexa 488 (green) and AChR (red) in intracellular puncta, showing that the AChR-BTX-biotin-streptavidin complexes are internalized. Red arrowheads indicate intracellular puncta that contained only receptors (likely unlabeled receptors that are in the process of insertion or BTX-biotin labeled receptors in the process of recycling). Green arrowheads indicate intracellular puncta that contained only streptavidin-Alexa 488. (G-O) Example of a neuromuscular junction on a muscle section (labeled as described above) immunostained for AChRs and EEA1. (G-I) Eight confocal slices at 2 μm intervals were collapsed onto a single image plane. In the overlay image, green indicates anti-AChR immunostaining and red indicates anti-EEA1 immunostaining. (J-L) The boxed regions of panels G-I are shown at higher power. (M-O) Z-stack of fluorescence intensity taken at various depths along the white line indicated in panels J-L. The top of the section is to the right, and the width of these panels corresponds to a total depth of 20 μm.

Having shown that the Alexa from AChR-BTX-biotin-streptavidin-Alexa complexes can be internalized, we next tested whether biotin that had lost streptavidin could also be observed inside of muscle fibers. We first showed that the anti-biotin antibody we were using can effectively stain AChR-BTX-biotin complexes (Figure 3.5 A), but not AChR-BTX-biotin-streptavidin-Alexa 488 complexes (Figure 3.5 B-D). Thus if muscles are pretreated with BTX-biotin and streptavidin-Alexa, this antibody will label only receptor complexes that have been stripped of streptavidin. Confocal images of muscle sections saturated with BTX-biotin-streptavidin and fixed and processed 4 days later showed that staining with both the anti-AChR antibody and the anti-biotin antibody labeled the entire synaptic region, and both fluorescent labels were also found co-localized in small spots in the vicinity of the junction (Figure 3.5 E-J). Approximately 40% of the intracellular spots were labeled by both antibodies, and the rest were labeled only by the anti-receptor antibody. An alternate approach was also used to confirm the presence of free biotin within puncta. Longitudinal sections of mouse sternomastoid

muscle saturated 4 days previously with BTX-biotin followed with streptavidin-Alexa 594 or unlabeled streptavidin were fixed and permeabilized as described above, and labeled with anti-receptor antibody and streptavidin-Alexa 488. The number of green fluorescent puncta was similar to the number obtained when anti-biotin antibody was used.
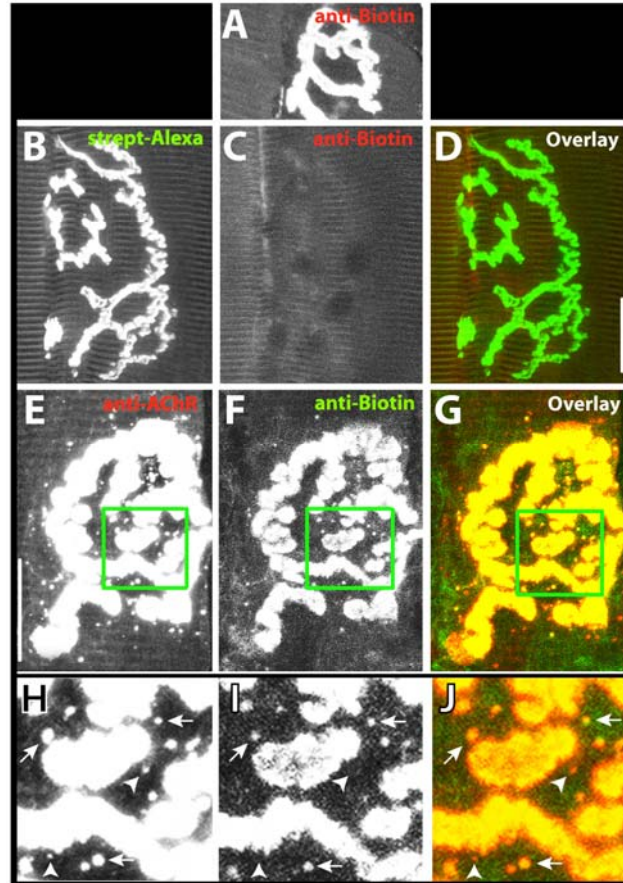
Figure 3.5. Confocal images of AChR-BTX-biotin complexes in intracellular compartments. (A) Example of a neuromuscular junction labeled with BTX-biotin followed by anti-biotin-Alexa 488 or 594. This staining was a positive control to demonstrate that this antibody is able to effectively label biotin in complex with AChR. (B) Example of a neuromuscular junction that was labeled with biotin-bungarotoxin followed by a saturating dose of streptavidin-Alexa 488 and then immediately fixed. (C) When the same synapse was immunostained with anti-biotin-Alexa 594, no red fluorescence was observed. The absence of staining with anti-biotin indicates that this antibody can only interact with BTX-biotin when it has been stripped of streptavidin. (D) Overlay of images in (B) and (C). (E) Example of a synapse on a muscle initially incubated with BTX-biotin/ streptavidin and then fixed and sectioned 4 days later and immunostained with anti-AChR and an Alexa 594 conjugated secondary antibody. (F) The same synapse as in (E) labeled with anti-biotin-Alexa 488. (G) Overlay of images in (E) and (F). (H-J) The boxed areas from panels (E-G) at higher magnification and viewed at a camera gain sufficient to saturate the signal from synaptic AChRs in order to accentuate the signal coming from the internal spots. Arrowheads indicate spots of fluorescence that stained positive for AChR but not for biotin, while arrows indicate spots where both labels were colocalized. Scale bar, 20 μm.

In summary, we see AChR-BTX-biotin complexes that have been stripped of their streptavidin labels both in intracellular vesicles and on the cell surface *in vivo*. Because we have seen no indication that dissociation occurs on the cell surface, the likely sequence is that the AChR-BTX-biotin-streptavidin complex is endocytosed into vesicles, the streptavidin is stripped off of the complex and degraded and then the AChR-BTX-biotin complex is returned to the surface. For these and other reasons considered in the Discussion, we will refer to the pool of receptors that can be relabeled with a second color of streptavidin-Alexa as "recycled receptors".

Time-lapse imaging of synaptic AChR recycling

Having found that receptors are able to recycle, we next wanted to determine how quickly recycled receptors were incorporated into the postsynaptic membrane. To do this, sternomastoid muscles of 3 mice were labeled with a low dose of BTX-biotin (5 µg/ml, 2 min) (to ensure that synaptic activity remained fully functional (Lingle and Steinbach, 1988)) followed by a saturating dose of streptavidin-Alexa 488. A dose of streptavidin-Alexa 594 (30 min) was then added to ensure the saturation of all biotin sites (Figure 3.6 A,B). Every 2 hours a fresh dose of streptavidin-Alex 594 was added to the muscle to label recycled receptors. Using high detector gain with a CCD camera, we were able to see a clear red fluorescence signal at 2 hours. In all 10 synapses imaged the fluorescence signal increased in intensity after each new strep-Alexa 594 application (Figure 3.6 C-F). This result suggests that recycled receptors are rapidly inserted into the membrane.
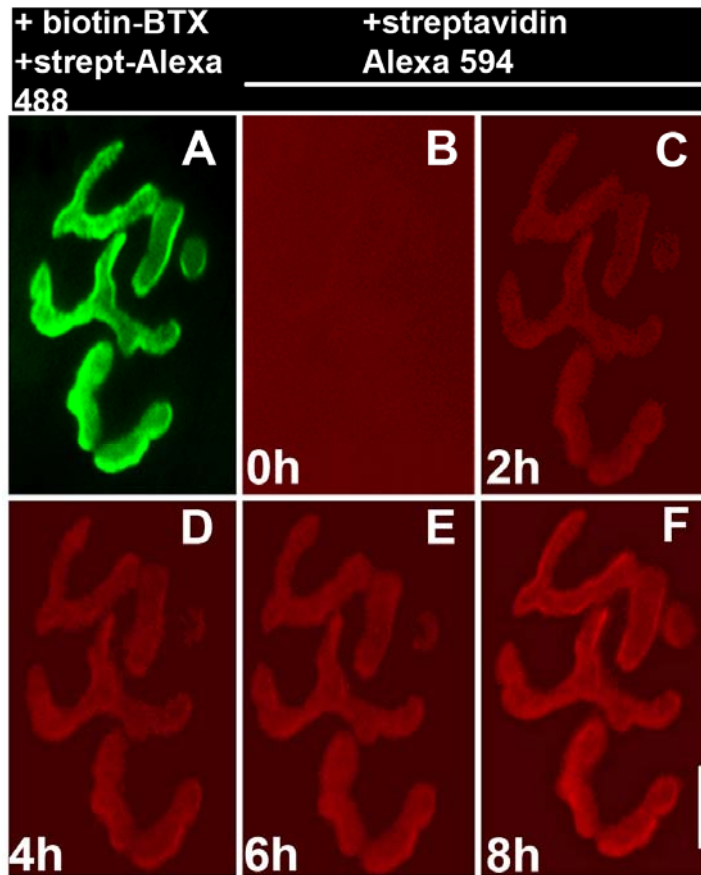
Figure 3.6. Time-lapse imaging of the appearance of recycled receptors. (A) In a living adult mouse, a neuromuscular junction of the sternomastoid muscle was labeled with a low dose of BTX-biotin followed by a saturating dose of streptavidin-Alexa 488 (green). (B) The junction was then immediately bathed with a saturating dose of streptavidin-Alexa 594 (red) and viewed at substantially higher gain. The absence of any red labeling indicates that all biotins were initially saturated with streptavidin-Alexa 488. (C-F) The same neuromuscular junction imaged every 2 hours for 8 hours, after application of new streptavidin-Alexa 594 (red) to the sternomastoid muscle before each time point. Scale bar, 20 μm.

Effect of synaptic activity on the recycled and new AChR pools

To quantitate the number of recycled and new receptors inserted into the same synapse over time, we used the same fluorophore in three distinct labeling steps, which allowed us to distinguish each receptor pool, and then we assayed fluorescence intensity using an established *in vivo* quantitative fluorescence method (Turney et al., 1996; Akaaboune et al., 1999). The sternomastoid muscle of 6 mice was saturated with an

initial dose of BTX-biotin (5 µg/ml, 1.5 h) followed by streptavidin-Alexa 594 (red) (10 µg/ml, 2.5 h) to saturate biotin sites. The fluorescence intensity of superficial neuromuscular junctions was then assayed at time 0, and then at a second time point 8 hours, 1 day, 3 days or 4 days later (Figure 3.7 A,B). At 4 days we found that junctions labeled at t0 with a saturating dose of BTX-biotin/ streptavidin-Alexa 594 had lost 53% ±3 SD (n=30) of their original fluorescence. To quantitate the amount of receptors that were recycled over time, we applied a second saturating dose of streptavidin-Alexa 594, and measured the resulting increase in fluorescence intensity. We found that at 4 days the fluorescence from the recycled receptors equaled 26% ±5 SD (n=29) of the original fluorescence (Figure 3.7 A,B).

To quantitate the contribution of the new receptors added to these same synapses during the 4 days the sternomastoid muscle was then labeled with a fresh saturating dose of BTX-biotin followed with a fresh saturating dose of streptavidin-Alexa 594. We found that an additional 24% ±5 SD (n=29) of the original fluorescence was recovered (Figure 3.7 A,B). In summary, four days after a single transient application of BTX-biotin the sum of remaining original (pre-existing), new and recycled receptors was very close to 100% of the original signal, and the contribution of newly inserted receptors and recycled receptors were nearly equal at about 25% of original fluorescence each.

When the contributions of original, recycled and new receptors were examined at earlier time points after the initial labeling (Figure 3.7 B), several interesting characteristics became apparent. At one day after a one-time bungarotoxin AChR blockade, the contribution of recycled receptors was less (18% ±5 SD of original fluorescence recovered, n=25) than that of new receptors (22% ±5 SD of original

fluorescence recovered, n=20, p< 0.005). This effect was even more pronounced at 8 hours with recycled receptors contributing 9% ±3 SD of original fluorescence (n=30) and new receptors accounting for 17% ±7 SD (n=20, P<0.0001) (Figure 3.7 B).
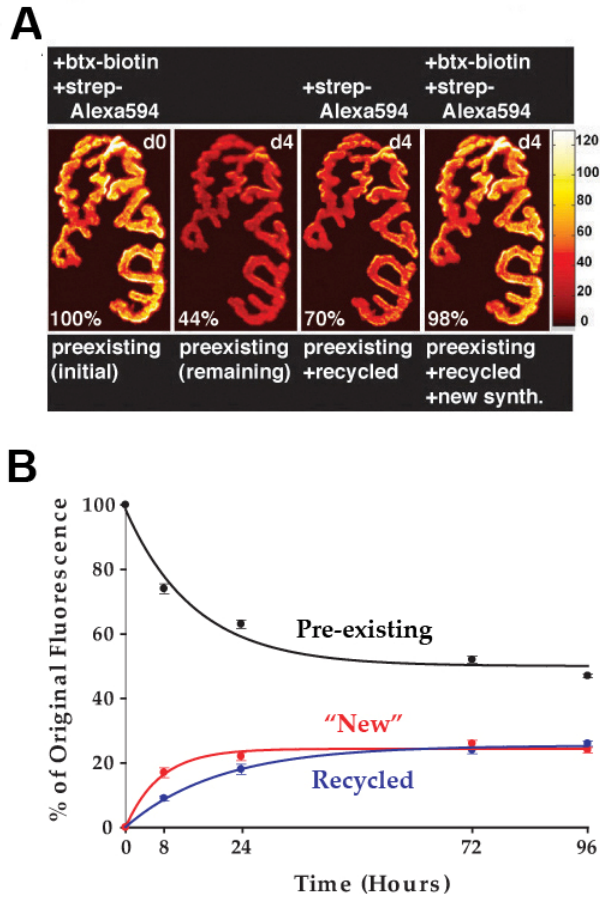
Figure 3.7. Quantification of original, recycled and new receptors at the neuromuscular junction following transient activity blockade. These pseudo-color images provide a linear representation of the density of AChRs (white-yellow, high density; red-black, low density). (A) Example of a mouse neuromuscular junction labeled with a saturating dose of BTX-biotin followed immediately by a saturating dose of streptavidin-Alexa 594, imaged, and then re-imaged 4 days later. The total fluorescence intensity (a measure of the total number of AChRs) was expressed as 100% at the initial labeling (first panel from the left, day 0) and normalized to this on each successive view. Second panel from the left represents the pre-existing receptors remaining after 4 days when more than 50% of the initial fluorescence is lost. To quantitate the recycled receptors, streptavidin-Alexa 594 (red) fluorophore was then added to the muscle. The third panel from the left thus represents the sum of pre-existing and recycled receptors after 4 days. New receptors were identified by next adding a saturating concentration of BTX-biotin followed by a saturating dose of streptavidin-Alexa 594 (red) as shown in the fourth panel. The fluorescence from these new receptors is added to the pre-existing and recycled receptors to determine the total receptor density after 4 days. (B) Graph summarizing the amount of original receptors remaining after various times, and the proportion of new and recycled receptors that were inserted into the synapse; obtained from many junctions with the approach shown in (A). Each data point represents the mean percentage of original fluorescence intensity (±SEM).

Receptors in the pools defined as pre-existing and recycled both have BTX bound and so do not function, but the receptors in the new pool are unlabeled and therefore unblocked and functional. In the NMJ it is known that a large safety factor exists that enables synapses to be fully functional with only 10-20% of receptors being unblocked (Lingle and Steinbach, 1988). Therefore, it would be expected that by 8 hours, the 17% of the total receptors that are new and unblocked would be sufficient to restore super-threshold endplate potentials and muscle spiking activity. It thus seemed likely that the changes in the rate of receptor recycling in transiently blocked NMJs (1.5 h one-time bungarotoxin treatment) are the consequence of the initial activity blockade by BTX and subsequent restoration of neuromuscular transmission by new unlabeled and unblocked AChRs.

To further examine the role of synaptic activity on the insertion of recycled and new receptors, we monitored the appearance of receptors in continuously blocked synapses, in which AChRs are reported to be lost at an accelerated rate (Salpeter and Loring, 1985; Martyn et al., 1992; Akaaboune et al., 1999). To test the effect of activity cessation on receptor trafficking, we chronically blocked synaptic transmission with curare (a poison that reversibly blocks AChRs), and so indirectly blocked muscle spiking. The longest this treatment could be carried out without mortality was 8 hours, plus a two hour treatment to label either recycled receptors, or new receptors but not both. However, this was sufficiently long to resolve several interesting differences from the one-time labeling of AChRs with saturating bungarotoxin, in which blockade is transient and muscle activity recovers over time (Figure 3.8). First, as expected from previous studies, the removal of original receptors was more pronounced (on average falling to 65% of the

initial fluorescence at 8 hours as compared to 74% in animals receiving a one time block with BTX). Second, the rate of appearance of new AChRs decreased to about 1/3 that observed when synaptic transmission was restored after a few hours, but remained at observable levels (4.5% ±2 SD, n=20). Most dramatically, the contribution of the recycled receptors decreased to nearly undetectable levels (0.4% ±1 SD of original fluorescence, n=60) (Figure 3.8 A,B).
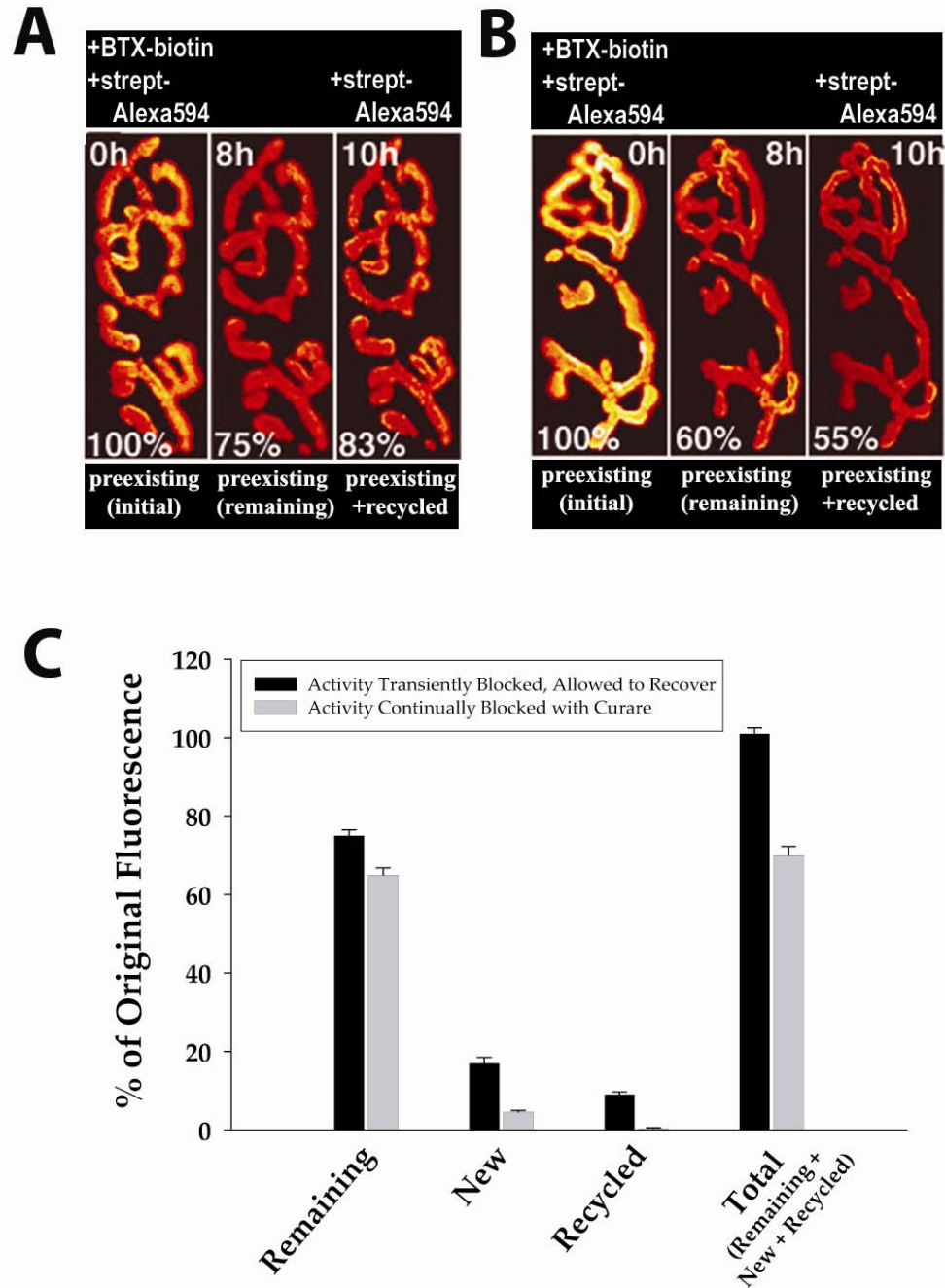
Figure 3.8. Quantification of original, recycled and new receptors at the neuromuscular junction following a transient and maintained activity blockade. (**A**) Assessment of the extent of recycling after 8 hours following an initial transient blockade of activity with BTX-biotin. (**B**) Assessment of the extent of recycling after 8 hours following a maintained blockade of activity with curare. (**C**) Graph summarizing results obtained from many synapses studied as in (A and B). The data show the mean ± SEM. For all four conditions, the difference between the two experimental groups was significant (p< 0.001). These experiments were not carried beyond 8 hours, because of mouse mortality from the long term curare treatment. It thus was not possible to measure recycling and new receptors at the same synapses. The insertion of new receptors was therefore measured in a parallel experiment using BTX-Alexa 594

Discussion

These results are based on the surprising finding that at sternomastoid muscle synapses in living mice, streptavidin dissociates unexpectedly rapidly from AChR-BTX-biotin complexes. The dissociation of purified streptavidin from biotin in test tube assays is extremely slow, because of their extraordinarily high affinity (Chilkoti and Stayton, 1995). However, our observation that biotin-streptavidin dissociation occurs at an accelerated rate *in vivo* is not unprecedented: avidin-biotin complexes have been previously reported to dissociate after their intraperitoneal injection into live animals (Fraenkel-Conrat and Fraenkel-Conrat, 1952; Wei et al., 1971; Lee et al., 1972; Lee et al., 1973b; Lee et al., 1973a). One potential molecular mechanism for enhanced dissociation comes from an older study that reported that although the avidin-biotin complex is highly resistant to elevated temperature, acidic or basic pH and proteases, the weak oxidizing environment provided by 0.3% H_2O_2 can readily cause dissociation (Gyorgy, 1943), which could allow the specific liberation of the streptavidin-Alexa tag from the AChR-BTX-biotin complex without affecting the AChR-BTX bond. A second potential mechanism for enhancing unbinding is suggested by recent studies conducted on purified proteins. When added to complexes of biotin and streptavidin, two different classes of proteins have been demonstrated to have the ability to rapidly displace the streptavidin from the biotin (Subramanian et al., 1997; Morris and Raney, 1999). In both cases the extra protein (a helicase in one study and a monoclonal antibody in the other) can be thought of as a chaperone, placing the streptavidin in a non-native conformation that enhances unbinding. It seems plausible that the combination of low pH, an oxidizing environment, and perhaps some modification in the conformation of streptavidin by

unknown factors within recycling vesicles could be responsible for the observed dissociation of streptavidin-Alexa from biotin. This mechanism would also be consistent with the absence of dissociation on the cell surface, as this is a relatively reducing environment at nearly neutral pH.

The cellular location of dissociation of streptavidin from biotin

For several reasons, we believe that the dissociation of streptavidin from biotin takes place within intracellular vesicles rather than on the cell surface. First, we saw no evidence for streptavidin-biotin dissociation occurring on the cell surface of fixed muscle tissue (even when transplanted into an *in vivo* milieu), from AChR ghost clusters or from clusters of AChRs on living aneural muscle cells in culture. Second, we could readily observe AChR-BTX-biotin complexes that had been stripped of streptavidin in intracellular vesicles near synaptic sites in sternomastoid muscles. Third, when the rate of internalization of receptors was greatly decreased by electrical stimulation of the muscle, we could no longer detect dissociation of streptavidin from biotin. Finally, when the same labeling protocol was applied to AChE, a component of the synaptic cleft localized in the extracellular matrix rather in the plasma membrane, there was no evidence of streptavidin-biotin dissociation. This last observation implies that AChE is recycled very slowly or not at all. Insertion of AChE into the basal lamina requires collagen (ColQ) (Feng et al., 1999), so one possible explanation for the failure to recycle is that AChE-Fasciculin2-biotin-streptavidin complexes are internalized after detaching from ColQ and therefore unable to insert back into the basal lamina. Whatever the reason for the lack of streptavidin unbinding from AChE complexes over time, these findings provide

compelling evidence that local surface events are not responsible for the biotin-streptavidin dissociation observed with AChRs at the living neuromuscular synapse.

A final reason for favoring vesicles as the site of the biotin-streptavidin dissociation is that a vesicular intermediate provides a ready explanation for the observation that the ability to recycle receptors to the cell surface can be dissociated from the ability to endocytose. Under two situations in which there was no synaptic activity (aneural cultures of C2C12 myotubes and *in vivo* synapses chronically blocked with curare), internalization of receptors was readily detected as expected from previous results (St John and Gordon, 2001) and yet we saw no indication that there was any recycling (no vacant streptavidin binding sites on the cell surface). Regarding the failure to observe receptor recycling in cultured C2C12 myotubes, it has been shown previously that a large subsurface "hidden" pool of receptors exists in cultured chick and rat myotubes, but that such a pool is absent in innervated muscle (Devreotes and Fambrough, 1975). This pool comprises up to 30% of the total AChR complement of cultured myotubes, and was found to derive partially from the surface of the muscle as opposed to newly synthesized receptors (Devreotes and Fambrough, 1975). As with AChRs at inactive synapses in living mice, these cultured muscle fibers are apparently lacking a signal that allows the internalized receptors to return to the cell surface.

Both the *in vitro* and *in vivo* results could be readily explained if the insertion of vesicles containing receptors available for recycling are delivered to the cell surface only when there is synaptic activity. An obvious candidate for mediating the activity dependent signal is intracellular calcium, as it is the most common signal that regulates exocytosis in both secretory and nonsecretory cells (Chavez et al., 1996). At central

nervous system synapses, Ca^{2+} influx into the postsynaptic cell through NMDA receptors is involved in AMPA receptor recycling in cortical and hippocampal neurons (Carroll et al., 1999b; Luscher et al., 1999). Such alteration in AMPA and NMDA receptor numbers in the postsynaptic density are proposed to account for changes in synaptic strength (Malinow and Malenka, 2002; Malinow, 2003). Indeed, the activity-dependent cycling of AMPA receptors at the post-synaptic membrane underlies many aspects of synaptic plasticity (Malinow and Malenka, 2002; Malinow, 2003; Park et al., 2004). At the NMJ, AChRs allow the entry of calcium in addition to sodium and potassium, so it is conceivable that blocking the receptors could inhibit Ca^{2+} influx and thus block a signal required for receptor recycling.

What is the extent of AChR recycling at normally functioning synapses?

Our experiments have demonstrated that AChR recycling occurs at the neuromuscular junction of living mice, and that chronically inhibiting synaptic activity with curare drastically decreases the amount of detectable recycling. Although measurements of changes in fluorescence intensity over time were made with great precision, there are several important caveats to the interpretation of our results that cause us to be cautious about extrapolating these data to estimate the rates of internalization and recycling of native receptors when activity is unmodified.

First, only receptors that have been internalized have the possibility of recycling. If the internalization rate is slow, it will be difficult or impossible to detect recycling, even if the cellular mechanisms that cause recycling are fully functional.

Second, it is necessary to bind the bulky ligands BTX-biotin and streptavidin-Alexa in order to detect recycling. It is unclear to what extent the binding of streptavidin

would alter the life history of receptors. For instance, it is widely accepted that antibody binding to AChR can accelerate the rate of internalization and degradation (Fumagalli et al., 1982), perhaps as a consequence of crosslinking or due to other unknown factors. Streptavidin has four biotin binding sites, and so has the potential to cross link biotins on multiple toxin molecules, and thus indirectly crosslink receptors. However, the time course of the loss of fluorescence on cultured myotubes (where recycling was not observed) was not significantly different when receptors were directly labeled with BTX-Alexa or indirectly labeled with α-BTX-biotin and then with streptavidin-Alexa. This indicates that either steric factors prevented the streptavidin from crosslinking receptors, or that receptors crosslinked by streptavidin do not have an altered rate of internalization beyond any effect of BTX alone.

Third, the amount of recycling we detect is a minimum estimate and the actual amount could be greater. There are two possible ways that receptors could recycle without being detected by the methods we used. Any receptor that is endocytosed and returned to the cell surface without losing either its BTX-biotin or its streptavidin Alexa will be counted as part of the preexisting pool, even though it has recycled. Similarly, any receptor that loses its BTX-biotin and then recycles will be counted as part of the new pool. At present there are no available methods that would allow us to determine whether either of these two types of events occur at a sufficient frequency to significantly increase the actual recycling rate above what we measured. Regardless of these caveats, it is clear that under the conditions used for some of the experiments presented in this paper, at least 25% of the synaptic receptors on the cell surface are recycled over a 4-day period.

The existence of a recycled pool of AChRs requires that a number of earlier experiments on the life history of AChRs be reinterpreted. For instance, a substantial number of experiments using fluorescently labeled BTX have shown that the half-life of fluorescence loss at synapses in living mice is approximately 7 days after a one time blockade with bungarotoxin (Salpeter and Loring, 1985; Andreose et al., 1993; Caroni et al., 1993; Akaaboune et al., 1999; Akaaboune et al., 2002). This had been interpreted as the half-life of receptors on the cell surface, but our results suggest that each receptor can recycle back to the cell surface (perhaps several times) before it is degraded, and that junctional AChRs are therefore being internalized from the surface at a significantly faster rate ($t_{1/2}\sim$ 4 days after one-time blockade) than previously mentioned. The results reported here suggest that despite the stability of the synaptic structure over the lifetime of the animal (Balice-Gordon and Lichtman, 1990), receptors are highly dynamic and are constantly exchanged between the plasmalemma and internal compartments, in addition to being frequently shuttled between junctional and extra-junctional regions (Akaaboune et al., 2002).

Together, our results suggest a model for the regulation of the postsynaptic receptor density at the neuromuscular junction in live animals involving two separate pathways: a receptor recycling pathway and a new receptor pathway. When postsynaptic transmission is functional, both the recycled and the new receptor pathways contribute significantly to the postsynaptic density (Figure 3.9 A). In the absence of postsynaptic activity, however, internalized AChRs are shifted from a recycling pathway to a degradative pathway (Figure 3.9 B). The new receptor insertion pathway is also affected by the absence of postsynaptic activity, but continues to deliver receptors at a reduced

rate. We do not know, however, whether new and recycled receptors are added directly to the junction or are inserted into the perijunctional region and then migrate into the junction to be anchored. It would be of considerable interest to see whether different patterns of activity can alter the proportion of new and recycled receptors at synapses in live animals.
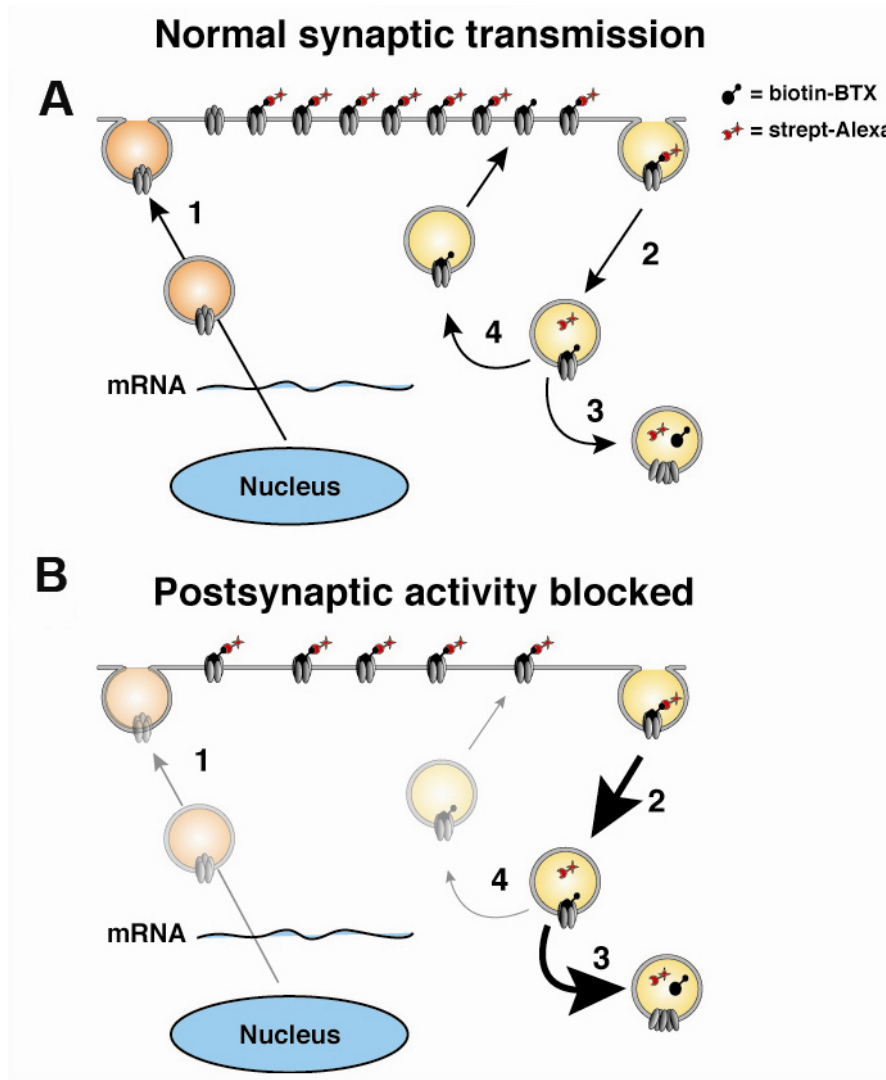
Figure 3.9. A proposed model suggesting the way activity affects the insertion of recycled and new AChRs at the neuromuscular junction. (A) During normal synaptic transmission, the recycled (4) and new receptor (1) pathways contribute equally to the synaptic density. (B) In the absence of postsynaptic activity, the recycled and new receptor pools decrease. After internalization (2) the receptors presumably shift from the recycling pathway to the degradative (3) pathway.

Supplemental Figures
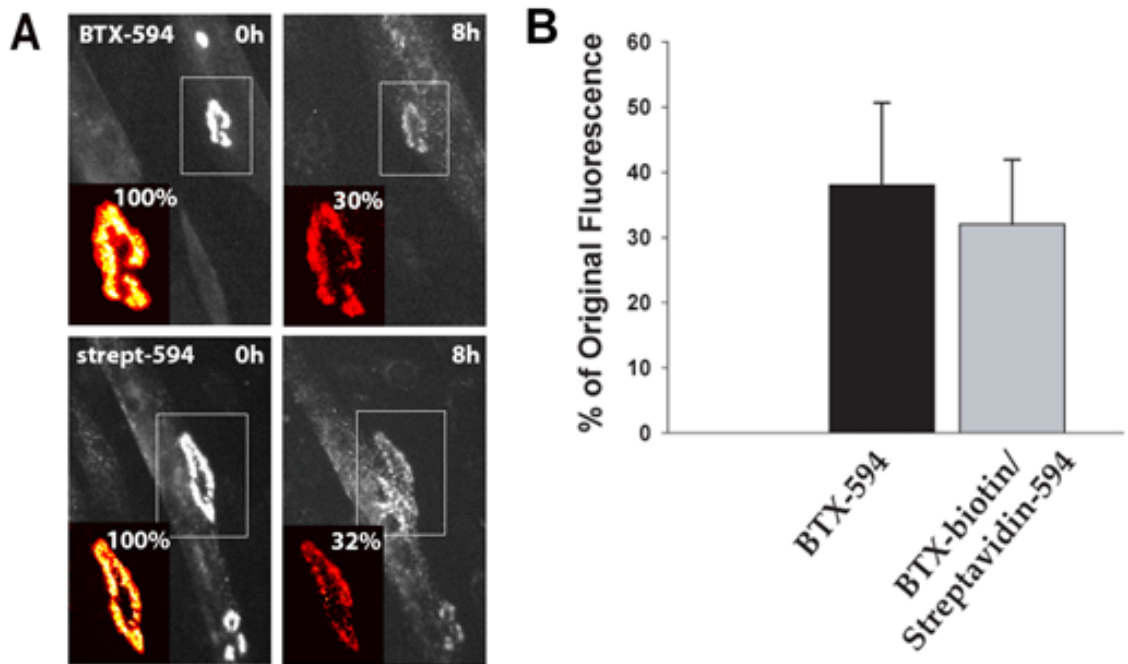
Figure S3.1. There was no significant difference between the rate of loss of AChR labeling assessed with fluorescent BTX or with fluorescent Streptavidin/biotin-BTX. (A) C2C12 myotubes were saturated with bungarotoxin-Alexa 594 (top panels) and individual clusters were imaged. Eight hours later the same clusters were re-imaged and fluorescence was quantified. In the bottom panels, C2C12 myotubes were saturated with bungarotoxin-biotin followed immediately by streptavidin-Alexa 594. Individual clusters were imaged after labeling and at 8 hours and their fluorescence was assayed. (B) Graph represents the fluorescence remaining at BTX-Alexa (38% ±12.0 SD, n= 11 clusters/3 cultures) or BTX-biotin-streptavidin-Alexa (33% ±10.0 SD, n= 14 clusters/3 cultures). The amount of fluorescence remaining detected with the two labeling schemes was not significantly different (p > 0.2). The data show the mean ± SEM.
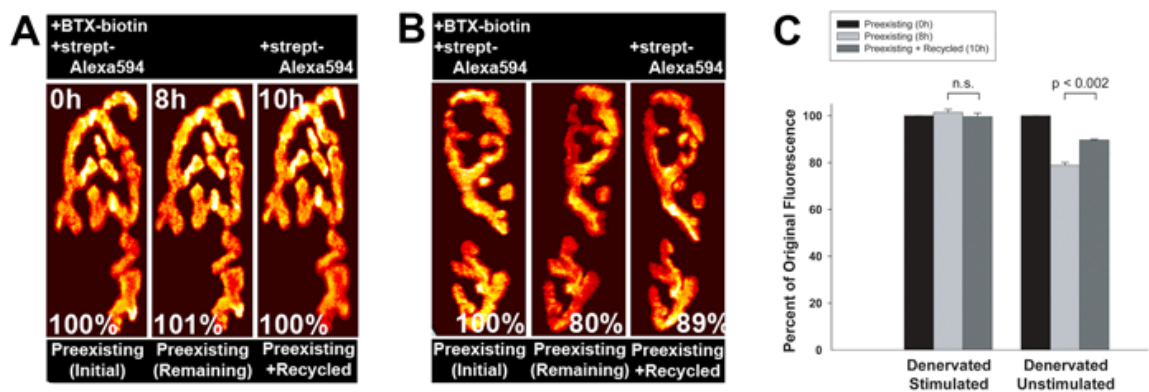
Figure S3.2. Streptavidin/biotin BTX dissociation does not occur on stimulated denervated muscle. (A) Denervated muscle was labeled with bungarotoxin-biotin/streptavidin-Alexa 594 to saturation, and the fluorescence at an individual synapse was imaged and quantified (first panel). After initial imaging the muscle was stimulated for the duration of the experiment. After 8 hours the same synapse was located and imaged and the fluorescence was again quantified (second panel). To identify any receptors that had been recycled during the period of stimulation, new streptavidin-Alexa 594 was added to the muscle and the synapse was again imaged and fluorescence was quantified (third panel). (B) Control denervated muscle not stimulated but labeled and imaged exactly as described in A. (C) Summary of the data obtained from many synapses as in (A) and (B). Note that stimulation of the sternomastoid muscle prevented fluorescence loss and that there was no evidence for recycling AChR, while the fluorescence in unstimulated muscle NMJs lost ~20% of their original fluorescence over 8 hours, and the addition of new streptavidin-Alexa 594 resulted in a significant increase in fluorescence intensity. Values represent mean ±SEM.

Acknowledgements

Chapter IV

The Dynamics of Recycled Acetylcholine Receptors at the Neuromuscular Junction *In Vivo*

Emile G. Bruneau and Mohammed Akaaboune

Abstract

At the peripheral neuromuscular junction (NMJ), a significant number of nicotinic acetylcholine receptors (AChRs) recycle back into the postsynaptic membrane after internalization to intermingle with not yet internalized "pre-existing" AChRs. However the way these receptor pools are maintained and regulated at the NMJ in living animals remains unknown. Here, we demonstrate that recycled receptors in functional synapses are removed ~4 times faster than "pre-existing" receptors and that most removed recycled receptors are replaced by new recycled ones. In denervated NMJ, the recycling of AChRs is significantly depressed and their removal rate increased, while direct muscle stimulation prevents their loss. Furthermore, we show that protein tyrosine phosphatase inhibitors cause the selective accumulation of recycled AChRs in the peri-synaptic membrane without affecting the "pre-existing" AChR pool. The inhibition of serine/threonine phosphatases, however, has no effect on AChR recycling. These data show that recycled receptors are remarkably dynamic and suggest a potential role for tyrosine dephosphorylation in the insertion and maintenance of recycled AChRs at the

postsynaptic membrane. These findings may provide insights into long-term recycling processes at less accessible synapses in the central nervous system in vivo.

Introduction

At central synapses, recycling of postsynaptic receptors plays a critical role in synaptic plasticity. For example, during long-term potentiation, synaptic strength is enhanced by an increased recruitment of recycled AMPA receptors from intracellular endosomal compartments to the postsynaptic membrane (Contractor and Heinemann, 2002; Ehlers, 2000; Lee et al., 2004; Luscher et al., 1999; Park et al., 2004). At the peripheral neuromuscular junction (NMJ) it was long assumed that acetylcholine receptors (AChRs) remain stable in the post-synaptic membrane until they are internalized and degraded in the lysosomes (Gardner and Fambrough, 1979). In this scheme, insertion of newly synthesized receptors would be responsible for maintaining AChR density in the post-synaptic membrane over time. Recent work from our lab has shown, however, that a significant number of internalized AChRs are not degraded, but instead return back into the postsynaptic membrane where they intermingle with AChRs that have not yet been internalized and retain their initial fluorescent tag (referred to hereafter as "pre-existing" AChRs) (Bruneau et al., 2005). However, the way these AChR pools are maintained and regulated remains to be determined.

The involvement of phosphorylation in the trafficking, insertion and maintenance of ionotropic receptors in central synapses has been extensively studied, and has been found to play an important role in regulating synaptic changes that lead to either long-term potentiation or long-term depression (Carroll et al., 1999; Ehlers, 2000; Hayashi et al., 2000; Lee et al., 2000; Malinow and Malenka, 2002). At the neuromuscular junction,

a large body of work demonstrates that phosphatases are involved in AChR anchoring and clustering in vivo and in vitro (Grady et al., 2003; Huganir et al., 1984; Li et al., 2004; Mei and Si, 1995; Wallace, 1994; Wallace et al., 1991), however the role of phosphorylation/dephosphorylation events in AChR recycling at the neuromuscular junction in vivo has not previously been investigated.

In order to investigate the dynamics of recycled and "pre-existing" AChR pools and the potential role of phosphorylation/dephosphorylation in AChR recycling, we monitored recycled and "pre-existing" AChRs by using a sequential labeling method that we previously used to selectively identify recycled and "pre-existing" receptor pools in the postsynaptic membrane (Bruneau et al., 2005). In this work, we report that recycled receptors are removed more quickly than "pre-existing" receptors from the same postsynaptic membrane of functional synapses, and demonstrate that denervation decreases the insertion of recycled AChRs and increases their removal rate. In addition, we found that tyrosine phosphatase inhibitors, but not serine/threonine phosphatase inhibitors, cause the aberrant peri-synaptic accumulation of recycled AChRs.

Materials and Methods

Live animal imaging. All animal usage followed methods approved by the University of Michigan Committee on the Use and Care of Animals. Adult female mice (20-27 grams, NSA, Harlan Sprague Dawley, Indianapolis, IN) were anesthetized with an intra-peritoneal injection of ketamine and xylazine (KX) (17.38 mg/ml). Sternomastoid muscle exposure and neuromuscular junction imaging was performed as previously described in detail (Akaaboune et al., 1999; Lichtman et al., 1987; van Mier and Lichtman, 1994). Briefly, the anesthetized mouse was placed on its back on the stage of a customized

epifluorescence microscope, and neuromuscular junctions were viewed under a coverslip with water immersion objectives (20X and 60X UAPO 0.7 NA, Olympus BW51, Optical Analysis Corporation, NH) and a digital CCD camera (Retiga EXi, Burnaby, BC, Canada). Mice were intubated and ventilated for the duration of the imaging sessions. For imaging at multiple time points, the mouse was sutured after each session and allowed to fully recover before the next imaging session.

Labeling of distinct AChR pools. The labeling protocol was performed as described by Bruneau et al., 2005. Briefly, the sternomastoid muscle was bathed first with fully substituted BTX-biotin (5 µg/ml, 1 hour, Molecular Probes, Eugene, OR) to label AChRs and then with streptavidin conjugated to Alexa 488 (green) (10 µg/ml, 3 hours, Molecular Probes, Eugene, OR) to saturate all biotin sites. To ensure that all biotin sites were saturated, a distinct color of streptavidin-Alexa (streptavidin-Alexa 594, 10 µg/ml, 10-20 minutes) was added to the sternomastoid muscle, and synapses were imaged. The absence of (red) streptavidin-Alexa 594 staining indicated that all biotin sites were initially saturated with streptavidin-Alexa 488. Three to four days later the mouse was re-anesthetized, and the sternomastoid muscle was re-exposed and bathed with streptavidin-Alexa 594 to label the AChRs that had recycled back to the muscle surface as AChR-BTX-biotin complexes. The muscle was washed out continuously for 15 minutes with Ringer's solution. A brief chase of unlabeled streptavidin (10 minutes) was added to the sternomastoid muscle to prevent the unlikely binding to recycled AChRs of any residual fluorescent streptavidin that remained in the milieu after the extensive washing. This labeling procedure would prevent any erroneous estimation of receptor removal. The doubly-labeled superficial synapses were then imaged (IPLAB software, Scanalytics,

VA). At subsequent time points, the same synapses were relocated and imaged. In this way, we were able to distinguish the "pre-existing" (BTX-biotin labeled receptors retaining their initial streptavidin) and recycled receptor pools. It is worth noting that at the time of recycled AChRs labeling, a significant number of receptors in the NMJ are new, functional receptors, which are sufficient to allow normal synaptic transmission (Bruneau et al., 2005; Lingle and Steinbach, 1988). All controls for the specificity of biotin-streptavidin dissociation were worked out previously by Bruneau et al., 2005

To determine the loss rate of newly synthesized receptors, the sternomastoid muscle was incubated with unlabeled-BTX (5 µg/ml, 1.5 hours) to saturate all surface receptors (a second dose of fluorescent-BTX was used to verify that all AChRs were saturated). Four to five days after initial labeling, newly inserted receptors were labeled with BTX-biotin at a sub-saturating dose (5 µg/ml for 20 minutes) so that synaptic transmission remained functional, followed by a saturating dose of streptavidin-Alexa 488 (green). Superficial synapses were imaged and fluorescence loss was monitored over days.

Surgical procedures. Sternomastoid muscles were denervated by excising a 5 mm piece of the sternomastoid nerve to prevent re-innervation. To determine the effect of denervation on the number of receptors recycled at the postsynaptic membrane, mice denervated 6-8 days earlier were anesthetized and the sternomastoid muscle was exposed and labeled with biotin-bungarotoxin followed with a single saturating dose of streptavidin-Alexa 594 and superficial synapses were imaged as described above. Three days later, the animal was re-anaesthetized and the same synapses were imaged and the loss of fluorescence was measured. The sternomastoid muscle was bathed again with

fresh streptavidin-Alexa 594 (to label recycled AChRs) and synapses were imaged and the fluorescence intensity was assayed. For comparison, a similar labeling protocol was used for innervated synapses.

To determine the removal rate of recycled and "pre-existing" AChRs in denervated muscle, the sternomastoid muscle of mice denervated 6-8 days earlier was labeled with biotin-bungarotoxin followed with a single saturating dose of streptavidin-Alexa 488. Three days later the sternomastoid was exposed and synapses were labeled with a single saturating dose of streptavidin-Alexa 594 (to label all receptors that had recycled over that time) and then superficial synapses were imaged and their fluorescence intensities were measured, and the decrease in fluorescence of both AChR pools was monitored over time.

To determine the effect of muscle action potentials on AChR turnover, immediately after recycled receptor labeling in denervated NMJs, the muscle was directly stimulated with a Grass SD5 stimulator connected to two platinum wires at either side of the muscle. The stimulus pulses (3 ms bipolar pulses of 6-9 V at 10 Hz for 1 second duration every 2 seconds) elicited maximal twitching and therefore action potentials in all muscle fibers. Mice were continuously ventilated and maintained under anesthesia by intraperitoneal injections of KX every 2 hours for the duration of the experiment. To minimize evaporation a coverslip was placed over the exposed muscle.

Quantitative fluorescence imaging. The fluorescence intensity of labeled receptors at neuromuscular junctions was assayed using a quantitative fluorescence imaging technique, as described by Turney and colleagues (Turney et al., 1996), with minor modifications. This technique incorporates compensation for image variation that may be

caused by spatial and temporal changes in the light source and camera between imaging sessions by calibrating the images with a non-fading reference standard. A key feature of the quantitative imaging approach used in the current study is that it involves repetitive imaging of the same fluorescent ligands (streptavidin-Alexa 594 and streptavidin-Alexa 488). Thus, as long as we verified that labeling had reached saturation and that the image pixel intensity was not saturated, it was relatively trivial to get an accurate quantitative measurement of the relative number of AChRs.

Pharmacology. The agents tested were prepared as a stock solution and 500 µl of the stock was placed directly onto the sternomastoid muscle for 9 hours. During the experiment, the animal was intubated with a ventilator to avoid asphyxiation. To inhibit tyrosine phosphatase activity, we used 2 agents: phenylarsine oxide (2 mM, Sigma, St. Louis) and pervanadate (5-10 mM). Pervanadate solution was prepared by mixing 1.7% H_2O_2 and sodium orthovanadate (Sigma, St. Louis) at 1:50 for 10 minutes before adding it to the sternomastoid muscle (Madhavan et al., 2005). To inhibit serine/threonine phosphatases, we used okadaic acid (10 µM - 100 µM, Sigma, St. Louis). To verify the effectiveness of okadaic acid in vivo, at the end of the imaging session, the sternomastoid muscle that had been bathed with okadaic acid was removed from the mouse and homogenized in RIPA buffer. The supernatant was then exposed to a direct fluorescence-based assay for detecting serine/threonine phosphatase activity (RediPlate[TM] 96 EnzChek serine/threonine phosphatases Assay Kit (Molecular Probes, Eugene, OR)). The serine/threonine phosphatase assay was done according to the protocol provided with the kit. Briefly, appropriate buffers for the serine/threonine phosphatases PP1 and PP2A were added to a 96-well microplate preloaded with inhibitors of phosphatases other than

106

serine/threonine phosphatases and the fluorogenic substrate DiFMUP (6,8-difluoro-4-methyl-umbelliferyl phosphate), which generates DiFMU. The serine/threonine phosphate substrate (DiFMUP) was then fully solubilized and homogenates from treated and untreated muscle were added to the wells. The fluorescence emitted by DiFMU was then measured using a fluorescence microplate reader using excitation at 355 ± 20 nm and emission 460 ± 12.5 nm.

Confocal Microscopy. The sternomastoid muscle was saturated with biotin-bungarotoxin followed by a single saturating dose of streptavidin-Alexa 488 (10 μg/ml, 3 hours). Three to four days later the animal was re-anaesthetized and streptavidin-Alexa 594 was added to the sternomastoid muscle to label recycled AChRs. Two to three days later the animal was perfused transcardially with 2% PFA and the sternomastoid muscle was removed and longitudinally sectioned. Twenty μm muscle sections were blocked with 10% BSA and 0.5 % Triton X-100 and then bathed with monoclonal anti-receptor antibody (mAb 35) followed by an anti-rat secondary antibody conjugated to Alexa 647. Muscle sections were scanned with a confocal microscope (Olympus fluoview) and imaged. The z-stacks were then collapsed and contrast was adjusted with Photoshop to maximally resolve intracellular fluorescent spots.

Results

Recycled and "pre-existing" AChR removal at the neuromuscular junction of living mice

Recent work from our lab has shown that a significant number of receptors recycle back to synapses after internalization (Bruneau et al., 2005); here we wanted to know whether recycled receptors are as stable in the synapse as "pre-existing" receptors

(receptors retaining their streptavidin-Alexa 488 after initial labeling). To this end, the sternomastoid muscle of living mice was labeled with bungarotoxin-biotin (BTX-biotin), followed by a single saturating dose of streptavidin-Alexa 488 (strept-488) to saturate all biotin sites. To ensure that all biotin sites were labeled, the muscle was exposed to a second color of fluorescent streptavidin (strept-594). Images of superficial synapses showed no staining with strept-594, indicating that all biotin sites were saturated with strept-488. The animal was then allowed to recover. Three to four days after the initial labeling, strept-594 was added to label recycled receptors that had lost their strept-488 but retained BTX-biotin and images were taken immediately (day 0). The dissociation of streptavidin from AChR-BTX-biotin does not occur spontaneously on the muscle surface but rather only after the complex (AChR-BTX-biotin/strept-488) is internalized (Bruneau et al., 2005). Both "pre-existing" AChRs that retained BTX-biotin/strept-488 after the initial labeling and recycled AChRs labeled with BTX-biotin/strept-594 could then be imaged separately and the changes in their fluorescence intensities monitored over time. As shown in Figure 4.1A, recycled and "pre-existing" AChRs were intermingled in the same postsynaptic membrane. One to three days after labeling recycled AChRs with strept-594, both recycled and "pre-existing" AChRs were re-imaged once or multiple times and then their fluorescence intensities were assayed. We found that after 1 day the fluorescence intensity of recycled receptors (receptors tagged with BTX-biotin/strept-594) decreased to 59% (±5 s.d., n=25) of their original fluorescence, corresponding to a $t_{1/2}$ of ~ 1.3 days. At 2 and 3 days, the remaining fluorescence intensities were 36% (±6 s.d., n=20) and 16% (±2 s.d., n=15) of original fluorescence, respectively. At the same synapses over the same times, however, the fluorescence intensity of AChRs labeled with

BTX-biotin/strept-488 decreased to only 84% (±6 s.d., n=20) of original fluorescence after 1 day ($t_{1/2} \sim 4$ days), and after 2 and 3 days fluorescence decreased to 68% (±9 s.d., n=10) and 54% (±4 s.d., n=15), respectively (Figure 4.1 B,C). Similar results were obtained if strept-594 was used initially to label "pre-existing" receptors and strept-488 was used to label recycled AChRs.
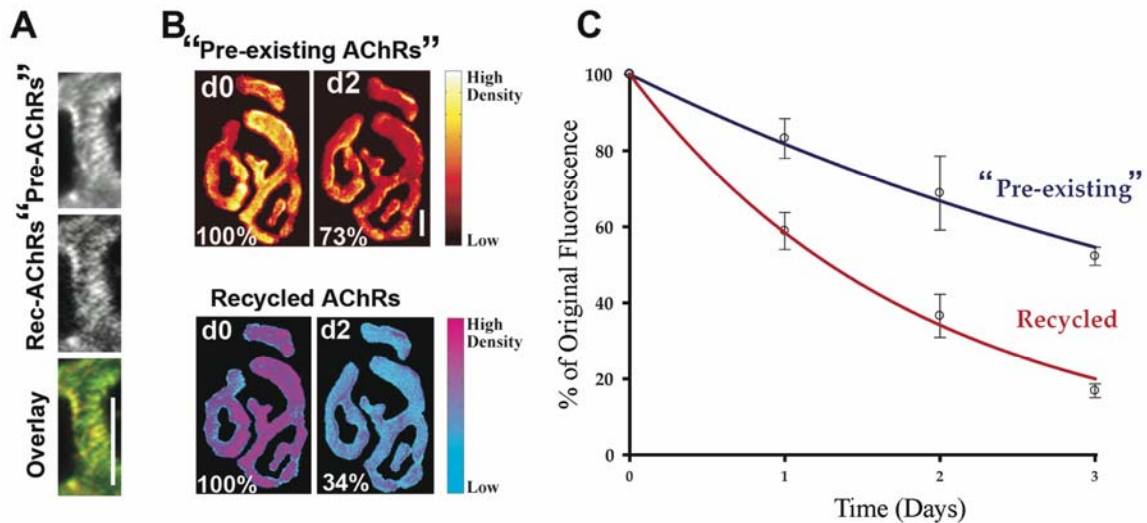
Figure 4.1. Recycled and "pre-existing" AChRs are removed at different rates from the same synapse. The sternomastoid muscle was labeled with BTX-biotin/strept-488 and 3-4 days later was incubated with strept-594 to selectively label recycled AChRs. (**A**) High resolution image of a neuromuscular junction branch shows that recycled and "pre-existing" (receptors retaining their strept-Alexa 488 after initial labeling) AChRs are intermingled in the postsynaptic membrane. Scale bar, 20μm. (**B**) Example of mouse neuromuscular junction where "pre-existing" and recycled AChRs were labeled with distinct fluorophores and both fluorescence intensities were measured immediately after strept-594 labeling of recycled AChRs (day 0) and 2 days later. The total fluorescence intensity of each AChR pool is normalized to 100% at initial imaging. Pseudo-color images provide a linear representation of the density of AChRs. Scale bar, 20μm. (**C**) Graph summarizes the results obtained from all junctions with the approach shown in (B). Each data point represents the mean percentage of fluorescence intensity (±s.d.). Note that recycled receptors are removed significantly faster than "pre-existing" receptors.

To examine the removal rate of newly inserted receptors, the sternomastoid muscle was saturated with BTX and the animal was allowed to recover. Four to five days later the sternomastoid was then bathed with a low dose of BTX-biotin/strept-488 to label newly synthesized receptors. The superficial synapses were imaged and re-imaged 1 and

2 days later. We found that the fluorescence from newly synthesized receptors decreased to 79% (±5 s.d., n=14) of original fluorescence after 1 day, and to 69% (±10 s.d., n=7) of original fluorescence after 2 days. These data indicate that the removal rate of newly synthesized receptors is significantly slower than recycled receptors ($p<0.0001$).

Given the rapid loss of recycled receptors from the postsynaptic membrane, we next examined whether this loss is matched by the insertion of new recycled receptors over the same time period. To do this, the sternomastoid muscle of 3 mice was labeled with BTX-biotin followed by a saturating dose of strept-488, and 3 to 4 days later the animal was anaesthetized and the sternomastoid muscle was bathed with a saturating dose of strept-594 to specifically label the recycled receptors, as described above. The superficial synapses were then imaged, and the animal was allowed to recover. Two days later, the same synapses were re-imaged and the fluorescence of each synapse was measured at each data point. The sternomastoid muscle was then bathed with a saturating dose of fresh strept-594 to label receptors that had been recycled over the given time period. When we measured the fluorescence intensity at 2 days, we found the fluorescence remaining from the recycled pool (labeled with strept-594) was 35% (±6 s.d., n=17) of the original fluorescence. When re-labeled with new strept-594, the fluorescence intensity returned to 99% (±17 s.d., n=10) of the initial recycled AChR fluorescence (Figure 4.2 A,B). This result indicates that the insertion of new recycled receptors matches the loss of recycled receptors from the postsynaptic membrane.
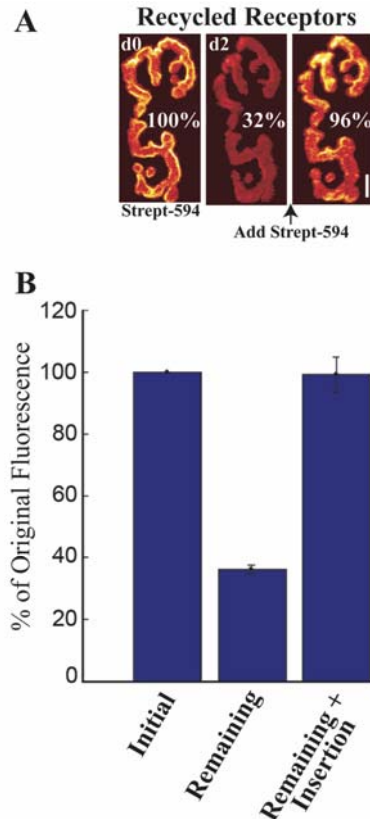
Figure 4.2. Insertion of newly recycled AChRs matches the removal of recycled receptors. The sternomastoid muscle was labeled with BTX-biotin followed by a saturating dose of strept-488, and 3 to 4 days later the animal was anaesthetized and the sternomastoid muscle was bathed with a saturating dose of strept-594 to specifically label the recycled receptors and superficial synapses were immediately imaged (d0). The same synapses were imaged again 2 days later and the loss of recycled receptors was determined. The sternomastoid muscle was bathed with fresh strept-594 and synapses were relocated and imaged to determine the insertion of newly recycled AChRs. Scale bar, 20μm. (**A**) Example of a mouse neuromuscular junction that was imaged three times over 2 days to determine the loss and insertion of recycled AChRs. (**B**) Graph summarizes the results of recycled AChR loss and insertion after 2 days obtained from junctions with the approach shown in (A) (±s.d.). Note that nearly all AChRs from the recycled pool that were lost over 2 days were replaced by newly recycled receptors that had re-inserted into the NMJ over this time.

Targeting of recycled AChRs to stable fluorescent intracellular vesicles after internalization

Previously we have shown that receptors that are removed from synapses are internalized in intracellular endocytic vesicles (Akaaboune et al., 1999; Bruneau et al., 2005). Since recycled and "pre-existing" receptors intermingle at the same postsynaptic

membrane but turn over at such different rates (Figure 4.1), we wanted to know whether recycled and "pre-existing" receptors, after their removal from the postsynaptic membrane, are internalized in the same or distinct intracellular vesicles. To examine this, the sternomastoid muscle was labeled with BTX-biotin/strept-488 (green), and 3-4 days later the recycled receptors were labeled with strept-594 (red), as described in Methods. When recycled and "pre-existing" AChRs were re-imaged 2 or more days later, we were surprised to find that 100% of the vesicles that contained red fluorescence from recycled receptors also contained green fluorescence from "pre-existing" receptors (n= 50 synapses) (Figure 4.3 A). This result prompted us to monitor the formation and accumulation of both green and red intracellular puncta using time-lapse imaging. To do this, the sternomastoid muscle was labeled with BTX-biotin/strept-488, and 3-4 days later the receptors that had recycled over this time were labeled with strept-594, as described above. When superficial synapses were imaged immediately after strept-594 (red) labeling, the AChRs labeled with green strept-488 were concentrated in the postsynaptic membrane and also in internal compartments represented by small spots of fluorescence in the vicinity of the junction (Figure 4.3 B, top panels). When the same synapse was imaged 8 hours later, we found that some of the green spots remained while others had disappeared. At this time point faint red fluorescent spots began to be detected, but appeared only at the stable spots of green fluorescence (Figure 4.3 B, middle panels). At 28 hours, while many of the green fluorescent spots had disappeared, stable spots that contained both strept-488 and strept-594 remained (Figure 4.3 B, bottom panels). These results indicate either that the removed recycled receptors were directly and specifically targeted to stable vesicles already containing internalized AChR-BTX-biotin/strept-488

112

complexes, or that the fluorescent puncta observed in the intracellular vesicles were from streptavidin-Alexa tags that had been removed from both receptor pools after internalization (see discussion).
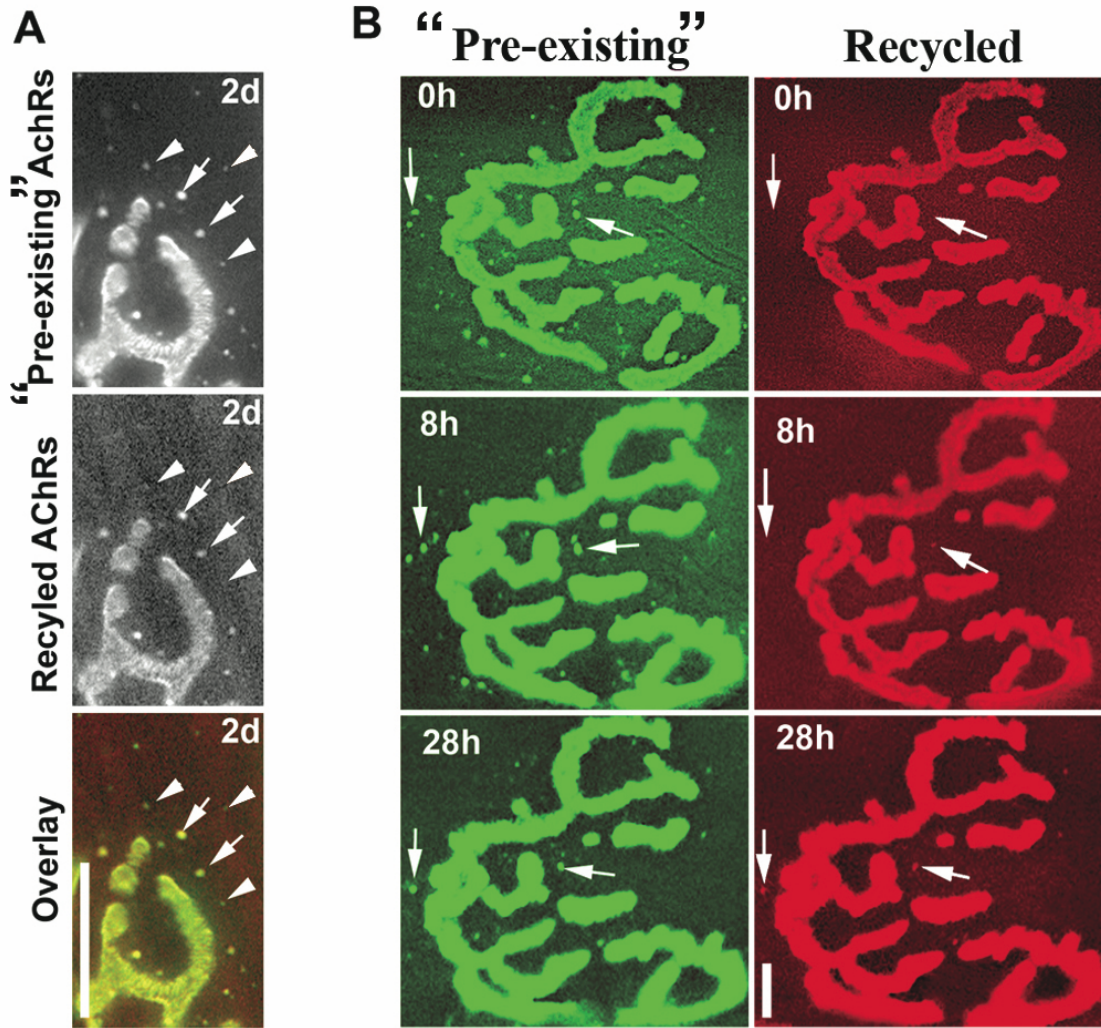
Figure 4.3. Fluorescent tags from recycled receptors are endocytosed and targeted to vesicles containing strept-488 from "pre-existing" AChRs. Sternomastoid muscle was labeled with BTX-biotin/strept-488, and recycled receptors were labeled 3 days later with strept-594. (**A**) Example of recycled and "pre-existing" AChRs imaged 2 days after recycled receptor labeling. Note that 100% of the vesicles containing red fluorescence from recycled AChRs also have green signals from "pre-existing" AChRs (arrows), while some of the green fluorescent spots lack red signal (arrowheads). Scale bar, 20μm. (**B**) Time-lapse imaging of a mouse neuromuscular junction labeled as in (A) and then imaged multiple times over the next 28 hours. Note that a number of the vesicles containing strept-488 from the "pre-existing" AChRs at time 0 are stable over the next 28 hours (arrows), while others are transient. The strept-594 labels from recycled receptors are selectively targeted to the stable vesicles containing fluorescent label from "pre-existing" receptors. Scale bar, 20μm.

If the red and green fluorescence observed in stable vesicles are from streptavidin-Alexa tags that have been removed from their receptor complexes and then sequestered, then we would expect that at least a subset of these vesicles may lack AChRs. To investigate this possibility, the sternomastoid muscle was labeled with BTX-biotin/strept-488 (green) and three days later was incubated with strept-594 (red) to label recycled receptors. Two days later, the animal was perfused with paraformaldehyde and the muscle was dissected, sectioned and immuno-stained with the anti-AChR antibody mAb 35 (pseudo-color, blue). Interestingly, some green/red fluorescent vesicles were devoid of receptors, suggesting that the streptavidin-Alexa tags had indeed been removed and sequestered, possibly in degradative vesicles. Other vesicles contained fluorescent streptavidin tags and receptors, potentially indicating complexes that were in the process of recycling or degradation. A third subset of puncta contained receptors only without any fluorescent streptavidin tags, indicating receptors in the process of insertion, or receptors in the later stages of recycling that already had their strept-Alexa tags removed (Figure 4.4).
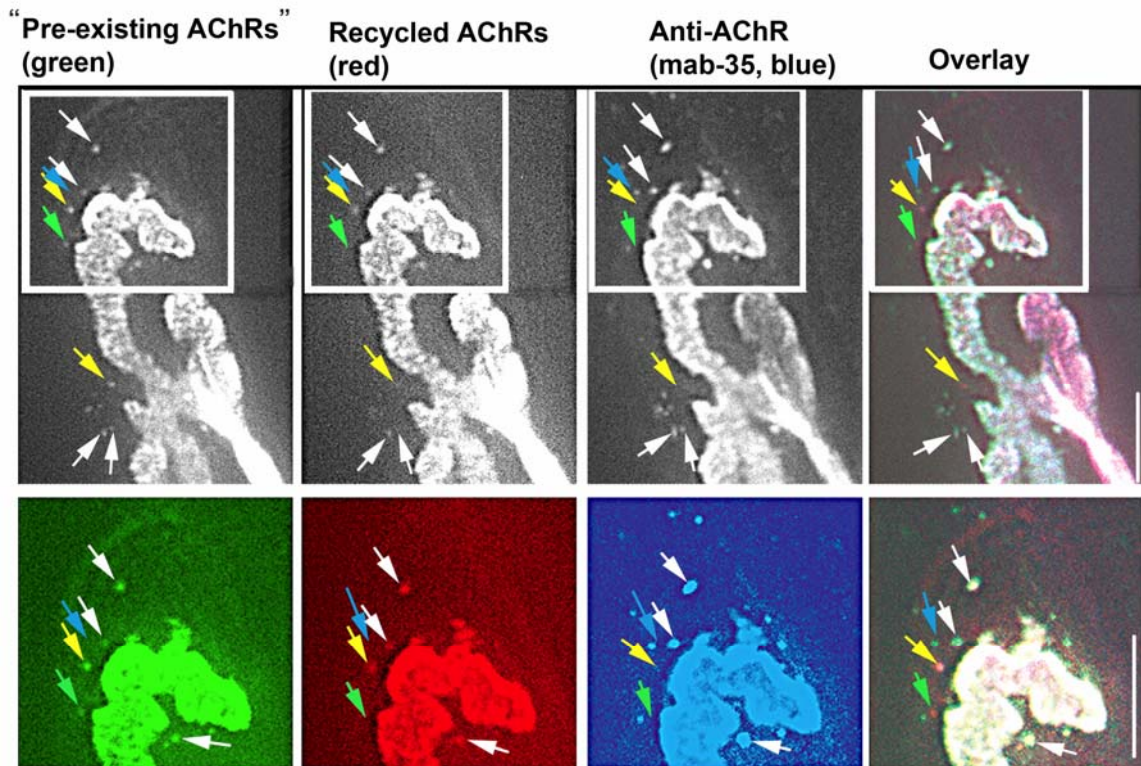
Figure 4.4. Confocal images of a triply-labeled neuromuscular junction. The sternomastoid muscle of a live animal was labeled with BTX-biotin/strept-488 (green) and bathed 3 days later with strept-594 (red) to label recycled receptors. Two days after recycled receptor labeling the animal was perfused with 2% PFA, the sternomastoid muscle was sectioned and immunostained with anti-AChR. Green arrows indicate accumulation of only green fluorescent streptavidin that has been removed from "pre-existing" AChRs after internalization, which may correspond to degradative vesicles. Yellow arrows indicate accumulation of green and red streptavidin tags removed from pre-existing and recycled receptors after internalization, which likely also correspond to degradative vesicles. Blue arrows indicate vesicles containing AChRs, but lacking any streptavidin Alexa tags. These vesicles may correspond to internalized AChRs in later stages of recycling and/or degradation, or newly synthesized receptors in the process of insertion. White arrows indicate vesicles containing receptors and their streptavidin tags after internalization. The colors in the overlay of the three fluorescent labels were altered and adjusted in Photoshop to maximize contrast. Inset from top panels shown in panels below. Scale bar, 20μm.

These results, combined with the observation from time-lapse imaging (Figure 4.3) suggests that stable vesicles may contain fluorescent products (indicated by yellow arrows) and the more dynamic vesicles may correspond to cycling AChRs (indicated by white arrows).

Effect of denervation and muscle stimulation on recycled AChR dynamics

Given the rapid removal rate of recycled AChRs, we next asked whether this loss rate could further be affected by muscle denervation. We first asked whether denervation has any effect on the insertion of recycled AChRs into the postsynaptic membrane. To this end, innervated NMJs and junctions denervated 6-8 days earlier were labeled with a single saturating dose of BTX-biotin and then all biotin sites were saturated with strept-594 (red). The superficial synapses were imaged and 3 days later the animal was re-anesthetized, the sternomastoid muscle was exposed, and the same synapses were relocated and re-imaged to measure the loss of their original fluorescence. To quantify the number of recycled AChRs that had been inserted after initial labeling, new strept-594 (red) was added to the sternomastoid muscle and the same synapses were re-imaged. Interestingly, we found that only 8% (±3.8 s.d., n=20) of the original fluorescence had recovered at denervated synapses after 3 days (Figure 4.5 A,B), which is significantly less than the insertion rate of recycled receptors in innervated junctions (25% of original fluorescence ±7.1 s.d., n=20) (Figure 4.5 C,D).
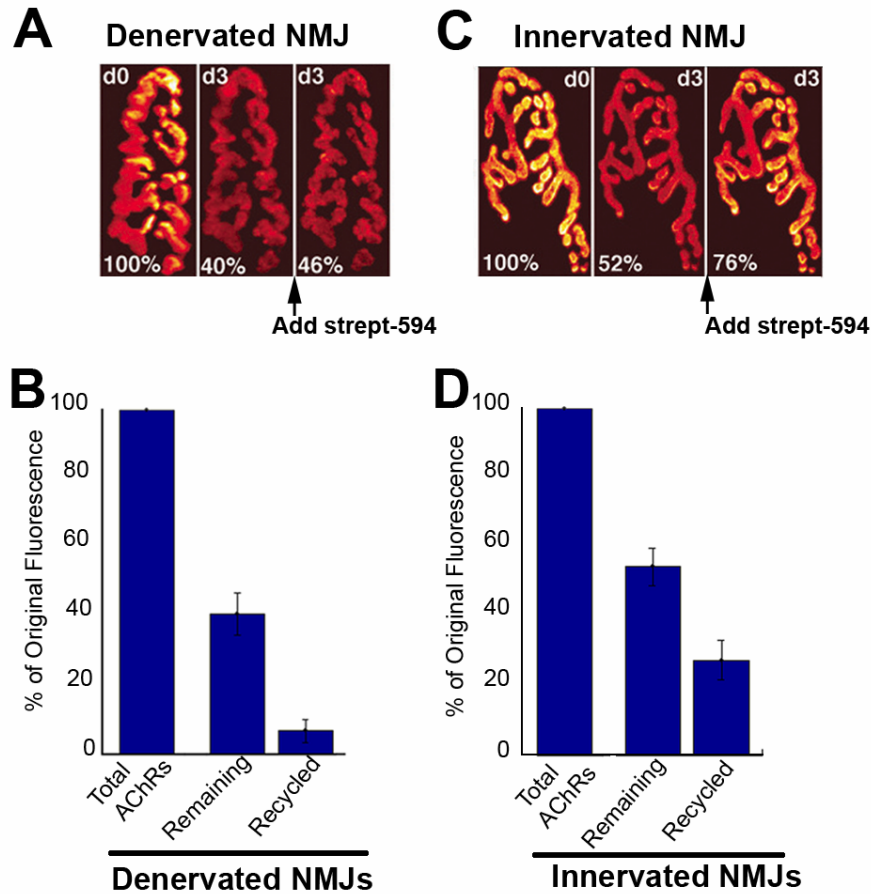
Figure 4.5. Muscle denervation affects the contribution of recycled AChRs. (**A**) Example of a denervated neuromuscular junction that was labeled with BTX-biotin/strept-594 and imaged immediately. Three days later the same synapse was imaged again (to measure the loss of fluorescence) and incubated with strept-594 to selectively label recycled AChRs. Note that 60% of original fluorescence was lost after 3 days, while very little fluorescence was gained after strept-594 was added (6% of original fluorescence), indicating that recycling of AChR is significantly decreased in denervated muscle. All three panels are displayed on the same intensity scale. (**B**) Graph summarizes results obtained from many junctions with the approach shown in (A). Each data point represents the mean percentage of fluorescence intensity (±s.d.). (**C**) Example of an innervated mouse synapse measured over 3 days, showing that a significant number of recycled AChRs return back to the postsynaptic membrane. (**D**) Graph summarizes measurements obtained from many synapses.

Next, we asked whether recycled and "pre-existing" AChRs have similar removal rates in denervated muscle. To test this idea directly, junctions denervated 6-8 days earlier were labeled with BTX-biotin/strept-488. The animals were allowed to recover and three days later the recycled AChRs were labeled with strept-594, and superficial synapses were imaged immediately and re-imaged 1 and 2 days later. We found that after

117

only 1 day the strept-594 fluorescence intensity (labeled recycled AChRs) decreased dramatically to 35% ($\pm$ 5 s.d., n=17) of original fluorescence (corresponding to a $t_{1/2}$ ~15 hours, nearly 2 times faster than the $t_{1/2}$ of recycled AChRs at innervated synapses). Loss of fluorescence continued, decreasing to 16% ($\pm$3 s.d., n=9) after 2 days. At the same time the strept-488 fluorescence from "pre-existing" receptors decreased to 70% ($\pm$6 s.d., n=10) after 1 day ($t_{1/2}$ ~ 1.9 days, also nearly 2 times faster than the $t_{1/2}$ at innervated synapses) and 43% ($\pm$6 s.d., n=9) of their original fluorescence after 2 days (Figure 4.6 A,B). These results indicate that denervation increases the already rapid removal of recycled receptors from the postsynaptic membrane, and has a similar effect on both recycled and "pre-existing" AChRs, nearly doubling the rate of removal of each receptor pool.
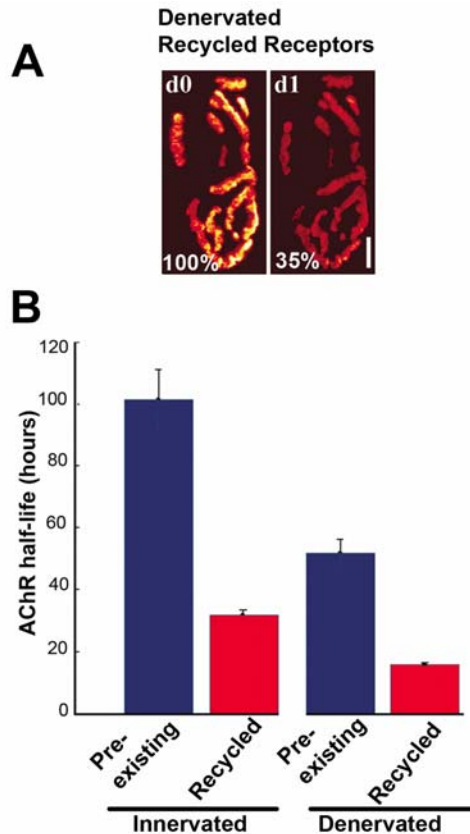
Figure 4.6. Denervation increases the removal rates of recycled and "pre-existing" AChRs at the neuromuscular junction. AChRs at denervated neuromuscular junctions were labeled with BTX-biotin/strept-488, and recycled AChRs were labeled 3 days later with strept-594. Fluorescence signals from both receptor pools were then imaged, and imaged again 1 day later. (**A**) Example of a denervated neuromuscular junction in which recycled AChRs were monitored over 1 day. (**B**) Graph shows the lifetime of recycled and "pre-existing" AChRs from the same synapses as assessed by the change in fluorescence intensities over a 1 day period. Note that in innervated synapses recycled AChRs had an average t1/2 of 28 hours, whereas "pre-existing" AChRs had an average $t_{1/2}$ of ~102 hours. In denervated synapses, recycled AChR half-life dropped to ~15 hours and "pre-existing" AChR half-life decreased by the same proportion to ~48 hours.

Since the above experiments indicate that muscle activity is important for receptor stability, we next tested whether direct muscle stimulation could prevent the rapid removal of recycled AChRs from the postsynaptic membrane. Denervated sternomastoid muscle was saturated (6-8 days after denervation) with BTX-biotin/strept-488, and 3 days later was saturated with strept-594 to specifically label recycled AChRs. Superficial synapses were imaged and muscle action potentials were then elicited via stimulating

electrodes placed at either end of the muscle (3 ms bipolar pulses of 6 to 9 V at 10 Hz for 1 s duration every 2 s for the entire 8 hour period). For the duration of the experiment, the mouse was intubated and ventilated to prevent asphyxia. The result was dramatic: the loss of recycled AChRs observed in denervated muscles over the 8 hours (66% of original fluorescence remaining ±5 s.d., n=8) was almost completely prevented after stimulation of denervated muscles (94% of original fluorescence remaining ±6 s.d., n=16) (Figure 4.7 C-E). This result indicates that muscle action-potentials are sufficient to prevent the loss of recycled receptors.
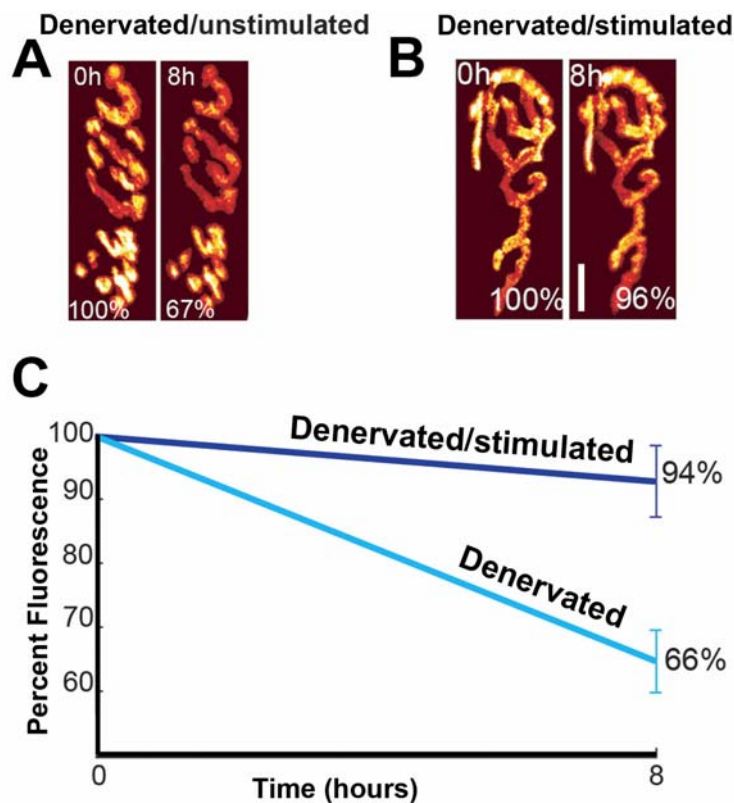
Figure 4.7. Muscle stimulation prevents loss of recycled AChRs from denervated NMJs. (A) Three days after initial labeling with BTX-biotin/strept-488, recycled AChRs on denervated muscle were labeled with strept-594 and immediately imaged and imaged again 8 hours later and the loss of fluorescence was measured. **(B)** Example of a NMJ illustrating that stimulation of denervated muscle prevents the loss of recycled receptors from the synapse. Scale bar, 20μm. **(C)** Graph summarizes results obtained from many synapses. Note that after 8 hours ~66% of fluorescence from recycled receptors remained in denervated synapses; however when denervated muscle was chronically stimulated, this loss of fluorescence was nearly abolished.

Proper localization of recycled receptors requires tyrosine phosphatase activity

Because phosphorylation and dephosphorylation events are associated with postsynaptic receptor cycling in central synapses (Ehlers, 2000; Esteban et al., 2003; Malinow and Malenka, 2002), we next tested whether AChR recycling also depends upon phosphorylation/dephosphorylation events. To do this, the sternomastoid muscle was labeled with BTX-biotin/strept-488 (green), and then the muscle was bathed continuously with a phosphatase inhibitor. The mice were anesthetized and ventilated to prevent asphyxia. After 9 hours of incubation with the drug, strept-594 (red) was added to the sternomastoid muscle to label receptors that had been recycled back to the membrane after initial labeling. We found a striking alteration in receptor localization at synapses when the muscle was treated with phenylarsine oxide (PAO), a known inhibitor of tyrosine phosphatases (Fletcher et al., 1993; Moult et al., 2006; Moult et al., 2002). In contrast to untreated control muscles where the recycled surface receptors are restricted to the junctional area as the original receptors, PAO treatment resulted in red labeling in the peri-synaptic region as well as the junctional region (Figure 4.8 B,C). The presence of red signal in the peri-synaptic region is specific to recycled receptors labeled with strept-594 (red) because at 9 hours no "pre-existing" receptors (green) were detected outside of the original synapse (Figure 4.8 A). In another set of experiments we used another common tyrosine phosphatase inhibitor, pervanadate (Madhavan et al., 2005; Moult et al., 2006). This treatment caused the same peri-synaptic staining of recycled AChRs (Figure 4.8 E,F) without affecting the synaptic localization of "pre-existing" AChRs (Figure 4.8 D). These results indicate that tyrosine phosphatase activity is involved in proper localization of recycled receptors.

121

To investigate the potential role of serine/threonine phosphatases on receptor recycling, the sternomastoid muscle of 4 mice was labeled (as described above) and then bathed with different concentrations of okadaic acid (10 µM – 100µM), a specific inhibitor of serine/threonine phosphatases 1 and 2A (Pahan et al., 1998). Nine hours later, when the muscle was labeled with strept-594, specific staining was observed only in the junctional zone, indicating that the targeting of recycled receptors does not require serine/threonine phosphatases (Figure 4.8 G-I). The effectiveness of this drug in vivo was tested at the end imaging session by removing and homogenizing the sternomastoid muscle and testing the activity of PP1 and P2A phosphatases using a serine/threonine phosphatase assay kit. When the muscle was incubated in 10µM of okadaic acid, most of the serine/threonine phosphatase activity (>70%) was inhibited compared to untreated muscle. When 100 µM was used all serine/threonine phosphatases activity was inhibited and the muscle also presented some signs of swelling.

Discussion

In this study we report that at fully functional synapses, recycled AChRs turn over more rapidly than "pre-existing" or newly synthesized AChRs that are co-localized in the same postsynaptic membrane. The absence of muscle activity significantly decreases the number of recycled AChRs and increases the already rapid removal rate of recycled AChRs, while direct muscle stimulation completely prevents receptor loss. In addition, this work provides evidence for the possible involvement of tyrosine dephosphorylation in the insertion or maintenance of recycled AChRs at synaptic sites.
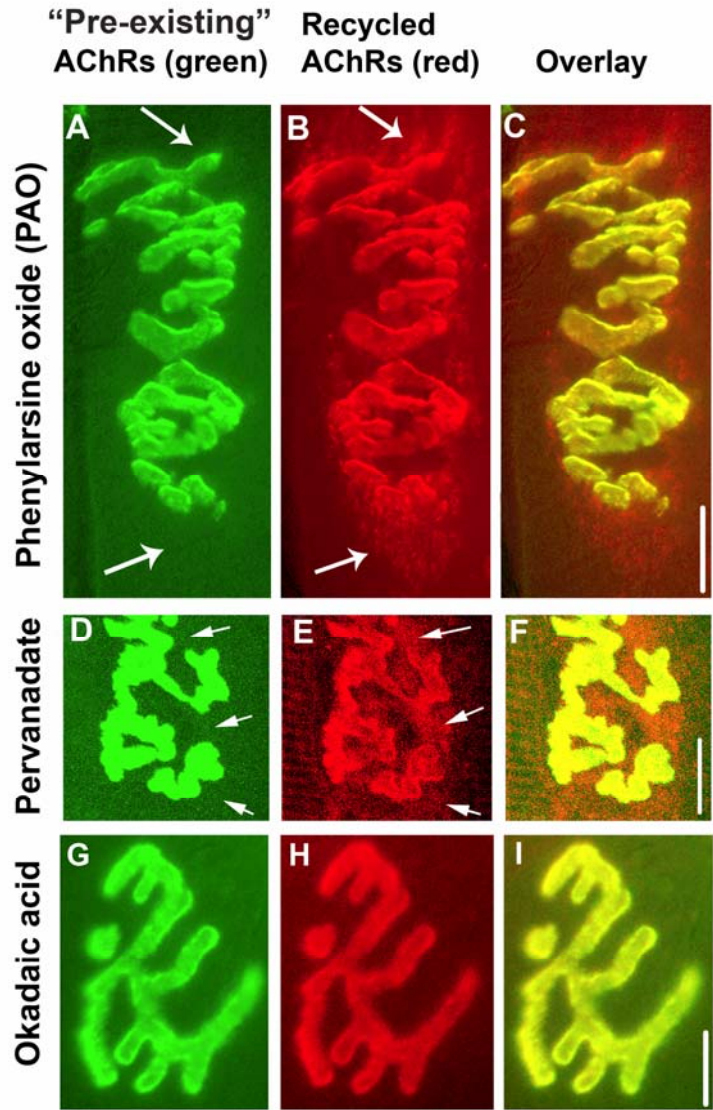
Figure 4.8. Tyrosine phosphatase inhibition causes the accumulation of recycled receptors in the peri-synaptic membrane. (**A**) Example of a living adult mouse neuromuscular junction previously saturated with BTX-biotin/strept-488 (green) at time 0 and viewed at high detector gain. The muscle was continuously bathed in tyrosine phosphatase inhibitor (PAO), and imaged 9 hours later. (**B**) The junction was then incubated with strept-594 (red) to determine if PAO affects AChR recycling. Peri-synaptic areas were labeled with red strept-594 (arrows), indicating that some of the recycled receptors were miss-targeted when tyrosine phosphatases were inhibited pharmacologically. (**C**) Overlay of "pre-existing" and recycled receptors. Similar results were obtained when an alternate tyrosine phosphatase inhibitor, pervanadate, was instead applied to the sternomastoid muscle (D-F). Note that while recycled receptors (red) appear in the peri-synaptic area after tyrosine phosphatase inhibition, "pre-existing" receptors (green) remain restricted to the synapse. (**G-I**) Example of an adult mouse neuromuscular junction labeled using the same labeling procedure as above and bathed for the duration of the experiment with okadaic acid, a serine/threonine phosphatase inhibitor. Recycled receptors were identified by adding strept-594 (red) after 9 hours. Note that recycled receptors were properly targeted to the synapse. (**I**) Overlay of "pre-existing" and recycled receptors. Images were adjusted for brightness and contrast using Adobe Photoshop.

One interesting finding of this work is that the lifetime of recycled receptors is far shorter than that of initially labeled and "pre-existing" AChRs, even though all these AChRs are intermingled in the same postsynaptic membrane. It is unlikely that the difference in receptors lifetime obtained in our studies is due to BTX binding itself, since we are comparing the removal rates of receptors that are both tagged with BTX. However, it must be acknowledged that the use of BTX, which specifically and irreversibly binds to AChRs, also blocks AChRs function. Although there is no direct evidence about whether bungarotoxin binding itself changes the behavior of AChRs, a number of previous studies suggest that labeled receptors behave normally as long as the neuromuscular junction activity is not totally blocked (Akaaboune et al., 1999; Lingle et al., 1988). While it has been shown previously that gamma and epsilon subunits of AChRs are able to turn over at different rates, it is also unlikely that differences in loss rates are due to differences in the subunit composition of receptors (gamma vs. epsilon) because innervated adult synapses only express the epsilon subunit (Burden, 1977; Missias et al., 1996; Yumoto et al., 2005). This implies that an unknown mechanism exists which specifically alters recycled AChR stability.

It is possible that during the process of receptor intracellular trafficking (in early endosomes or specialized recycling endosomes) alterations or modifications of AChR subunits or receptor-associated proteins may occur. Such alterations might affect the interaction of receptors with postsynaptic scaffolding proteins, which in turn may affect their stability once inserted in the postsynaptic membrane. For example, it has been suggested that phosphorylation events are involved in the stabilization of AChRs (Caroni et al., 1993) and inhibition of these events has been shown to increase receptor removal

124

and prevent receptor clustering, despite ongoing muscle activity (Ferns et al., 1996; Fuhrer et al., 1997; Wallace, 1994; Wallace et al., 1991). At central synapses, it has been shown that a coordination of phosphorylation and dephosphorylation events may regulate synaptic strength (Moult et al., 2006; Raymond et al., 1993; Raymond et al., 1994; Roche et al., 1994); it is possible that similar mechanisms may be involved at the neuromuscular junction. This possibility is supported by our results, which show that inhibition of tyrosine phosphatase activity can cause selective disruption of receptor recycling, resulting in labeling outside of the usually sharp NMJ boundary, while "pre-existing" receptors remain intact within the NMJ. This suggests that phosphorylation of receptors or associated proteins at tyrosine sites during trafficking might cause miss-targeting of recycled receptors or increase their mobility once they have recycled into the postsynaptic membrane. It is also conceivable that tyrosine phosphatase inhibitors could selectively increase the insertion and accumulation of recycled receptors to the peri-junctional region. Interestingly, previous work has made the same observation in synapses of frog nerve/muscle co-cultures treated with tyrosine phosphatase inhibitors, which they attributed to the dissociation and migration of "pre-existing" receptors into the peri-synaptic region (Dai and Peng, 1998). Because we were able to distinguish between "pre-existing" and recycled pools of receptors, our results argue that tyrosine phosphatase inhibition does not cause dissociation of "pre-existing" receptors, but rather specifically interferes with the delivery of internalized receptors back into the NMJ or their maintenance at the postsynaptic membrane.

Muscle activity appears to be critical for the insertion and stability of recycled AChRs in the postsynaptic membrane. Our results indicate that the contribution of

recycled AChRs is significantly depressed in denervated muscle synapses compared to innervated synapses. The inhibition of recycling is not affected within the first week of denervation, however (data not shown). It is possible that during the first week of muscle denervation, the insertion of recycled receptors is maintained by spontaneous release of acetylcholine neurotransmitter by Schwann cells (Brett et al., 1982; Dennis and Miledi, 1974), which might explain why the number of synaptic receptors only begins to decline ~9 days after muscle denervation (Andreose et al., 1995). Consistent with this, we have previously shown that spontaneous release of neurotransmitter is sufficient to prevent the loss of receptors from synapses (Akaaboune et al., 1999). This result suggests that the decrease in receptor number at denervated muscle synapses over time could be attributed to the decrease in delivery of the recycled receptor pool back to the postsynaptic membrane. Interestingly, the absence of muscle activity following denervation not only increases the removal rate of "pre-existing" AChRs but also accelerates the already rapid removal of the receptors that have recycled back into the membrane. This indicates that recycled receptors, despite their rapid loss, can still be controlled by synaptic activity. In agreement with our previous findings, which showed that stimulation of denervated muscle prevents the removal of "pre-existing" AChRs (Bruneau et al., 2005), we found here that muscle stimulation also prevents the removal of recycled receptors. Consistent with these results, muscle stimulation alone has been reported to reversibly increase the metabolic stability of receptors at synapses that are denervated early in development and can prevent the decrease of AChR half-life observed at surgically denervated and blocked endplates (Akaaboune et al., 1999; Brenner and Rudin, 1989; Rotzler and Brenner, 1990). However, the way in which neuromuscular transmission or muscle action potentials

126

regulate AChR behavior is not understood. It is possible that muscle contraction caused by direct stimulation causes an increase of calcium influx either through ligand-gated or L-type channels, or that it causes calcium release directly from intracellular stores. In support of this idea, previous studies have shown that blockade of L-type channels affects AChR stability (Rotzler et al., 1991).

At functional neuromuscular synapses, recycled receptors are continually inserted into the post synaptic membrane. However, it is unclear what proportion of the recycled receptor pool derives from "pre-existing" or previously recycled AChRs and how many times receptors are able to recycle back before being degraded. If receptors recycle only one time, then a fraction of the pre-existing pool must enter the recycling pathway over time to maintain the recycled receptor pool. The observation that red streptavidin from recycled AChRs co-localizes in intracellular vesicles with the previously internalized green fluorescent label from "pre-existing" receptors is intriguing (see Figs 4.3, 4.4). This result suggests two possibilities: first, recycled AChRs could have a tag that directly shuttles them to stable degradation vesicles containing previously internalized "pre-existing" AChRs. In this scheme, it is tempting to speculate that the stable spots of fluorescence are part of the accumulated degradation products, implying that AChRs might recycle only one-time before being targeted for degradation. Alternatively, it is possible that AChRs may recycle more than one time and that the stable fluorescent vesicles may correspond to accumulations of fluorescent tag that recycled and "pre-existing" AChRs lose intracellularly while in the process of recycling. The absence of receptors in some vesicles suggests that these are indeed sites of degradation which may correspond to stable vesicles observed in time-lapse imaging; the more dynamic vesicles

127

are either in the process of recycling or early in the degradation pathway. While this result suggests that receptors may be able to cycle many times, losing their streptavidin tag each time, the question of how many times a receptor can cycle before being degraded is not resolved here and requires the development of new techniques to study.

Acknowledgements

Chapter V

Acetylcholine Receptor Clustering is required for the Accumulation and Maintenance of Post-Synaptic Scaffolding Proteins

Previously published in Current Biology

Emile G. Bruneau, Daniel S. Brenner, John Y. Kuwada, and Mohammed Akaaboune

Introduction

The maintenance of a high density of post-synaptic receptors is essential for proper synaptic function. At the neuromuscular junction, acetylcholine receptor (AChR) aggregation is induced by nerve clustering factors and mediated by scaffolding proteins (Sanes and Lichtman, 2001). While the mechanisms underlying AChR clustering have been extensively studied (Gautam et al., 1999; Lin et al., 2001; Beeson et al., 2006; Okada et al., 2006), the role that the receptors themselves play in the clustering process and how they are organized with scaffolding proteins is not well understood.

Here we report that the exposure of AChRs labeled with Alexa 594 conjugates to relatively low-powered laser light caused an effect similar to chromaphore-assisted light inactivation (CALI) (Jay, 1988; Beermann and Jay, 1994), which resulted in the unexpected dissipation of the illuminated AChRs from clusters on cultured myotubes. This technique enabled us to demonstrate that AChR removal from illuminated regions induced the removal of scaffolding proteins and prevented the accumulation of new AChRs and associated scaffolding proteins. Further, the dissipation of clustered AChRs

129

and scaffold was spatially restricted to the illuminated region and had no effect on neighboring, non-illuminated AChRs. These results provide direct evidence that AChRs are essential for the local maintenance and accumulation of intracellular scaffolding proteins, and suggest that the scaffold is organized into distinct modular units at AChR clusters.

Materials and Methods

GFP fusion construct. The rapsyn-GFP fusion construct was kindly provided by Dr. Jonathan Cohen (Harvard Medical School).

Cell culture. C2C12 myoblasts (ATCC, Manassas, VA) were grown on uncoated or laminin-coated dishes, as described previously (Bruneau et al., 2005b; Bruneau and Akaabourne, 2007). Cells were transfected at 70-100% confluence with 1 μg of rapsyn-GFP using FUGENE6 transfection reagent (Roche, Basel, Switzerland) and differentiated the next day. Cells were imaged 3-4 days after differentiation. Mouse primary myotubes were grown in 20% FBS, differentiated in 10% FBS/10% HS and imaged 1 week later.

Live cell imaging. Primary mouse muscle cells or C2C12 myotubes were incubated for 1.5 h in 5 μg/ml of fluorescent bungarotoxin (bungarotoxin-Alexa 488, 555, tetramethyrhodamine, 594 or 647), or in bungarotoxin conjugated to biotin (1.5 h, 5 μg/ml) followed by streptavidin-Alexa 488 or 594 (1.5 h, 10 μg/ml). Since anti-AChR (mAb35) antibody is too large to label AChRs that are induced to cluster by laminin (clusters form between the laminin and muscle membrane), non-laminin dishes plated with C2C12 myotubes were labeled with anti-AChR (2.5 hours) followed by anti-rat-Alexa 594 secondary antibody (2.5 hours). This effectively labeled clustered AChRs that were not between the muscle membrane and dish surface. After labeling, cells were

washed and then imaged under an upright epifluorescent or scanning confocal microscope. Each laser-illumination experiment was performed at least once in the presence of unlabeled bungarotoxin to ensure that photo-unbinding was controlled for. After initial images were taken, the fluorescence was removed from individual clusters either with an 8 mW Argon laser (488 nm) mounted to the epifluorescent microscope (laser beam was passed through a neutral density filter and focused to a < 5 μm spot, with a beam power of 2 mW at the specimen plane, as measured by a laser power meter (Lasercheck, Edmond Optics, Barrington, NJ)), or a diode-pumped solid state (DPSS) scanning laser (561 nm) on a confocal microscope (imaged at 400 Hz and 1024x1024 resolution, < 2 mW at specimen plane). From 6 - 20 hours after laser illumination, cells were labeled again with either the same fluorescent bungarotoxin, or bungarotoxin conjugated to a distinct fluorescent ligand.

To assay the effect of temporary membrane damage on AChR dissipation from clusters, FM1-43 (25 nM) was added to cultures prior to imaging and images were taken every minute after laser illumination for ~ 10 minutes (Bansal et al., 2003).

For time-lapse imaging of rapsyn-GFP, myotubes were transfected with rapsyn-GFP and then AChRs were labeled with bungarotoxin-Alexa 594 (1.5 h, 5 μg/ml). Individual clusters were then exposed to either the confocal Argon laser bleach the rapsyn-GFP, or to the DPSS to illuminate the Alexa 594. Images were then taken every hour after the addition of new doses of bungarotoxin-Alexa 594. After 6 hours the cells were fixed and labeled with anti-AChR antibody.

Immunofluorescence. Myotubes were fixed at various times after laser exposure with 2% paraformaldehyde and then treated for 20 minutes with 1% triton X-100 and 10%

bovine serum albumin in phosphate buffered solution. Cells were then incubated with mouse anti-rapsyn (mAb 1234, Sigma, St. Louis, MO), mouse anti-β-dystroglycan or mouse anti-utrophin (MANDAG2 clone 7D11 and MANCHO3 clone 8A4, Developmental Studies Hybridoma Bank, Iowa City, IA) primary antibody overnight and goat anti-mouse-Alexa594 or 488 secondary antibodies (Invitrogen Molecular Probes, Eugene, OR), as well as rat anti-receptor primary (mAb 35, Developmental Studies Hybridoma Bank) and anti-rat-Alexa647 secondary (Invitrogen Molecular Probes) antibodies. For experiments in which phalloidin-FITC was used, the phalloidin-FITC (1 µg/ml, 15 minutes) was added after antibody labeling. Cells were then imaged either with a 20x UAPO 0.7 NA objective (Olympus BW51, Optical Analysis Corporation, NH) of an upright fluorescent microscope using a digital CCD camera (Retiga EXi, Burnaby, BC, Canada), or with a 40x immersion objective on a scanning confocal microscope (TCS SP5, Leica Microsystems, Wetzlar, Germany). For quantitative immunofluorescence determination, the background fluorescence from images was approximated by selecting a boundary region around the cluster and subtracting it from the original image; the mean total fluorescence intensity (which corresponds to density) was then measured, as previously described (Turney et al., 1996; Akaaboune et al., 1999). The mean fluorescence from the bleached cluster was compared to the mean fluorescence of at least one of the closest neighboring, unbleached clusters. Image analysis was performed using a procedure written for Matlab (The Mathworks, Natick, MA), and images were processed using Adobe Photoshop.

Results

Characterization of photo-dissipation of AChRs from individual clusters

Evidence for laser-induced AChR dissipation was obtained from the following experiments: AChRs on primary mouse myotubes (Supplementary Fig. S5.1) or on C2C12 myotubes cultured on plastic or laminin-coated plates were saturated with bungarotoxin-Alexa 594 (BTX-594), and entire clusters or small regions of individual clusters were bleached either with an Argon (488 nm) laser mounted to an upright epifluorescent microscope or with a DPSS (561 nm) scanning laser on a confocal microscope. When the cells were imaged 6 hours later (or 20 hours later, see Supplementary Figure S5.2), we were surprised to find that there was neither recovery of fluorescence at bleached clusters from laterally migrating BTX-594 labeled receptors, nor any new receptor labeling above background (after the addition of a distinctly colored fluorescent BTX conjugate), even if not all of the fluorescence was removed (Figure 5.1A, arrowheads) (see also Supplementary Figure S3). At the same time, the accumulation of receptors occurred normally at neighboring unbleached clusters (Figure 5.1A). Further, when only small regions within BTX-594 labeled receptor clusters were illuminated with a focused laser, only background AChR staining was observed at the bleached region after the addition of the same or distinctly colored fluorescent BTX (see arrowheads, Figure 5.1B), while the accumulation of newly synthesized receptors at neighboring, unbleached clusters and unbleached regions within the illuminated cluster were completely unaffected (Figures 5.1A and B). The same effect was observed when AChRs were labeled with bungarotoxin conjugated to biotin (BTX-biotin) and streptavidin-Alexa-594 (strept-594) (Figure 5.1C), while AChRs labeled with anti-AChR

antibody (mAb35) and secondary antibody conjugated to Alexa 594 were not disrupted by laser illumination (Figure 5.1D). This indicates that the distance between Alexa 594 and the AChR may be crucial to Alexa 594-mediated AChR dissociation. Finally, dissipation of BTX-594 labeled receptors also occurred on clusters that had been treated with c-terminal agrin (data not shown), indicating that the dissipation of AChRs can occur even in the presence of a neural clustering factor.

To test whether the removal of AChRs was specific to the Alexa 594 fluorophore, cultured C2C12 myotubes were labeled with BTX-488 or BTX-555 and receptor clusters were imaged and then laser illuminated for long enough to bleach all the fluorescence from individual clusters (~ 3 seconds per cluster). Six hours after original bleaching we found that the recovery of original fluorescence from the lateral migration of surface receptors, and the accumulation of new receptors that were subsequently labeled with a distinct BTX conjugate, were both readily apparent around the circumference of the bleached clusters, as previously reported (Bruneau et al., 2005b) (Figures 5.1E and F) (it should be noted that continued exposure of BTX-488 or BTX-555 labeled clusters to high-intensity laser light for >60 seconds sometimes resulted in partial disruption of the cluster). Similarly, receptor accumulation at bleached sites was normal if receptors were labeled with BTX-tetramethylrhodamine or BTX-647 (data not shown).
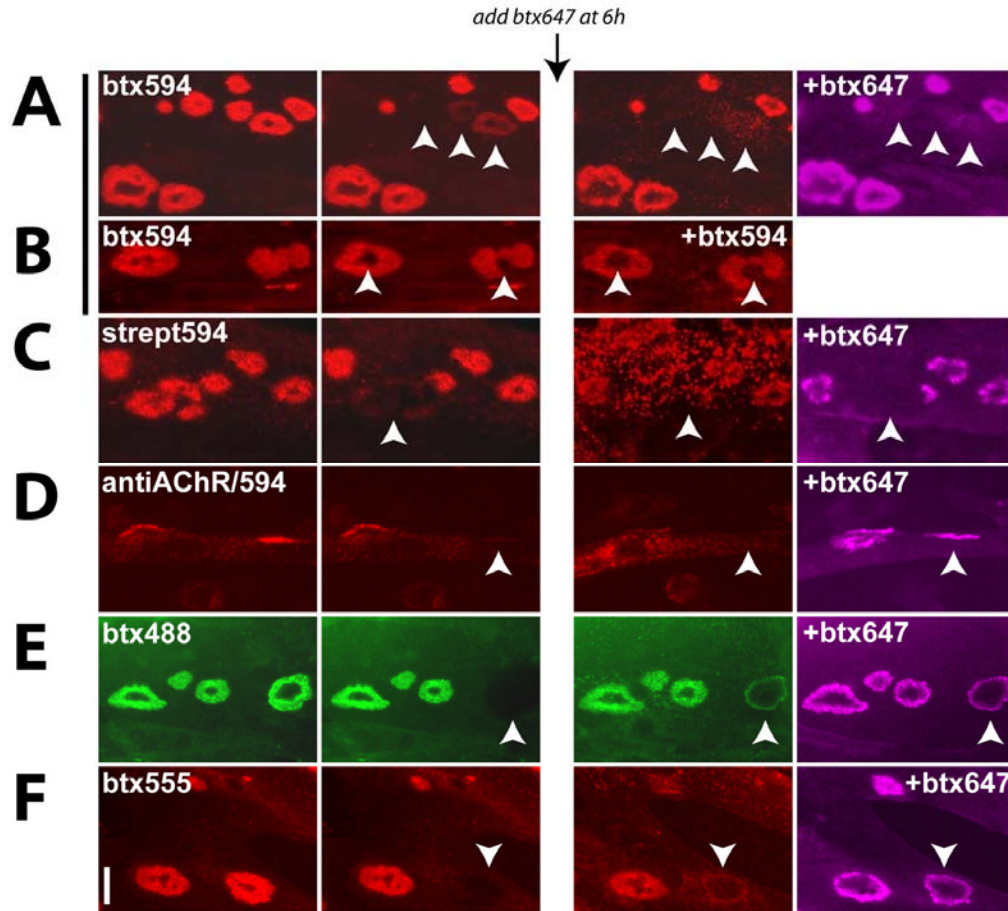
Figure 5.1. Alexa 594-mediated dissipation of illuminated AChR clusters on cultured myotubes. C2C12 myotubes were incubated in fluorescent bungarotoxin-Alexa 488, 555 or 594 or bungarotoxin-biotin/streptavidin-Alexa 594, and individual labeled clusters on the myotube surface were imaged and then illuminated with an Argon laser (488 nm). Six hours later, the cells were incubated in bungarotoxin-Alexa 647 (BTX-647) or BTX-594 and then imaged again to identify newly synthesized receptors inserted over this time. **(A)** Example of a myotube labeled with BTX-594 in which 3 clusters were illuminated for various times to cause different amounts of bleaching (arrowheads). Six hours later, after the addition of BTX-647, no originally labeled or newly inserted receptors had accumulated at any of the illuminated cluster sites, while high density accumulation at unbleached control clusters was normal. **(B)** Small regions within AChR clusters on myotubes labeled with BTX-594 were illuminated and then re-labeled 6 hours later with new BTX-594. Note that the accumulation of newly synthesized AChRs was only prevented at the illuminated spots, indicating that the disruption of AChR clustering following laser illumination is a local effect. **(C)** The accumulation of newly synthesized receptors was also prevented when AChR clusters labeled with bungarotoxin-biotin/streptavidin-Alexa 594 were illuminated. Note that the direct internalization and accumulation of streptavidin-Alexa 594 in intracellular puncta after labeling dramatically increases intracellular fluorescence. **(D)** When AChRs on living myotubes were labeled with anti-AChR antibody and secondary antibody conjugated to Alexa 594, bleached, and then labeled 6 hours later with BTX-647, we found that AChRs were inserted normally. **(E and F)** Examples of myotubes that were labeled with bungarotoxin-Alexa 488 or 555 and then illuminated with the same Argon laser used above. Six hours after laser exposure the illuminated clusters had recovered significant amounts of fluorescence around the periphery of the cluster (as previously reported (Kummer et al., 2004; Bruneau et al., 2005b)) both from the lateral migration of originally labeled receptors, and the insertion of new receptors, indicating that laser illumination of BTX-488 or BTX-555 labeled AChRs did not noticeably alter AChR accumulation. Scale bar = 20 μm.

135

The dissipation of BTX-594 labeled AChRs from clusters was not due to laser damage of the muscle membrane (Supplemental Figure S5.4), however when an AChR antibody which does not compete for AChR binding with bungarotoxin was added immediately after AChR-BTX-594 illumination, the fluorescent intensity at bleached clusters was decreased to ~60% that of neighboring, unbleached clusters, implying that AChR dissipation might be mediated by a change in receptor conformation (Supplemental Figure S5.5).

AChRs are required for the maintenance and accumulation of post-synaptic scaffolding proteins at individual clusters.

To investigate whether receptors are necessary for the maintenance of the post-synaptic scaffold, we examined the localization of rapsyn, β-dystroglycan, utrophin and actin following laser illumination of BTX-594 labeled receptor clusters. We focused on these proteins because they have been shown to serve as a link between the AChR and the intracellular cytoskeleton (James et al., 1996; Sanes and Lichtman, 2001; Galkin et al., 2002; Huebsch and Maimone, 2003; Dobbins et al., 2006). To do this, receptors on cultured myotubes were labeled with BTX-594 and then entire clusters or small regions within individual clusters were illuminated with the DPSS (561 nm) laser of a scanning confocal microscope. Six hours later, cells were fixed and immunostained with anti-AChR (mAb35) antibody, and one of the following: anti-rapsyn, anti-β-dystroglycan, anti-utrophin, anti-actin (JLA20) (which we found to bind specifically to scaffold-specific actin) or phalloidin-FITC (which has been shown previously to bind to cytoskeletal actin (Shepard et al., 2004)) (Supplementary Figure S5.6). We found that the removal of the BTX-594 labeled AChRs from the entire illuminated cluster or from a

small illuminated region within a cluster was accompanied by the disappearance of rapsyn, β-dystroglycan, utrophin and scaffold-specific actin from the same bleached sites (Figures 5.2A-D). The underlying cytoskeleton (labeled with phalloidin-FITC), however, was unaffected (Figure 5.2E). Illumination of BTX-488 labeled AChRs at individual clusters either with the Argon laser, or exposure of these clusters to the confocal DPSS laser for the same amounts of time that were used for BTX-594 mediated dissipation, had no effect on the migration of AChRs into bleached regions, or the accumulation of either AChRs or rapsyn at the cluster after 6 hours (Figure 5.2F). These data indicate that AChRs are required for the maintenance and accumulation of rapsyn, β-dystroglycan, utrophin and actin molecules at clusters in the muscle membrane.
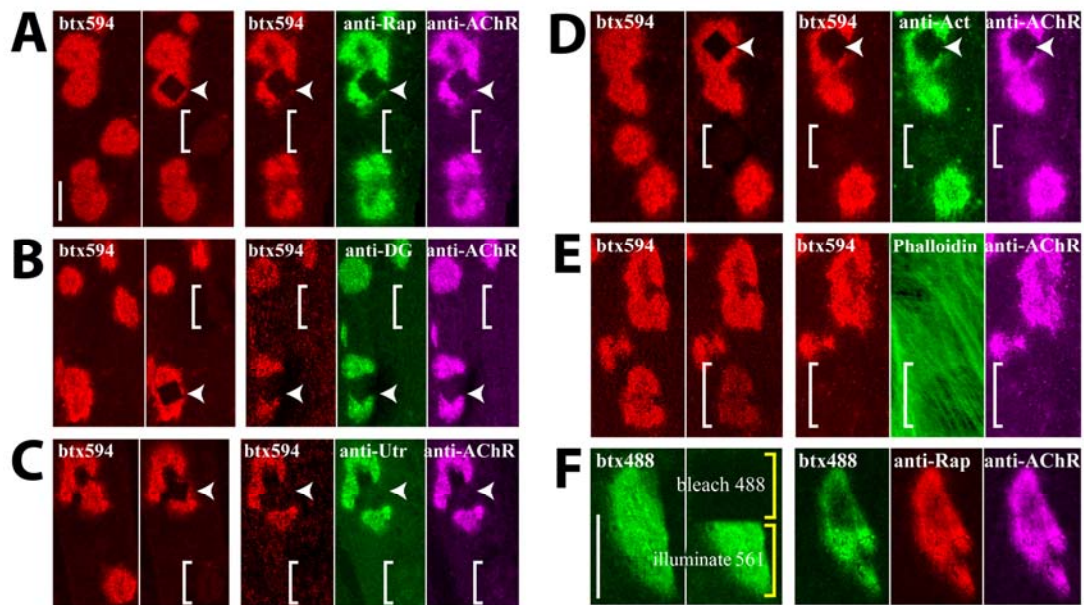
Figure 5.2. Laser illumination of bungarotoxin-Alexa 594 labeled clusters results in the complete dissipation of the AChR scaffold. Myotubes were labeled with bungarotoxin-Alexa 594 and then individual clusters (open bracket) and regions of individual clusters (arrowheads) were illuminated with a scanning confocal microscope using DPSS (561 nm) laser emission. Six hours later the myotubes were fixed and labeled with anti-AChR antibody and one of the following: anti-rapsyn (Rap), anti-β-dystroglycan (DG), anti-utrophin (Utr), anti-actin (Act) or Phalloidin-FITC. **(A-D)** Since antibodies label both existing proteins and the proteins inserted during the 6 hour incubation, complete lack of staining from Rap, DG, Utr and Act at whole illuminated clusters or illuminated regions within clusters indicates that the elimination of AChRs results in the local dissipation of the intracellular scaffold, and also prevents the insertion of new scaffolding proteins. **(E)** The presence of normal phalloidin staining

after 6 hours at illuminated sites in which AChR clusters have been induced to dissipate indicates that the underlying cytoskeleton is unaffected by this laser illumination. Note that for (A-E) different levels of illumination/bleaching were able to induce complete dissipation. **(F)** Clusters labeled with bungarotoxin-Alexa 488 were also bleached with either the Argon (488 nm) or DPSS (561 nm) laser of the scanning confocal microscope and then fixed and labeled as above. Note that complete bleaching of the Alexa 488 with the Argon laser or exposure of the cluster to the DPSS laser (for the same amount of time used to dissociate clusters in (A-E)) did not result in receptor dissipation. Each confocal image was taken on a single plane on the muscle surface. Scale bars = 20 μm.

Time-lapse imaging of intracellular scaffolding protein dissipation

To examine the time-course of removal of labeled AChRs and AChR-scaffold proteins from illuminated clusters, we monitored AChR and associated scaffolding proteins at various time points after laser illumination. As an initial step, we examined the removal of rapsyn from illuminated clusters by transfecting myotubes with rapsyn-GFP and then labeling the AChRs on these cells with BTX-594. The GFP or the Alexa 594 from individual clusters was then excited using the Argon or DPSS lasers of a confocal microscope, respectively. In this way we were able to simultaneously follow rapsyn-GFP removal over time from clusters that were illuminated with the DPSS (561 nm) laser (which induced BTX-594-labeled AChRs to dissipate, but did not bleach the rapsyn-GFP) and determine the insertion of rapsyn-GFP into clusters that were illuminated briefly with the Argon (488 nm) laser (which bleached the GFP but left labeled AChRs relatively unbleached) on the same myotube. At clusters where only AChR-Alexa 594 was excited, time-lapse imaging revealed that rapsyn-GFP fluorescence decreased rapidly after only 1.5 hours, and was nearly undetectable after 3.5 hours. In contrast to visible internalized Alexa 594 puncta, no internal GFP signal was seen at these clusters. At the same time, insertion of rapsyn-GFP into clusters in which the GFP (and not the Alexa 594) was bleached with the Argon laser was normal and similar to previous reports (Bruneau and Akaabourne, 2007) (Figure 5.3). These data indicate that net rapsyn dissipation (the combination of rapsyn removal and the prevention of new rapsyn

138

insertion) occurs very rapidly from clusters following photo-dissipation of clustered AChRs.
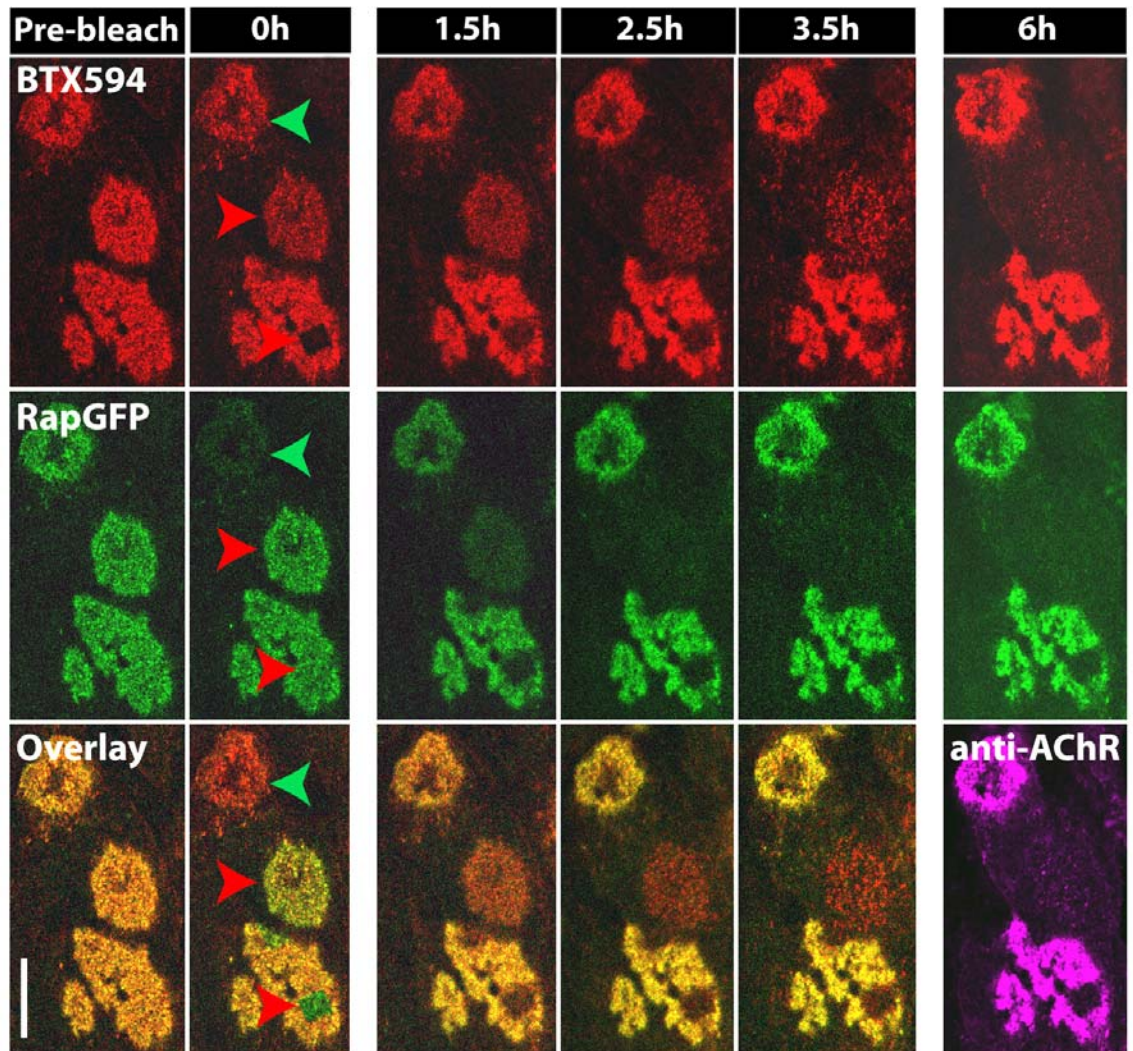
Figure 5.3. Time-lapse imaging of rapsyn-GFP following laser-induced AChR dissipation. Myotubes were transfected with rapsyn-GFP and labeled with bungarotoxin-Alexa 594. Individual clusters were imaged and then illuminated either with a brief exposure to the Argon (488 nm) laser to bleach the GFP fluorescence (green arrowheads) or more prolonged exposure to the DPSS (561 nm) laser to excite Alexa 594 fluorescence (red arrowheads). The same clusters were then imaged from 0 to 3.5 hours later after fresh applications of new bungarotoxin-Alexa 594 between imaging time points. Cells were then fixed and labeled with anti-AChR antibody after 6 hours. At clusters in which only rapsyn-GFP was bleached (green arrowhead), rapsyn-GFP fluorescence rapidly recovered, and fluorescence had nearly reached original levels when cells were fixed 6 hours later. At clusters in which the Alexa 594 fluorescence was illuminated and AChRs were therefore induced to dissociate (red arrowheads), rapsyn-GFP fluorescence rapidly decreased over time as rapsyn dissipated from the bleached cluster, and rapsyn-GFP was completely absent from the cluster site after cells were fixed at 6 hours. The absence of anti-AChR staining at 6 hours indicates that complete cluster dissipation had occurred. Each confocal image was taken on a single plane of the muscle surface. Scale bar = 20 μm.

139

To confirm the above results and extend them to the other scaffolding proteins, BTX-594 labeled receptor clusters were illuminated, fixed 1 hour later and then immunostained with anti-rapsyn, anti-utrophin, anti-β-dystroglycan or anti-actin (JLA20) antibodies. We found that rapsyn, utrophin, β-dystroglycan and actin immunofluorescence at bleached clusters had all decreased after only 1 hour to nearly half the amount at neighboring, unbleached control clusters (48 ± 13%, n=7; 53 ± 6%, n=6; 51 ± 10%, n=19; and 51 ± 8%, n=13, respectively) (Figures 5.4A and B). When cells were fixed immediately after bleaching, negligible changes in antibody binding for scaffolding components were seen (see supplementary Figure S5.5 and data not shown). When cells were fixed 2 hours after illumination, bright intracellular puncta made quantification difficult, and at time points after 2 hours the immunofluorescence from all antibodies was too dim to quantify; immunofluorescence was completely absent at illuminated clusters after 6 hours.
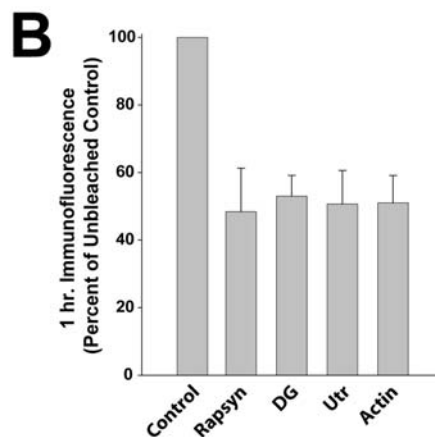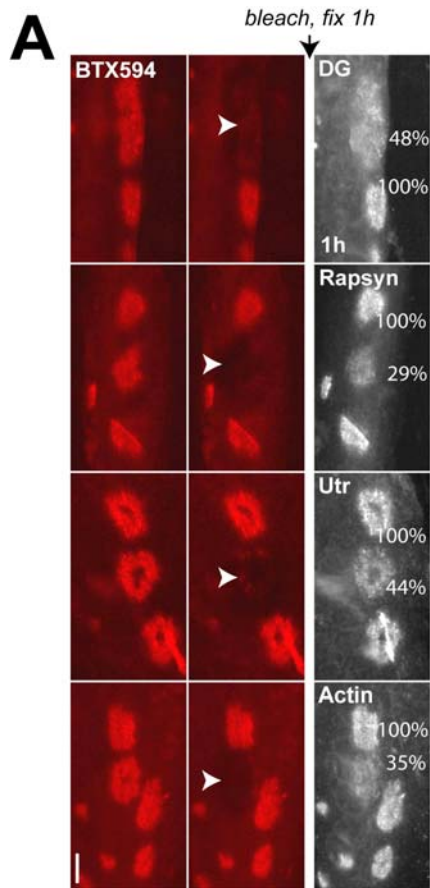
Figure 5.4. Rapsyn, β-dystroglycan, utrophin and actin are all removed at similar rates from illuminated clusters. Myotube cultures were labeled with bungarotoxin-Alexa 594 and imaged, and then individual clusters were illuminated with an Argon (488 nm) laser. One hour later the cells were fixed, immunostained with antibodies for rapsyn, β-dystroglycan, utrophin and actin, and imaged again. The average immunofluorescence from each bleached cluster was then compared to the average immunofluorescence at a neighboring, unbleached control cluster. **(A)** Representative images from individual myotubes show that after 1 hour, approximately half of the population of each scaffolding protein at bleached clusters had been removed. **(B)** Graph represents the quantification of immunofluorescence from all antibodies 1 hour after illumination. Note that the immunofluorescence from each protein decreased similarly. All data represented as mean ± SD. Scale bar = 20 μm.

Discussion

This work demonstrates that low-power laser illumination of the Alexa 594 fluorophore conjugated to bungarotoxin not only causes the removal of the AChRs and simultaneous or subsequent loss of scaffold proteins from illuminated regions, but also prevents the accumulation of new synaptic proteins at that region. This phenomenon is spatially restricted to the illuminated region, leaving unbleached regions of the same cluster unaffected.

The effect observed here is similar to chromaphore-assisted light inactivation (CALI) in which illumination of a specific protein/fluorophore pair causes the inactivation of the labeled protein. CALI has been shown to result from the generation of free radicals which alter proteins only within a very close proximity (less than 100 Å) (Beck et al., 2002; Marek and Davis, 2002). Consistent with this, we found that the Alexa 594 mediated dissipation only occurred if the fluorophore was relatively close to the AChR (separated by BTX or BTX-biotin-streptavidin), but not if the fluorophore was conjugated to a secondary antibody. Further, even if the laser light was intense enough to temporarily damage the muscle membrane, it still did not alter AChR clustering in regions immediately adjacent to the illuminated region.

Although it is not clear how illumination of the Alexa 594 fluorophore is able to induce the dissipation of clustered receptors, it is possible that the absorption of photons by the fluorophore could cause structural modification of the AChR (as suggested by Supplementary Figure S5.5). While it is possible that the illuminated and structurally modified AChRs remain stuck in the membrane, our data are more consistent with a model in which subsequent un-tethering of affected AChRs from the cluster site could

then lead to an AChR density below a critical level necessary to signal the accumulation of AChRs, which would lead to the dispersal of all clustered AChRs at the illuminated region, and the prevention of newly synthesized AChR accumulation. Whatever the mechanism by which laser illumination causes Alexa 594-labeled AChR dissipation, we used this as a tool to directly investigate the role of the AChR in the maintenance and integrity of the intracellular scaffold. When receptors were induced to disperse, all other proteins of the scaffold examined were also removed from the cluster, and newly synthesized proteins were not accumulated at the illuminated region. Consistent with this observation, rapsyn fails to cluster in AChR-deficient muscles in zebrafish (Ono et al., 2001; Ono et al., 2004) and in C2C12 myotubes lacking AChRs (Marangi et al., 2001), and mice lacking the adult epsilon AChR subunit fail to form mature synapses and show marked decreases in scaffolding proteins (Missias et al., 1997).

One concern with all laser illumination studies is that the laser may be causing non-specific cell damage. The following data indicate that this is likely not the case in the present study: First, although laser illumination caused AChR dissipation it did not result in muscle membrane damage (Supplemental Figure S5.3); second, at clusters that were induced to dissipate, the intracellular actin cytoskeleton was not altered after laser illumination (Figure 3E); third, AChRs that were within microns of the laser illumination (even extensive illumination that temporarily damaged the muscle membrane) were not affected; fourth, exposing rapsyn-GFP to high laser power for prolonged time did not disrupt rapsyn insertion; fifth, illumination of BTX-488 labeled AChRs with the Argon or DPSS scanning confocal laser using the same parameters that caused dissipation of BTX-594 labeled AChRs did not alter AChR clustering or rapsyn localization (Figure 5.3F);

finally, 6 hours after laser exposure the background fluorescence from new fluorescent BTX at illuminated regions was similar to staining from diffuse AChRs elsewhere on the muscle surface (Figure 5.1, S5.1 and S5.2), and even non-labeled AChRs within illuminated regions were dissipated following laser illumination (Figure S5.3), indicating that receptors were able to move freely into and out of the laser-illuminated membrane. These observations suggest that laser illumination caused the selective dissociation of clustered receptors, which in turn resulted in the local disassembly of the intracellular scaffold without disrupting either the intracellular cytoskeleton or membrane integrity or fluidity.

Here we show directly that AChRs are not only necessary for the clustering of rapsyn in mammalian myotubes, but that a threshold density of AChRs likely provides a critical signal which enables proteins of the dystrophin-glycoprotein complex and intracellular scaffold to remain aggregated and which allows the accumulation of newly synthesized proteins into the existing cluster. The fact that Alexa 594-mediated dissipation occurs only within small illuminated sections of individual clusters further implies that the high density of AChRs provide a local clustering signal. Together these data indicate that the post-synaptic scaffold may be organized not as a matrix of cross-linked proteins, but as discrete units of intracellular scaffolding proteins associated with individual receptors (Supplemental Figure S5.7). Consistent with this model, local removal of clustered AChRs and scaffold proteins has been observed during synaptic re-modeling during development or after nerve damage (Culican et al., 1998; Sanes and Lichtman, 2001). It will be interesting to see if AChR dissipation is responsible for precipitating these types of synaptic re-modeling events.
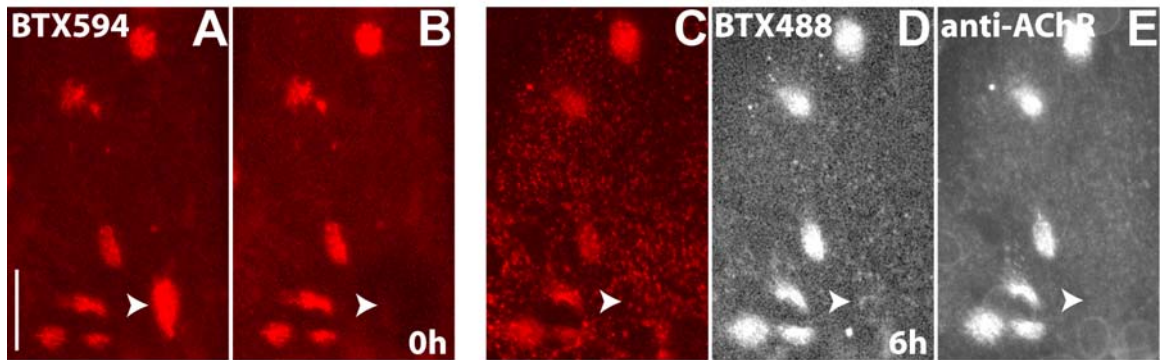
Figure S5.1. Bungarotoxin-Alexa 594 induced dissipation of AChRs from clusters on primary mouse myotubes. Primary muscle cells were plated on mitrigel and labeled after differentiation with bungarotoxin-Alexa 594. **(A, B)** Shown is a single fiber on which one cluster was laser illuminated (arrowhead). **(C-E)** Six hours later cells were fixed and labeled with a distinct fluorescent bungarotoxin conjugate to identify all new receptors inserted over this time, and anti-AChR antibody to label all AChRs. Note that the dissipation of AChRs and prevention of new receptor insertion occurred only at the bleached cluster. Scale bar = 20 μm.
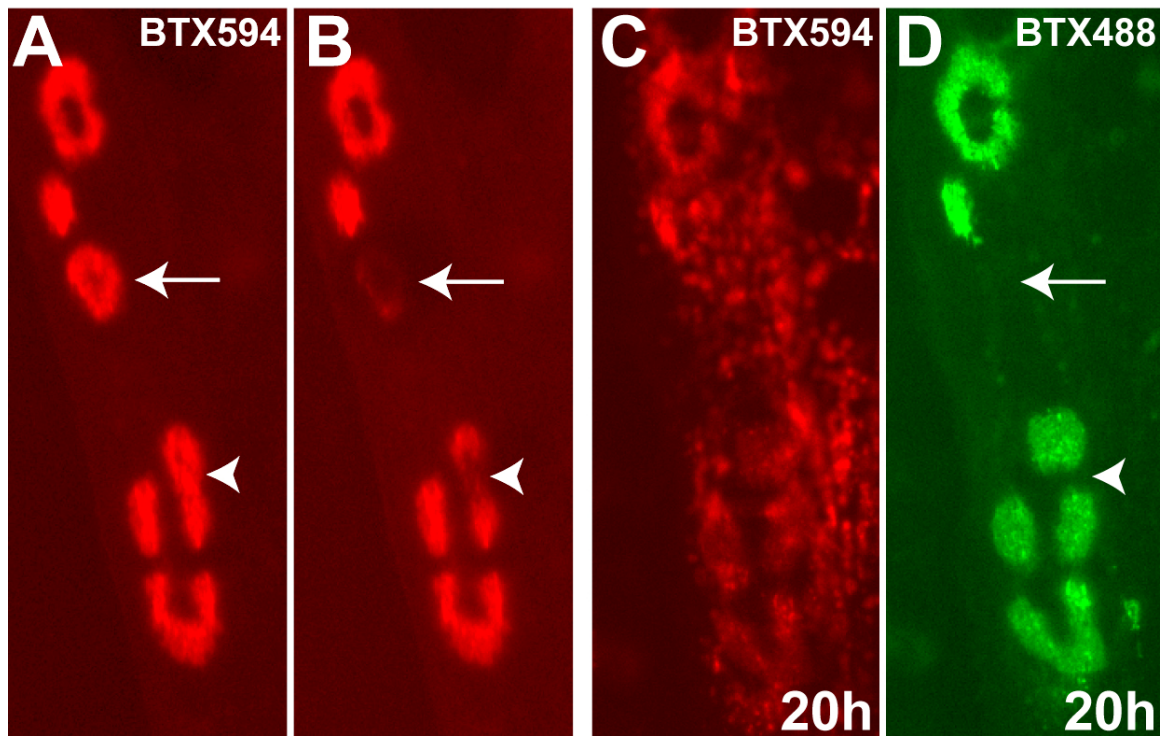
Figure S5.2. Cluster dissipation persists over time. (A) C2C12 myotubes were incubated with bungarotoxin-Alexa 594 and individual clusters or regions of clusters were imaged. **(B)** Individual clusters (arrows) or small regions within clusters (arrowheads) were then laser illuminated and re-imaged. **(C, D)** Twenty hours later the myotubes were incubated with a distinct fluorescently tagged bungarotoxin-Alexa 488 to label receptors that had been inserted into the membrane after initial labeling. Note that after 20 hours most of the original fluorescence (red) was eliminated from all clusters (C), and that although background labeling of diffuse AChRs was present at illuminated regions, high intensity fluorescence from the accumulation of newly inserted AChRs (green) was absent only from the regions that were illuminated (D), indicating that the accumulation of newly synthesized AChRs at laser illuminated regions was prevented. Scale bar = 20 μm.

146
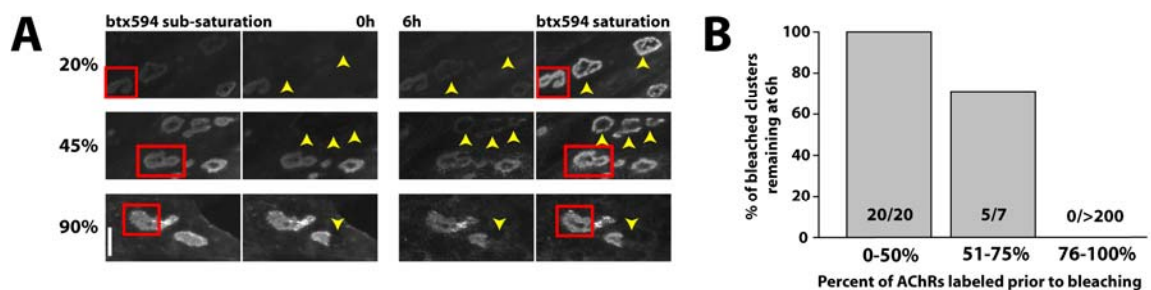
Figure S5.3. Bleaching of unsaturated clusters causes complete AChR cluster dissipation. C2C12 myotubes were incubated for variable periods of time with bungarotoxin-Alexa 594 to label only a proportion of the AChRs at individual clusters. **(A)** Images show clusters that were labeled with a sub-saturating dose of bungarotoxin-Alexa 594 (BTX-594 incubation between 2 and 15 minutes) and then bleached (arrowheads). After 6 hours, a saturating dose of bungarotoxin was then applied (1.5 hours) and the fluorescence of unbleached control clusters at 6 hours was compared to their fluorescence at 0 hours to determine the amount of original saturation (red boxed clusters). Percent of saturation at original labeling is indicated at the left. **(B)** Graph summarizes data from a number of clusters imaged as in (A). Note that for clusters in which fewer than 50% of AChRs were labeled prior to bleaching, complete cluster dissipation was not observed in any of the 20 clusters examined. If 50-75% of AChRs were labeled prior to bleaching, 2 of the 7 clusters examined were completely dissipated 6 hours after laser illumination. Labeling of greater than 75% of AChRs resulted in the complete dissipation not only of labeled and illuminated AChRs, but of all non-labeled AChRs in the illuminated region (n > 200). Scale bar = 20 μm.

147
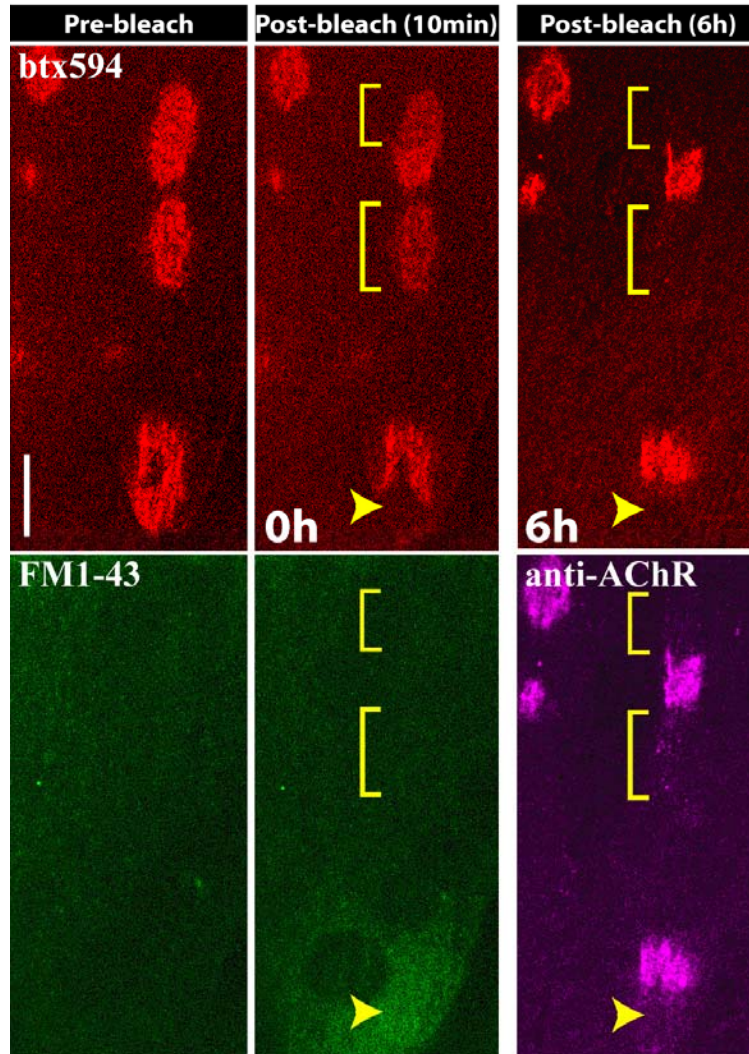
Figure S5.4. Temporary muscle membrane damage is not responsible for AChR cluster dissipation. FM1-43 is a lipid soluble dye that does not fluoresce unless incorporated into newly forming membranes. This dye has been used previously to label endo-membrane following temporary muscle membrane damage in response to high intensity laser light (Miyake et al., 2001; Bansal et al., 2003). In muscle fibers, FM1-43 fluorescence stabilizes after minutes due to surface membrane resealing, but persists in membranes that are deficient in components necessary for membrane recovery. To determine if laser illumination necessary to induce AChR dissipation was causing temporary muscle membrane damage, C2C12 myotube clusters were labeled with BTX-594 and incubated with FM1-43. In the presence of FM1-43, individual clusters or regions of clusters were illuminated with a DPSS (561 nm) laser of a scanning confocal microscope and then membrane damage was assessed with the FM1-43 assay described above. Shown here is a myotube in which temporary muscle membrane damage was intentionally initiated with prolonged focal laser exposure (arrowhead), as indicted by FM1-43 labeling. Other clusters on the same cell were exposed to the laser briefly enough to avoid membrane damage (open brackets), as indicated by the absence of FM1-43 labeling. Six hours later cells were fixed, labeled with anti-AChR antibodies and imaged with confocal microscopy. Note that the dissipation of bleached and unbleached AChRs and the lack of accumulation of newly synthesized AChRs at all illuminated regions were not due to temporary muscle membrane damage. Each confocal image was taken on a single plane on the muscle surface, and image brightness was adjusted using Adobe photoshop to enhance background fluorescence. Scale bar = 20 μm.
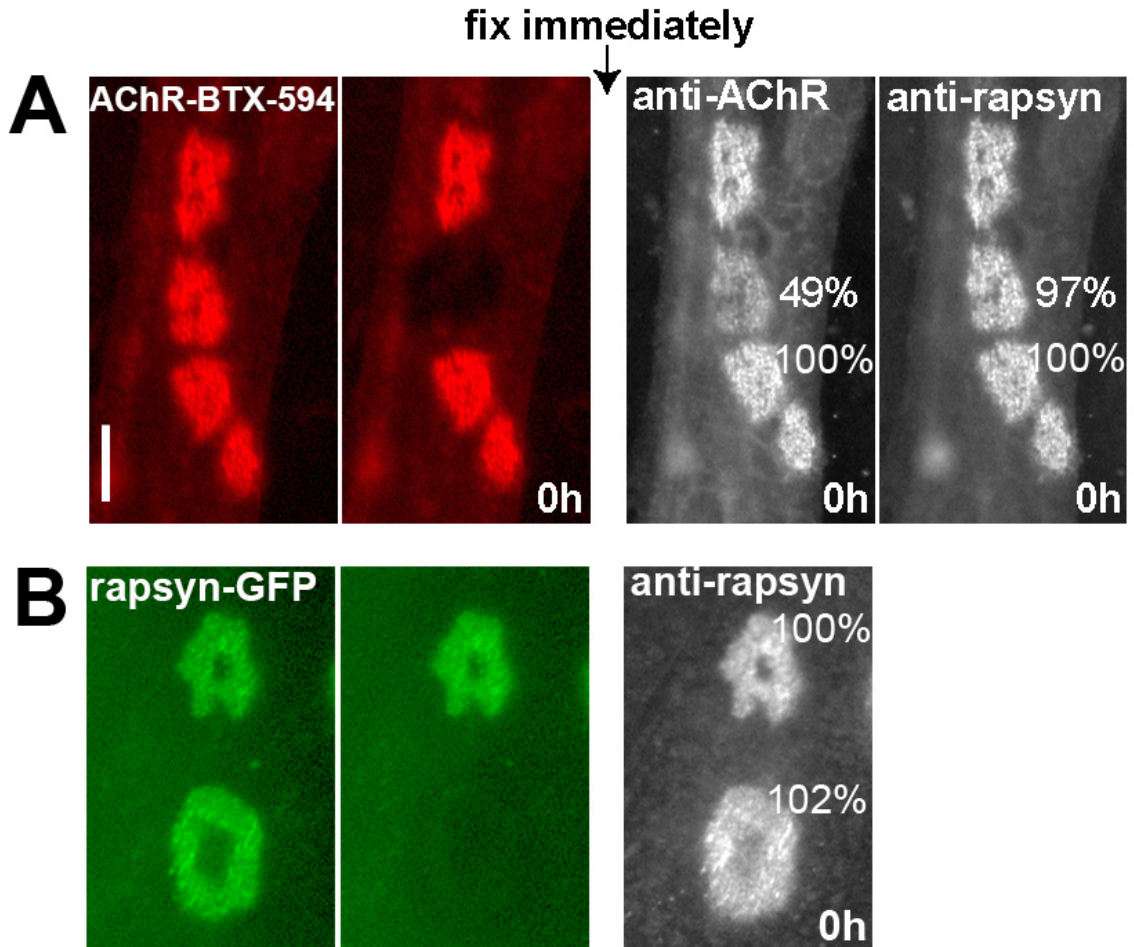
Figure S5.5. Exposure of bungarotoxin-Alexa 594 labeled AChRs to laser illumination decreases anti-receptor antibody binding. (A) C2C12 myotubes were incubated with bungarotoxin-Alexa 594 and imaged. Individual clusters were then laser illuminated immediately after fixation in 2% paraformaldehyde (see arrowheads), and the muscle culture was immunostained with anti-AChR (mAb35) and anti-rapsyn antibodies. Quantitative immunofluorescence indicated that anti-AChR binding was significantly compromised in the laser illuminated cluster compared to neighboring, unbleached control clusters, while anti-rapsyn staining was normal. Similar results were obtained if the cells were instead fixed prior to laser illumination. Data from a number of experiments performed as above showed that labeling at bleached clusters was decreased to $58 \pm 11\%$ (S.D., n=85) of unbleached control clusters when bleached immediately prior to fixation, and $61 \pm 13\%$ (S.D., n=17) when bleached immediately after fixation. **(B)** C2C12 myotubes were transfected with a rapsyn-GFP fusion protein, and clusters expressing rapsyn-GFP were imaged. The GFP fluorescence from individual clusters was then laser illuminated, and cells were fixed and immunostained with anti-rapsyn antibodies. Note that anti-rapsyn immunofluorescence was unaffected by GFP illumination. Together these data indicate that the laser illumination of fluorescent Alexa 594 is able to alter antibody binding to AChRs, while illumination of fluorescent GFP has no effect on antibody binding to rapsyn. It is possible that the decrease in anti-AChR binding could be due to structural modification of the AChR induced by the laser illumination of the Alexa 594 fluorophore. Scale bar = 20 μm.

149
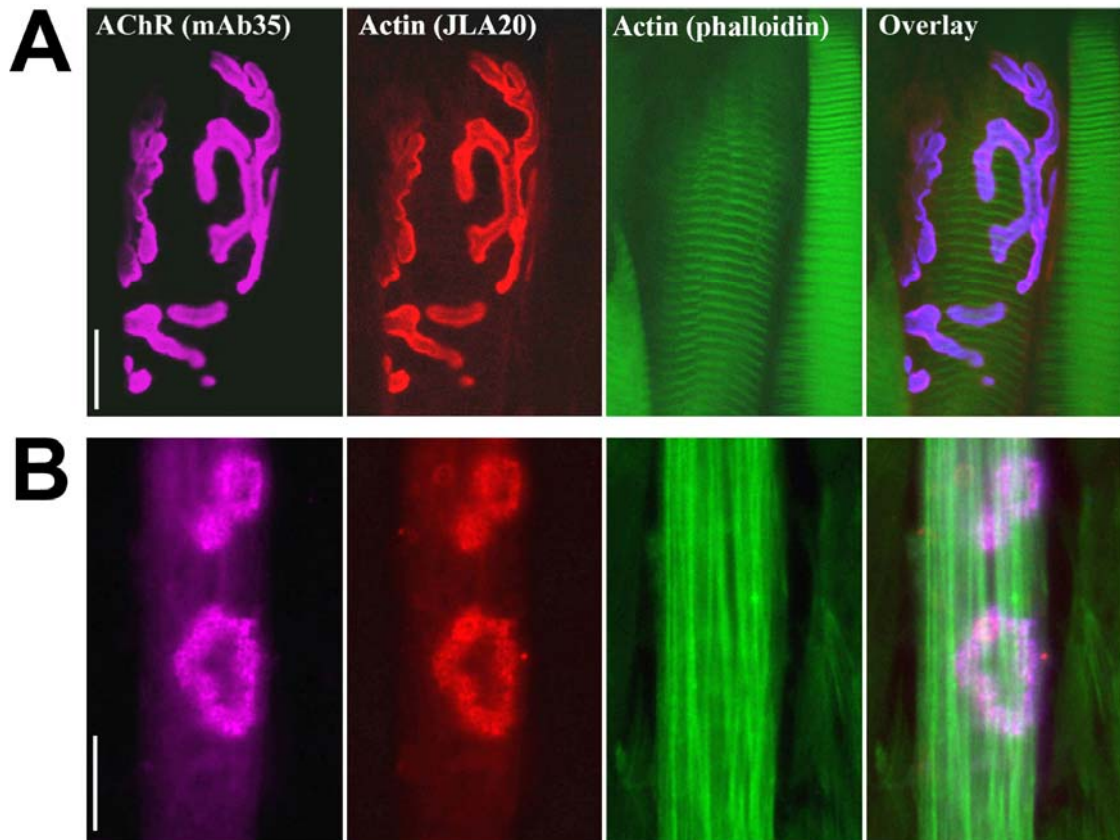
Figure S5.6. JLA20 and Phalloidin label distinct actin populations on C2C12 muscle cells *in vitro* and sternomastoid muscle fibers *in vivo*. Muscle cells were labeled with anti-AChR antibody, anti-actin antibody (JLA20) and FITC-phalloidin and then imaged with a scanning confocal microscope. **(A)** Top panels represent collapsed confocal images of a sternomastoid muscle that was fixed in the animal, sectioned longitudinally and then immunostained and imaged. Note that JLA20 immunostaining co-localizes with AChRs specifically at the neuromuscular junction and is absent from the intracellular cytoskeleton, while phalloidin labels the actin filaments of the cytoskeleton and is absent from the neuromuscular junction. **(B)** Bottom panels show collapsed confocal images of a C2C12 myotube immunostained as described above. Similar to the neuromuscular junction in the top panels, JLA20 labeling was restricted to AChR clusters while phalloidin labeled the actin fibers of the intracellular cytoskeleton. The switch of cytoskeletal actin orientation in the muscle fiber from parallel to perpendicular represents a normal developmental transition between immature and mature muscle fibers. Scale bar = 20 μm.
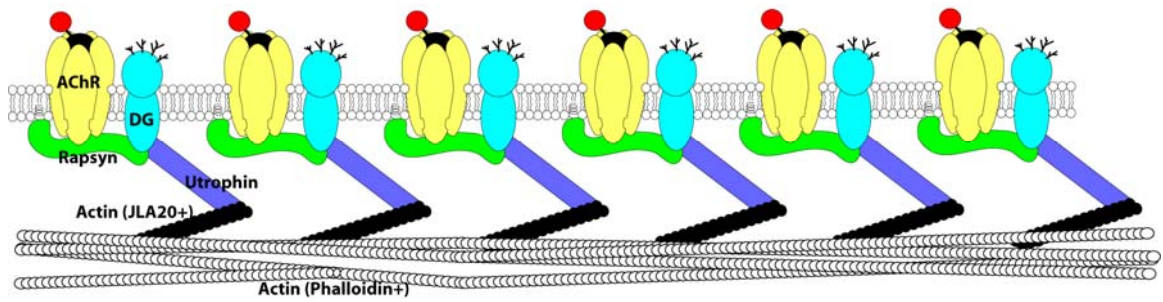
Figure S5.7. A model for the modular organization of AChRs and proteins of the post-synaptic scaffold. In this simplified model, each AChR is linked separately to proteins of the dystrophin-glycoprotein complex through their interaction with rapsyn. Each AChR could then be removed as a unit along with the individual scaffolding proteins associated with it. In this model, local AChR density is critical for the maintenance of a high density of receptors and scaffolding proteins.

Acknowledgments

Chapter VI

The Dynamics of the Rapsyn Scaffolding Protein at Individual Acetylcholine Receptor Clusters

Emile G. Bruneau and Mohammed Akaaboune

Abstract

Rapsyn, a cytoplasmic receptor-associated protein, is required for the clustering of acetylcholine receptors (AChRs). While AChR dynamics have been extensively studied, little is known about the dynamics of rapsyn. Here, we used a rapsyn-GFP fusion protein and quantitative fluorescent imaging to study the dynamics of rapsyn in transfected C2C12 myotubes. First, we found that rapsyn-GFP expression at clusters did not alter AChR aggregation, function or turnover. Quantification of rapsyn immuno-fluorescence indicated that the expression of rapsyn-GFP proteins at clusters does not increase the overall rapsyn density compared to untransfected myotube clusters. Using time-lapse imaging and fluorescence recovery after photobleaching, we demonstrated that the recovery of rapsyn-GFP fluorescence at clusters was very fast, with a halftime of about ~ 1.5 h (~ 3 times faster than AChRs). Inhibition of protein kinase C (PKC) significantly altered receptor insertion, but it had no effect on rapsyn insertion. When cells were treated with the broad-spectrum kinase inhibitor staurosporine, receptor insertion was decreased even further. However, inhibition of protein kinase A (PKA) had no effect on

insertion of either rapsyn or receptors. Finally, when cells were treated with neural agrin, rapsyn and AChRs were both directed away from pre-existing clusters and accumulated together in new small clusters. These results demonstrate the remarkable dynamism of rapsyn, which may underlie the stability and maintenance of the post-synaptic scaffold and suggest that the insertion of different postsynaptic proteins may be operating independently.

Introduction

The efficacy of synaptic transmission depends upon the high density and number of postsynaptic neurotransmitter receptors at sites of neurotransmitter release (Sanes and Lichtman, 2001; Carroll and Zukin, 2002). This density can be maintained in several ways. For example, phosphorylation/dephosphorylation events mediated by different kinases are able to alter receptor synthesis and dynamics (Si et al., 1998; Sanes and Lichtman, 2001; Sadasivam et al., 2005; Wang et al., 2005), and a number of postsynaptic scaffolding proteins have been found to be essential either for the clustering or the maintenance of postsynaptic receptors at cluster sites at both central and peripheral synapses (Feng et al., 1998b; Sanes and Lichtman, 2001; Akaaboune et al., 2002; Grady et al., 2003; Henley, 2003; Kim and Sheng, 2004; Bruneau and Akaaboune, 2006b).

The formation of the postsynaptic receptor density is best studied at the neuromuscular junction (NMJ). Among the molecules involved in the clustering of AChRs is rapsyn. Rapsyn (43 kD) was initially purified from the torpedo electric organ and is thought to be associated with AChRs in a 1:1 stoichiometry at the muscle surface (Frail et al., 1988; Noakes et al., 1993). Rapsyn is responsible for mediating the effect of agrin, a neuronal clustering factor that activates the muscle-specific kinase (MuSK) and

154

initiates AChR clustering in a tyrosine kinase-dependent manner (Apel et al., 1997; Fuhrer et al., 1999; Mohamed and Swope, 1999; Mittaud et al., 2001; Mohamed et al., 2001). In mice lacking rapsyn, receptor clustering does not occur and NMJs fail to form (Gautam et al., 1995). Rapsyn mutations also cause AChR deficiency in patients with congenital myasthenia syndrome (McConville and Vincent, 2002; Ohno et al., 2002; Muller et al., 2006), highlighting the importance of rapsyn for the formation and organization of the post-synaptic receptor density. While the availability of highly specific receptor ligands has enabled the study of AChR dynamics on the living muscle *in vitro* and *in vivo* (Akaaboune et al., 1999; Bruneau et al., 2005b), study of scaffolding protein dynamics at the post-synaptic density has been hindered by their inaccessibility to extracellular ligands.

In this study, we investigated the dynamics of rapsyn at individual clusters on cultured myotubes. Our interest specifically in rapsyn stems from its close association with AChRs and its role in receptor clustering at the post-synaptic membrane. By monitoring the fluorescence of rapsyn-GFP fusion proteins clustered on the surface of transfected C2C12 myotubes, we were able to determine that rapsyn is markedly more dynamic than AChRs and is not affected by pharmacological manipulation that alters AChR dynamics, even though both rapsyn and AChRs are similarly modulated by the nerve clustering factor, agrin.

Materials and Methods

GFP fusion construct. The rapsyn-GFP fusion construct was kindly provided by Dr. Jonathan Cohen (Harvard Medical School).

Cell culture. To generate laminin-coated dishes, 5 μg/mL of poly-ornithine (Sigma, St Louis, MO) was added to 35 mm culture dishes and allowed to evaporate overnight. The following day 10 μg/mL of EHS Laminin (Invitrogen, CA) in L-15 media supplemented with 0.2% sodium bicarbonate was added to the dishes, and they were placed in an incubator overnight until ready for plating. C2C12 myoblasts (ATCC, Manassas, VA) were plated and then grown in 20% fetal bovine serum with penicillin and streptomycin in DMEM. Cells were transfected at 70-100% confluence with 1 μg of rapsyn-GFP using FUGENE6 transfection reagent (Roche, Basel, Switzerland). Cells were then differentiated by replacing the FBS solution with 5% horse serum media with penicillin and streptomycin in DMEM. Media was changed every 2 days and cells were imaged 3-4 days after differentiation.

Immuno-fluorescence microscopy. Transfected myotubes were fixed with 2% paraformaldehyde and then treated for 20 minutes with 1% triton X-100 in phosphate buffered solution. Cells were then incubated with mouse anti-rapsyn primary (mAb 1234, Sigma, St. Louis, MO) and goat anti-mouse-Alexa 594 secondary antibodies (Invitrogen Molecular Probes, Eugene, OR). After extensive washing, cells were imaged. Background fluorescence was approximated by selecting a boundary region around the cluster and subtracting it from the original image, and the mean of the total fluorescence intensity (which corresponds to density) was measured. Image analysis was performed by using a procedure written for Matlab (The Mathworks, Natick, MA) (Martinez-Pena y Valenzuela et al., 2005). The acquisition and quantification of images were done with the experimenter blind to rapsyn-GFP expression at each cluster.

Electrophysiology. A rapsyn-GFP transfected myotube was located and a whole cell patch clamp recording was obtained under voltage-clamp. The AChR agonist carbachol (100 μM) was then ejected into the media with a puffer pipette placed near the patched cell and the resulting inward current was measured. As a control for the specificity of carbachol, the AChR antagonist curare (10 μM) was applied by perfusion into the cell media to block these inward currents. Measurements were made as above on untransfected myotubes for comparison.

Receptor loss. AChR loss was determined by labeling AChRs of untransfected myotubes or myotubes expressing rapsyn-GFP with bungarotoxin-Alexa 594 (5 μg/ml, 1 h). Initial images of rapsyn-GFP and/or clustered receptors were taken, and 4 hours later the same clusters were found and re-imaged. The loss of fluorescence was then assayed using quantitative fluorescence imaging (Turney et al., 1996; Akaaboune et al., 1999). Clusters expressing different levels of GFP were then grouped into three categories according to mean GFP expression: low (0-25th percentile of mean fluorescence), medium (26th-49th percentile) and high (50-100th percentile).

Fluorescent recovery after photobleaching. To determine the insertion of rapsyn into receptor clusters over time, the green fluorescence at individual rapsyn-GFP expressing clusters was removed by illuminating the cluster with an Argon laser passed through a neutral density filter that blocked 50% of the light. Laser illumination of myotube clusters has been shown previously not to affect receptor dynamics or muscle cell integrity (Akaaboune et al., 2002; Bruneau et al., 2005b). The recovery of fluorescence was assayed and the amount of fluorescence recovered at each cluster was measured.

To determine the insertion of AChRs into clusters over time, receptors on untransfected myotubes were saturated with bungarotoxin-Alexa 488 (BTX-488) (5μg/ml, 1 h) (Molecular Probes, Eugene, OR) and the green fluorescence was completely removed with an Argon laser. Since newly synthesized receptors inserted into the cluster over time were unlabeled, BTX-488 was then added before each time point to label these receptors, excess BTX-488 was washed away, and the clusters were again imaged (as described by Bruneau et al, 2005). In this way the total insertion of receptors (both previously labeled receptors that had laterally migrated into the cluster, and the newly labeled receptors that had been inserted into the cluster) could be determined and compared to the insertion + lateral migration of rapsyn-GFP. For the purposes of this paper, "insertion" will refer to the accumulation of proteins at clusters both through direct incorporation from intracellular locations and from the lateral migration of surface-associated proteins.

Agrin Treatment. To determine the effect of agrin on rapsyn-GFP expression at clusters, myotubes grown on laminin-coated dishes transfected with rapsyn-GFP were incubated with BTX-594 to label all AChRs. After initial images were taken, 100 ng/ml of C-terminal agrin (R & D Systems, Minneapolis, MN) was added to the culture dish. At 4 and 8 hours, images were taken to determine the location of rapsyn-GFP and AChRs.

Kinase Inhibition. To determine the effect of various kinase inhibitors on rapsyn-GFP insertion over time, the GFP signal from clusters on myotubes transfected with rapsyn-GFP was carefully removed with an Argon laser and one of the following drugs was added to the media: 100 nM H-89 (to block PKA), 20 μM H-89 (to inhibit both PKA and PKC), 10 nM Calphostin C (to inhibit PKC) or 20 nM staurosporine (to block a broad

158

spectrum of kinases, including PKA and PKC) (drug specificity obtained from the manufacturer: Sigma, St. Louis, MO). Images were taken immediately before and after photobleaching, and 4 hours later the same clusters were re-imaged, and the fluorescent intensity at bleached and non-bleached clusters was determined. Rapsyn-GFP recovery was determined by comparing the GFP signal at bleached clusters after 4 hours to their fluorescence immediately prior to bleaching. Since the expression of rapsyn-GFP was variable over time and between different myotubes in these experiments, rapsyn-GFP insertion at each cluster was normalized to the changes in expression (if any) at control, unbleached clusters on the same myotube. Overall changes in expression in each culture dish were comparable across all treatment groups.

We also performed a series of experiments to determine the loss and insertion of receptors at individual clusters in the presence of the same pharmacological agents. To measure the insertion rate of receptors, untransfected myotubes were saturated with BTX-488 (5 μg/ml, 1 h) and the fluorescence was carefully removed from individual clusters with an Argon laser. Initial images were taken, and one of the above kinase inhibitors was added to the cultures. Four hours later, after incubating with new BTX-488 to label new receptors inserted since initial imaging, the same clusters were found and imaged. The insertion of AChRs was determined by comparing cluster fluorescence at 4 hours to the original fluorescence prior to bleaching.

To measure the loss rate of receptors, untransfected myotubes were saturated with BTX-488 (5 μg/ml, 1 h) and individual clusters were immediately imaged and incubated with one of the above mentioned inhibitors. The same clusters were then re-imaged 4 hours later and their fluorescence intensity was measured.

159

Results

Rapsyn-GFP does not affect acetylcholine receptor clustering, function or removal rate.

First, in order to verify that rapsyn-GFP was able to localize to laminin-associated AChR clusters on our cultured myotubes, we transiently transfected C2C12 myoblasts with a rapsyn-GFP fusion protein (Ramarao and Cohen, 1998). Three to four days after differentiation into myotubes, cultured cells were bathed with bungarotoxin conjugated to Alexa 594 (BTX-594) to label AChRs and receptor clusters were imaged. Rapsyn-GFP clusters were found to always perfectly co-localize with AChRs (Figure 6.1A).

We also wanted to determine if the insertion and accumulation of rapsyn-GFP at laminin-induced receptor clusters affected AChR function. To examine this question, we compared inward current across the muscle membrane in response to the application of the AChR agonist, carbachol, on myotubes expressing rapsyn-GFP and non-transfected myotubes. Under direct visual control we obtained a whole cell patch on a myotube, clamped voltage and stimulated with carbachol. We found that the inward currents were similar in both transfected and untransfected cells, and were both completely blocked by addition of the AChR antagonist curare (Figure 6.1B). These results indicate that the surface expression of rapsyn-GFP does not disrupt receptor function.

Next, we asked whether the overall density of rapsyn molecules at clusters (endogenous rapsyn + exogenous rapsyn-GFP) was increased by rapsyn-GFP expression in transfected myotubes. To examine this, myotube cultures that were transfected with rapsyn-GFP were fixed and permeabilized, and then immuno-stained with an anti-rapsyn antibody. We used an anti-rapsyn antibody that has been shown previously to recognize both rapsyn and rapsyn-GFP fusion proteins (Gervasio and Phillips, 2005). Since

160

transfection efficiency of myotubes in each culture dish was variable, we were able to use the same culture dish to determine the relative number of rapsyn molecules at non-transfected clusters and at rapsyn-GFP expressing clusters over a wide range of expression levels (Figure 6.1C). Quantitative analysis of the mean fluorescence intensity of anti-rapsyn immunostaining revealed that the average density of total rapsyn at rapsyn-GFP expressing clusters was 12.5 ±3.2 SD. (arbitrary units), n=198. This is nearly identical to the density at clusters containing only endogenous rapsyn (11.8 ±3.2 SD, n=123) (Figure 6.1C-E). Even over a nearly 10 fold range of rapsyn-GFP expression at clusters, the difference in total rapsyn density was negligible (Figure 6.1E). It is possible that the number of rapsyn-GFP molecules at transfected clusters is negligible compared to the total number of endogenous rapsyn molecules. In this case the presence of exogenous rapsyn-GFP would not detectibly alter overall rapsyn density. Alternatively, it is possible that exogenous rapsyn-GFP replaces the endogenous rapsyn allowing overall rapsyn density at clusters to remain constant (see discussion).

Finally, we wanted to determine whether rapsyn-GFP expression levels at clusters had any effect on AChR stability. To do this, transfected myotubes were saturated with BTX-594 and receptor loss was monitored at clusters expressing low, medium and high levels of rapsyn-GFP on two separate myotube cultures. After 4 hours, we found that 65% ±15 SD, (n = 29) of fluorescently labeled AChRs remained at clusters expressing low rapsyn-GFP fluorescence, 60% ±13 SD, (n = 42) remained at clusters expressing medium rapsyn-GFP and 62% ±15 SD (n = 44) remained at clusters expressing high rapsyn-GFP. These results are similar to fluorescence remaining after 4 hours at AChR

clusters expressing no rapsyn-GFP (63% ±17 SD, n = 77) (Figure 6.2A-C). This indicates

that rapsyn-GFP expression has no effect on AChR stability in our culture system.
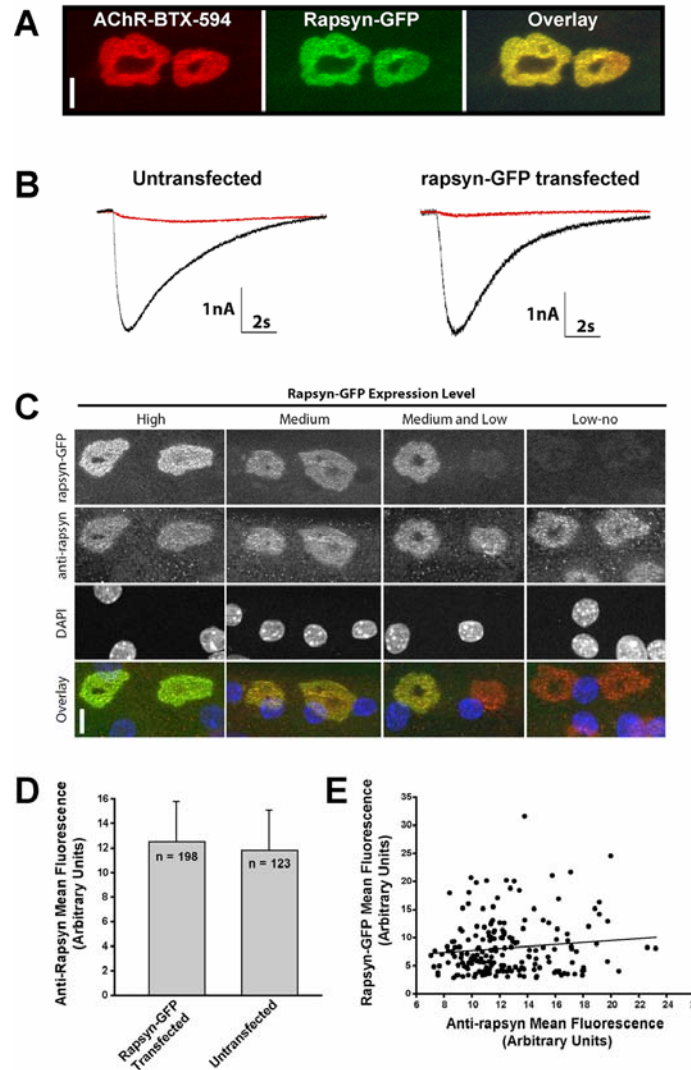
Figure 6.1. Rapsyn-GFP cluster expression does not alter AChR clustering, stability or activity.
(A) Example of a myotube transfected with rapsyn-GFP and labeled with bungarotoxin-Alexa 594.
Shown are representative clusters in which rapsyn-GFP perfectly co-localizes with acetylcholine
receptors. Scale bar = 20 μm. **(B)** Untransfected myotubes and myotubes expressing rapsyn-GFP
responded similarly to the application of the AChR agonist, carbachol, and this response was blocked
after the addition of the AChR antagonist, curare, indicating that AChR function is not disrupted by
rapsyn-GFP. **(C)** Example of myotubes expressing different levels of rapsyn-GFP at clusters that were
labeled with anti-rapsyn antibodies and DAPI to stain nuclei. Images illustrate that overall rapsyn
density is the same in rapsyn-GFP expressing clusters and in clusters that do not express rapsyn-GFP.
Scale bar = 20 μm. **(D)** Histogram showing the mean fluorescence intensity of anti-rapsyn staining from
many clusters of non-transfected myotubes and myotubes transfected with rapsyn-GFP. Note that the
mean fluorescence is comparable in both transfected and untransfected myotube clusters. Histograms
represent mean fluorescent intensity ±SD. **(E)** Quantification of rapsyn immuno-fluorescence and
rapsyn-GFP for many clusters on transfected myotubes. As shown by the scatter plot, rapsyn-GFP
fluorescent expression at clusters did not correlate with total rapsyn density.
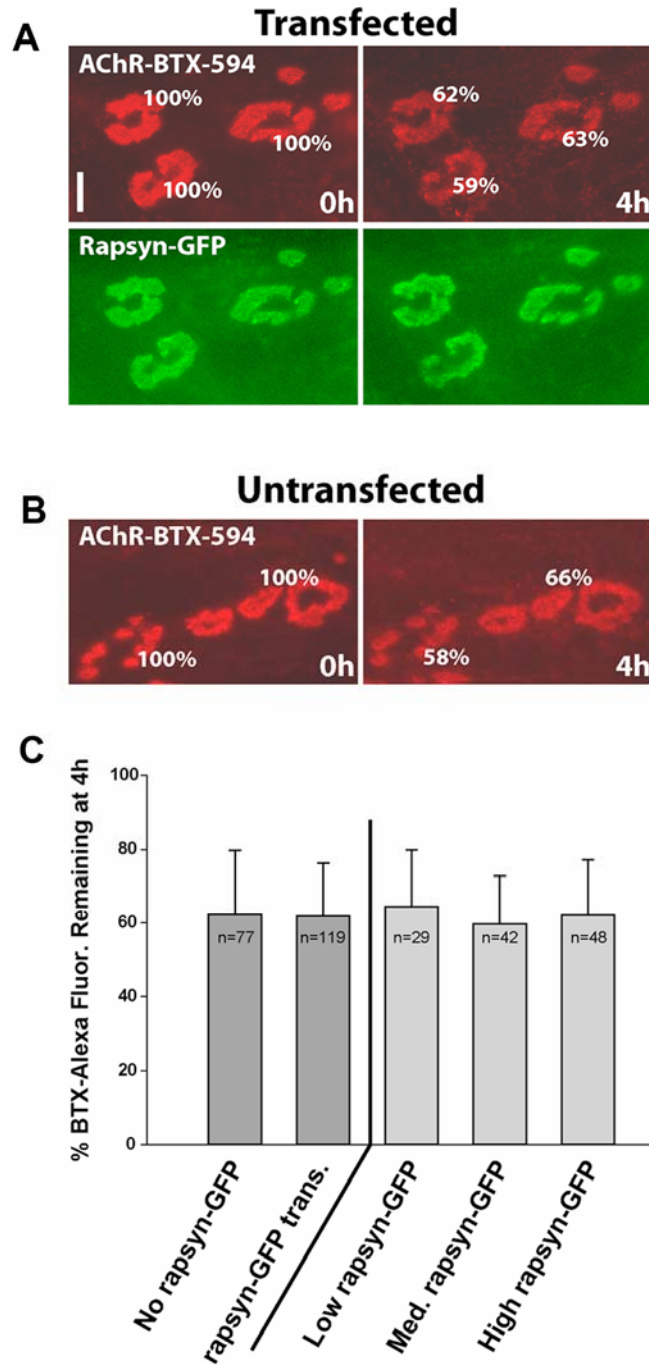
Figure 6.2. The cluster expression of rapsyn-GFP has no effect on AChR removal. Non-transfected myotubes and myotubes transfected with rapsyn-GFP were labeled with BTX-Alexa 594 and the loss of AChR-BTX-594 was monitored over 4 hours. **(A)** Example of clustered AChRs on rapsyn-GFP transfected myotubes that were labeled with BTX-594, imaged, and imaged again 4 hours later to determine the receptor loss rate. **(B)** Clustered AChRs on untransfected myotubes were labeled as above and also followed over 4 hours. **(C)** Histogram summarizes data obtained from many clusters on transfected and untransfected myotubes. Note that the change in fluorescently labeled AChR levels monitored over 4 hours on untransfected myotubes and at myotube clusters expressing a wide range of rapsyn-GFP were not significantly different ($p > 0.3$). All values represent mean ±SD.

163

Recovery rate of rapsyn-GFP at individual myotube clusters.

Having found that rapsyn-GFP has no effect on the clustering, function or turnover of AChRs, we wanted to determine the lifetime of rapsyn at individual clusters. To do this, transfected myotubes expressing rapsyn-GFP were imaged and then the GFP at individual clusters was removed with an Argon laser. Confirmation of the removal of fluorescence was done by acquiring a second image (Figure 3A). We then monitored the recovery of fluorescence at bleached clusters over time from a number of cultures (data from 3-5 culture dishes at each time point). We found that rapsyn clusters recovered fluorescence very rapidly, gaining 61% ($\pm$11 SD, n = 40) of original fluorescence after only 2 hours, 71% ($\pm$19 SD, n = 56) after 4 hours, and 75% ($\pm$18 SD, n = 58) after 6 hours (Figure 6.3A,B). The recovery at each data point was nearly identical for rapsyn-GFP clusters from myotubes not grown on laminin (2h: 63% $\pm$12 SD, n = 35; 4h: 73% $\pm$17 SD, n = 15; 6h: 78% $\pm$21 SD, n = 33) (Figure 3A, B). This recovery was not due to reversible bleaching of GFP, because no fluorescence was observed after bleaching rapsyn-GFP clusters on fixed myotubes. In addition we found that the recovery of rapsyn-GFP over 4 hours was not affected by rapsyn-GFP expression levels (Figure 6.3C).

Given this rapid rate of rapsyn insertion, and past reports suggesting that rapsyn is co-transported with AChRs to the cell surface (Marchand et al., 2000; Marchand et al., 2002), we wanted to determine the rate of AChR insertion into individual clusters using the same FRAP method. To do this, myotubes were bathed with a single saturating dose of BTX-488 and then all fluorescence was carefully removed from individual clusters with an Argon laser. After 2, 4 or 6 hours a second dose of BTX-488 was added to label all AChRs that had been inserted into clusters over this time. We found that 15% ($\pm$4 SD, n = 30) of original fluorescence was returned to the clusters after 2 hours, 25% ($\pm$7 SD, n

= 54) after 4 hours, and 28% (±9 SD, n = 39) after 6 hours (data obtained from 3-5 cultures per data point) (Figure 6.3A,B). The number of AChR molecules inserted over time was therefore significantly lower than the number of rapsyn-GFP molecules inserted over the same time period (see discussion).

Given the large amount of rapsyn-GFP recovery during the first 2 hours, we wanted to monitor more closely the insertion of rapsyn-GFP immediately after photobleaching. To do this, rapsyn-GFP clusters on transfected myotubes were bleached, and time-lapse imaging was used to monitor the fluorescent recovery every 15 minutes at room temperature. We found that rapsyn-GFP recovery was 11% ±4 SD, 17 % ±5 SD, 23% ±9 SD and 27 % ±11 SD at 15, 30, 45, 60 min (n=15 clusters/3 culture dishes) (Figure 6.3D,E). The rapid recovery of fluorescence observed in clusters is not due to reversible bleaching of the fluorophore, as rapsyn-GFP clusters on fixed myotubes that are bleached show no spontaneous fluorescence recovery, even over days (data not shown). We also found that the labeling of AChRs with BTX-647 also had no effect on rapsyn insertion dynamics, as rapsyn insertion measured by FRAP was identical at rapsyn-GFP expressing clusters that were not labeled with any BTX, and at rapsyn-GFP expressing clusters that were saturated with BTX-647 prior to photobleaching (data not shown).
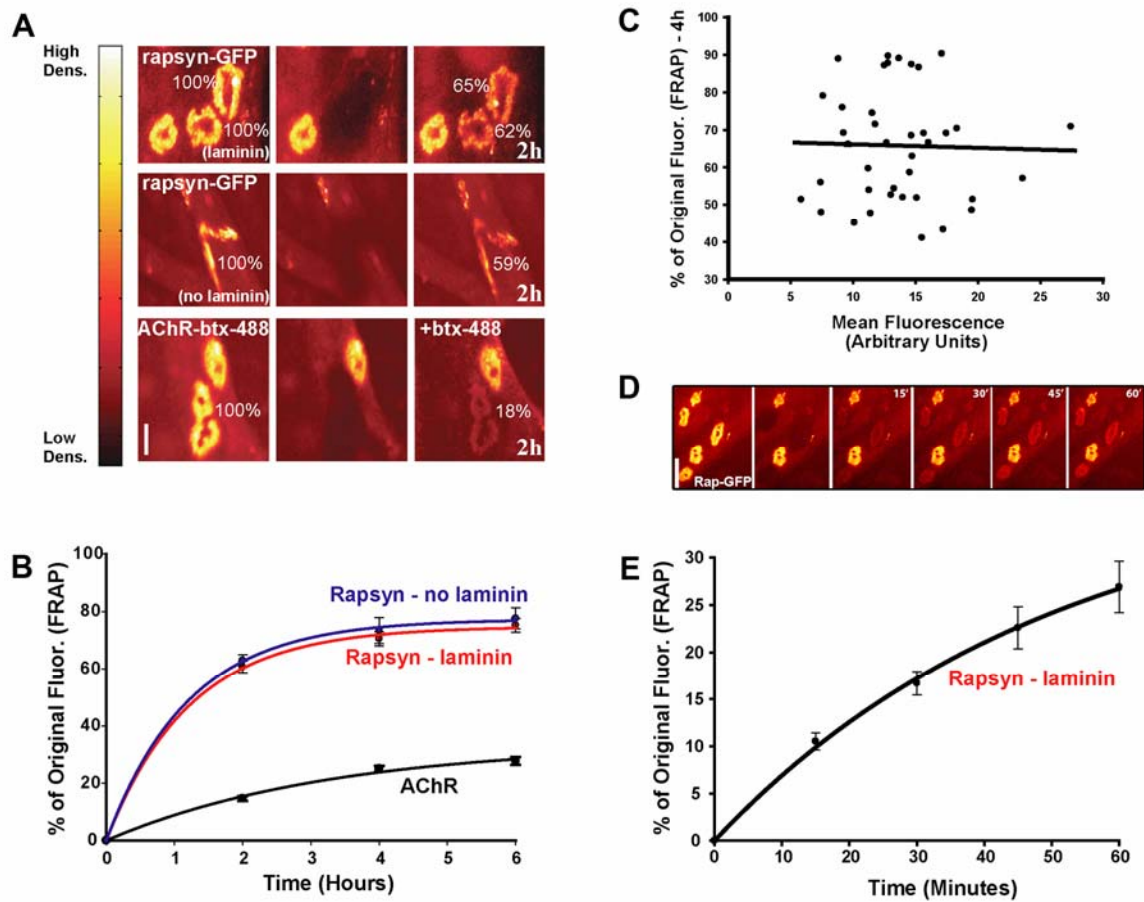
Figure 6.3. Rapsyn is inserted rapidly into individual clusters. (A) The insertion of rapsyn-GFP into individual clusters on myotubes grown either on laminin-coated dishes or uncoated dishes was measured by determining the fluorescent recovery after photobleaching using quantitative fluorescent imaging. The insertion of rapsyn-GFP into bleached laminin-associated clusters (top panels) and non-laminin clusters (middle panels) is rapid and nearly identical over two hours in both cases. In contrast, acetylcholine receptor clusters that were labeled with bungarotoxin-Alexa 488, bleached, and then incubated in new bungarotoxin-488 (bottom panels) show far fewer inserted AChRs over the same time period. **(B)** Graph summarizes the data from the recovery of rapsyn and AChRs at 2, 4 and 6 hour time points. **(C)** The rate of rapsyn-GFP insertion is independent of the level of rapsyn-GFP expression. **(D)** Sample images from a time-lapse experiment in which the fluorescent recovery at a number of clusters was determined every 15 minutes for 60 minutes. **(E)** Results from 3 experiments performed as in (D) (n=15 clusters). Note that the recovery of fluorescence is > 25% after 1 hour even though cells were maintained at room temperature for the duration of the experiment. All graph points for (B) and (E) represent mean ± SEM, and all data were fit well by single exponential curves. Scale bars = 20 μm.

166

The clustering of AChRs and rapsyn are altered similarly by agrin treatment

In order to determine if rapsyn and AChRs are regulated similarly despite the difference in dynamics, we attempted to manipulate AChR stability and insertion using the neuronal clustering factor, agrin. Our previous results showed that when agrin was added to myotubes grown on a laminin substrate, most new receptors were not directed into pre-existing laminin-induced clusters but instead formed numerous small aggregates on the entire muscle surface (Bruneau et al., 2005b). Since rapsyn is required for the clustering of AChRs, and its interaction with the receptor is highly regulated and increased by agrin (Moransard et al., 2003), we wanted to know whether newly inserted rapsyn molecules are also directed away from pre-existing laminin-associated clusters and into new, agrin-induced clusters when agrin is added to the cultures. To investigate this issue, transfected myotubes expressing rapsyn-GFP were labeled with BTX-594, imaged, treated with agrin and then imaged again 4 and 8 hours later. Over the time-course of our study we found that rapsyn clustering was altered similarly to AChRs, being directed away from the same regions on laminin-associated clusters and inserted into the same agrin-induced clusters (Figure 6.4).
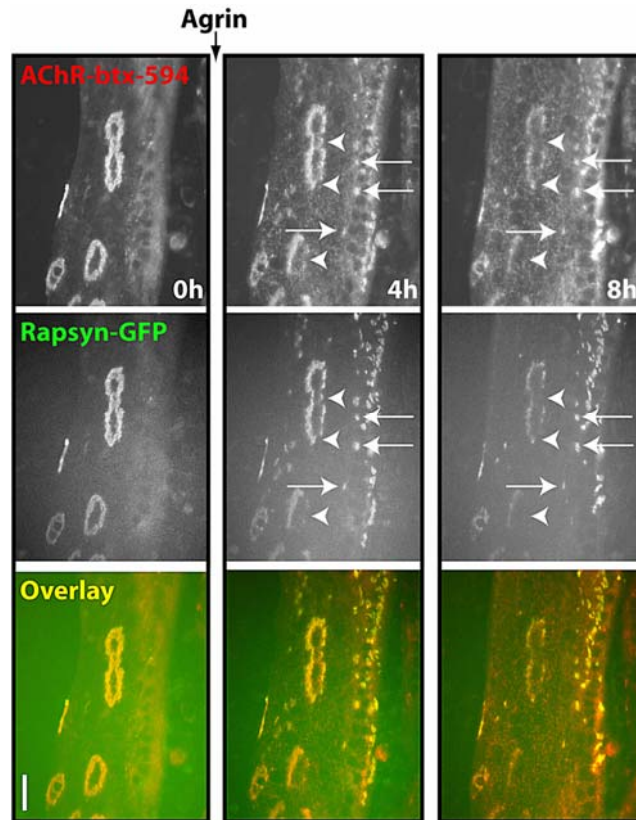
Figure 6.4. Agrin redirects both AChRs and rapsyn away from pre-existing laminin clusters and into new agrin-induced clusters. Myotubes expressing rapsyn-GFP were incubated with BTX-594 to label all AChRs. Agrin was then added to the culture media and rapsyn and receptors were imaged 4 and 8 hours later. Note that both AChRs and rapsyn were directed away from some locations on the pre-existing laminin-associated clusters (arrowheads) and were also aggregated together into new, agrin-induced clusters (arrows). Scale bar = 20 μm.

Effect of kinase inhibition on Rapsyn-GFP and AChR dynamics.

Having found that AChRs and rapsyn respond similarly to agrin treatment, we wanted to extend our analysis to determine if alterations in kinase activity could affect rapsyn and AChRs in a similar manner. Previous studies have shown that agrin-induced clustering of AChRs can be inhibited by the broad spectrum kinase inhibitor, staurosporine (Wallace, 1994; Ferns et al., 1996; Marangi et al., 2002). To further investigate the role of kinase activity on receptor and rapsyn dynamics at single clusters, we performed a series of experiments using various kinase inhibitors. As a first step we

used the broad spectrum kinase inhibitor, staurosporine. To study the effect of staurosporine on receptor insertion, cultured myotubes were labeled with BTX-488, and clusters were imaged and photobleached. Cells were then incubated with 20 nM staurosporine and 4 hours later the cells were bathed with new BTX-488 to label all new receptors. We found that the number of AChRs accumulated at bleached clusters was significantly decreased to 18 % (±5 SD, n=15, p<0.0001) of the original receptor density, compared to 28% (±6 SD, n=20) for control clusters (Figure 6.5A,B).

Since staurosporine inhibits PKC, PKA and other kinases, we wanted to more specifically determine the effect of PKA and PKC on receptor insertion. To do this, myotubes were labeled with BTX-488 as above and the recovery of fluorescence in bleached clusters was monitored in the presence of 100nM H-89 (to specifically block PKA), 20 nM H-89 (to block PKA and PKC) or 10 nM Calphostin C (to specifically block PKC). We found that 100 nM H-89 had no effect on receptor insertion (27% ±8 SD, n=20) compared to controls. However, in the presence of 20 μM H-89, the accumulation of new receptors at bleached clusters decreased to 23% (±4 SD, n=21, p<0.005). Similar results were obtained when PKC was more specifically inhibited by 10 nM Calphostin C (21% ±6 SD, n=20, p<0.005). At higher concentration of Calphostin C (> 50 nM), most cells were dead after 4 hours. These experiments suggest that PKC activity is somehow involved in the insertion of receptors (Figure 6.5B).

Next we asked whether AChR loss was also affected by kinase inhibition. To answer this question, cells were labeled with BTX-488 and individual receptor clusters were imaged and then incubated with one of the same drugs used in the above experiments before being imaged again at 4 hours. At clusters on untreated control

myotubes, 72% of original fluorescence remained after 4 hours (±8 SD, n=15). When cells were treated with 100 nM H-89, 20 μM H-89 or 10 nM Calphostin C, there was no difference in receptor loss compared to control (68% ± 9 SD, n=23; 71% ± 10, n=10; 73% ± 12, n=20) (Figure 5D). However, incubation in 20 nM staurosporine resulted in an increase in receptor removal from clusters, with only 52% of original fluorescence remaining at clusters after 4 hours (±10 SD, n=21, p<0.0001) (Figures 6.5C,D). These results suggest that staurosporine, in addition to inhibiting AChR insertion, increases receptor removal from clusters in a non PKC/PKA-dependent manner.

Finally, we investigated whether rapsyn-GFP insertion is similarly affected by kinase inhibition. To do this, myotubes expressing rapsyn-GFP at clusters were imaged and the fluorescence was removed from individual clusters using an Argon laser. Bleached clusters were then imaged and staurosporine (20 nM), H-89 (100 nM or 20 μM) or Calphostin C (10 nM) were added to the cultures, and the rate of rapsyn-GFP insertion into the bleached clusters was determined at 4 hours. We found that bleached clusters regained 67% (±15 SD, n = 37), 64% (±15 SD, n = 10), 67% (±15 SD, n = 16) and 76% (±11 SD, n = 19) of their original fluorescence, respectively (Figure 6.5E,F). The insertion at bleached clusters was normalized to the changes in expression (if any) at control, unbleached clusters on the same myotube. It should be noted that higher concentrations (200 nM) of staurosporine did result in a significant decrease in rapsyn-GFP insertion over 2 hours (clusters were too dim to be imaged after 4 hours) that was similar to the decrease in AChR insertion measured over the same time period. However, it seems likely that this was due to decreased cell viability, as has been observed previously (Wallace, 1994).
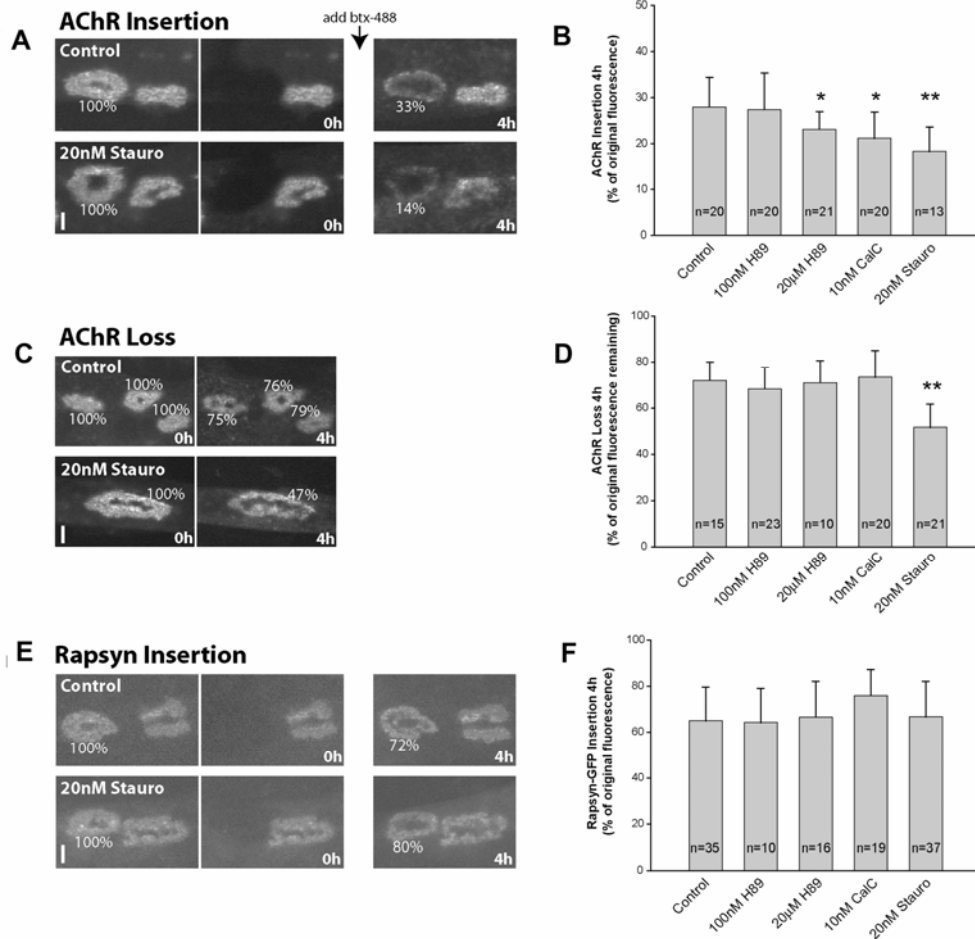
Figure 6.5. Kinase inhibitors alter AChR dynamics, but not the dynamics of rapsyn-GFP.
Laminin-associated clusters on rapsyn-GFP transfected myotubes were bleached, and on non-transfected myotubes AChRs were labeled with BTX-488 before bleaching individual clusters. Cells were then incubated in either 100 nM H-89, 20 μM H-89, 10 nM Calphostin C or 20 nM staurosporine. Myotubes were imaged and the fluorescence at each cluster was compared to its original fluorescence. **(A)** Example of clusters that were bleached on either control or 20 nM staurosporine treated myotubes. **(B)** Graph summarizes data obtained from many clusters in untreated control cultures and in cultures incubated with one of the above drugs. Note that PKA inhibition alone had no effect on AChR insertion, while the blockade of PKC (with higher concentrations of H-89 and with Calphostin C) resulted in a significant decrease in AChR insertion. Inhibition of a broader spectrum of kinases along with PKC by staurosporine caused a slightly greater inhibition of AChR insertion. **(C)** Representative clusters showing loss of receptors from control myotubes or myotubes treated with 20 nM staurosporine. **(D)** AChR loss from individual clusters in the presence of the same kinase inhibitors shows that only incubation with staurosporine caused a decrease in overall receptor density remaining at clusters after 4 hours, indicating that the blockade of kinases other than PKA and PKC with staurosporine treatment resulted in the accelerated removal of AChRs from clusters. **(E)** Representative images of control and staurosporine-treated myotubes that are expressing rapsyn-GFP. **(F)** Clusters expressing rapsyn-GFP were bleached, and the insertion of rapsyn was measured by determining the recovery in fluorescence over time in the presence of the same drugs as used above. Note that the insertion of rapsyn-GFP was not altered by any of the drug treatments. Insertion into clusters was normalized to the changes in fluorescence at neighboring, unbleached clusters on the same myotube. All bar graphs represent mean ±SD. * indicates p-values < 0.005, ** indicates p-values < 0.0001 on a Student's T-test. Scale bars = 10 μm.

171

Discussion

In this study, we investigated the dynamics of rapsyn in cultured myotubes and found that rapsyn is remarkably dynamic compared to AChRs. Further, although the localization of both rapsyn and receptor were similarly affected by agrin treatment, their dynamics were differentially regulated by kinase inhibition.

One unexpected finding from this work is the rapid recovery of rapsyn-GFP fluorescence at individual clusters after photobleaching. For a number of reasons, we believe that the fused GFP is not interfering with rapsyn function, and that the recovery in fluorescence observed in our studies therefore reflects the turnover rate of rapsyn. First, it has been shown previously that the rapsyn-GFP construct used in the present studies is indistinguishable from wild-type rapsyn in its ability to associate with and cluster AChRs in heterologous cells (Ramarao and Cohen, 1998). Second, the present work demonstrates that rapsyn-GFP expression at clusters does not alter receptor function, clustering or turnover in muscle cells. Third, the rapid recovery of fluorescence after photobleaching was independent of rapsyn-GFP expression at myotube clusters (Figure 3). Finally, the accumulation of rapsyn-GFP at clusters was regulated by agrin in a similar manner as AChRs. Consistent with these observations, it has been shown that fluorescent rapsyn also recovers rapidly after photobleaching in QT-6 cells (Gervasio and Phillips, 2005). The remarkable dynamism of rapsyn at surface clusters is further supported by biochemical studies which show that the metabolic turnover of rapsyn is short compared to AChRs, with a metabolic half-life of ~ 3 hours (Frail et al., 1989). Since our studies were done on aneural receptor clusters, it is possible that the turnover of rapsyn might be decreased under the influence of the nerve. Further studies investigating the dynamics of

172

rapsyn at the NMJ will be necessary to determine if rapsyn is indeed stabilized by innervation. Although we cannot definitively exclude the possibility that GFP may diminish the affinity of rapsyn for the AChR or other scaffold proteins, these results argue strongly that rapsyn-GFP behaves as endogenous rapsyn, and that rapsyn therefore turns over very rapidly in muscle cells.

While our studies indicate that the acetylcholine receptor-associated protein turns over more rapidly than AChRs, recent studies on the turnover of receptor-associated proteins at glutamatergic synapses have yielded analogous results. For example, PSD-95, a dynamic protein affiliated with the AMPA and NMDA receptors (Rutter and Stephenson, 2000; Chetkovich et al., 2002; Choi et al., 2002; El-Husseini Ael et al., 2002; Schnell et al., 2002; Cai et al., 2006), when tagged with GFP and measured with FRAP was shown to turn over very rapidly relative to the glutamate receptors with which it associates (Rasse et al., 2005; Sharma et al., 2006a). This result opens the possibility that the rapid turnover of rapsyn observed in muscle cells in the present study may be similar to the behavior of receptor-associated proteins in the central nervous system.

Previously it has been shown that AChRs and rapsyn are transported together in the same intracellular vesicles from the Golgi complex to the membrane surface both in COS cells co-transfected with AChRs and rapsyn, and at the mature torpedo electric organ (a structure analogous to the mammalian NMJ) (Marchand et al., 2000; Marchand et al., 2002). While the ratio of rapsyn to receptor during intracellular trafficking remains undetermined, estimates from our results suggest that multiple rapsyn molecules may accompany each AChR to the membrane surface in aneural myotubes.

In addition to highlighting the difference in turnover between receptors and rapsyn, the present study also shows that the expression of exogenous rapsyn at clusters does not increase receptor stability. The effect of exogenous rapsyn on AChR dynamics has previously been studied in heterologous cells. In these studies, the effect of rapsyn on AChR stability was determined by comparing the degradation of radioactive-bungarotoxin in heterologous cells devoid of endogenous rapsyn to cells transfected with rapsyn cDNA (15,29,30). They found that the metabolic half-life of receptors was increased upon co-expression with rapsyn. A recent study also indicates that the over-expression rapsyn through electroporation of rapsyn-GFP into muscle cells *in vivo* can stabilize receptors (Gervasio and Phillips, 2005). This *in vivo* result is further supported by findings that mutant rapsyn results in a decrease in receptor stability in some forms of myasthenia gravis (Ohno et al., 2002). By contrast, our results indicate that rapsyn-GFP expression at clusters did not alter AChR stability. This result can be explained by two possibilities. First it is conceivable that that exogenous rapsyn-GFP is able to replace endogenous rapsyn at clusters without increasing rapsyn density, as demonstrated by quantitative immuno-fluorescence (Figure 1C-E). It is also possible that despite the strong GFP fluorescence signal, the number of exogenous rapsyn-GFP molecules inserted at clusters was negligible compared to the density of endogenous rapsyn. It is important to mention that the anti-rapsyn antibody used for assaying the total rapsyn content has been shown to recognize both endogenous rapsyn and exogenous rapsyn-GFP (Gervasio and Phillips, 2005).

Despite the difference in turnover between rapsyn and AChRs, our work indicates that both rapsyn and AChRs are subject to similar modulation following treatment with

174

neural agrin. Previously, work from our lab has shown that when AChRs at laminin-associated clusters are treated with agrin, most new receptors are not directed into pre-existing laminin-induced clusters but instead form numerous small aggregates on the entire muscle surface (Bruneau et al., 2005b). The present work extends this observation and demonstrates that when agrin is added to myotubes, rapsyn-GFP is directed into the new aggregates to co-localize with AChRs, suggesting that rapsyn and AChRs are responding to agrin similarly and simultaneously. It is possible that the redirection of AChRs into small aggregates is driven by the rapsyn, since rapsyn is the bridge between biological activity following agrin treatment and receptor clustering. This idea is supported by experiments showing that AChRs fail to associate with cytoskeletal proteins in agrin treated myotubes devoid of rapsyn (Fuhrer et al., 1999; Mittaud et al., 2001). In fact, AChRs fail to cluster at all *in vitro* or *in vivo* when rapsyn is not present (Apel et al., 1995; Gautam et al., 1995; Ramarao and Cohen, 1998). On the other hand, there is also reason to believe that rapsyn could instead follow AChRs to clusters. For example, in the absence of receptors, rapsyn fails to cluster (Marangi et al., 2001; Ono et al., 2001) (Bruneau et al., unpublished results).

Although rapsyn and AChR are intimately associated and similarly directed by agrin, the mechanisms regulating their delivery and removal from individual clusters are at least partially distinct. While PKA inhibition with 100 nM H-89 had no effect on the insertion of rapsyn or AChRs, or on the loss of AChRs from individual clusters, inhibition of PKC with higher concentrations of H-89 (20 μM) or 10 nM Calphostin C significantly decreased AChR insertion without affecting AChR loss or rapsyn insertion. The broad-spectrum kinase inhibitor staurosporine was able to further decrease AChR

insertion, and resulted also in the increase in AChR removal without altering rapsyn insertion. Previous work has shown that the *in vivo* inhibition of PKC by Calphostin C injection retards the development of neuromuscular synapses (Lanuza et al., 2002). Although our cells are aneural, they were plated on laminin, which has been shown to mimic, at least in some respects, the development of the neuromuscular junction (Kummer et al., 2004). Therefore, it is possible that the mechanism by which PKC inhibition decreases AChR insertion in our system could account for the alterations in post-synaptic growth observed when PKC is blocked *in vivo* by the same pharmacological agent. The fact that staurosporine increases the removal of AChRs in addition to decreasing their insertion implies that staurosporine may act to increase AChR dispersal through a non-PKA/PKC-dependent mechanism. In support of this conclusion, it has been shown previously that non-PKC-dependent tyrosine phosphorylation contributes to receptor clustering. For example, Src class kinases promote the phosphorylation of the beta subunit and increase the association of AChRs with the intracellular cytoskeleton (Fuhrer and Hall, 1996; Mohamed and Swope, 1999; Mohamed et al., 2001; Sadasivam et al., 2005), and agrin-induced receptor clusters are removed rapidly in the absence of Src class kinases (Mohamed et al., 2001).

Our results show that rapsyn-GFP insertion was not affected by any of the kinase inhibitors used. This may indicate that the synthesis and delivery of rapsyn to individual clusters is independent of the phosphorylation either of rapsyn or of proteins that are necessary for rapsyn exocytosis. Previous reports have shown that receptors and rapsyn are co-transported in the same vesicle and inserted into the plasma membrane. It is possible that the difference in the amount of receptor and rapsyn insertion when cultured

cells were treated with PKC inhibitor could therefore be due to impaired transcription of receptors compared rapsyn.

Acknowledgements

Chapter VIII

Conclusion

Summary

In this thesis I have described a body of work that has investigated the dynamics and regulation of acetylcholine receptors and scaffolding proteins, as well as the interactions between these post-synaptic protein populations, both *in vitro* in cultured myotubes, and *in vivo* in the living mouse neuromuscular junction. While AChR dynamics have been studied for over 3 decades at the mouse neuromuscular junction with radio-labeled bungarotoxin, the availability of fluorescently conjugated bungarotoxin and recent advances in fluorescence microscopy have enabled a mini-renaissance in our understanding of AChR dynamics and the regulated development of the neuromuscular synapse. It is in this context that I began my work in Mohammed Akaaboune's lab. The highlights of my work include the following: the identification of an interaction between agrin and substrate laminin that causes a shift in clustering that is reminiscent of the shift from pre-patterned AChR clusters to agrin-induced neuromuscular junctions; the identification of a previously unknown recycled receptor pool *in vivo*, which we found to be highly dynamic and regulated by post-synaptic activity, but that is absent *in vitro*; characterization of a novel method by which to induce the dissipation of Alexa 594 labeled AChRs with low-intensity laser light, which enabled us to determine that AChRs are critical organizing components of the post-synaptic scaffold; analysis of rapsyn

dynamics *in vitro*, which showed that rapsyn is more dynamic than the receptors to which it binds, and indicated that the turnover of rapsyn and AChRs are differently regulated by phosphorylation. The background of the field and my specific contributions to our current understanding are summarized in the following sections.

Synaptic development

Although neural agrin has been identified as the nerve clustering factor essential for the development of the mature neuromuscular junction (McMahan, 1990; Reist et al., 1992), the spontaneous clustering of AChRs and scaffolding components occurs even in aneural cultured myotubes. Agrin-independent clustering of post-synaptic components requires rapsyn and the receptors themselves and has been shown to be induced by the extracellular matrix protein, laminin (Montanaro et al., 1998; Marangi et al., 2002). During development AChR clusters also form prior to innervation near the site of eventual innervation, raising the possibility that pre-patterned junctions may be replaced by agrin-induced AChR clusters upon innervation. Although recent work suggests that nerves can be induced to grow to pre-patterned clusters of MuSK (Kim and Burden, 2008), high resolution time-lapse imaging is not possible *in utero*, so the question of whether incoming nerve terminals grow to the pre-patterned junctions or whether they replace these junctions with new AChR clusters is still not clearly understood. In my work I used an *in vitro* system to examine this question (Bruneau et al., 2005b). To do this I first cultured C2C12 myotubes on a laminin substrate to stimulate the formation of large, topologically complex AChR clusters and then identified receptor clusters by incubating the cells with fluorescent bungarotoxin. By adding soluble agrin to the media and then adding new fluorescent bungarotoxin to the cell cultures at later time points, I

179

was then able to track the formation of new clusters and the fate of originally imaged laminin-induced clusters. From these studies I found that new, agrin induced clusters grew quickly over the course of hours, while laminin-induced clusters rapidly dissipated. The addition of agrin therefore resulted in the re-distribution of receptors to new, agrin-induced clusters and re-directed the insertion of new receptors to these clusters. While the mechanism by which agrin negates laminin clustering is not known, this data supports a model of agrin-induced NMJ formation in which pre-patterned AChR clusters are replaced by new, agrin-induced clusters after innervation during synaptic development *in vivo*.

Receptor dynamics

Once the synapse is formed and the cluster has gained a more mature, pretzel-shaped topology, receptor density and cluster architecture is maintained over months. Beginning nearly 40 years ago AChR turnover studies relied mostly on radio-labeling, which required the removal of the muscle to assay receptor density (Fertuck and Salpeter, 1974, 1976). A common finding from these studies was that two populations of AChRs existed at the NMJ: one that turns over rapidly and one that turns over more slowly. More recently the availability of fluorescent bungarotoxin conjugates and the development of quantitative fluorescent imaging allowed the investigation of receptor density over time at the same junction in the living muscle. These studies demonstrated that the synaptic dwell-time of AChRs is dependent upon synaptic activity: when the synapse is active, synaptic turnover is slow, and when synaptic activity is blocked, turnover increases (Akaaboune et al., 1999). This indicates that rather than two different populations of receptors with distinct turnover rates, AChR turnover is activity-dependent, with turnover

decreasing over time when synaptic activity slowly recovers as new, unlabeled (and thus unblocked) AChRs are progressively inserted into the synapse. In addition to synaptic activity, recent evidence also indicates that scaffolding proteins are involved in AChR turnover. For example, the rate of AChR removal is significantly increased in mice deficient in dystrobrevin, and AChRs are stabilized in the membrane after co-transfection with rapsyn in heterologous cells (Wang et al., 1999b; Akaaboune et al., 2002).

While it has been recognized for many years that the insertion, lateral mobility and removal of receptors provides a dynamic equilibrium that enables the AChR density to remain relatively constant, underlying this was an assumption that unlike receptors in central synapses, AChRs make a one way trip to be degraded following removal from the membrane. This question had not been directly investigated, though, since there was no method with which to study receptor recycling *in vivo*. This limitation was overcome in our lab by using a two-step labeling method (Bruneau et al., 2005a; Bruneau and Akaaboune, 2006a). In this technique, AChRs *in vivo* were labeled first with btx-biotin and then strept-Alexa. The binding at later time points of new strept-Alexa indicated that these labeled AChRs had lost their original strept-Alexa tag while retaining their btx-biotin label. Since a number of controls determined that this biotin-streptavidin dissociation does not happen at the muscle surface, this result indicated that a significant number of AChRs were internalized, stripped of their strep-Alexa tag and then returned to the muscle surface. We found that this AChR recycling mechanism was rapid and robust, inserting recycled AChRs into the synapse within 2 hours and inserting a large number of receptors into the synapse over time. Following post-synaptic activity blockade receptor recycling was inhibited, and even more suppressed than the insertion

of newly synthesized receptors. Surprisingly, we found also that recycled AChRs turn over more rapidly than non-recycled AChRs despite being intermingled in the same post-synaptic membrane, arguing that the recycled receptor pool is specifically regulated. In agreement with this idea, we found that recycled AChRs are selectively mistargeted to perisynaptic sites by phosphatase inhibition. Finally, receptor recycling was found to be absent *in vitro*, indicating that the activation of recycling may be activated by innervation. Together these studies identified and characterized a previously unknown receptor recycling mechanism that provides a significant portion of the AChRs at the mature NMJ and enables post-synaptic receptor density to remain constant over time.

Receptor-scaffold interactions

Anchoring the AChR in place at the NMJ is a complex of proteins that collectively make up the post-synaptic scaffold. Naturally occurring mutations, genetic knockouts and protein truncations have revealed the essential role that a number of these proteins play in the initiation of AChR clustering. For example, MuSK, Dok-7 and rapsyn knockouts do not form mature neuromuscular junctions at motor nerve terminals, and muscle cells from these mice do not form spontaneous clusters when cultured *in vitro* (Gautam et al., 1995; DeChiara et al., 1996; Okada et al., 2006). Other post-synaptic density (PSD) proteins affect AChR density more subtly. Deletions in utrophin, for example, disrupt AChR organization by decreasing post-synaptic folding, but have little effect on AChR density or turnover (Deconinck et al., 1997; Grady et al., 1997). Alpha-dystrobrevin knockouts, on the other hand, show a dramatic decrease in post synaptic AChR density and an increase in AChR turnover (Akaaboune et al., 2002). Even while these knockout mice indicate that a complex network of post-synaptic proteins enable

proper AChR clustering, it was not clear whether AChRs are required for the establishment and maintenance of the scaffolding complex.

It was in this context that I stumbled upon an interesting interaction between low-power laser emission and bungarotoxin Alexa 594 conjugates that resulted in the dissipation of AChRs from illuminated spots (Bruneau et al., 2008). This serendipitous discovery enabled me to directly investigate a number of AChR-scaffolding protein interactions. From these studies I found first that the laser-induced dissipation of AChRs from individual clusters on C2C12 myotubes resulted in the complete dissipation of rapsyn, dystroglycan, utrophin and scaffold-specific actin from the illuminated clusters without affecting the muscle membrane or intracellular cytoskeleton. This indicates that AChRs are not only necessary for the formation of post-synaptic scaffolds in skeletal muscle cells, but that a high density of AChRs is required to maintain the post-synaptic scaffold and enable new scaffolding proteins to accumulate at that spot. Further, since dissipation of AChRs and associated scaffolding proteins occurred only from illuminated regions, even from small regions within individual clusters, it seems likely that the AChRs and scaffolding proteins are organized not as a complex network of cross-linked proteins, but rather as modular units of AChRs and their associated scaffolding components that can be untethered from surrounding scaffold and locally removed. Finally, not all receptors in a given region needed to be labeled with btx-594 and illuminated in order for the entire AChR density and intracellular scaffold to dissipate. This indicates that a critical density of AChRs may be required in order for the local intracellular scaffolding proteins to accumulate and be maintained. Since these studies

183

were performed on muscle cell cultures, it remains to be seen whether this effect will be applicable *in vivo*.

Receptor-associated protein dynamics

Over the past decades, AChR dynamics have been extensively studied, while the movement and regulation of scaffolding proteins have received little attention. Since many lines of evidence indicate that dynamic changes in the post-synaptic apparatus (receptors and associated scaffolding proteins) may underlie synaptic plasticity during development, learning and memory, recent work has turned towards investigating the dynamics of the intracellular receptor scaffold.

What remains unclear about the scaffold is the stability and potential regulation of the scaffolding proteins with which the receptors associate. The lack of information about scaffolding protein dynamics is largely due to the inaccessibility of intracellular proteins to fluorescent ligands such as bungarotoxin, which has enabled detailed investigation of AChR dynamics both *in vitro* and *in vivo*. We sought to circumvent this limitation by introducing rapsyn-GFP fusion proteins into cells so that we could use the same quantitative fluorescent microscopy techniques that we have used previously to characterize AChR dynamics. By transfecting C2C12 myotubes with rapsyn-GFP and using FRAP, we were able to investigate rapsyn dynamics *in vitro* (Bruneau and Akaabourne, 2007). The principle, and surprising, finding from these studies was that rapsyn turns over at laminin-induced clusters approximately 4 times more rapidly than the receptors to which it binds. The second main finding from this work was that receptor insertion and removal are affected by kinase inhibitors, while rapsyn dynamics are not. Together these findings challenge the view that the intracellular receptor scaffold is a

static and stable structure, and provides evidence that receptor and rapsyn dynamics are regulated by distinct mechanisms. Analogously, recent studies on receptor-associated proteins at glutamatergic synapses have also been shown to turn over more rapidly than the receptors to which they associate, and that scaffolding protein turnover can be regulated by distinct mechanisms.

Future directions: Rapsyn *in vivo*

Expanding on the results above and utilizing all the molecular biology, cellular biology and live animal quantitative fluorescence microscopy that I have acquired in my graduate studies is a final, ongoing project to determine the turnover and regulation of rapsyn *in vivo*. Some significant progress has been made in this project, and clear future directions for the continuation of this research have emerged.

To determine the turnover of rapsyn *in vivo*, I had to first insert rapsyn-GFP into living mouse muscles. Using electroporation I have now successfully inserted plasmids containing a rapsyn-GFP fusion protein construct into the mouse sternomastoid muscle without damaging the muscle fibers. Expression of the rapsyn-GFP at synapses appears to be stable, even over months, with an average loss of fluorescence of <3% per day at any given synapse when measured at 3, 6, 21 or 42 days (Figure 7.1). Similar to the FRAP studies of rapsyn-GFP turnover *in vitro*, I have also been able to successfully measure the recovery of GFP fluorescence over time at individual synapses expressing rapsyn-GFP. As with protein turnover *in vitro*, we have found that rapsyn turns over ~4 times more rapidly than AChRs at the same synapse. These experiments were performed both in fully active muscles that were incubated with a sub-saturating dose of btx-594, and in muscles that were incubated with a saturating dose of btx-594 which transiently

185

blocks post-synaptic muscle activity (Figure 7.2). As has been shown previously, complete inhibition of post-synaptic activity is able to increase AChR turnover at synapses, while an incomplete block of less than ~20% of the AChRs at the synapse allows normal muscle activity and slower AChR turnover. Although the effect of muscle activity blockade on AChR turnover was clearly evident, the insertion of rapsyn at functional and transiently blocked synapses was similar. This suggested that changes in activity which dramatically alter AChR turnover at synaptic sites may not have an effect on rapsyn dynamics.
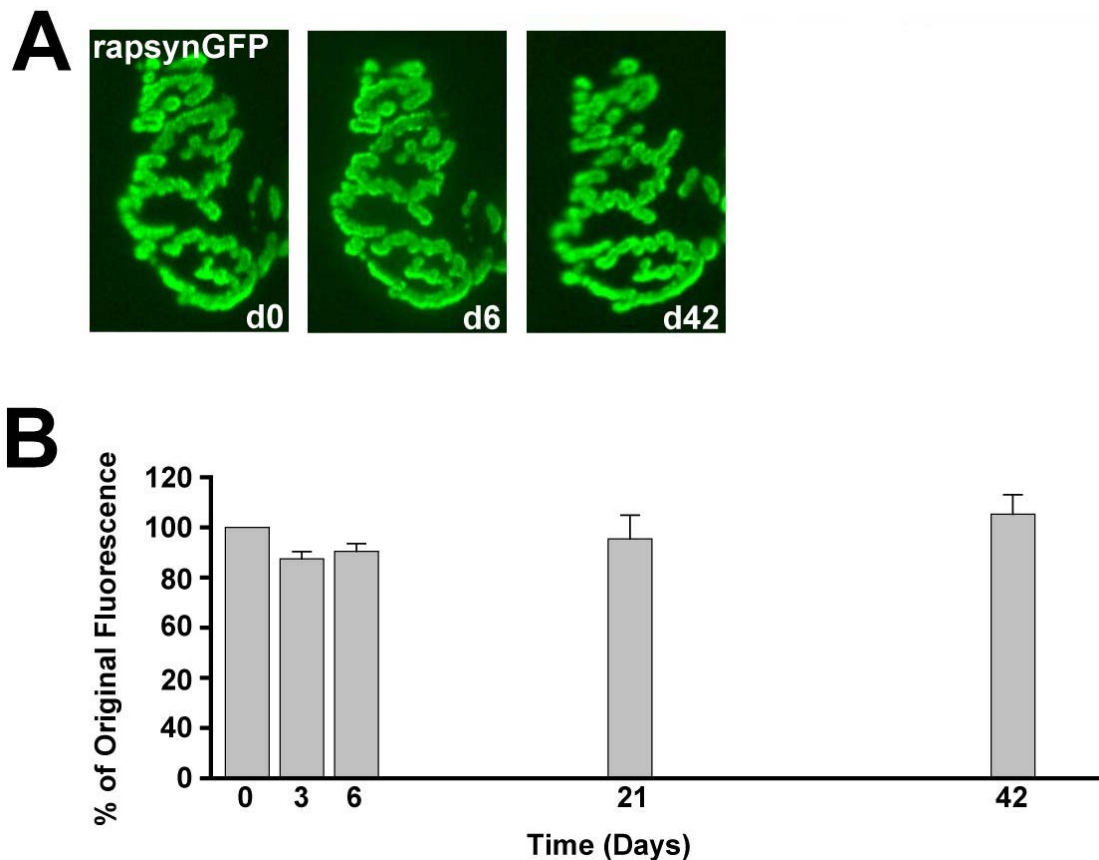
Figure 7.1. Rapsyn-GFP expression is stable over weeks at individual synapses in vivo following electroporation. Mouse sternomastoid muscle was electroporated with rapsyn-GFP and 4 weeks later the muscle was exposed and imaged (d0). At various time points over the following 6 weeks the muscle was re-exposed and the same synapses were imaged. (A) A representative synapse imaged at multiple time points over 6 weeks. Images were all taken using the same imaging parameters. (B) Quantitative fluorescence data from a number of synapses imaged as in (A). All data represented as mean ±S.D.
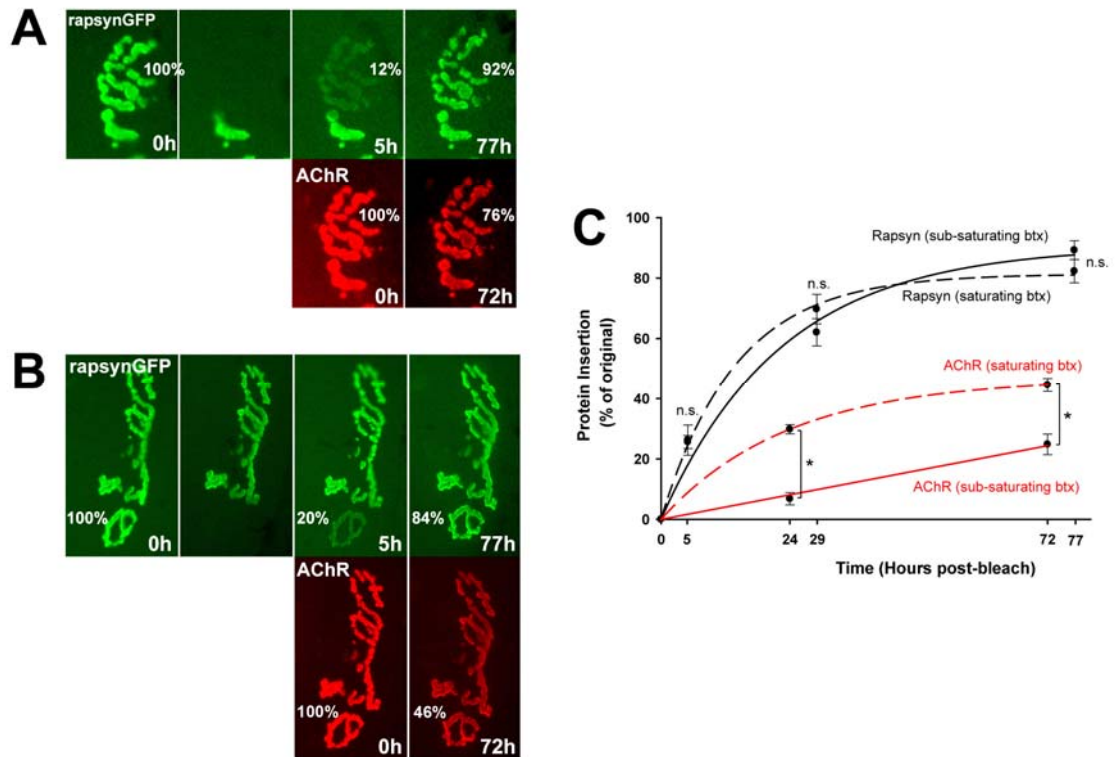
Figure 7.2. Synaptic Turnover of Rapsyn-GFP is Significantly more Rapid than the Turnover of AChRs at the Same Synapse. Sternomastoid muscles of living mice were electroporated with rapsyn-GFP. At least 4 weeks later the muscles were re-exposed, synapses expressing rapsyn-GFP were imaged and then fluorescence from discrete sections of individual junctions was removed with a laser. Muscles were then incubated immediately in either **(A)** saturating or **(B)** non-saturating doses of Btx-biotin followed by a saturating dose of strept-594. After labeling, synapses were imaged and initial fluorescence from AChRs and recovered fluorescence from rapsyn-GFP was measured. After 1 and/or 3 days the muscle was re-exposed and the same synapses were again imaged. **(C)** Data from many synapses measured as in (A) and (B). Since overall AChR density remains constant over these time periods (Bruneau et al., 2005a), receptor loss was converted to receptor insertion for ease of comparison with rapsyn-GFP insertion. Note that AChR removal/insertion is dramatically altered at saturated (post-synaptic activity blocked) vs. unsaturated (post-synaptic activity not blocked) synapses, while rapsyn insertion is unaffected by activity blockade at these same synapses. All data represent mean ±S.D.

To directly test if rapsyn turnover is subject to modulation by post-synaptic activity blockade, we performed the following experiments: first, we examined rapsyn insertion using the same methods as above in muscle that had been denervated 8 days previously that were then labeled with btx-594. As shown previously, muscle denervation resulted in a dramatic increase in AChR removal 1 and/or 3 days later (Figure 7.3A). Consistent with the role of post-synaptic activity on AChR turnover from synapses,

AChR removal from denervated synapses was best described by a linear function (since post-synaptic activity was chronically absent), while removal from innervated control synapses was best fit by 2 functions (as complete post-synaptic blockade was only transient in these synapses). The first question we asked was whether AChR removal was altered by the presence of rapsyn-GFP at these denervated synapses. It has been shown previously that the overexpression of rapsyn is able to decrease AChR loss in experimental myasthenia gravis (Losen et al., 2005; Martinez-Martinez et al., 2007). If the presence of rapsyn-GFP results in an overall increase in rapsyn density at electroporated synapses, then we suspected that AChR removal might be slowed. We found, however, that AChR removal was unaffected at synapses expressing rapsyn-GFP (Figure 7.3B). This indicates either that increased rapsyn does not prevent AChR loss following denervation, or that rapsyn-GFP may replace endogenous rapsyn at synapses in our system to keep rapsyn density constant at the synapse, consistent with our results *in vitro* (Bruneau and Akaabourne, 2007). We also investigated the overall change in rapsyn-GFP density at synapses on denervated muscles. Although overall AChR and rapsyn transcription increase following denervation, the expression of each protein at synaptic sites decreases. Since the rapsyn-GFP construct is driven by a CMV promoter rather than a rapsyn promoter, we were interested to see what effect denervation had on the synaptic expression rapsyn. We found that overall rapsyn-GFP density decreased dramatically over 3 days in denervated synapses (Figure 7.3A, B). Consistent with our previous work (Bruneau et al., 2008), this suggests that AChRs may be critical for maintaining rapsyn density *in vivo*. Finally, we also examined rapsyn dynamics at denervated synapses with FRAP. When fluorescent recovery at bleached regions was

normalized to the fluorescence at unbleached control regions of the same synapse, recovery was similar to the normalized recovery of fluorescence at synapses on the non-denervated control muscle in the same animal (Figure 7.3A, C). When we examined rapsyn-GFP insertion prior to normalization, the insertion of rapsyn (46 ± 20% (s.d.) of original fluorescence, n = 9) was nearly half the insertion at innervated synapses (83 ± 14% (s.d.) of original fluorescence, n = 14) over the same time period. Interestingly, when btx-594 was added at the end of the experiment, the resulting increase in fluorescence from btx-594 binding to newly inserted receptors was similar for both denervated (32 ± 11% (s.d.) of original fluorescence, n = 14) and innervated (33 ± 6% (s.d.) of original fluorescence, n = 7) muscles. These data indicate that rapsyn insertion may be altered by denervation while receptor insertion is not. In light of the fact that nerve trophic factors may be necessary to induce and maintain AChR recycling, these preliminary results suggest that rapsyn turnover may also be regulated by trophic factors. At the least, these results are interesting and warrant further investigation.

As a second test for the effect of activity on rapsyn insertion, we examined AChR and/or rapsyn turnover at rapsyn-GFP expressing synapses that were either unblocked or chronically blocked with a saturating dose of btx-594 followed by constant incubation with curare. For synapses that were incubated with btx-594, both GFP and Alexa 594 fluorescence were removed from synapses and the muscles were re-incubated with new btx-594 at the end of the experiment to label the new, unblocked AChRs that were inserted over the experimental period. Animals were maintained on a ventilator for the duration of the experiment to prevent asphyxiation. Similar to previous studies, we found that chronic inhibition of post-synaptic activity almost completely prevented AChR

insertion during the 8 hours of blockade. Interestingly, for both conditions the insertion of rapsyn-GFP was similar (Figure 7.4). Although preliminary, these studies indicate that the turnover of rapsyn from synaptic sites is significantly more rapid than the turnover of AChRs, and that unlike the AChR, rapsyn dynamics may be unaffected by changes in post-synaptic activity.
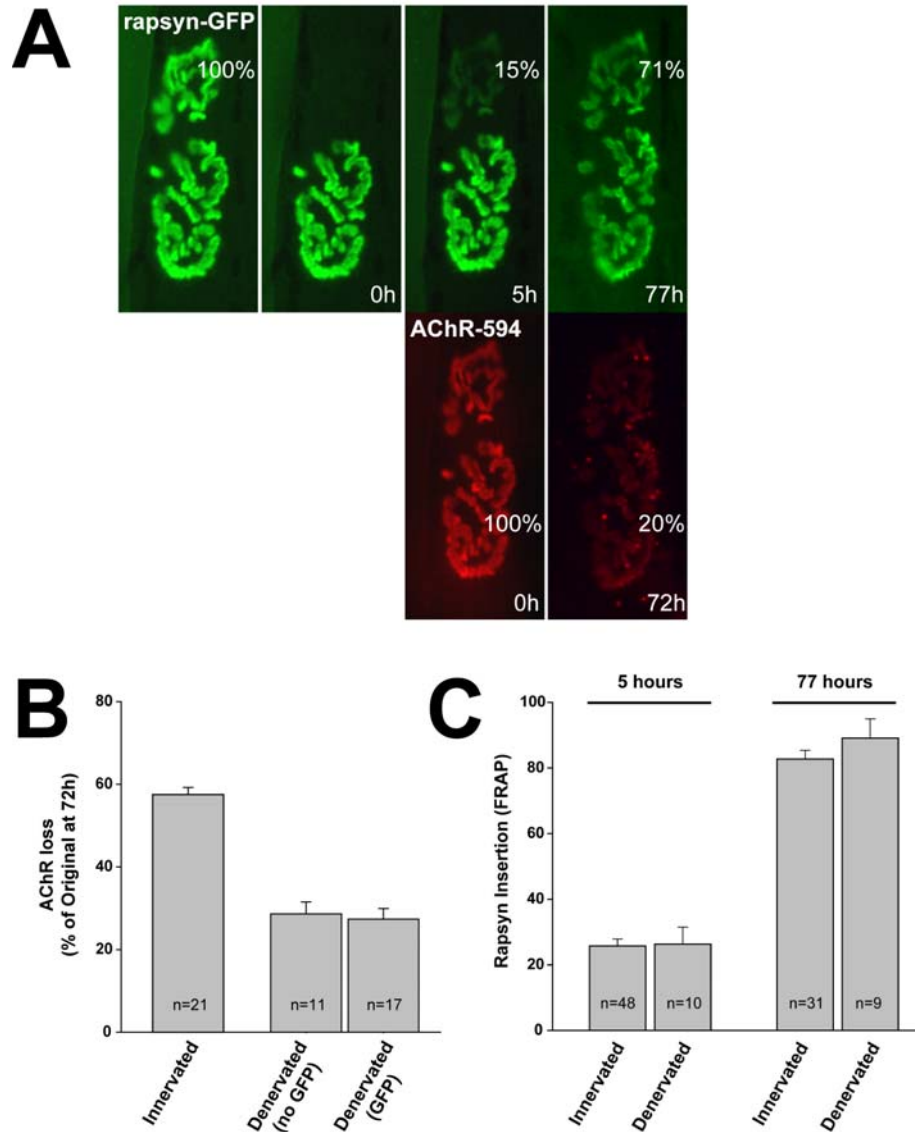
Figure 7.3. Normalized Rapsyn-GFP Synaptic Turnover is Unaffected by Denervation. Four days after rapsyn-GFP electroporation of both sternomastoid muscles, the left muscle of a number of mice was denervated by surgically by removing a 5 mm section of the sternomastoid nerve. Eight days later the fluorescence was removed from discrete regions of individual synapses expressing rapsyn-GFP by carefully tracing the region with a laser. The muscles were then incubated in a saturating dose of Btx-594 and images of synapses expressing rapsyn-GFP and synapses devoid of rapsyn-GFP were taken on both denervated and control muscles. **(A)** Sample image of a synapse expressing rapsyn-GFP on a denervated muscle. FRAP calculated at bleached synaptic regions is relative to original fluorescence at 0h and normalized (in parenthesis) to unbleached regions of the same synapse at each time point. Note that the presence of rapsyn-GFP does not prevent the accelerated receptor loss at denervated synapses. **(B)** Quantification of receptor loss from denervated synapses either devoid of or expressing rapsyn-GFP shows that rapsyn-GFP expression does not slow AChR loss. **(C)** Data obtained from many experiments performed as described above show that rapsyn-GFP insertion (normalized to unbleached regions of the same synapse at each time point) after 5 hours and 3 days is similar at innervated and denervated synapses. All data represented as mean ± SD.
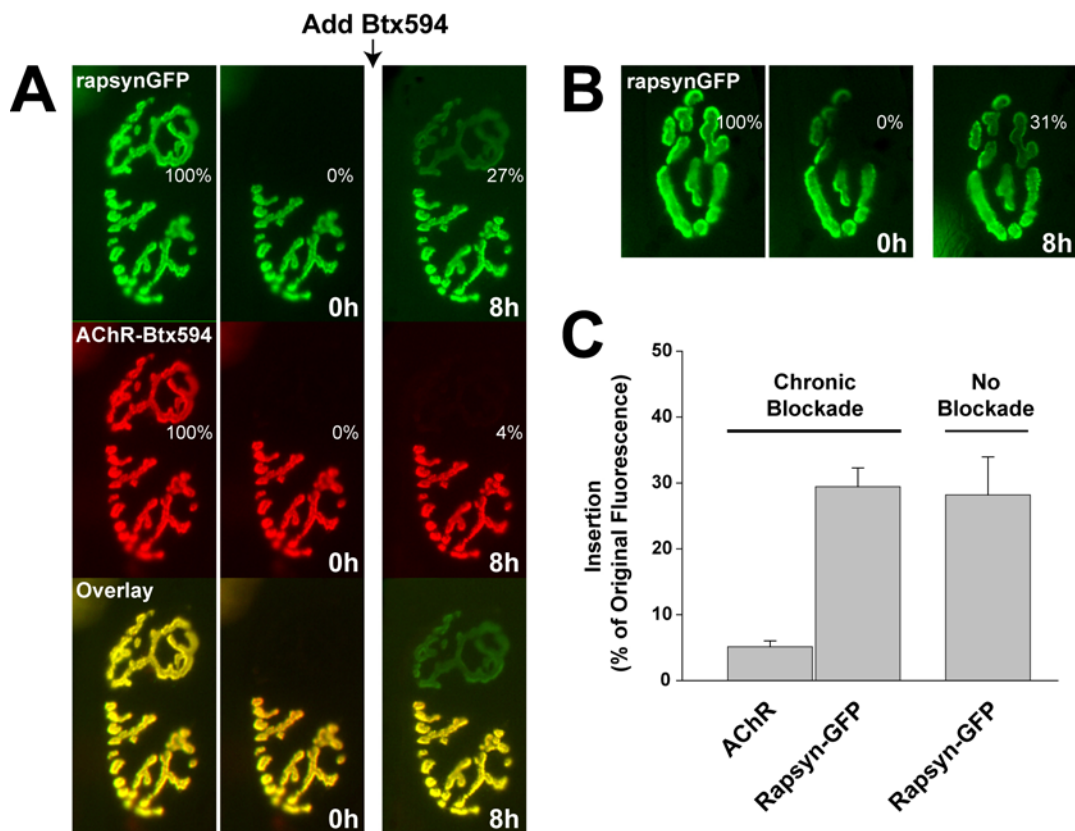
Figure 7.4. Rapsyn-GFP synaptic turnover is not altered by post-synaptic activity blockade. Sternomastoid muscles of living mice were electroporated with rapsyn-GFP, and at least 4 weeks later the muscles were surgically exposed. **(A)** Muscles were incubated with a saturating dose of btx-594 and initial images were taken. The GFP fluorescence from rapsyn-GFP and the Alexa 594 fluorescence from AChR-btx-594 were removed from discrete sections of individual synapses with a laser and the muscle was immediately incubated in the AChR antagonist, curare, for the duration of the experiment. After 8 hours fresh btx-594 was applied to label any newly inserted receptors (and also any receptors that had lost their btx-594 tag after photo-unbinding), and images were again obtained. Note that rapsyn insertion is far greater than AChR insertion/re-binding at the same synapse. **(B)** A sample image of a synapse that was imaged and bleached of rapsyn-GFP fluorescence in the absence of any post-synaptic activity blockade. **(C)** Data obtained from 7 and 13 synapses from experiments done as in (A) and (B), respectively. Data represents mean ± SD.

192

In preparation for the final stage of this work, we have begun to develop an shRNA construct that will allow us to replace rapsyn with rapsyn-GFP at individual synapses. The reasons for pursuing this line of investigation are many-fold: for example, it will provide a powerful control that will enable us to determine if rapsyn-GFP serves as an effective mimic of endogenous rapsyn, and it will enable us to ask a number of novel questions about the role of rapsyn density on AChR synaptic dynamics. As a first step I have created a rapsyn-GFP construct that contains 5 silent point mutations at the wobble positions within the rapsyn gene that is targeted by the shRNA oligomer (rapsyn5*-GFP), rendering the mRNA transcript of this rapsyn5*-GFP invisible to the shRNA. A control GFP-dystrobrevin construct has also been created to test the effectiveness of the shRNA rapsyn *in vivo*. The control will be performed by inserting the GFP-DB gene sequence into the shRNA plasmid at a second cloning site that allows the fusion protein to be driven by a CMV promoter. Since the GFP-DB construct codes for both DB-1, which is expressed selectively at synaptic sites, and DB-2, which is expressed extrasynaptically, this will allow effective identification of electroporated fibers containing the rapsyn shRNA. Electroporated muscles will be immediately incubated in btx-594 (to label all AChRs) and fasciculin2-647 (to label all AChEs), and the quantitative fluorescence at individual synapses will be assayed. The DB-2 labeling will allow us to identify electroporated muscle fibers, and the fasciculin2-647 labeling will enable us to locate synaptic sites even if rapsyn knock-down results in the complete dissipation of synaptic AChRs, since the extracellular AChE molecules labeled with fasciculin2 have been shown to remain even after nerve retraction has induced the post-synaptic cluster to disperse. Subsequent labeling days or weeks later with new btx-594 will enable us to

assess the rate of receptor dissipation, which should provide an estimate of rapsyn knock-down since rapsyn is required for AChR clustering. However, since rapsyn dissipation from synapses may precede AChR dispersion, we will also use quantitative immunohisochemistry of muscles fixed at various times after electroporation to determine the rapsyn density at muscles expressing GFP-DB (and rapsyn shRNA) and at neighboring fibers on the same muscle that are not electroporated with rapsyn shRNA/GFP-DB. Our initial experiments have shown that individual synapses expressing GFP-DB can be identified within 24 hours of electroporation and can be labeled with btx-594 and fasciculin2-647 and imaged at later time points, verifying the feasibility of this approach (Figure 7.5).
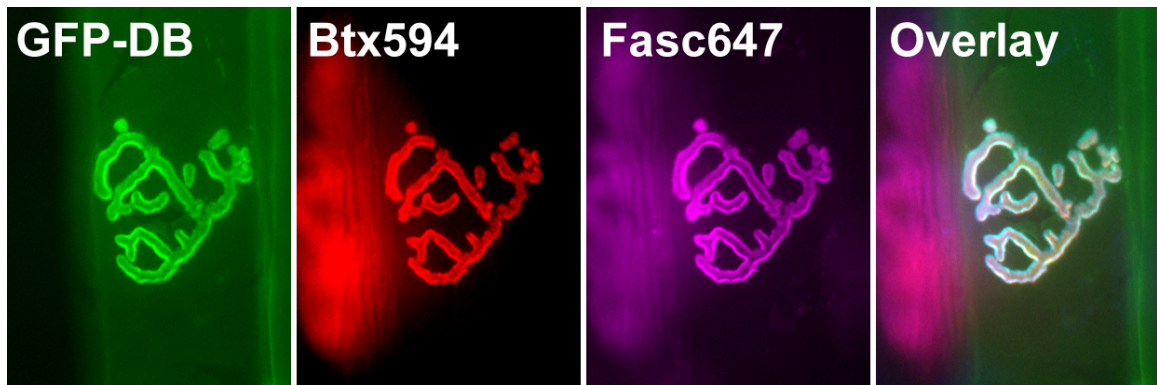
Figure 7.5. Triple-labeling of dystrobrevin, acetylcholine receptors and acetylcholinesterase at the neuromuscular junction. Sternomastoid muscles of living mice were electroporated with GFP-dystrobrevin (GFP-DB) and then incubated with btx-594 (to label all AChRs) and Fasciculin2-647 (to label all AChEs). Note that the dystrobrevin isoforms label both the junction and the muscle surface, as indicated by green staining at the synapse and along the length of the muscle fiber.

After determining the time of maximum rapsyn knock-down with these control experiments, we will electroporate muscles with the rapsyn shRNA/rapsyn5*-GFP construct, and then incubate the sternomastoid muscle with a saturating dose of btx-biotin/strept-594 at a time point after maximum knock-down to label all superficial

AChRs. Subsequent imaging of Alexa 594 fluorescence 1 and/or 3 days later will enable us to determine the rate of receptor loss at synapses expressing exogenous rapsyn5*-GFP and at synapses on neighboring, non-electroporated fibers containing only endogenous synaptic rapsyn. Imaging after sequential labeling with new strept-594 and then new Btx-biotin/strept-594 will enable us to determine AChR recycling and AChR insertion, respectively, at synapses containing only rapsyn5*-GFP and at synapses containing only endogenous rapsyn. This will enable us to compare AChR removal, insertion and recycling at synapses exclusively expressing exogenous rapsyn5*-GFP and at synapses exclusively expressing endogenous rapsyn on different fibers on the same sternomastoid muscle. Finally, in a separate set of experiments, synapses containing rapsyn5*-GFP and synapses containing only endogenous rapsyn will be labeled with btx-594 and the Alexa 594 fluorescence from individual synapses will be removed with a laser. Recovery of fluorescence over time will then be assessed to determine the rate of receptor migration from extrasynaptic to synaptic regions. Together, these experiments will allow us to definitively determine if exogenous rapsyn-GFP mimics the AChR clustering function of endogenous rapsyn. Further, if AChR dynamics correlate with the density of exogenous rapsyn-GFP expression at synapses (determined by average synaptic GFP fluorescence), this would indicate that rapsyn density is able to regulate AChR density at synapses, potentially serving as a mechanism by which synaptic plasticity may be governed.

A second set of experiments will determine rapsyn-GFP turnover using FRAP analysis of rapsyn-GFP after 1 and/or 3 days. If these results are similar to the results obtained at clusters on muscles electroporated with only rapsyn-GFP, which presumably contain mixed populations of endogenous rapsyn and exogenous rapsyn-GFP, the RNAi

data will be pooled with data already obtained. If the data obtained from the rapsyn shRNA/rapsyn5*-GFP FRAP experiments are different, then this data will replace the data obtained in rapsyn-GFP electroporation experiments.

If the shRNA approach is successful, it opens the door to a number of exciting future options. For example, the replacement of endogenous rapsyn with various rapsyn constructs containing common mutations which cause myasthenic syndrome could allow us to examine the effect of these mutant rapsyn proteins on receptor and rapsyn dynamics and the maintenance of the post-synaptic apparatus, while the insertion of various GFP-dystrobrevin constructs into adbn$^{-/-}$ mice could allow analogous studies on the dynamics of dystrobrevin and the effect of dystrobrevin on the maintenance of the intracellular scaffold. This represents an exciting potential future and an interesting extension of the work that I have completed in my PhD studies, which may expand our understanding of the dynamic post-synaptic structure in the intact, living muscle *in vivo*.

References

Adams ME, Kramarcy N, Krall SP, Rossi SG, Rotundo RL, Sealock R, Froehner SC (2000) Absence of alpha-syntrophin leads to structurally aberrant neuromuscular synapses deficient in utrophin. J Cell Biol 150:1385-1398.

Adesnik H, Nicoll RA, England PM (2005) Photoinactivation of native AMPA receptors reveals their real-time trafficking. Neuron 48:977-985.

Akaaboune M, Culican SM, Turney SG, Lichtman JW (1999) Rapid and reversible effects of activity on acetylcholine receptor density at the neuromuscular junction in vivo. Science 286:503-507.

Akaaboune M, Grady RM, Turney S, Sanes JR, Lichtman JW (2002) Neurotransmitter receptor dynamics studied in vivo by reversible photo-unbinding of fluorescent ligands. Neuron 34:865-876.

Andreose JS, Xu R, Lomo T, Salpeter MM, Fumagalli G (1993) Degradation of two AChR populations at rat neuromuscular junctions: regulation in vivo by electrical stimulation. J Neurosci 13:3433-3438.

Apel ED, Roberds SL, Campbell KP, Merlie JP (1995) Rapsyn may function as a link between the acetylcholine receptor and the agrin-binding dystrophin-associated glycoprotein complex. Neuron 15:115-126.

Apel ED, Glass DJ, Moscoso LM, Yancopoulos GD, Sanes JR (1997) Rapsyn is required for MuSK signaling and recruits synaptic components to a MuSK-containing scaffold. Neuron 18:623-635.

Archibald K, Perry MJ, Molnar E, Henley JM (1998) Surface expression and metabolic half-life of AMPA receptors in cultured rat cerebellar granule cells. Neuropharmacology 37:1345-1353.

Ashby MC, De La Rue SA, Ralph GS, Uney J, Collingridge GL, Henley JM (2004) Removal of AMPA receptors (AMPARs) from synapses is preceded by transient endocytosis of extrasynaptic AMPARs. J Neurosci 24:5172-5176.

Axelrod D, Ravdin P, Koppel DE, Schlessinger J, Webb WW, Elson EL, Podleski TR (1976) Lateral motion of fluorescently labeled acetylcholine receptors in membranes of developing muscle fibers. Proc Natl Acad Sci U S A 73:4594-4598.

Balice-Gordon RJ, Lichtman JW (1990) In vivo visualization of the growth of pre- and postsynaptic elements of neuromuscular junctions in the mouse. J Neurosci 10:894-908.

Bansal D, Miyake K, Vogel SS, Groh S, Chen CC, Williamson R, McNeil PL, Campbell KP (2003) Defective membrane repair in dysferlin-deficient muscular dystrophy. Nature 423:168-172.

Banwell BL, Ohno K, Sieb JP, Engel AG (2004) Novel truncating RAPSN mutations causing congenital myasthenic syndrome responsive to 3,4-diaminopyridine. Neuromuscul Disord 14:202-207.

Barnes EM, Jr. (2000) Intracellular trafficking of GABA(A) receptors. Life Sci 66:1063-1070.

Barria A, Malinow R (2002) Subunit-specific NMDA receptor trafficking to synapses. Neuron 35:345-353.

Bartoli M, Ramarao MK, Cohen JB (2001) Interactions of the rapsyn RING-H2 domain with dystroglycan. J Biol Chem 276:24911-24917.

Bear MF, Malenka RC (1994) Synaptic plasticity: LTP and LTD. Curr Opin Neurobiol 4:389-399.

Beck S, Sakurai T, Eustace BK, Beste G, Schier R, Rudert F, Jay DG (2002) Fluorophore-assisted light inactivation: a high-throughput tool for direct target validation of proteins. Proteomics 2:247-255.

Bedford FK, Kittler JT, Muller E, Thomas P, Uren JM, Merlo D, Wisden W, Triller A, Smart TG, Moss SJ (2001) GABA(A) receptor cell surface number and subunit stability are regulated by the ubiquitin-like protein Plic-1. Nat Neurosci 4:908-916.

Beermann AE, Jay DG (1994) Chromophore-assisted laser inactivation of cellular proteins. Methods Cell Biol 44:715-732.

Beeson D, Higuchi O, Palace J, Cossins J, Spearman H, Maxwell S, Newsom-Davis J, Burke G, Fawcett P, Motomura M, Muller JS, Lochmuller H, Slater C, Vincent A, Yamanashi Y (2006) Dok-7 mutations underlie a neuromuscular junction synaptopathy. Science 313:1975-1978.

Bevan S, Steinbach JH (1977) The distribution of alpha-bungarotoxin binding sites of mammalian skeletal muscle developing in vivo. J Physiol 267:195-213.

Bevan S, Steinbach JH (1983) Denervation increases the degradation rate of acetylcholine receptors at end-plates in vivo and in vitro. J Physiol 336:159-177.

Bezakova G, Rabben I, Sefland I, Fumagalli G, Lomo T (2001) Neural agrin controls acetylcholine receptor stability in skeletal muscle fibers. Proc Natl Acad Sci U S A 98:9924-9929.

Bingol B, Schuman EM (2004) A proteasome-sensitive connection between PSD-95 and GluR1 endocytosis. Neuropharmacology 47:755-763.

Blanpied TA, Scott DB, Ehlers MD (2002) Dynamics and regulation of clathrin coats at specialized endocytic zones of dendrites and spines. Neuron 36:435-449.

Bliss TV, Lomo T (1973) Long-lasting potentiation of synaptic transmission in the dentate area of the anaesthetized rabbit following stimulation of the perforant path. J Physiol 232:331-356.

Bogdanov Y, Michels G, Armstrong-Gold C, Haydon PG, Lindstrom J, Pangalos M, Moss SJ (2006) Synaptic GABAA receptors are directly recruited from their extrasynaptic counterparts. Embo J 25:4381-4389.

Borden LA, Czajkowski C, Chan CY, Farb DH (1984) Benzodiazepine receptor synthesis and degradation by neurons in culture. Science 226:857-860.

Borgdorff AJ, Choquet D (2002) Regulation of AMPA receptor lateral movements. Nature 417:649-653.

Braithwaite SP, Xia H, Malenka RC (2002) Differential roles for NSF and GRIP/ABP in AMPA receptor cycling. Proc Natl Acad Sci U S A 99:7096-7101.

Bredt DS, Nicoll RA (2003) AMPA receptor trafficking at excitatory synapses. Neuron 40:361-379.

Brown TC, Tran IC, Backos DS, Esteban JA (2005) NMDA receptor-dependent activation of the small GTPase Rab5 drives the removal of synaptic AMPA receptors during hippocampal LTD. Neuron 45:81-94.

Bruneau E, Sutter D, Hume RI, Akaaboune M (2005a) Identification of nicotinic acetylcholine receptor recycling and its role in maintaining receptor density at the neuromuscular junction in vivo. J Neurosci 25:9949-9959.

Bruneau EG, Akaaboune M (2006a) The dynamics of recycled acetylcholine receptors at the neuromuscular junction in vivo. Development 133:4485-4493.

Bruneau EG, Akaaboune M (2006b) Running to Stand Still: Ionotropic Receptor Dynamics at Central and Peripheral Synapses. Mol Neurobiol 34:137-152.

Bruneau EG, Akaaboune M (2007) The dynamics of the rapsyn scaffolding protein at individual acetylcholine receptor clusters. J Biol Chem.

Bruneau EG, Brenner DI, Kuwada JY, Akaaboune M (2008) Acetylcholine receptor clustering is required for the accumulation and maintenance of scaffolding proteins. Curr Biol.

Bruneau EG, Macpherson PC, Goldman D, Hume RI, Akaaboune M (2005b) The effect of agrin and laminin on acetylcholine receptor dynamics in vitro. Dev Biol 288:248-258.

Burden SJ, DePalma RL, Gottesman GS (1983) Crosslinking of proteins in acetylcholine receptor-rich membranes: association between the beta-subunit and the 43 kd subsynaptic protein. Cell 35:687-692.

Bursztajn S, Berman SA, McManaman JL, Watson ML (1985) Insertion and internalization of acetylcholine receptors at clustered and diffuse domains on cultured myotubes. J Cell Biol 101:104-111.

Cai C, Li H, Rivera C, Keinanen K (2006) Interaction between SAP97 and PSD-95, two Maguk proteins involved in synaptic trafficking of AMPA receptors. J Biol Chem 281:4267-4273.

Caroni P, Rotzler S, Britt JC, Brenner HR (1993) Calcium influx and protein phosphorylation mediate the metabolic stabilization of synaptic acetylcholine receptors in muscle. J Neurosci 13:1315-1325.

Carroll RC, Zukin RS (2002) NMDA-receptor trafficking and targeting: implications for synaptic transmission and plasticity. Trends Neurosci 25:571-577.

Carroll RC, Lissin DV, von Zastrow M, Nicoll RA, Malenka RC (1999a) Rapid redistribution of glutamate receptors contributes to long-term depression in hippocampal cultures. Nat Neurosci 2:454-460.

Carroll RC, Beattie EC, Xia H, Luscher C, Altschuler Y, Nicoll RA, Malenka RC, von Zastrow M (1999b) Dynamin-dependent endocytosis of ionotropic glutamate receptors. Proc Natl Acad Sci U S A 96:14112-14117.

Cartaud A, Coutant S, Petrucci TC, Cartaud J (1998) Evidence for in situ and in vitro association between beta-dystroglycan and the subsynaptic 43K rapsyn protein. Consequence for acetylcholine receptor clustering at the synapse. J Biol Chem 273:11321-11326.

Charrier C, Ehrensperger MV, Dahan M, Levi S, Triller A (2006) Cytoskeleton regulation of glycine receptor number at synapses and diffusion in the plasma membrane. J Neurosci 26:8502-8511.

Chavez RA, Miller SG, Moore HP (1996) A biosynthetic regulated secretory pathway in constitutive secretory cells. J Cell Biol 133:1177-1191.

Chen F, Qian L, Yang ZH, Huang Y, Ngo ST, Ruan NJ, Wang J, Schneider C, Noakes PG, Ding YQ, Mei L, Luo ZG (2007) Rapsyn interaction with calpain stabilizes AChR clusters at the neuromuscular junction. Neuron 55:247-260.

Chen L, Chetkovich DM, Petralia RS, Sweeney NT, Kawasaki Y, Wenthold RJ, Bredt DS, Nicoll RA (2000) Stargazin regulates synaptic targeting of AMPA receptors by two distinct mechanisms. Nature 408:936-943.

Chetkovich DM, Chen L, Stocker TJ, Nicoll RA, Bredt DS (2002) Phosphorylation of the postsynaptic density-95 (PSD-95)/discs large/zona occludens-1 binding site of stargazin regulates binding to PSD-95 and synaptic targeting of AMPA receptors. J Neurosci 22:5791-5796.

Choi J, Ko J, Park E, Lee JR, Yoon J, Lim S, Kim E (2002) Phosphorylation of stargazin by protein kinase A regulates its interaction with PSD-95. J Biol Chem 277:12359-12363.

Chung HJ, Steinberg JP, Huganir RL, Linden DJ (2003) Requirement of AMPA receptor GluR2 phosphorylation for cerebellar long-term depression. Science 300:1751-1755.

Chung HJ, Huang YH, Lau LF, Huganir RL (2004) Regulation of the NMDA receptor complex and trafficking by activity-dependent phosphorylation of the NR2B subunit PDZ ligand. J Neurosci 24:10248-10259.

Chung HJ, Xia J, Scannevin RH, Zhang X, Huganir RL (2000) Phosphorylation of the AMPA receptor subunit GluR2 differentially regulates its interaction with PDZ domain-containing proteins. J Neurosci 20:7258-7267.

Colledge M, Dean RA, Scott GK, Langeberg LK, Huganir RL, Scott JD (2000) Targeting of PKA to glutamate receptors through a MAGUK-AKAP complex. Neuron 27:107-119.

Collingridge GL, Isaac JT, Wang YT (2004) Receptor trafficking and synaptic plasticity. Nat Rev Neurosci 5:952-962.

Connolly CN, Uren JM, Thomas P, Gorrie GH, Gibson A, Smart TG, Moss SJ (1999a) Subcellular localization and endocytosis of homomeric gamma2 subunit splice variants of gamma-aminobutyric acid type A receptors. Mol Cell Neurosci 13:259-271.

Connolly CN, Kittler JT, Thomas P, Uren JM, Brandon NJ, Smart TG, Moss SJ (1999b) Cell surface stability of gamma-aminobutyric acid type A receptors. Dependence on protein kinase C activity and subunit composition. J Biol Chem 274:36565-36572.

Cornish T, Chi J, Johnson S, Lu Y, Campanelli JT (1999) Globular domains of agrin are functional units that collaborate to induce acetylcholine receptor clustering. J Cell Sci 112 (Pt 8):1213-1223.

Cote PD, Moukhles H, Lindenbaum M, Carbonetto S (1999) Chimaeric mice deficient in dystroglycans develop muscular dystrophy and have disrupted myoneural synapses. Nat Genet 23:338-342.

Culican SM, Nelson CC, Lichtman JW (1998) Axon withdrawal during synapse elimination at the neuromuscular junction is accompanied by disassembly of the postsynaptic specialization and withdrawal of Schwann cell processes. J Neurosci 18:4953-4965.

Dahan M, Levi S, Luccardini C, Rostaing P, Riveau B, Triller A (2003) Diffusion dynamics of glycine receptors revealed by single-quantum dot tracking. Science 302:442-445.

DeChiara TM, Bowen DC, Valenzuela DM, Simmons MV, Poueymirou WT, Thomas S, Kinetz E, Compton DL, Rojas E, Park JS, Smith C, DiStefano PS, Glass DJ, Burden SJ, Yancopoulos GD (1996) The receptor tyrosine kinase MuSK is required for neuromuscular junction formation in vivo. Cell 85:501-512.

Deconinck AE, Potter AC, Tinsley JM, Wood SJ, Vater R, Young C, Metzinger L, Vincent A, Slater CR, Davies KE (1997) Postsynaptic abnormalities at the neuromuscular junctions of utrophin-deficient mice. J Cell Biol 136:883-894.

Denzer AJ, Brandenberger R, Gesemann M, Chiquet M, Ruegg MA (1997) Agrin binds to the nerve-muscle basal lamina via laminin. J Cell Biol 137:671-683.

Devreotes PN, Fambrough DM (1975) Acetylcholine receptor turnover in membranes of developing muscle fibers. J Cell Biol 65:335-358.

Dobbins GC, Zhang B, Xiong WC, Mei L (2006) The role of the cytoskeleton in neuromuscular junction formation. J Mol Neurosci 30:115-118.

Dong H, O'Brien RJ, Fung ET, Lanahan AA, Worley PF, Huganir RL (1997) GRIP: a synaptic PDZ domain-containing protein that interacts with AMPA receptors. Nature 386:279-284.

Ebert V, Scholze P, Fuchs K, Sieghart W (1999) Identification of subunits mediating clustering of GABA(A) receptors by rapsyn. Neurochem Int 34:453-463.

Ehlers MD (2000) Reinsertion or degradation of AMPA receptors determined by activity-dependent endocytic sorting. Neuron 28:511-525.

Ehrlich I, Malinow R (2004) Postsynaptic density 95 controls AMPA receptor incorporation during long-term potentiation and experience-driven synaptic plasticity. J Neurosci 24:916-927.

El-Husseini Ael D, Schnell E, Dakoji S, Sweeney N, Zhou Q, Prange O, Gauthier-Campbell C, Aguilera-Moreno A, Nicoll RA, Bredt DS (2002) Synaptic strength regulated by palmitate cycling on PSD-95. Cell 108:849-863.

Erickson JW, Cerione RA (2001) Multiple roles for Cdc42 in cell regulation. Curr Opin Cell Biol 13:153-157.

Essrich C, Lorez M, Benson JA, Fritschy JM, Luscher B (1998) Postsynaptic clustering of major GABAA receptor subtypes requires the gamma 2 subunit and gephyrin. Nat Neurosci 1:563-571.

Fambrough DM (1979) Control of acetylcholine receptors in skeletal muscle. Physiol Rev 59:165-227.

Fambrough DM, Hartzell HC (1972) Acetylcholine receptors: number and distribution at neuromuscular junctions in rat diaphragm. Science 176:189-191.

Feng G, Steinbach JH, Sanes JR (1998a) Rapsyn clusters neuronal acetylcholine receptors but is inessential for formation of an interneuronal cholinergic synapse. J Neurosci 18:4166-4176.

Feng G, Krejci E, Molgo J, Cunningham JM, Massoulié J, Sanes JR (1999) Genetic analysis of collagen Q: roles in acetylcholinesterase and butyrylcholinesterase assembly and in synaptic structure and function. J Cell Biol 144:1349-1360.

Feng G, Tintrup H, Kirsch J, Nichol MC, Kuhse J, Betz H, Sanes JR (1998b) Dual requirement for gephyrin in glycine receptor clustering and molybdoenzyme activity. Science 282:1321-1324.

Ferns M, Deiner M, Hall Z (1996) Agrin-induced acetylcholine receptor clustering in mammalian muscle requires tyrosine phosphorylation. J Cell Biol 132:937-944.

Ferns MJ, Campanelli JT, Hoch W, Scheller RH, Hall Z (1993) The ability of agrin to cluster AChRs depends on alternative splicing and on cell surface proteoglycans. Neuron 11:491-502.

Fertuck HC, Salpeter MM (1974) Localization of acetylcholine receptor by 125I-labeled alpha-bungarotoxin binding at mouse motor endplates. Proc Natl Acad Sci U S A 71:1376-1378.

Fertuck HC, Salpeter MM (1976) Quantitation of junctional and extrajunctional acetylcholine receptors by electron microscope autoradiography after 125I-alpha-bungarotoxin binding at mouse neuromuscular junctions. J Cell Biol 69:144-158.

Fraenkel-Conrat J, Fraenkel-Conrat H (1952) Metabolic fate of biotin and of avidin-biotin complex upon parenteral administration. Biochim Biophys Acta 8:66-70.

Frail DE, McLaughlin LL, Mudd J, Merlie JP (1988) Identification of the mouse muscle 43,000-dalton acetylcholine receptor-associated protein (RAPsyn) by cDNA cloning. J Biol Chem 263:15602-15607.

Frail DE, Musil LS, Buonanno A, Merlie JP (1989) Expression of RAPsyn (43K protein) and nicotinic acetylcholine receptor genes is not coordinately regulated in mouse muscle. Neuron 2:1077-1086.

Fuhrer C, Hall ZW (1996) Functional interaction of Src family kinases with the acetylcholine receptor in C2 myotubes. J Biol Chem 271:32474-32481.

Fuhrer C, Gautam M, Sugiyama JE, Hall ZW (1999) Roles of rapsyn and agrin in interaction of postsynaptic proteins with acetylcholine receptors. J Neurosci 19:6405-6416.

Fuhrmann JC, Kins S, Rostaing P, El Far O, Kirsch J, Sheng M, Triller A, Betz H, Kneussel M (2002) Gephyrin interacts with Dynein light chains 1 and 2, components of motor protein complexes. J Neurosci 22:5393-5402.

Fumagalli G, Engel AG, Lindstrom J (1982) Ultrastructural aspects of acetylcholine receptor turnover at the normal end-plate and in autoimmune myasthenia gravis. J Neuropathol Exp Neurol 41:567-579.

Galkin VE, Orlova A, VanLoock MS, Rybakova IN, Ervasti JM, Egelman EH (2002) The utrophin actin-binding domain binds F-actin in two different modes: implications for the spectrin superfamily of proteins. J Cell Biol 157:243-251.

Gardner JM, Fambrough DM (1979) Acetylcholine receptor degradation measured by density labeling: effects of cholinergic ligands and evidence against recycling. Cell 16:661-674.

Gardoni F, Mauceri D, Fiorentini C, Bellone C, Missale C, Cattabeni F, Di Luca M (2003) CaMKII-dependent phosphorylation regulates SAP97/NR2A interaction. J Biol Chem 278:44745-44752.

Gautam M, DeChiara TM, Glass DJ, Yancopoulos GD, Sanes JR (1999) Distinct phenotypes of mutant mice lacking agrin, MuSK, or rapsyn. Brain Res Dev Brain Res 114:171-178.

Gautam M, Noakes PG, Mudd J, Nichol M, Chu GC, Sanes JR, Merlie JP (1995) Failure of postsynaptic specialization to develop at neuromuscular junctions of rapsyn-deficient mice. Nature 377:232-236.

Gervasio OL, Phillips WD (2005) Increased ratio of rapsyn to ACh receptor stabilizes postsynaptic receptors at the mouse neuromuscular synapse. J Physiol 562:673-685.

Gervasio OL, Armson PF, Phillips WD (2007) Developmental increase in the amount of rapsyn per acetylcholine receptor promotes postsynaptic receptor packing and stability. Dev Biol 305:262-275.

Gesemann M, Denzer AJ, Ruegg MA (1995) Acetylcholine receptor-aggregating activity of agrin isoforms and mapping of the active site. J Cell Biol 128:625-636.

Giesemann T, Schwarz G, Nawrotzki R, Berhorster K, Rothkegel M, Schluter K, Schrader N, Schindelin H, Mendel RR, Kirsch J, Jockusch BM (2003) Complex formation between the postsynaptic scaffolding protein gephyrin, profilin, and Mena: a possible link to the microfilament system. J Neurosci 23:8330-8339.

Gomes AR, Correia SS, Carvalho AL, Duarte CB (2003) Regulation of AMPA receptor activity, synaptic targeting and recycling: role in synaptic plasticity. Neurochem Res 28:1459-1473.

Goto H, Terunuma M, Kanematsu T, Misumi Y, Moss SJ, Hirata M (2005) Direct interaction of N-ethylmaleimide-sensitive factor with GABA(A) receptor beta subunits. Mol Cell Neurosci 30:197-206.

Grady RM, Merlie JP, Sanes JR (1997) Subtle neuromuscular defects in utrophin-deficient mice. J Cell Biol 136:871-882.

Grady RM, Zhou H, Cunningham JM, Henry MD, Campbell KP, Sanes JR (2000) Maturation and maintenance of the neuromuscular synapse: genetic evidence for roles of the dystrophin--glycoprotein complex. Neuron 25:279-293.

Grady RM, Akaaboune M, Cohen AL, Maimone MM, Lichtman JW, Sanes JR (2003) Tyrosine-phosphorylated and nonphosphorylated isoforms of alpha-dystrobrevin: roles in skeletal muscle and its neuromuscular and myotendinous junctions. J Cell Biol 160:741-752.

Green DP, Miledi R, Perez de la Mora M, Vincent A (1975) Acetylcholine receptors. Philos Trans R Soc Lond B Biol Sci 270:551-559.

Green NM (1990) Avidin and streptavidin. Methods Enzymol 184:51-67.

Groc L, Heine M, Cognet L, Brickley K, Stephenson FA, Lounis B, Choquet D (2004) Differential activity-dependent regulation of the lateral mobilities of AMPA and NMDA receptors. Nat Neurosci 7:695-696.

Grosshans DR, Clayton DA, Coultrap SJ, Browning MD (2002) LTP leads to rapid surface expression of NMDA but not AMPA receptors in adult rat CA1. Nat Neurosci 5:27-33.

Gu Y, Hall ZW (1988) Immunological evidence for a change in subunits of the acetylcholine receptor in developing and denervated rat muscle. Neuron 1:117-125.

Gyorgy PaR, C.S. (1943) The Liberation of Biotin from the Avidin-Biotin Complex. Proc Soc Exp Biol Med 53.

Hanley JG, Henley JM (2005) PICK1 is a calcium-sensor for NMDA-induced AMPA receptor trafficking. Embo J 24:3266-3278.

Hanley JG, Khatri L, Hanson PI, Ziff EB (2002) NSF ATPase and alpha-/beta-SNAPs disassemble the AMPA receptor-PICK1 complex. Neuron 34:53-67.

Hanus C, Vannier C, Triller A (2004) Intracellular association of glycine receptor with gephyrin increases its plasma membrane accumulation rate. J Neurosci 24:1119-1128.

Hanus C, Ehrensperger MV, Triller A (2006) Activity-dependent movements of postsynaptic scaffolds at inhibitory synapses. J Neurosci 26:4586-4595.

Harvey K, Duguid IC, Alldred MJ, Beatty SE, Ward H, Keep NH, Lingenfelter SE, Pearce BR, Lundgren J, Owen MJ, Smart TG, Luscher B, Rees MI, Harvey RJ (2004) The GDP-GTP exchange factor collybistin: an essential determinant of neuronal gephyrin clustering. J Neurosci 24:5816-5826.

Hashimoto K, Fukaya M, Qiao X, Sakimura K, Watanabe M, Kano M (1999) Impairment of AMPA receptor function in cerebellar granule cells of ataxic mutant mouse stargazer. J Neurosci 19:6027-6036.

Hayashi T, Huganir RL (2004) Tyrosine phosphorylation and regulation of the AMPA receptor by SRC family tyrosine kinases. J Neurosci 24:6152-6160.

Hayashi Y, Shi SH, Esteban JA, Piccini A, Poncer JC, Malinow R (2000) Driving AMPA receptors into synapses by LTP and CaMKII: requirement for GluR1 and PDZ domain interaction. Science 287:2262-2267.

Henley JM (2003) Proteins interactions implicated in AMPA receptor trafficking: a clear destination and an improving route map. Neurosci Res 45:243-254.

Henry MD, Campbell KP (1996) Dystroglycan: an extracellular matrix receptor linked to the cytoskeleton. Curr Opin Cell Biol 8:625-631.

Henry MD, Campbell KP (1999) Dystroglycan inside and out. Curr Opin Cell Biol 11:602-607.

Herring D, Huang R, Singh M, Robinson LC, Dillon GH, Leidenheimer NJ (2003) Constitutive GABAA receptor endocytosis is dynamin-mediated and dependent on a dileucine AP2 adaptin-binding motif within the beta 2 subunit of the receptor. J Biol Chem 278:24046-24052.

Heynen AJ, Yoon BJ, Liu CH, Chung HJ, Huganir RL, Bear MF (2003) Molecular mechanism for loss of visual cortical responsiveness following brief monocular deprivation. Nat Neurosci 6:854-862.

Hollmann M, Heinemann S (1994) Cloned glutamate receptors. Annu Rev Neurosci 17:31-108.

Huebsch KA, Maimone MM (2003) Rapsyn-mediated clustering of acetylcholine receptor subunits requires the major cytoplasmic loop of the receptor subunits. J Neurobiol 54:486-501.

Huh KH, Wenthold RJ (1999) Turnover analysis of glutamate receptors identifies a rapidly degraded pool of the N-methyl-D-aspartate receptor subunit, NR1, in cultured cerebellar granule cells. J Biol Chem 274:151-157.

Jacob TC, Bogdanov YD, Magnus C, Saliba RS, Kittler JT, Haydon PG, Moss SJ (2005) Gephyrin regulates the cell surface dynamics of synaptic GABAA receptors. J Neurosci 25:10469-10478.

Jacobson C, Cote PD, Rossi SG, Rotundo RL, Carbonetto S (2001) The dystroglycan complex is necessary for stabilization of acetylcholine receptor clusters at neuromuscular junctions and formation of the synaptic basement membrane. J Cell Biol 152:435-450.

James M, Nguyen TM, Wise CJ, Jones GE, Morris GE (1996) Utrophin-dystroglycan complex in membranes of adherent cultured cells. Cell Motil Cytoskeleton 33:163-174.

Jay DG (1988) Selective destruction of protein function by chromophore-assisted laser inactivation. Proc Natl Acad Sci U S A 85:5454-5458.

Jia Z, Agopyan N, Miu P, Xiong Z, Henderson J, Gerlai R, Taverna FA, Velumian A, MacDonald J, Carlen P, Abramow-Newerly W, Roder J (1996) Enhanced LTP in mice deficient in the AMPA receptor GluR2. Neuron 17:945-956.

Jin W, Ge WP, Xu J, Cao M, Peng L, Yung W, Liao D, Duan S, Zhang M, Xia J (2006) Lipid binding regulates synaptic targeting of PICK1, AMPA receptor trafficking, and synaptic plasticity. J Neurosci 26:2380-2390.

Kalia LV, Salter MW (2003) Interactions between Src family protein tyrosine kinases and PSD-95. Neuropharmacology 45:720-728.

Kassner PD, Conroy WG, Berg DK (1998) Organizing Effects of Rapsyn on Neuronal Nicotinic Acetylcholine Receptors. Mol Cell Neurosci 10:258-270.

Kew JN, Richards JG, Mutel V, Kemp JA (1998) Developmental changes in NMDA receptor glycine affinity and ifenprodil sensitivity reveal three distinct populations of NMDA receptors in individual rat cortical neurons. J Neurosci 18:1935-1943.

Kim CH, Lisman JE (2001) A labile component of AMPA receptor-mediated synaptic transmission is dependent on microtubule motors, actin, and N-ethylmaleimide-sensitive factor. J Neurosci 21:4188-4194.

Kim CH, Chung HJ, Lee HK, Huganir RL (2001) Interaction of the AMPA receptor subunit GluR2/3 with PDZ domains regulates hippocampal long-term depression. Proc Natl Acad Sci U S A 98:11725-11730.

Kim CH, Takamiya K, Petralia RS, Sattler R, Yu S, Zhou W, Kalb R, Wenthold R, Huganir R (2005) Persistent hippocampal CA1 LTP in mice lacking the C-terminal PDZ ligand of GluR1. Nat Neurosci 8:985-987.

Kim E, Sheng M (2004) PDZ domain proteins of synapses. Nat Rev Neurosci 5:771-781.

Kim E, Niethammer M, Rothschild A, Jan YN, Sheng M (1995) Clustering of Shaker-type K+ channels by interaction with a family of membrane-associated guanylate kinases. Nature 378:85-88.

Kim E, Naisbitt S, Hsueh YP, Rao A, Rothschild A, Craig AM, Sheng M (1997) GKAP, a novel synaptic protein that interacts with the guanylate kinase-like domain of the PSD-95/SAP90 family of channel clustering molecules. J Cell Biol 136:669-678.

Kim JH, Liao D, Lau LF, Huganir RL (1998) SynGAP: a synaptic RasGAP that associates with the PSD-95/SAP90 protein family. Neuron 20:683-691.

Kim N, Burden SJ (2008) MuSK controls where motor axons grow and form synapses. Nat Neurosci 11:19-27.

Kim S, Nelson PG (2000) Involvement of calpains in the destabilization of the acetylcholine receptor clusters in rat myotubes. J Neurobiol 42:22-32.

Kins S, Betz H, Kirsch J (2000) Collybistin, a newly identified brain-specific GEF, induces submembrane clustering of gephyrin. Nat Neurosci 3:22-29.

Kirsch J, Wolters I, Triller A, Betz H (1993) Gephyrin antisense oligonucleotides prevent glycine receptor clustering in spinal neurons. Nature 366:745-748.

Kittler JT, Arancibia-Carcamo IL, Moss SJ (2004) Association of GRIP1 with a GABA(A) receptor associated protein suggests a role for GRIP1 at inhibitory synapses. Biochem Pharmacol 68:1649-1654.

Kittler JT, Rostaing P, Schiavo G, Fritschy JM, Olsen R, Triller A, Moss SJ (2001) The subcellular distribution of GABARAP and its ability to interact with NSF suggest a role for this protein in the intracellular transport of GABA(A) receptors. Mol Cell Neurosci 18:13-25.

Kittler JT, Chen G, Honing S, Bogdanov Y, McAinsh K, Arancibia-Carcamo IL, Jovanovic JN, Pangalos MN, Haucke V, Yan Z, Moss SJ (2005) Phospho-dependent binding of the clathrin AP2 adaptor complex to GABAA receptors regulates the efficacy of inhibitory synaptic transmission. Proc Natl Acad Sci U S A 102:14871-14876.

Kneussel M (2002) Dynamic regulation of GABA(A) receptors at synaptic sites. Brain Res Brain Res Rev 39:74-83.

Kneussel M, Brandstatter JH, Laube B, Stahl S, Muller U, Betz H (1999) Loss of postsynaptic GABA(A) receptor clustering in gephyrin-deficient mice. J Neurosci 19:9289-9297.

Kneussel M, Brandstatter JH, Gasnier B, Feng G, Sanes JR, Betz H (2001) Gephyrin-independent clustering of postsynaptic GABA(A) receptor subtypes. Mol Cell Neurosci 17:973-982.

Knuesel I, Mastrocola M, Zuellig RA, Bornhauser B, Schaub MC, Fritschy JM (1999) Short communication: altered synaptic clustering of GABAA receptors in mice lacking dystrophin (mdx mice). Eur J Neurosci 11:4457-4462.

Kong XC, Barzaghi P, Ruegg MA (2004) Inhibition of synapse assembly in mammalian muscle in vivo by RNA interference. EMBO Rep 5:183-188.

Kumar S, Kralic JE, O'Buckley TK, Grobin AC, Morrow AL (2003) Chronic ethanol consumption enhances internalization of alpha1 subunit-containing GABAA receptors in cerebral cortex. J Neurochem 86:700-708.

Kummer TT, Misgeld T, Lichtman JW, Sanes JR (2004) Nerve-independent formation of a topologically complex postsynaptic apparatus. J Cell Biol 164:1077-1087.

Kuriu T, Inoue A, Bito H, Sobue K, Okabe S (2006) Differential control of postsynaptic density scaffolds via actin-dependent and -independent mechanisms. J Neurosci 26:7693-7706.

Lan JY, Skeberdis VA, Jover T, Grooms SY, Lin Y, Araneda RC, Zheng X, Bennett MV, Zukin RS (2001) Protein kinase C modulates NMDA receptor trafficking and gating. Nat Neurosci 4:382-390.

Lanuza MA, Garcia N, Santafe M, Gonzalez CM, Alonso I, Nelson PG, Tomas J (2002) Pre- and postsynaptic maturation of the neuromuscular junction during neonatal synapse elimination depends on protein kinase C. J Neurosci Res 67:607-617.

Lau LF, Mammen A, Ehlers MD, Kindler S, Chung WJ, Garner CC, Huganir RL (1996) Interaction of the N-methyl-D-aspartate receptor complex with a novel synapse-associated protein, SAP102. J Biol Chem 271:21622-21628.

Lavezzari G, McCallum J, Lee R, Roche KW (2003) Differential binding of the AP-2 adaptor complex and PSD-95 to the C-terminus of the NMDA receptor subunit NR2B regulates surface expression. Neuropharmacology 45:729-737.

Lavezzari G, McCallum J, Dewey CM, Roche KW (2004) Subunit-specific regulation of NMDA receptor endocytosis. J Neurosci 24:6383-6391.

Lee HM, Wright LD, McCormick DB (1972) Metabolism of carbonyl-labeled 14 C-biotin in the rat. J Nutr 102:1453-1463.

Lee HM, Wright LD, McCormick DB (1973a) Metabolism, in the rat, of biotin injected intraperitoneally as the avidin-biotin complex. Proc Soc Exp Biol Med 142:439-442.

Lee HM, McCall NE, Wright LD, McCormick DB (1973b) Urinary excretion of biotin and metabolites in the rat. Proc Soc Exp Biol Med 142:642-644.

Lee SH, Simonetta A, Sheng M (2004) Subunit rules governing the sorting of internalized AMPA receptors in hippocampal neurons. Neuron 43:221-236.

Lee SH, Liu L, Wang YT, Sheng M (2002) Clathrin adaptor AP2 and NSF interact with overlapping sites of GluR2 and play distinct roles in AMPA receptor trafficking and hippocampal LTD. Neuron 36:661-674.

Leonard AS, Davare MA, Horne MC, Garner CC, Hell JW (1998) SAP97 is associated with the alpha-amino-3-hydroxy-5-methylisoxazole-4-propionic acid receptor GluR1 subunit. J Biol Chem 273:19518-19524.

Levi S, Logan SM, Tovar KR, Craig AM (2004) Gephyrin is critical for glycine receptor clustering but not for the formation of functional GABAergic synapses in hippocampal neurons. J Neurosci 24:207-217.

Lichtman JW, Magrassi L, Purves D (1987) Visualization of neuromuscular junctions over periods of several months in living mice. J Neurosci 7:1215-1222.

Lin JW, Ju W, Foster K, Lee SH, Ahmadian G, Wyszynski M, Wang YT, Sheng M (2000) Distinct molecular mechanisms and divergent endocytotic pathways of AMPA receptor internalization. Nat Neurosci 3:1282-1290.

Lin W, Burgess RW, Dominguez B, Pfaff SL, Sanes JR, Lee KF (2001) Distinct roles of nerve and muscle in postsynaptic differentiation of the neuromuscular synapse. Nature 410:1057-1064.

Lin Y, Skeberdis VA, Francesconi A, Bennett MV, Zukin RS (2004) Postsynaptic density protein-95 regulates NMDA channel gating and surface expression. J Neurosci 24:10138-10148.

Lingle CJ, Steinbach JH (1988) Neuromuscular blocking agents. Int Anesthesiol Clin 26:288-301.

Losen M, Stassen MH, Martinez-Martinez P, Machiels BM, Duimel H, Frederik P, Veldman H, Wokke JH, Spaans F, Vincent A, De Baets MH (2005) Increased expression of rapsyn in muscles prevents acetylcholine receptor loss in experimental autoimmune myasthenia gravis. Brain 128:2327-2337.

Lu W, Ziff EB (2005) PICK1 interacts with ABP/GRIP to regulate AMPA receptor trafficking. Neuron 47:407-421.

Lu W, Man H, Ju W, Trimble WS, MacDonald JF, Wang YT (2001) Activation of synaptic NMDA receptors induces membrane insertion of new AMPA receptors and LTP in cultured hippocampal neurons. Neuron 29:243-254.

Luscher B, Keller CA (2004) Regulation of GABAA receptor trafficking, channel activity, and functional plasticity of inhibitory synapses. Pharmacol Ther 102:195-221.

Luscher C, Xia H, Beattie EC, Carroll RC, von Zastrow M, Malenka RC, Nicoll RA (1999) Role of AMPA receptor cycling in synaptic transmission and plasticity. Neuron 24:649-658.

Luthi A, Chittajallu R, Duprat F, Palmer MJ, Benke TA, Kidd FL, Henley JM, Isaac JT, Collingridge GL (1999) Hippocampal LTD expression involves a pool of AMPARs regulated by the NSF-GluR2 interaction. Neuron 24:389-399.

Maimone MM, Enigk RE (1999) The intracellular domain of the nicotinic acetylcholine receptor alpha subunit mediates its coclustering with rapsyn. Mol Cell Neurosci 14:340-354.

Malenka RC (2003) Synaptic plasticity and AMPA receptor trafficking. Ann N Y Acad Sci 1003:1-11.

Malinow R (2003) AMPA receptor trafficking and long-term potentiation. Philos Trans R Soc Lond B Biol Sci 358:707-714.

Malinow R, Malenka RC (2002) AMPA receptor trafficking and synaptic plasticity. Annu Rev Neurosci 25:103-126.

Mammen AL, Huganir RL, O'Brien RJ (1997) Redistribution and stabilization of cell surface glutamate receptors during synapse formation. J Neurosci 17:7351-7358.

Marangi PA, Wieland ST, Fuhrer C (2002) Laminin-1 redistributes postsynaptic proteins and requires rapsyn, tyrosine phosphorylation, and Src and Fyn to stably cluster acetylcholine receptors. J Cell Biol 157:883-895.

Marangi PA, Forsayeth JR, Mittaud P, Erb-Vogtli S, Blake DJ, Moransard M, Sander A, Fuhrer C (2001) Acetylcholine receptors are required for agrin-induced clustering of postsynaptic proteins. Embo J 20:7060-7073.

Marchand S, Stetzkowski-Marden F, Cartaud J (2001) Differential targeting of components of the dystrophin complex to the postsynaptic membrane. Eur J Neurosci 13:221-229.

Marchand S, Bignami F, Stetzkowski-Marden F, Cartaud J (2000) The myristoylated protein rapsyn is cotargeted with the nicotinic acetylcholine receptor to the postsynaptic membrane via the exocytic pathway. J Neurosci 20:521-528.

Marchand S, Devillers-Thiery A, Pons S, Changeux JP, Cartaud J (2002) Rapsyn escorts the nicotinic acetylcholine receptor along the exocytic pathway via association with lipid rafts. J Neurosci 22:8891-8901.

Marek KW, Davis GW (2002) Transgenically encoded protein photoinactivation (FlAsH-FALI): acute inactivation of synaptotagmin I. Neuron 36:805-813.

Martinez-Martinez P, Losen M, Duimel H, Frederik P, Spaans F, Molenaar P, Vincent A, De Baets MH (2007) Overexpression of rapsyn in rat muscle increases acetylcholine receptor levels in chronic experimental autoimmune myasthenia gravis. Am J Pathol 170:644-657.

Martinez-Pena y Valenzuela I, Hume RI, Krejci E, Akaaboune M (2005) In vivo regulation of acetylcholinesterase insertion at the neuromuscular junction. J Biol Chem 280:31801-31808.

Martyn JA, White DA, Gronert GA, Jaffe RS, Ward JM (1992) Up-and-down regulation of skeletal muscle acetylcholine receptors. Effects on neuromuscular blockers. Anesthesiology 76:822-843.

Maselli RA, Dunne V, Pascual-Pascual SI, Bowe C, Agius M, Frank R, Wollmann RL (2003) Rapsyn mutations in myasthenic syndrome due to impaired receptor clustering. Muscle Nerve 28:293-301.

Mauceri D, Cattabeni F, Di Luca M, Gardoni F (2004) Calcium/calmodulin-dependent protein kinase II phosphorylation drives synapse-associated protein 97 into spines. J Biol Chem 279:23813-23821.

McConville J, Vincent A (2002) Diseases of the neuromuscular junction. Curr Opin Pharmacol 2:296-301.

McMahan UJ (1990) The agrin hypothesis. Cold Spring Harb Symp Quant Biol 55:407-418.

Meier J, Vannier C, Serge A, Triller A, Choquet D (2001) Fast and reversible trapping of surface glycine receptors by gephyrin. Nat Neurosci 4:253-260.

Meng Y, Zhang Y, Jia Z (2003) Synaptic transmission and plasticity in the absence of AMPA glutamate receptor GluR2 and GluR3. Neuron 39:163-176.

Meyer G, Kirsch J, Betz H, Langosch D (1995) Identification of a gephyrin binding motif on the glycine receptor beta subunit. Neuron 15:563-572.

Migaud M, Charlesworth P, Dempster M, Webster LC, Watabe AM, Makhinson M, He Y, Ramsay MF, Morris RG, Morrison JH, O'Dell TJ, Grant SG (1998) Enhanced long-term potentiation and impaired learning in mice with mutant postsynaptic density-95 protein. Nature 396:433-439.

Miller JB (1984) Regulation of acetylcholine receptors in the mouse muscle cell line, C2. Exp Cell Res 154:256-269.

Mishina M, Takai T, Imoto K, Noda M, Takahashi T, Numa S, Methfessel C, Sakmann B (1986) Molecular distinction between fetal and adult forms of muscle acetylcholine receptor. Nature 321:406-411.

Missias AC, Chu GC, Klocke BJ, Sanes JR, Merlie JP (1996) Maturation of the acetylcholine receptor in skeletal muscle: regulation of the AChR gamma-to-epsilon switch. Dev Biol 179:223-238.

Missias AC, Mudd J, Cunningham JM, Steinbach JH, Merlie JP, Sanes JR (1997) Deficient development and maintenance of postsynaptic specializations in mutant mice lacking an 'adult' acetylcholine receptor subunit. Development 124:5075-5086.

Mittaud P, Marangi PA, Erb-Vogtli S, Fuhrer C (2001) Agrin-induced activation of acetylcholine receptor-bound Src family kinases requires Rapsyn and correlates with acetylcholine receptor clustering. J Biol Chem 276:14505-14513.

Miyake K, McNeil PL, Suzuki K, Tsunoda R, Sugai N (2001) An actin barrier to resealing. J Cell Sci 114:3487-3494.

Mohamed AS, Swope SL (1999) Phosphorylation and cytoskeletal anchoring of the acetylcholine receptor by Src class protein-tyrosine kinases. Activation by rapsyn. J Biol Chem 274:20529-20539.

Mohamed AS, Rivas-Plata KA, Kraas JR, Saleh SM, Swope SL (2001) Src-class kinases act within the agrin/MuSK pathway to regulate acetylcholine receptor phosphorylation, cytoskeletal anchoring, and clustering. J Neurosci 21:3806-3818.

Montanaro F, Gee SH, Jacobson C, Lindenbaum MH, Froehner SC, Carbonetto S (1998) Laminin and alpha-dystroglycan mediate acetylcholine receptor aggregation via a MuSK-independent pathway. J Neurosci 18:1250-1260.

Moransard M, Borges LS, Willmann R, Marangi PA, Brenner HR, Ferns MJ, Fuhrer C (2003) Agrin regulates rapsyn interaction with surface acetylcholine receptors, and this underlies cytoskeletal anchoring and clustering. J Biol Chem 278:7350-7359.

Morris PD, Raney KD (1999) DNA helicases displace streptavidin from biotin-labeled oligonucleotides. Biochemistry 38:5164-5171.

Mu Y, Otsuka T, Horton AC, Scott DB, Ehlers MD (2003) Activity-dependent mRNA splicing controls ER export and synaptic delivery of NMDA receptors. Neuron 40:581-594.

Muller BM, Kistner U, Kindler S, Chung WJ, Kuhlendahl S, Fenster SD, Lau LF, Veh RW, Huganir RL, Gundelfinger ED, Garner CC (1996) SAP102, a novel postsynaptic protein that interacts with NMDA receptor complexes in vivo. Neuron 17:255-265.

Muller JS, Baumeister SK, Rasic VM, Krause S, Todorovic S, Kugler K, Muller-Felber W, Abicht A, Lochmuller H (2006) Impaired receptor clustering in congenital myasthenic syndrome with novel RAPSN mutations. Neurology.

Nakagawa T, Futai K, Lashuel HA, Lo I, Okamoto K, Walz T, Hayashi Y, Sheng M (2004) Quaternary structure, protein dynamics, and synaptic function of SAP97 controlled by L27 domain interactions. Neuron 44:453-467.

Neuhoff H, Sassoe-Pognetto M, Panzanelli P, Maas C, Witke W, Kneussel M (2005) The actin-binding protein profilin I is localized at synaptic sites in an activity-regulated manner. Eur J Neurosci 21:15-25.

Nicoll RA, Tomita S, Bredt DS (2006) Auxiliary subunits assist AMPA-type glutamate receptors. Science 311:1253-1256.

Nishimune A, Isaac JT, Molnar E, Noel J, Nash SR, Tagaya M, Collingridge GL, Nakanishi S, Henley JM (1998) NSF binding to GluR2 regulates synaptic transmission. Neuron 21:87-97.

Nitkin RM, Smith MA, Magill C, Fallon JR, Yao YM, Wallace BG, McMahan UJ (1987) Identification of agrin, a synaptic organizing protein from Torpedo electric organ. J Cell Biol 105:2471-2478.

Noakes PG, Phillips WD, Hanley TA, Sanes JR, Merlie JP (1993) 43K protein and acetylcholine receptors colocalize during the initial stages of neuromuscular synapse formation in vivo. Dev Biol 155:275-280.

Noel J, Ralph GS, Pickard L, Williams J, Molnar E, Uney JB, Collingridge GL, Henley JM (1999) Surface expression of AMPA receptors in hippocampal neurons is regulated by an NSF-dependent mechanism. Neuron 23:365-376.

Nong Y, Huang YQ, Salter MW (2004) NMDA receptors are movin' in. Curr Opin Neurobiol 14:353-361.

Nong Y, Huang YQ, Ju W, Kalia LV, Ahmadian G, Wang YT, Salter MW (2003) Glycine binding primes NMDA receptor internalization. Nature 422:302-307.

O'Brien RJ, Kamboj S, Ehlers MD, Rosen KR, Fischbach GD, Huganir RL (1998) Activity-dependent modulation of synaptic AMPA receptor accumulation. Neuron 21:1067-1078.

O'Malley JP, Rubin LL, Salpeter MM (1993) Two populations of AChR in rat myotubes have different degradation rates and responses to cAMP. Exp Cell Res 208:44-47.

Ohno K, Sadeh M, Blatt I, Brengman JM, Engel AG (2003) E-box mutations in the RAPSN promoter region in eight cases with congenital myasthenic syndrome. Hum Mol Genet 12:739-748.

Ohno K, Engel AG, Shen XM, Selcen D, Brengman J, Harper CM, Tsujino A, Milone M (2002) Rapsyn mutations in humans cause endplate acetylcholine-receptor deficiency and myasthenic syndrome. Am J Hum Genet 70:875-885.

Okada K, Inoue A, Okada M, Murata Y, Kakuta S, Jigami T, Kubo S, Shiraishi H, Eguchi K, Motomura M, Akiyama T, Iwakura Y, Higuchi O, Yamanashi Y (2006) The muscle protein Dok-7 is essential for neuromuscular synaptogenesis. Science 312:1802-1805.

Ono F, Mandel G, Brehm P (2004) Acetylcholine receptors direct rapsyn clusters to the neuromuscular synapse in zebrafish. J Neurosci 24:5475-5481.

Ono F, Higashijima S, Shcherbatko A, Fetcho JR, Brehm P (2001) Paralytic zebrafish lacking acetylcholine receptors fail to localize rapsyn clusters to the synapse. J Neurosci 21:5439-5448.

Osten P, Khatri L, Perez JL, Kohr G, Giese G, Daly C, Schulz TW, Wensky A, Lee LM, Ziff EB (2000) Mutagenesis reveals a role for ABP/GRIP binding to GluR2 in synaptic surface accumulation of the AMPA receptor. Neuron 27:313-325.

Palmer CL, Cotton L, Henley JM (2005) The molecular pharmacology and cell biology of alpha-amino-3-hydroxy-5-methyl-4-isoxazolepropionic acid receptors. Pharmacol Rev 57:253-277.

Papadopoulos T, Korte M, Eulenburg V, Kubota H, Retiounskaia M, Harvey RJ, Harvey K, O'Sullivan GA, Laube B, Hulsmann S, Geiger JR, Betz H (2007) Impaired GABAergic transmission and altered hippocampal synaptic plasticity in collybistin-deficient mice. Embo J 26:3888-3899.

Park M, Penick EC, Edwards JG, Kauer JA, Ehlers MD (2004) Recycling endosomes supply AMPA receptors for LTP. Science 305:1972-1975.

Passafaro M, Piech V, Sheng M (2001) Subunit-specific temporal and spatial patterns of AMPA receptor exocytosis in hippocampal neurons. Nat Neurosci 4:917-926.

Penzes P, Johnson RC, Sattler R, Zhang X, Huganir RL, Kambampati V, Mains RE, Eipper BA (2001) The neuronal Rho-GEF Kalirin-7 interacts with PDZ domain-containing proteins and regulates dendritic morphogenesis. Neuron 29:229-242.

Perez-Otano I, Ehlers MD (2005) Homeostatic plasticity and NMDA receptor trafficking. Trends Neurosci 28:229-238.

Perez JL, Khatri L, Chang C, Srivastava S, Osten P, Ziff EB (2001) PICK1 targets activated protein kinase Calpha to AMPA receptor clusters in spines of hippocampal neurons and reduces surface levels of the AMPA-type glutamate receptor subunit 2. J Neurosci 21:5417-5428.

Phillips WD, Vladeta D, Han H, Noakes PG (1997) Rapsyn and agrin slow the metabolic degradation of the acetylcholine receptor. Mol Cell Neurosci 10:16-26.

Prybylowski K, Chang K, Sans N, Kan L, Vicini S, Wenthold RJ (2005) The synaptic localization of NR2B-containing NMDA receptors is controlled by interactions with PDZ proteins and AP-2. Neuron 47:845-857.

Quinlan EM, Philpot BD, Huganir RL, Bear MF (1999) Rapid, experience-dependent expression of synaptic NMDA receptors in visual cortex in vivo. Nat Neurosci 2:352-357.

Rabow LE, Russek SJ, Farb DH (1995) From ion currents to genomic analysis: recent advances in GABAA receptor research. Synapse 21:189-274.

Ramarao MK, Cohen JB (1998) Mechanism of nicotinic acetylcholine receptor cluster formation by rapsyn. Proc Natl Acad Sci U S A 95:4007-4012.

Ramarao MK, Bianchetta MJ, Lanken J, Cohen JB (2001) Role of rapsyn tetratricopeptide repeat and coiled-coil domains in self-association and nicotinic acetylcholine receptor clustering. J Biol Chem 276:7475-7483.

Rasse TM, Fouquet W, Schmid A, Kittel RJ, Mertel S, Sigrist CB, Schmidt M, Guzman A, Merino C, Qin G, Quentin C, Madeo FF, Heckmann M, Sigrist SJ (2005) Glutamate receptor dynamics organizing synapse formation in vivo. Nat Neurosci 8:898-905.

Reisel D, Bannerman DM, Schmitt WB, Deacon RM, Flint J, Borchardt T, Seeburg PH, Rawlins JN (2002) Spatial memory dissociations in mice lacking GluR1. Nat Neurosci 5:868-873.

Reist NE, Werle MJ, McMahan UJ (1992) Agrin released by motor neurons induces the aggregation of acetylcholine receptors at neuromuscular junctions. Neuron 8:865-868.

Roche KW, Standley S, McCallum J, Dune Ly C, Ehlers MD, Wenthold RJ (2001) Molecular determinants of NMDA receptor internalization. Nat Neurosci 4:794-802.

Rotzler S, Brenner HR (1990) Metabolic stabilization of acetylcholine receptors in vertebrate neuromuscular junction by muscle activity. J Cell Biol 111:655-661.

Rotzler S, Schramek H, Brenner HR (1991) Metabolic stabilization of endplate acetylcholine receptors regulated by Ca2+ influx associated with muscle activity. Nature 349:337-339.

Rouach N, Byrd K, Petralia RS, Elias GM, Adesnik H, Tomita S, Karimzadegan S, Kealey C, Bredt DS, Nicoll RA (2005) TARP gamma-8 controls hippocampal AMPA receptor number, distribution and synaptic plasticity. Nat Neurosci 8:1525-1533.

Rumbaugh G, Vicini S (1999) Distinct synaptic and extrasynaptic NMDA receptors in developing cerebellar granule neurons. J Neurosci 19:10603-10610.

Rumbaugh G, Sia GM, Garner CC, Huganir RL (2003) Synapse-associated protein-97 isoform-specific regulation of surface AMPA receptors and synaptic function in cultured neurons. J Neurosci 23:4567-4576.

Rumpel S, LeDoux J, Zador A, Malinow R (2005) Postsynaptic receptor trafficking underlying a form of associative learning. Science 308:83-88.

Rutter AR, Stephenson FA (2000) Coexpression of postsynaptic density-95 protein with NMDA receptors results in enhanced receptor expression together with a decreased sensitivity to L-glutamate. J Neurochem 75:2501-2510.

Sabatini DM, Barrow RK, Blackshaw S, Burnett PE, Lai MM, Field ME, Bahr BA, Kirsch J, Betz H, Snyder SH (1999) Interaction of RAFT1 with gephyrin required for rapamycin-sensitive signaling. Science 284:1161-1164.

Sadasivam G, Willmann R, Lin S, Erb-Vogtli S, Kong XC, Ruegg MA, Fuhrer C (2005) Src-family kinases stabilize the neuromuscular synapse in vivo via protein interactions, phosphorylation, and cytoskeletal linkage of acetylcholine receptors. J Neurosci 25:10479-10493.

Saiyed T, Paarmann I, Schmitt B, Haeger S, Sola M, Schmalzing G, Weissenhorn W, Betz H (2007) Molecular basis of gephyrin clustering at inhibitory synapses: role of G- and E-domain interactions. J Biol Chem 282:5625-5632.

Salpeter MM, Loring RH (1985) Nicotinic acetylcholine receptors in vertebrate muscle: properties, distribution and neural control. Prog Neurobiol 25:297-325.

Sanes JR (1997) Genetic analysis of postsynaptic differentiation at the vertebrate neuromuscular junction. Curr Opin Neurobiol 7:93-100.

Sanes JR, Lichtman JW (2001) Induction, assembly, maturation and maintenance of a postsynaptic apparatus. Nat Rev Neurosci 2:791-805.

Sans N, Prybylowski K, Petralia RS, Chang K, Wang YX, Racca C, Vicini S, Wenthold RJ (2003) NMDA receptor trafficking through an interaction between PDZ proteins and the exocyst complex. Nat Cell Biol 5:520-530.

Sans N, Wang PY, Du Q, Petralia RS, Wang YX, Nakka S, Blumer JB, Macara IG, Wenthold RJ (2005) mPins modulates PSD-95 and SAP102 trafficking and influences NMDA receptor surface expression. Nat Cell Biol 7:1079-1090.

Schmitt WB, Deacon RM, Seeburg PH, Rawlins JN, Bannerman DM (2003) A within-subjects, within-task demonstration of intact spatial reference memory and impaired spatial working memory in glutamate receptor-A-deficient mice. J Neurosci 23:3953-3959.

Schmitt WB, Sprengel R, Mack V, Draft RW, Seeburg PH, Deacon RM, Rawlins JN, Bannerman DM (2005) Restoration of spatial working memory by genetic rescue of GluR-A-deficient mice. Nat Neurosci 8:270-272.

Schnell E, Sizemore M, Karimzadegan S, Chen L, Bredt DS, Nicoll RA (2002) Direct interactions between PSD-95 and stargazin control synaptic AMPA receptor number. Proc Natl Acad Sci U S A 99:13902-13907.

Scott DB, Blanpied TA, Ehlers MD (2003) Coordinated PKA and PKC phosphorylation suppresses RXR-mediated ER retention and regulates the surface delivery of NMDA receptors. Neuropharmacology 45:755-767.

Scott DB, Blanpied TA, Swanson GT, Zhang C, Ehlers MD (2001) An NMDA receptor ER retention signal regulated by phosphorylation and alternative splicing. J Neurosci 21:3063-3072.

Scott DB, Michailidis I, Mu Y, Logothetis D, Ehlers MD (2004) Endocytosis and degradative sorting of NMDA receptors by conserved membrane-proximal signals. J Neurosci 24:7096-7109.

Sealock R, Wray BE, Froehner SC (1984) Ultrastructural localization of the Mr 43,000 protein and the acetylcholine receptor in Torpedo postsynaptic membranes using monoclonal antibodies. J Cell Biol 98:2239-2244.

Seidenman KJ, Steinberg JP, Huganir R, Malinow R (2003) Glutamate receptor subunit 2 Serine 880 phosphorylation modulates synaptic transmission and mediates plasticity in CA1 pyramidal cells. J Neurosci 23:9220-9228.

Sekine-Aizawa Y, Huganir RL (2004) Imaging of receptor trafficking by using alpha-bungarotoxin-binding-site-tagged receptors. Proc Natl Acad Sci U S A 101:17114-17119.

Sharma K, Fong DK, Craig AM (2006a) Postsynaptic protein mobility in dendritic spines: long-term regulation by synaptic NMDA receptor activation. Mol Cell Neurosci 31:702-712.

Sharma K, Fong DK, Craig AM (2006b) Postsynaptic protein mobility in dendritic spines: Long-term regulation by synaptic NMDA receptor activation. Mol Cell Neurosci.

Shepard AA, Dumka D, Akopova I, Talent J, Borejdo J (2004) Simultaneous measurement of rotations of myosin, actin and ADP in a contracting skeletal muscle fiber. J Muscle Res Cell Motil 25:549-557.

Shi S, Hayashi Y, Esteban JA, Malinow R (2001) Subunit-specific rules governing AMPA receptor trafficking to synapses in hippocampal pyramidal neurons. Cell 105:331-343.

Shi SH, Hayashi Y, Petralia RS, Zaman SH, Wenthold RJ, Svoboda K, Malinow R (1999) Rapid spine delivery and redistribution of AMPA receptors after synaptic NMDA receptor activation. Science 284:1811-1816.

Shyng SL, Salpeter MM (1989) Degradation rate of acetylcholine receptors inserted into denervated vertebrate neuromuscular junctions. J Cell Biol 108:647-651.

Si J, Tanowitz M, Won S, Mei L (1998) Regulation by ARIA/neuregulin of acetylcholine receptor gene transcription at the neuromuscular junction. Life Sci 62:1497-1502.

Sieghart W, Sperk G (2002) Subunit composition, distribution and function of GABA(A) receptor subtypes. Curr Top Med Chem 2:795-816.

Snyder EM, Philpot BD, Huber KM, Dong X, Fallon JR, Bear MF (2001) Internalization of ionotropic glutamate receptors in response to mGluR activation. Nat Neurosci 4:1079-1085.

Sola M, Kneussel M, Heck IS, Betz H, Weissenhorn W (2001) X-ray crystal structure of the trimeric N-terminal domain of gephyrin. J Biol Chem 276:25294-25301.

St John PA, Gordon H (2001) Agonists cause endocytosis of nicotinic acetylcholine receptors on cultured myotubes. J Neurobiol 49:212-223.

Standley S, Roche KW, McCallum J, Sans N, Wenthold RJ (2000) PDZ domain suppression of an ER retention signal in NMDA receptor NR1 splice variants. Neuron 28:887-898.

Stanley EF, Drachman DB (1983) Rapid degradation of "new" acetylcholine receptors at neuromuscular junctions. Science 222:67-69.

Stein V, House DR, Bredt DS, Nicoll RA (2003) Postsynaptic density-95 mimics and occludes hippocampal long-term potentiation and enhances long-term depression. J Neurosci 23:5503-5506.

Subramanian N, Subramanian S, Karande AA, Adiga PR (1997) A monoclonal antibody to avidin dissociates quaternary structure and curtails biotin binding to avidin and streptavidin. Arch Biochem Biophys 344:281-288.

Sugiyama JE, Glass DJ, Yancopoulos GD, Hall ZW (1997) Laminin-induced acetylcholine receptor clustering: an alternative pathway. J Cell Biol 139:181-191.

Takahashi T, Svoboda K, Malinow R (2003) Experience strengthening transmission by driving AMPA receptors into synapses. Science 299:1585-1588.

Tardin C, Cognet L, Bats C, Lounis B, Choquet D (2003) Direct imaging of lateral movements of AMPA receptors inside synapses. Embo J 22:4656-4665.

Tezuka T, Umemori H, Akiyama T, Nakanishi S, Yamamoto T (1999) PSD-95 promotes Fyn-mediated tyrosine phosphorylation of the N-methyl-D-aspartate receptor subunit NR2A. Proc Natl Acad Sci U S A 96:435-440.

Thomas P, Mortensen M, Hosie AM, Smart TG (2005) Dynamic mobility of functional GABAA receptors at inhibitory synapses. Nat Neurosci 8:889-897.

Tomita S, Fukata M, Nicoll RA, Bredt DS (2004) Dynamic interaction of stargazin-like TARPs with cycling AMPA receptors at synapses. Science 303:1508-1511.

Tomita S, Stein V, Stocker TJ, Nicoll RA, Bredt DS (2005a) Bidirectional synaptic plasticity regulated by phosphorylation of stargazin-like TARPs. Neuron 45:269-277.

Tomita S, Adesnik H, Sekiguchi M, Zhang W, Wada K, Howe JR, Nicoll RA, Bredt DS (2005b) Stargazin modulates AMPA receptor gating and trafficking by distinct domains. Nature 435:1052-1058.

Topinka JR, Bredt DS (1998) N-terminal palmitoylation of PSD-95 regulates association with cell membranes and interaction with K+ channel Kv1.4. Neuron 20:125-134.

Tovar KR, Westbrook GL (1999) The incorporation of NMDA receptors with a distinct subunit composition at nascent hippocampal synapses in vitro. J Neurosci 19:4180-4188.

Tovar KR, Westbrook GL (2002) Mobile NMDA receptors at hippocampal synapses. Neuron 34:255-264.

Triller A, Choquet D (2003) Synaptic structure and diffusion dynamics of synaptic receptors. Biol Cell 95:465-476.

Trinidad JC, Cohen JB (2004) Neuregulin inhibits acetylcholine receptor aggregation in myotubes. J Biol Chem 279:31622-31628.

Turney SG, Culican SM, Lichtman JW (1996) A quantitative fluorescence-imaging technique for studying acetylcholine receptor turnover at neuromuscular junctions in living animals. J Neurosci Methods 64:199-208.

Valenzuela DM, Stitt TN, DiStefano PS, Rojas E, Mattsson K, Compton DL, Nunez L, Park JS, Stark JL, Gies DR, et al. (1995) Receptor tyrosine kinase specific for the skeletal muscle lineage: expression in embryonic muscle, at the neuromuscular junction, and after injury. Neuron 15:573-584.

Valtschanoff JG, Burette A, Davare MA, Leonard AS, Hell JW, Weinberg RJ (2000) SAP97 concentrates at the postsynaptic density in cerebral cortex. Eur J Neurosci 12:3605-3614.

van Mier P, Lichtman JW (1994) Regenerating muscle fibers induce directional sprouting from nearby nerve terminals: studies in living mice. J Neurosci 14:5672-5686.

215

Vicini S, Wang JF, Li JH, Zhu WJ, Wang YH, Luo JH, Wolfe BB, Grayson DR (1998) Functional and pharmacological differences between recombinant N-methyl-D-aspartate receptors. J Neurophysiol 79:555-566.

Vogel Z, Christian CN, Vigny M, Bauer HC, Sonderegger P, Daniels MP (1983) Laminin induces acetylcholine receptor aggregation on cultured myotubes and enhances the receptor aggregation activity of a neuronal factor. J Neurosci 3:1058-1068.

Wallace BG (1988) Regulation of agrin-induced acetylcholine receptor aggregation by Ca++ and phorbol ester. J Cell Biol 107:267-278.

Wallace BG (1994) Staurosporine inhibits agrin-induced acetylcholine receptor phosphorylation and aggregation. J Cell Biol 125:661-668.

Wan Q, Xiong ZG, Man HY, Ackerley CA, Braunton J, Lu WY, Becker LE, MacDonald JF, Wang YT (1997) Recruitment of functional GABA(A) receptors to postsynaptic domains by insulin. Nature 388:686-690.

Wang H, Bedford FK, Brandon NJ, Moss SJ, Olsen RW (1999a) GABA(A)-receptor-associated protein links GABA(A) receptors and the cytoskeleton. Nature 397:69-72.

Wang JQ, Arora A, Yang L, Parelkar NK, Zhang G, Liu X, Choe ES, Mao L (2005) Phosphorylation of AMPA receptors: mechanisms and synaptic plasticity. Mol Neurobiol 32:237-249.

Wang ZZ, Mathias A, Gautam M, Hall ZW (1999b) Metabolic stabilization of muscle nicotinic acetylcholine receptor by rapsyn. J Neurosci 19:1998-2007.

Washbourne P, Bennett JE, McAllister AK (2002) Rapid recruitment of NMDA receptor transport packets to nascent synapses. Nat Neurosci 5:751-759.

Washbourne P, Liu XB, Jones EG, McAllister AK (2004) Cycling of NMDA receptors during trafficking in neurons before synapse formation. J Neurosci 24:8253-8264.

Weber PC, Ohlendorf DH, Wendoloski JJ, Salemme FR (1989) Structural origins of high-affinity biotin binding to streptavidin. Science 243:85-88.

Wei RD, Kou DH, Hoo SL (1971) Dissociation of avidin-biotin complex in vivo. Experientia 27:366-368.

Wenthold RJ, Prybylowski K, Standley S, Sans N, Petralia RS (2003) Trafficking of NMDA receptors. Annu Rev Pharmacol Toxicol 43:335-358.

Xia H, Hornby ZD, Malenka RC (2001) An ER retention signal explains differences in surface expression of NMDA and AMPA receptor subunits. Neuropharmacology 41:714-723.

Yang SH, Armson PF, Cha J, Phillips WD (1997) Clustering of GABAA receptors by rapsyn/43kD protein in vitro. Mol Cell Neurosci 8:430-438.

Yao WD, Gainetdinov RR, Arbuckle MI, Sotnikova TD, Cyr M, Beaulieu JM, Torres GE, Grant SG, Caron MG (2004) Identification of PSD-95 as a regulator of dopamine-mediated synaptic and behavioral plasticity. Neuron 41:625-638.

Young SH, Poo MM (1983) Rapid lateral diffusion of extrajunctional acetylcholine receptors in the developing muscle membrane of Xenopus tadpole. J Neurosci 3:225-231.

Yu W, Jiang M, Miralles CP, Li RW, Chen G, de Blas AL (2007) Gephyrin clustering is required for the stability of GABAergic synapses. Mol Cell Neurosci 36:484-500.

Zamanillo D, Sprengel R, Hvalby O, Jensen V, Burnashev N, Rozov A, Kaiser KM, Koster HJ, Borchardt T, Worley P, Lubke J, Frotscher M, Kelly PH, Sommer B,

Andersen P, Seeburg PH, Sakmann B (1999) Importance of AMPA receptors for hippocampal synaptic plasticity but not for spatial learning. Science 284:1805-1811.

Zhu JJ, Esteban JA, Hayashi Y, Malinow R (2000) Postnatal synaptic potentiation: delivery of GluR4-containing AMPA receptors by spontaneous activity. Nat Neurosci 3:1098-1106.